Observational study of physical properties of giant molecular clouds in W51

Shinji FUJITA

February 2017

Observational study of physical properties of giant molecular clouds in W51

Shinji FUJITA

Doctoral Program in Physics

Submitted to the Graduate School of

Pure and Applied Sciences

in Partial Fulfillment of the Requirements

for the Degree of Doctor of Philosophy in

Science

at the

University of Tsukuba

Abstract

It is known that massive stars, which play very important roles in the evolution of galaxies, are formed in Giant Molecular Clouds (GMCs). However, its formation mechanism has not been elucidated yet, and it is one of the major issue of the astronomy. Therefore, observational studies of GMC are considered to be indispensable for research on massive star formation. We focused on W51 which is one of the most active massive star forming region in the Galaxy. The characteristics of W51 are H II regions distributed throughout the region and molecular clouds with various velocities overlapping along the line of sight. We carried out the mapping observations of ^{12}CO, ^{13}CO and C^{18}O ($J = 1 - 0$) emission lines toward W51 with high angular resolutions ($\sim 18''$) as a part of the Nobeyama Radio Observatory Legacy Project, FOREST Ultra-wide Galactic plane survey In Nobeyama (FUGIN). This is the first ^{12}CO ($J = 1 - 0$) map which covers the entire region of W51 GMC. We analyzed the data by using the algorithm Dendrograms to investigate the internal structure of W51 GMC in detail.

First, in order to investigate the spacial variation of properties of W51, we decomposed W51 GMC into several clouds. As a result, we found that molecular clouds with tendency to make Young Stellar Objects (YSOs) with larger mass have the tendencies as follows. (1) The column density of hydrogen molecules is high and mass is large, (2) ^{13}CO ($J = 3 - 2$)/^{13}CO ($J = 1 - 0$) ratio is high, and (3) 8 μm intensity is high. These results are consistent with the scenario that molecular clouds with high column density of hydrogen molecules and large mass form massive stars, and its surrounding gas is heated by the radiation from the massive stars.

Then, we investigated the internal structure of the most complex molecular cloud in the eastern side of W51 (W51A) where star formation activity is very high. Cloud-Cloud Collisions (CCCs) are suggested as a cause of the active star formation in previous studies, and the central part (<10 pc) of this molecular cloud is called to be "starburst" because 17 O type stars were formed within 0.8 Myr. We found that ^{18}CO ($J = 1 - 0$)/^{13}CO ($J = 1 - 0$) ratio is high (> 0.2) and ^{13}CO ($J = 3 - 2$)/^{13}CO ($J = 1 - 0$) ratio is also high (> 1.3) in the collision site. These high ratios mean

high density and high temperature, respectively. In other words, in this region, it is considered that molecular clouds are compressed due to CCC and the radiation from the massive stars is heating the surround gas. The physical properties of molecular clouds were greatly changed by CCC. Also, apart from these CCCs, we found that many CCCs have occurred in W51. It is probable that star formation in W51 GMC is caused by CCCs (not single CCC) between its internal structures.

Furthermore, apart from these results, we also found that molecular clouds having an expanding shell-like structure centered on W51C (radius $\sim$ 30 pc) exist in W51A. This is a new result suggesting the possibility that molecular clouds have interacted with supernova remnants (SNR) W51C, not only in W51B but also in W51A. Acceleration of molecular clouds by supernova explosion is expected to be one of the factors that promote CCC inside GMC. Since the number of GMCs interacting with SNR is limited, W51 is a good target for such studies. In recent years, observational studies of GMCs in nearby galaxies have made significant progress thanks to the telescopes with high performance such as Atacama Large Millimeter/submillimeter Array (ALMA). This study provides important clues to the studies of the relationship between the internal structure of GMCs and star formation in galaxies.

Contents

List of Figures

List of Tables

Chapter 1

Introduction

1.1 Molecular Cloud

A molecular cloud is an interstellar cloud which mainly consists of hydrogen molecules (H_2) (Dust mass is $\sim 1\%$ of total mass of a molecular cloud). It is difficult to observe hydrogen molecules directly because low temperature ($\sim$ 10 K) hydrogen molecules do not emit radiation in any wavelength band. Therefore, we often use other molecules (e.g., carbon monoxide molecules (CO)) to measure the total mass of a molecular cloud assuming the abundance of the molecules. It is possible to derive not only molecular gas distribution and mass but also basic physical properties of molecular cloud such as temperature and density by spectroscopic observations of molecular emission lines. In addition, it is possible to know the motion along the line of sight of molecular gas from the shift of the frequency of the molecular emission lines (Doppler shift).

Since the critical density of CO ($J = 1 - 0$) is very low ($\sim 2 \times 10^3$ cm^{-3}), CO molecules are detected in many places in galaxies. In the Galaxy, molecular clouds are mainly distributed along spiral arms (Carina-Sagittarius arm, Perseus arm, Cygnus arm, etc.), and its total mass is $\sim 10^9\ M_\odot$ (e.g., Heyer & Dame 2015).

The relatively dense part of molecular clouds is called molecular cloud clump. In addition, the particularly high density part contained in clump is called molecular cloud core. Typically, the size and density of the clumps are $\sim 0.2 - 4$ pc and $\sim 10^2 - 10^4$ cm^{-3}, respectively, and the size and density of the cores are $\sim 0.1 - 0.4$ pc and $> 10^4$ cm^{-3}, respectively (Goldsmith 1987). The stars

are formed in molecular cloud cores. In particular, it is known that the massive cores related to massive mass stars ($> 8M_{\odot}$) are formed only in the molecular clouds with large size and mass called giant molecular clouds (GMCs) (e.g., Zinnecker & Yorke 2007).

1.2 Giant Molecular Cloud (GMC)

In general, molecular clouds with size of $\sim 10 - 100$ pc and mass of $\sim 10^4 - 10^6$ are called giant molecular clouds (GMCs). The typical size and mass are 40 pc and 4×10^5 $M_{\odot}$, respectively (Scoville & Sanders 1987). There are thousands of GMCs in the Galaxy (Solomon & Sanders 1980), and most of the molecular gas exist as GMCs. The nearest GMC from the sun is Orion-A GMC which is well studied (e.g., Bally 2008). The typical lifetime of a GMC is estimated to be roughly $20 - 30$ Myr (e.g., Blitz et al. 2007). The lifetime is from GMC formation to destruction due to influence from internal massive stars.

As mentioned above, not only low-mass stars but also massive stars (> 8 $M_{\odot}$) are formed inside GMCs. Since the formation mechanism of massive stars, which is very important for the evolution of galaxies, is still unclear, observational studies of GMCs are essential.

1.3 Massive star formation

Massive stars generally refer to stars with mass > 8 $M_{\odot}$. Since the luminosity of a massive star is very high (about $L \propto M^{3.5}$), it has a great influence on the surroundings (e.g., ionization, heating, and expansion of the H II regions). In addition, at the end of its lifetime, a supernova explosion occurs, releasing heavy elements and huge kinetic energy to the interstellar space. Therefore, massive stars have a significant impact on the evolution of galaxies.

However, the formation mechanism of massive stars has not yet revealed (e.g., Wolfire & Cassilelli 1987; Zinnecker & Yorke 2007; Tan et al. 2014). There are two theoretical models which have been studied actively. The first one is core accretion model. This is an extension of the formation mechanism of low-mass stars (Shu et al. 1987) in which massive stars are formed by mass accretion from accretion disks. The difficulty of this model is how such high accretion rate can be achieved.

The accretion rate required to form low mass stars is less than $10^{-5}\ M_\odot\ \mathrm{yr}^{-1}$, but very high values of $10^{-4} - 10^{-3}\ M_\odot\ \mathrm{yr}^{-1}$ are required to form massive stars (Wolfire & Cassilelli 1987). The second one is the competitive accretion model. In this model, gas is drawn chaotically from a wider region around the clump, without being massive cores, and massive stars are formed within a star cluster (e.g., Bonnell et al. 2001; Smith et al. 2011; Tan et al. 2014).

To understand how massive stars are formed, observational studies of the site of massive star formation is also effective. However, there are some problems; (1) the number of massive stars is much smaller than low mass stars, (2) the time scale of massive star formation is short, and (3) it is difficult to know the initial condition since massive stars destruct the parent cloud in which they were born.

1.4 W51

W51 is the most active star forming GMC in our Galaxy. It was first discovered by the observation of 21 cm radio continuum which is thermal emission (Westerhout 1958). As in Figure 1.2 and 1.1, W51 GMC is divided into two regions, W51A and W51B (e.g., Bieging 1975). Besides this, a supernova remnant W51C exists in south of W51B. W51C can be seen in non-thermal emission (Koo & Moon 1997b).

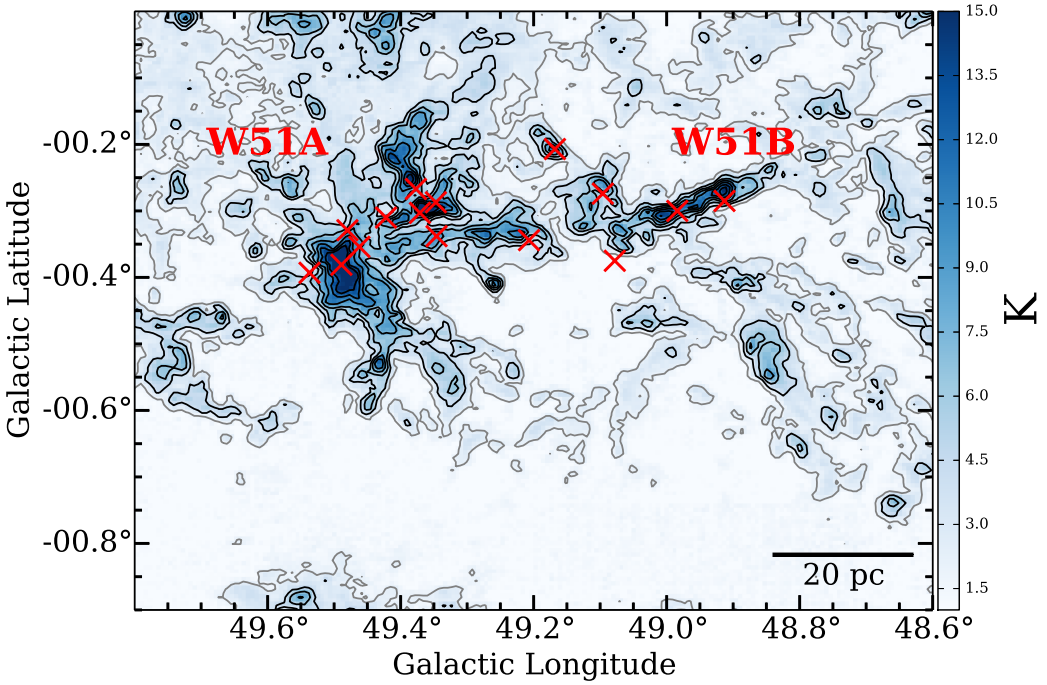

Figure 1.1: ^{13}CO ($J = 1 - 0$) $T_{\rm peak}$ map of W51 taken from the Galactic Ring Survey (GRS) archive data. The contour levels are [2 (gray), 4, 6, 8, 10, 12, 14 K]. The red crosses represent radio continuum sources listed in Koo (1997) ((l, b) = $(49.48, -0.329)$, $(49.462, -0.354)$, $(49.489, -0.381)$, $(49.537, -0.393)$, $(49.377, -0.267)$, $(49.371, -0.303)$, $(49.422, -0.310)$, $(49.347, -0.287)$, $(49.346, -0.338)$, $(49.207, -0.344)$, $(49.168, -0.207)$, $(49.096, -0.274)$, $(49.078, -0.375)$, $(48.984, -0.300)$, $(48.913, -0.285)$).

1.4.1 Location of W51 in the Milky Way

W51 is located at the constellation of Aquila and associated with the tangential point of Carina–Sagittarius spiral arm (e.g., Burton 1970). This means that we can see the cross-cut of the Galactic

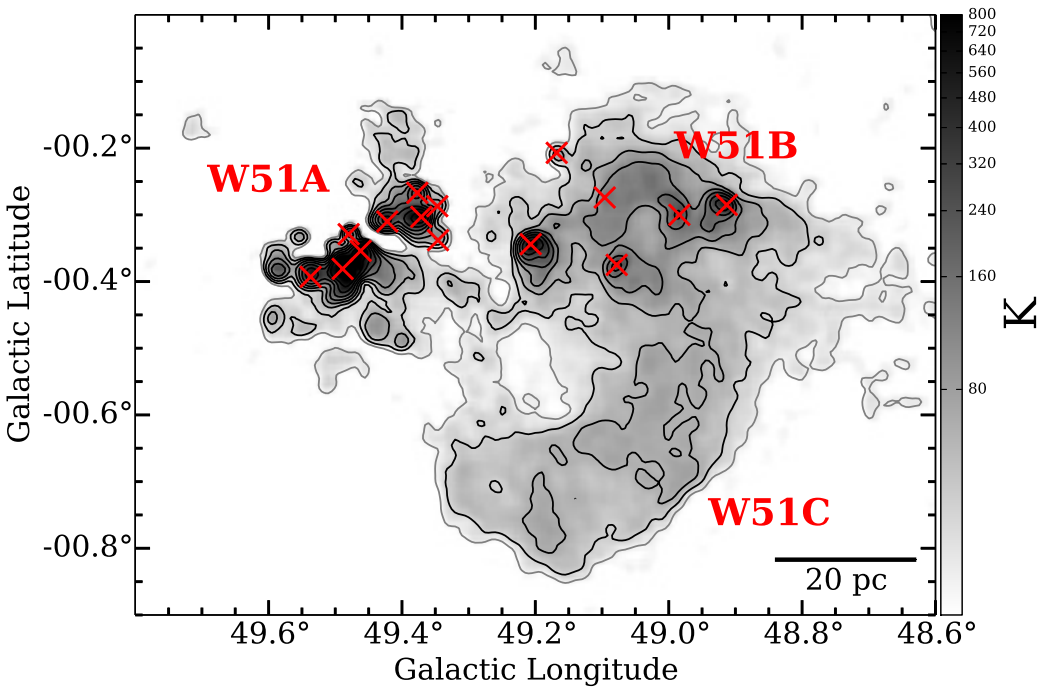

Figure 1.2: A 21 cm radio continuum map of W51 taken from the VLA Galactic Plane Survey (VGPS) archive data. The contour levels are [25 (gray), 40, 63, 100, 158, 251, 398, 631 K]. The red crosses represent radio continuum sources listed in Koo (1997).

spiral arm, although many components are overlapping along the line of sight. Studies on the tangential points in our Galaxy are summarized in Vallée (2014). We adopt the distance of $5.41^{+0.31}_{-0.28}$ kpc to W51 obtained from the measurement of the trigonometric parallax by Sato et al. (2010).

1.4.2 Size, mass and IR luminosity of W51 GMC

W51 GMC spread $\sim 100 \times 100$ pc including diffuse gas traced by ^{12}CO ($J = 1 - 0$) emission line. The total mass of W51 GMC is $\sim 7.1 \times 10^5$ $M_\odot$ (Carpenter & Sanders 1998, recalculated from a distance of 7.0 kpc to that of 5.4 kpc). The total far-infrared luminosity of W51 GMC is $> 10^6$ $L_\odot$ (Rengarajan 1984, recalculated from a distance of 7.6 kpc to that of 5.4 kpc). Most of this luminositiy comes from the central region of W51A (G49.5-0.4). W51A and W51B contain stellar mass of 1.76×10^4 $M_\odot$ and 1.4×10^4 $M_\odot$, respectively (Okumura et al. 2000; Kim et al. 2007).

1.4.3 Molecular clouds in W51

W51 GMC can be decomposed into "W51 complex" and "High Velocity Stream (HVS, $\sim$ 68 km s^{-1} cloud)" (e.g., Carpenter & Sanders 1998; Kang et al. 2010; Parsons et al. 2012). Figure 1.3 shows the ^{13}CO ($J = 3 - 2$) integrated intensity map of W51 taken from JCMT data (Parsons et al. 2012). The velocity range of W51 complex is approximately $45 - 65$ km s^{-1}, and that of HVS is $65 - 75$ km s^{-1}. In addition to these structures, molecular clouds at ~ 7 km s^{-1}, $-23 - 5$ km s^{-1} and $15 - 25$ km s^{-1} exist in this region. The emission line profile of ~ 7 km s^{-1} component is weak, narrow and spread over the entire mapped region. Therefore this component is undoubtedly a nearby molecular cloud (Carpenter & Sanders 1998). It is unclear whether the molecular clouds at $-23 - 5$ km s^{-1} and $15 - 25$ km s^{-1} are physically related to W51 GMC or not.

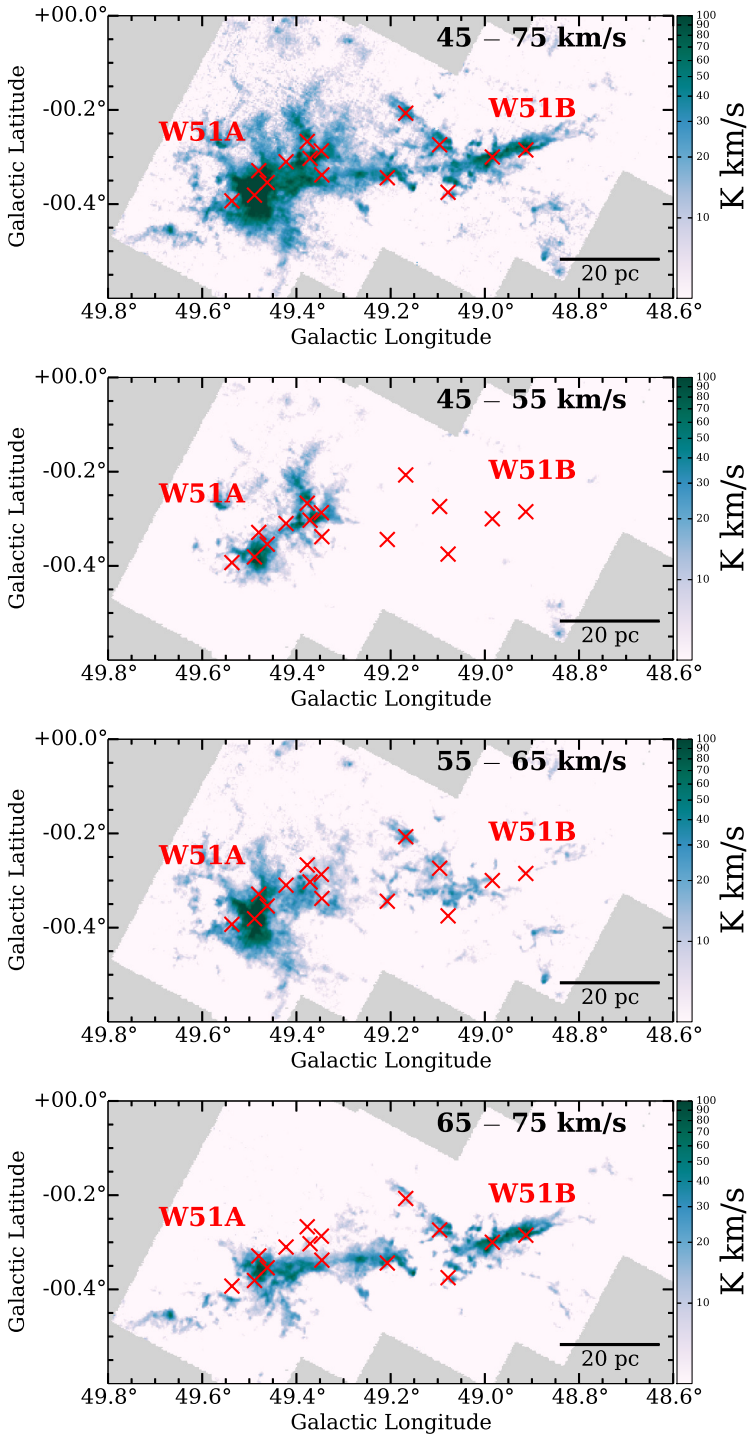

Figure 1.3: ^{13}CO ($J = 3 - 2$) integrated intensity map of W51 taken from JCMT data (Parsons et al. 2012). The integrated velocity range is displayed in the top right corner in each figure. The red crosses represent radio continuum sources listed in Koo (1997).

W51 complex

Molecular clouds in the W51 complex are very complicatedly distributed over several tens of pc in the velocity range of approximately $45 - 65$ km s^{-1}. The mass is $\sim 6.0 \times 10^5$ $M_\odot$ (Carpenter & Sanders 1998, recalculated from a distance of 7.0 kpc to that of 5.4 kpc). The clump-forming efficiency (CFE, defined as $M_{\rm dense}/(M_{\rm dense} + M_{\rm diffuse})$) is lower (11%) than HVS (Parsons et al. 2012).

The main H II regions are G49.4-0.3 and G49.5-0.4. Many compact radio sources are densely populated inside these H II regions. In G49.4-0.3, there are six subcomponents (Mehringer 1994). The average velocity of the ionized gas is 53 km s^{-1} (Pankonin et al. 1979). For G49.5-0.4, the bright radio sources W51d and W51e ($\sim$ compact H II regions) correspond to infrared sources IRS 2 ($(l, b) = (49.493, -0.385)$) and IRS 1 ($(l, b) = (49.482, -0.395)$), respectively. According to the observations of H109α (Wilson et al. 1970), the average velocity of the ionized gas is known to be 59 km s^{-1}. Observations of J, H, and K' broadband and Brγ narrowband (Okumura et al. 2000) revealed that 17 O stars are formed in last 0.8 Myr at the center of G49.5-0.4 (within $\sim$ 10 pc area). Therefore this region has been called "starburst". In addition, it is known that massive stars are still expected to form in this region because of its high Dense Gas Mass Fraction (DGMF, Ginsburg et al. 2015).

High Velocity Stream (HVS)

High Velocity Stream (HVS) is a molecular cloud spreading $\sim$ 10 pc $\times$ $\sim$ 100 pc centered at a velocity of 68 km s^{-1} and intersect with W51 complex on the sky (e.g., Burton 1970; Carpenter & Sanders 1998; Koo 1999; Okumura et al. 2001; Parsons et al. 2012). The mass is $\sim 1.1 \times 10^5$ $M_\odot$ (Carpenter & Sanders 1998, recalculated from a distance of 7.0 kpc to that of 5.4 kpc). Assuming the distance to the Galactic center of $R_0 = 8.4$ kpc and a circular rotation velocity of 254 km s^{-1} (Reid et al. 2009), the radial velocity of the tangential point of the Carina-Sagittarius spiral arm ($l = 49 - 51$ deg (Vallée 2014)) is $57 - 63$ km s^{-1}. The excess of the velocity of HVS is thought to be due to the streaming motions caused by a spiral density wave (Burton & Shane 1970; Koo 1999). The west side of HVS has an arc structure formed by expansion of H II regions, and star

formation was induced by *Collect & Collapse* (Elmegreen & Lada 1977) (Moon & Park 1998; Kang et al. 2010). However, star forming activities will decay because the DGMF of the clouds in this region is low (Ginsburg et al. 2015).

1.4.4 Young stellar objects in W51

Young Stellar Objects (YSOs) are stars in the earlier stages of their formation. There are four (five) classes in YSOs (Wilking et al. 1989). Class 0 and Class I are considered to be protostar stages and primitive stars covered with surrounding envelopes. Class 0 is a stage when the protostar is completely embedded in an optically thick envelope that are made of gas and dust. We can observe Class 0 objects at FIR and sub-mm emission. Class I is a stage that some radiation from the protostar can be observed at IR. Class II and Class III are considered to be in T Tauri star stage, and a circumstellar disk is formed (The stage of protostar is up to Class IIa. After that it is Class IIb). In Class II stage, the disk is optically thick. It has a protoplanetary disk composed of gas and dust. NIR, MIR excess and strong H_α emission are observed from the objects in Class II stage. In Class III stage, the gas is dispersed from the protoplanetary disk, and the disk is composed by only dust.

In W51, Kang et al. (2009) identified 737 YSO candidates at the area near W51 GMC by using the data of *Spitzer* IRAC, MIPS and 2MASS point source catalog. Based on the extinction of each YSO candidate, they concluded that 437 YSO candidates are associated with the W51 region.

1.4.5 Cloud–Cloud Collision in W51A

Recent simulational studies suggest that cloud-cloud collisions (CCCs) may play a role in massive star formation. Inoue & Fukui (2013) demonstrated that massive molecular cloud cores are formed in the shocked layer induced by CCC, by using three-dimensional, isothermal, magnetohydrodynamics (MHD) simulations with the effect of self-gravity. The core mass accretion rate in their simulations is high ($> 10^{-4}\ M_\odot \mathrm{yr}^{-1}$) enough to form massive stars. In observational studies, for example, Torii et al. (2015) suggest that the existence of O star in RCW 120 can be explained by the CCC scenario (Habe & Ohta 1992). For W51, previous studies have suggested that the active star formation in

W51A is due to CCC (e.g., Pankonin et al. 1979; Arnal & Goss 1985; Carpenter & Sanders 1998; Kang et al. 2009).

1.4.6 Supernova remnant (SNR) W51C

W51C is a middle aged ($\sim 3 \times 10^4$ yr), incomplete shell-type SNR (diameter of $\sim 30'$ in the radio continuum) and one of the most luminous γ-ray sources in the Galaxy (e.g., Koo et al. 1995; Koo & Moon 1997a; Koo & Moon 1997b; Abdo et al. 2009). This SNR is interacting with a molecular cloud in W51B (e.g., Green et al. 1997) and the γ-rays are naturally explained by π^0-decay (Abdo et al. 2009; Aleksić et al. 2012). The physical parameters of SNRs with fast-expanding H I shells (including W51C) are summarized in Park et al. (2013).

1.5 FUGIN (FOREST Ultra-wide Galactic plane survey In Nobeyama)

FUGIN (FOREST Ultra-wide Galactic plane survey In Nobeyama) is one of the legacy projects of NRO (Nobeyama Radio Observatory). This project aims to investigate the distribution, kinematics, and physical properties of both diffuse and dense molecular gas in the Galaxy from galactic scale to dense clump scale.

FUGIN has three strong points. Firstly, the angular resolution is the highest ($\sim 18''$) to date for the Galactic plane survey in the CO ($J = 1 - 0$) lines. This advantage makes it possible to find dense clumps located at further distance than the previous surveys. Secondly, the mapping region is very wide ($10^\circ \leq l \leq 50^\circ$, $b = \pm 1^\circ$ and $198^\circ \leq l \leq 236^\circ$, $b = \pm 1^\circ$) while the angular resolution is high. Many GMCs are included in this data. Thirdly, ^{12}CO, ^{13}CO, and C^{18}O ($J = 1 - 0$) emission lines were obtained simultaneously. There are few maps of ^{12}CO, ^{13}CO, and C^{18}O ($J = 1 - 0$) which cover the entire region of a GMC with high anglar resolution. Data with these advantages are very useful for studies of GMCs.

This project has taken place since 2013 with FOREST (FOur beam REceiver System on 45-m Telescope, Minamidani et al. 2016) receiver. FOREST is a 100 GHz–band (80–116 GHz), multi–beam (4–beam (2×2), the beam separation is $50''$ on the sky plane), dual–polarization (2–polarization), sideband-separating (2SB) SIS (Superconductor–Insulator–Superconductor) heterodyne receiver installed in the 45-m telescope at NRO.

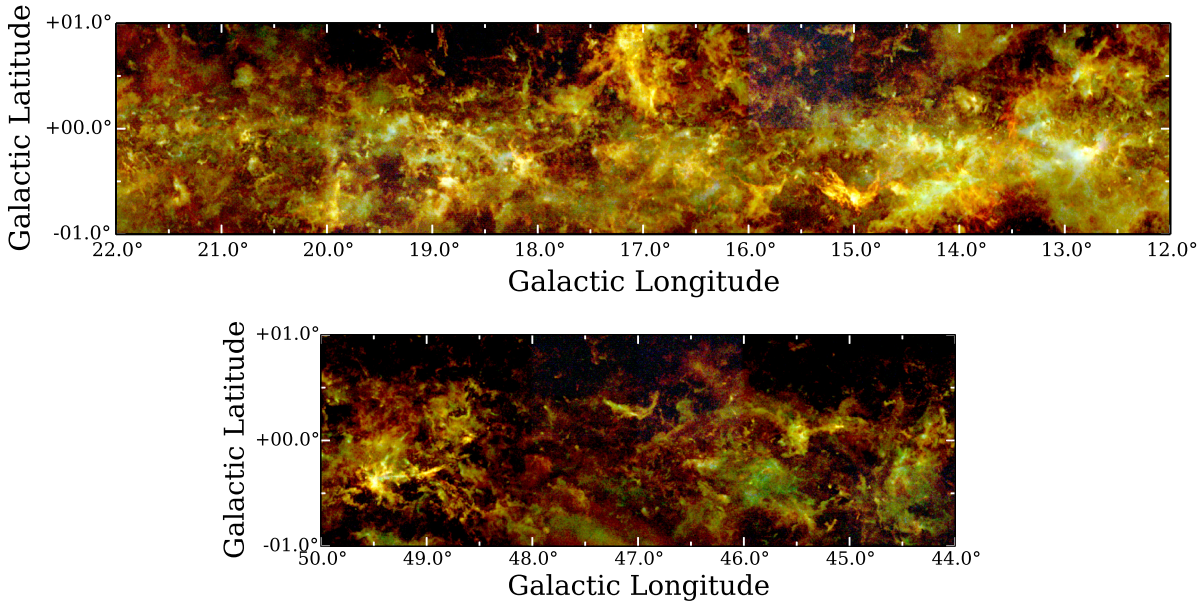

Figure 1.4: FUGIN RGB color map ($T_{\rm peak}$, until May 2015). Red: ^{12}CO ($J = 1 - 0$), scaled $1.5 - 20.0$ K. Green: ^{13}CO ($J = 1 - 0$), scaled $0.5 - 8.0$ K. Blue: C^{18}O ($J = 1 - 0$), scaled $0.5 - 4.0$ K. Note that, these images were roughly processed for thesis presentation.

1.6 The motivation of this thesis

Our final goal is to understand formation mechanism of massive stars in the Galaxy. Observational studies of GMCs are crucial for the purpose because GMCs are the site where massive stars are formed. Although there are many previous studies of GMCs, there are few studies using data that can be decomposed into the internal structures while covering the entire GMC. FUGIN data, which trace from diffuse gas to dense gas with a high angular resolution, enable us to do such studies.

In particular, W51 is the region where massive stars have been formed very actively at the central region (e.g., Okumura et al. 2000). Therefore, the ^{12}CO, ^{13}CO, and C^{18}O ($J = 1 - 0$) data of the entire region of W51 acquired with high angular resolution are very useful. Active star formation regions like W51 are also found in nearby galaxies (e.g., NGC604 in M33 (Muraoka et al. 2012)). If we can reveal the mechanism of the activation of massive star formation, we can make significant contribution on the studies of star formation and evolution of galaxies.

1.7 The structure of this thesis

In Chapter 2 (Observations), we explain the FUGIN W51 data. In Chapter 3 (Results), we present integrated intensity, channel map, $l - v$ diagram (Galactic longitude – velocity diagram), etc first. Then, the results of analysis using Dendrograms (Rosolowsky et al. 2008) and SCIMES (Colombo et al. 2015) will be explained. In Chapter 4 (Discussion), we first consider the Cloud-Cloud Collision (CCC) at the center of W51 and then discuss massive star formation in a Giant Molecular Cloud (GMC). After we summarize our results in Chapter 5, we present the channel maps that we will not present in Chapter 3 as Appendix. In addition, the shocked CO gas in W51B and the structure catalog of Dendrograms in W51 (^{13}CO ($J = 1 - 0$)) will be presented.

Chapter 2

Observations

The observations of W51 were carried out as a part of FUGIN (FOREST Ultra-wide Galactic plane survey In Nobeyama) project (1.5).

2.1 Observation summary of W51

We use the data in W51 region $l = 48^\circ$ – $50^\circ, b = -1^\circ$ – $+1^\circ (2^\circ \times 2^\circ)$ that were observed in 2014 and 2015. This mapping observations were made with the on-the- fly (OTF) mapping technique (Sawada et al. 2008). The telescope has a beam size of $\sim 15''$ (HPBW) at 115 GHz, and the main beam efficiencies are 45±2% and 43±2% at 110, and 115 GHz, respectively. In all analyses in this thesis, we use the data scaled in $T_{\rm mb}$. We observed a standard source W51main to check the performance of the telescope at least once per day. Based on these observations, the intensity variations are less than 10-20 %, 10 %, and 10 % for ^{12}CO ($J = 1 - 0$), ^{13}CO ($J = 1 - 0$), C^{18}O ($J = 1 - 0$), respectively.

We used SAM45 (Spectral Analysis Machine for the 45-m telescope: Kuno et al. 2011) with a frequency resolution of 244.14 kHz. The effective velocity resolution is 1.3 kms^{-1} at 115 GHz by considering the adopted window function and the typical system noise temperatures including atmosphere are ∼150 and ∼250 K at 110 and 115 GHz, respectively. Spatial grids of cube data are $8.5'' \times 8.5''$ and velocity grid is 0.65 km s^{-1} and $T_{\rm rms}$ are 1.5 K, 0.7 K and 0.7 K in $T_{\rm mb}$ scale for ^{12}CO ($J = 1 - 0$), ^{13}CO ($J = 1 - 0$), C^{18}O ($J = 1 - 0$), respectively. The map is made as mosaic

with $1^\circ \times 1^\circ$ sub-map (A sub-map consists of four maps: X-direction-a, X-direction-b, Y-direction-a and Y-direction-b.). The dumping speed corresponds to the spacing of $4''$ along the scan direction for the scan speed of $100''$/sec.

The primary parameters are listed in Table 2.1, and the $T_{\rm rms}$ map of W51 data is shown in Figure 2.1.

Table 2.1: Primary parameters for the observations and the data

Observed Date	March – May 2014 & April – May 2015
Observed Area	$l = 48^\circ$ – $50^\circ, b = -1^\circ$ – $+1^\circ (2^\circ \times 2^\circ)$
Telescope	NRO 45-m telescope
Receiver	FOREST
Observation Mode	On-The-Fly
Emission Lines	^{12}CO ($J = 1 - 0$), ^{13}CO ($J = 1 - 0$), C^{18}O ($J = 1 - 0$)
Spatial & Velocity Resolution	$\sim 18''$ (~ 0.4 pc for distance 5.4 kpc) & ~ 1.3 km s^{-1}
Spatial & Velocity Grid	$8.5''$ & 0.65 km s^{-1}
RMS ($T_{\rm mb}$ scale)	~ 1.5 K for ^{12}CO ($J = 1 - 0$), ~ 0.7 K for ^{13}CO ($J = 1 - 0$) & ~ 0.7 K for C^{18}O ($J = 1 - 0$)

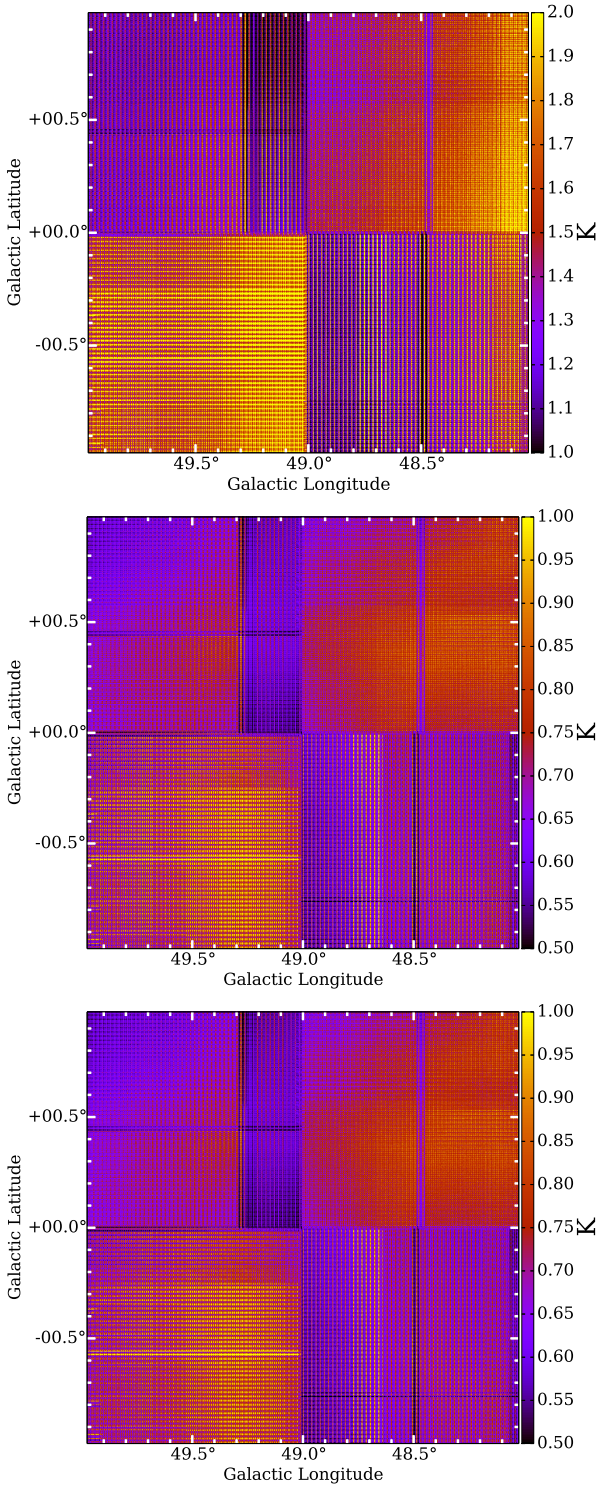

Figure 2.1: The $T_{\rm rms}$ map of W51 data. From the top, ^{12}CO ($J = 1 - 0$), ^{13}CO ($J = 1 - 0$) and C^{18}O ($J = 1 - 0$), respectively.

Chapter 3

Results

3.1 Distribution and kinematics of molecular gas in W51

3.1.1 Integrated intensity map

Figure 3.1 shows that the integrated intensity of ^{12}CO, ^{13}CO, and C^{18}O ($J = 1 - 0$). The velocity ($V_{\rm LSR}$) ranges of these integrated intensity are -20 – 80 kms^{-1}. FUGIN data cover the whole region of the JCMT ^{12}CO ($J = 3 - 2$), ^{13}CO ($J = 3 - 2$), and C^{18}O ($J = 3 - 2$) map (Parsons et al. 2012). We can see that W51 extends to about 100 pc $\times$ 100 pc in ^{12}CO ($J = 1 - 0$), which can trace diffuse gas including large clouds other than W51 complex and HVS. On the other hand, since ^{13}CO ($J = 1 - 0$) traces relatively dense gas, several clouds seen in ^{12}CO ($J = 1 - 0$) are not seen in the ^{13}CO ($J = 1 - 0$) map. The ^{13}CO ($J = 1 - 0$) data clearly show the break spot of HVS (about $(l, b) = (49.12, -0.32)$, break 2). C^{18}O ($J = 1 - 0$) which traces dense gas was detected in W51 complex and HVS almost exclusively.

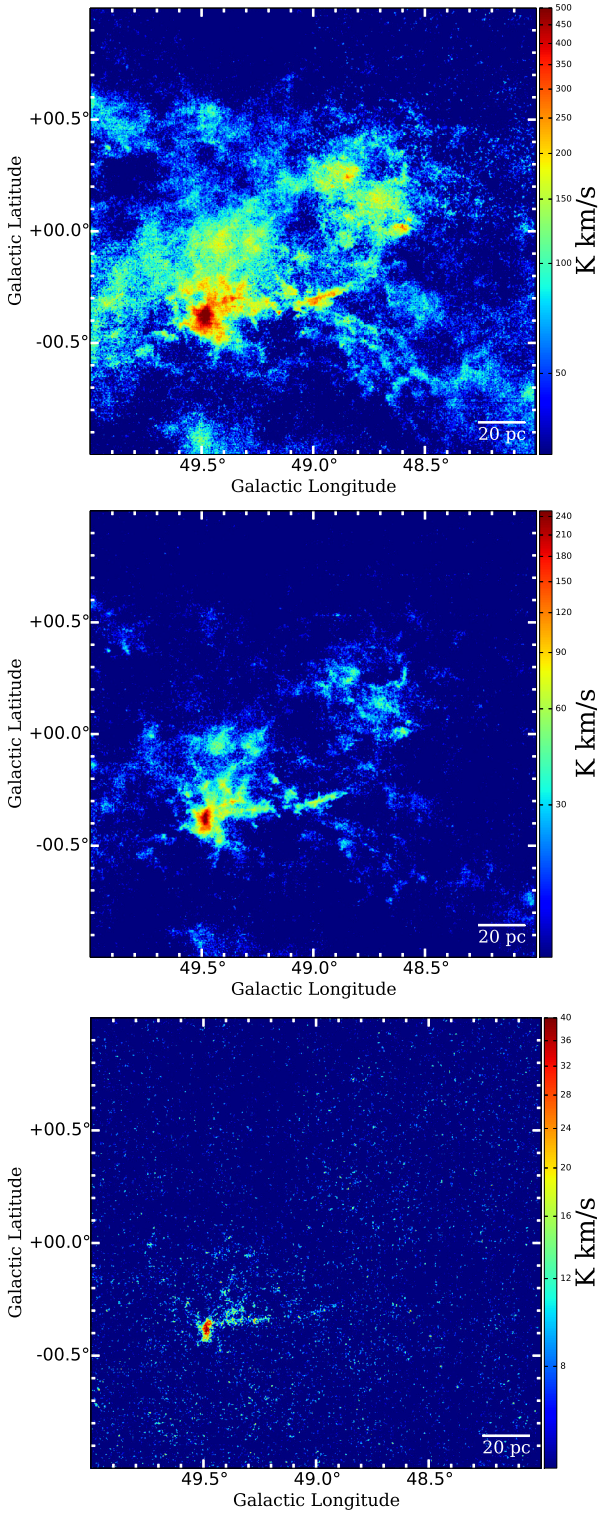

Figure 3.1: The integrated intensity map of ^{12}CO ($J = 1 - 0$), ^{13}CO ($J = 1 - 0$), and C^{18}O ($J = 1 - 0$). The integration velocity range is -20 to 80 kms^{-1}.

3.1.2 Channel maps

Figure 3.2, 3.3, and 3.4 show the ^{12}CO ($J = 1 - 0$), ^{13}CO ($J = 1 - 0$), and C^{18}O ($J = 1 - 0$) channel maps, respectively. The velocity spacing is 1.95 kms^{-1} (3 channels) and the velocity range is 44.0 – 73.2 kms^{-1}. To improve the signal to noise ratio of C^{18}O ($J = 1 - 0$) data, we convoluted the data of all lines to angular resolution of $36''$ in these figures. Although several clouds seen in ^{12}CO ($J = 1 - 0$) and ^{13}CO ($J = 1 - 0$) were detected in < 44.0 kms^{-1}, those are not presented here. In addition, the high velocity cloud (>83 km^{-1}) that was seen in JCMT ^{12}CO ($J = 3 - 2$) data and HI data (e.g., Koo & Moon 1997, Tian & Leahy 2013) is not detected significantly in the ^{12}CO ($J = 1 - 0$) data (see Appendix).

In the ^{12}CO ($J = 1 - 0$) map (Figure 3.2), we can see both diffuse and extended, and compact and intense structures. The ^{13}CO ($J = 1 - 0$) map (Figure 3.3) basically traces intense part of the ^{12}CO ($J = 1 - 0$) map. The ^{13}CO ($J = 1 - 0$)/^{12}CO ($J = 1 - 0$) intensity ratio map is presented in subsection (3.1.4). C^{18}O ($J = 1 - 0$) emission was detected in the intense part of W51A and High Velocity Stream (HVS, 68 kms^{-1} cloud).

In the 65.4, 67.4 and 69.3 km^{-1} panels, we can see the HVS and its breaks (e.g., Okumura et al. 2001, Parsons et al. 2012) clearly in not only the ^{12}CO ($J = 1 - 0$) map but also the ^{13}CO ($J = 1 - 0$) and C^{18}O ($J = 1 - 0$) maps. The velocity structure and intensity ratio of the HVS are presented in 4.1.4.

The GMC mapped in our observing area ($l = 48^\circ$ – $50^\circ, b = -1^\circ$ – $+1^\circ (2^\circ \times 2^\circ)$) are roughly divided into three regions: W51A, W51B, and the west region to the W51B (W51BW). Since it is probable that W51BW is associated with W51 (Nagayama et al. 2011), it is important to investigate W51BW to understand the whole region of W51.

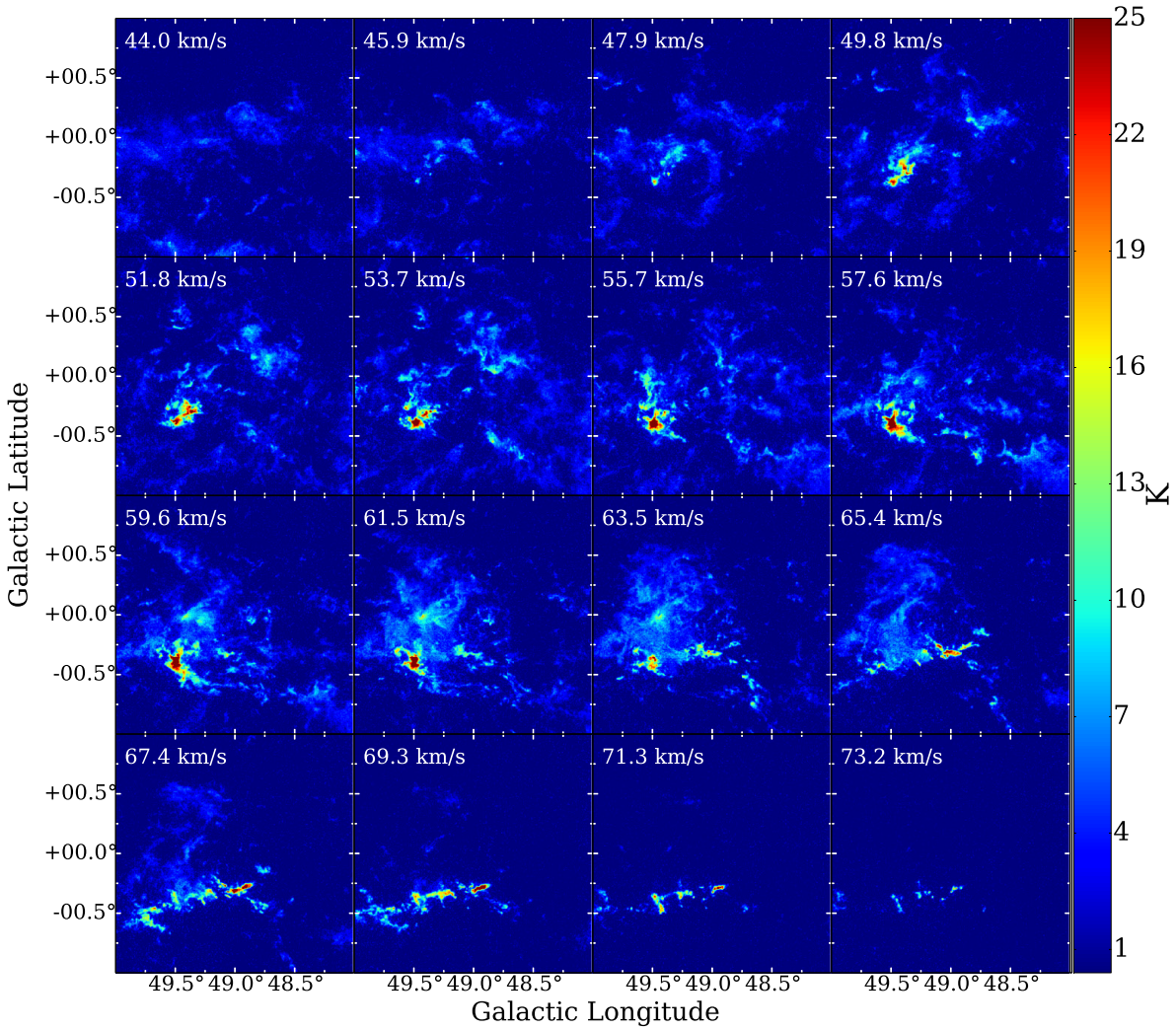

Figure 3.2: The channel map of ^{12}CO ($J = 1 - 0$) intensity ($T_{\rm mb}$ scale). Velocity range is 44.0 – 73.2 km s^{-1} and velocity spacings are 3 channels (1.95 km s^{-1}).

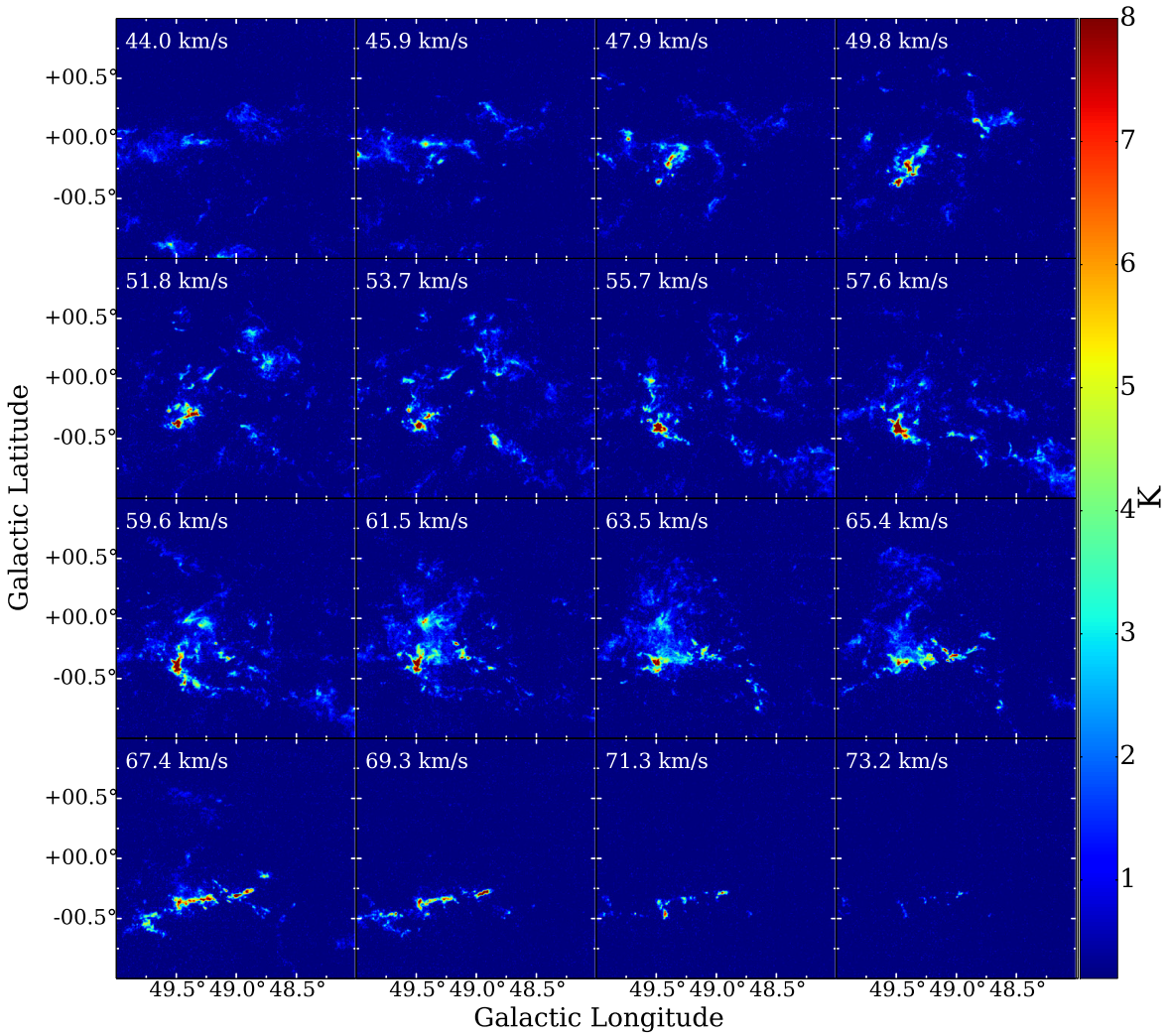

Figure 3.3: The channel map of ^{13}CO ($J = 1 - 0$) intensity ($T_{\rm mb}$ scale). Velocity range is 44.0 – 73.2 km s^{-1} and velocity spacings are 3 channels (1.95 km s^{-1}).

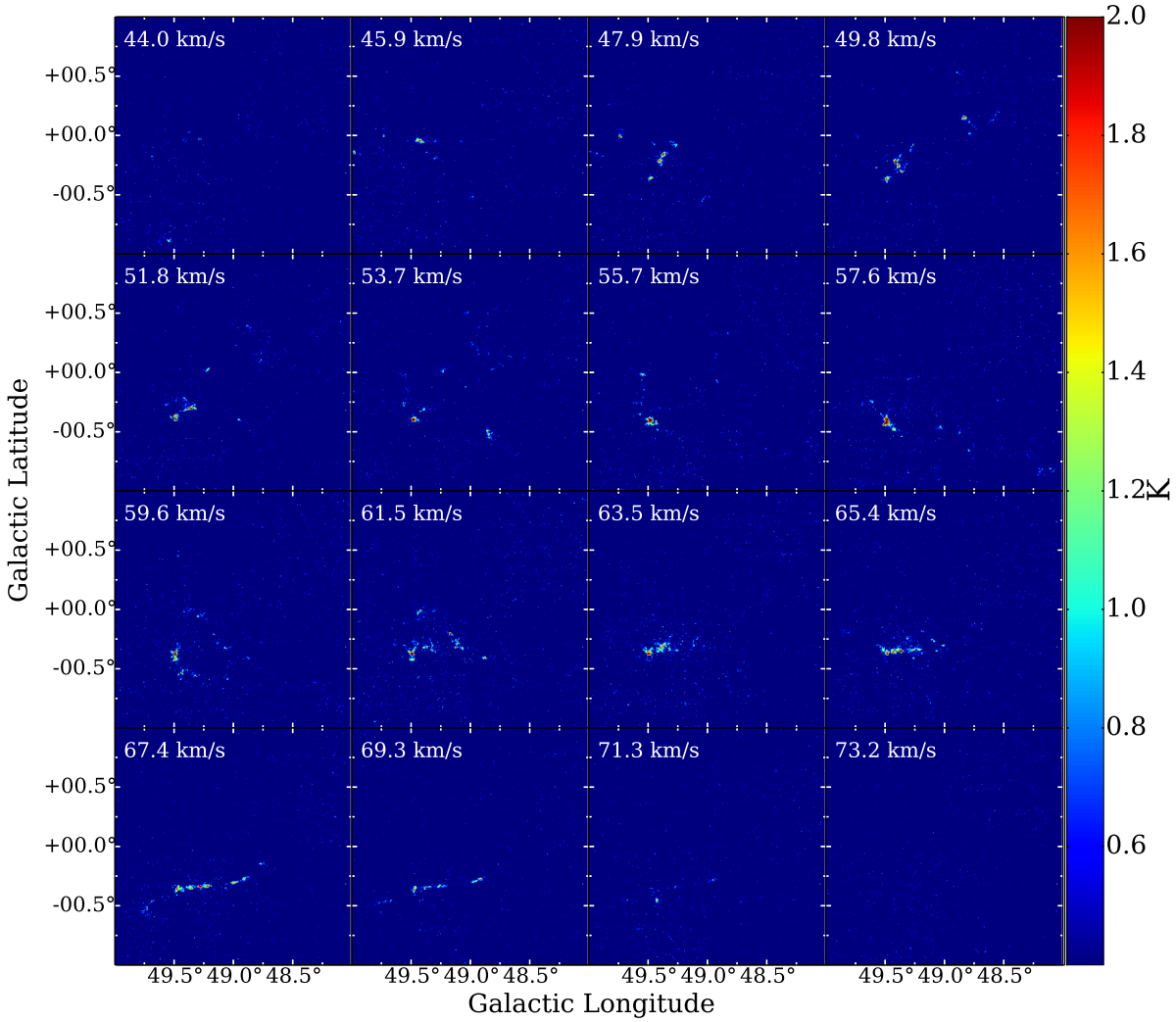

Figure 3.4: The channel map of $C^{18}O$ ($J = 1 - 0$) intensity (T_{mb} scale). Velocity range is 44.0 – 73.2 km s^{-1} and velocity spacings are 3 channels (1.95 km s^{-1}). This $C^{18}O$ ($J = 1 - 0$) map is spatially convolved.

3.1.3 Position–Velocity diagrams

Figure 3.5 shows Galactic Longitude – Velocity (L – V) diagrams of ^{12}CO ($J = 1 - 0$), ^{13}CO ($J = 1 - 0$), and C^{18}O ($J = 1 - 0$). The interval of the Galactic Latitude is 0.2° from +0.4° to -0.6°. We can see that there are several velocity components (7, 45, 50, 55, 60, 68 kms^{-1}) in the ^{12}CO ($J = 1 - 0$) map of W51A. 7 kms^{-1} cloud is a local molecular cloud and is not related to the W51 region (Carpenter & Sanders (1998)). Since many components overlap in projection both spatially and kinematically, the velocity structure is very complicated. In W51B ($49.3° > l > 48.7°$), there are 7, 34, 54, 68 kms^{-1} and other components. In $49.2° > l > 48.5°$, we can see some components of W51BW with velocity of 5–20 kms^{-1}. These clouds are presented as PC 7, 9, 10 in subsection 3.2.

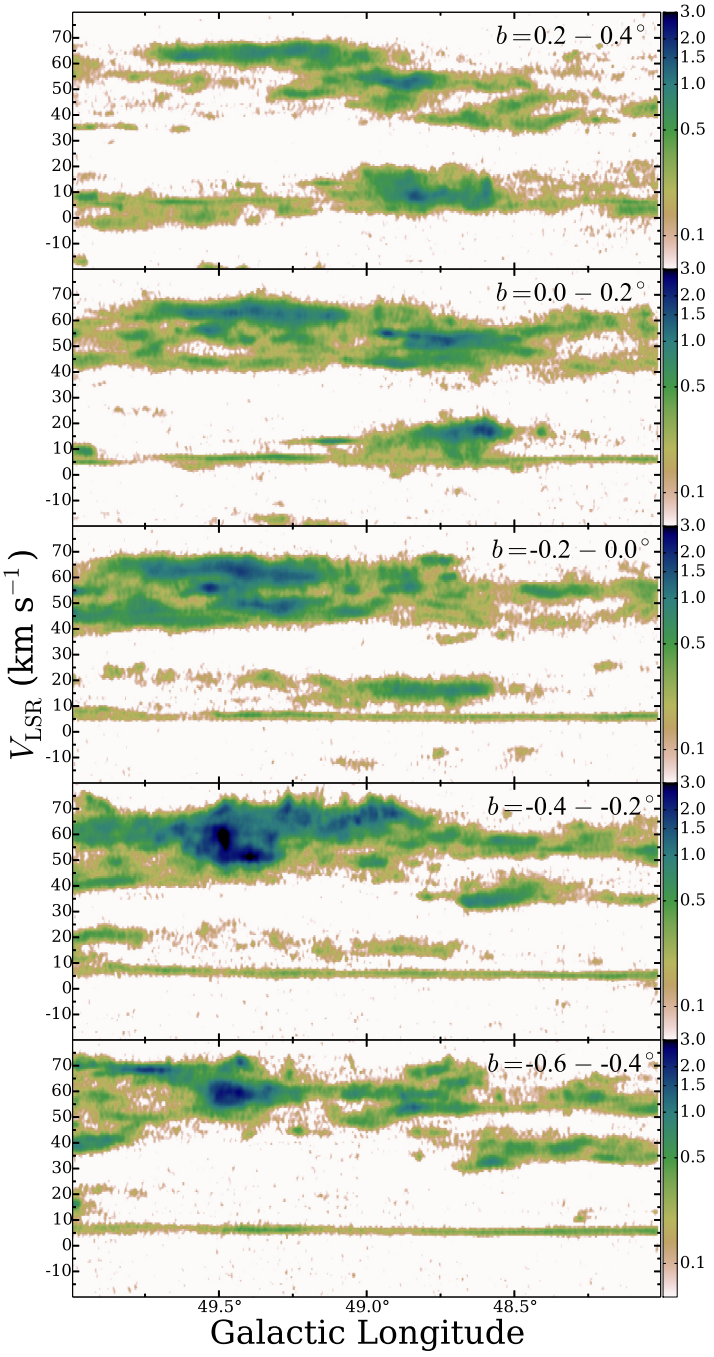

Figure 3.5: The L – V diagrams of ^{12}CO ($J = 1 - 0$), ^{13}CO ($J = 1 - 0$), and C^{18}O ($J = 1 - 0$) from the top. Color units are (K degree).

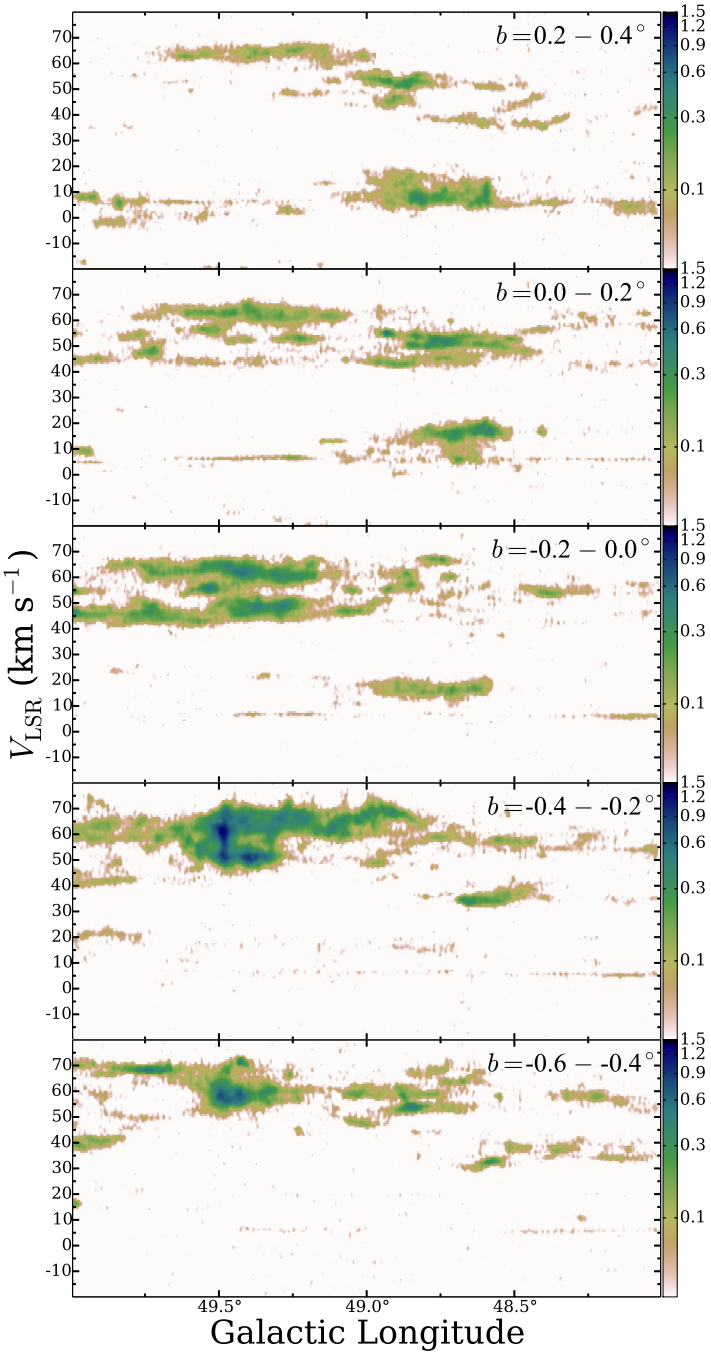

Figure 3.5: Continued.

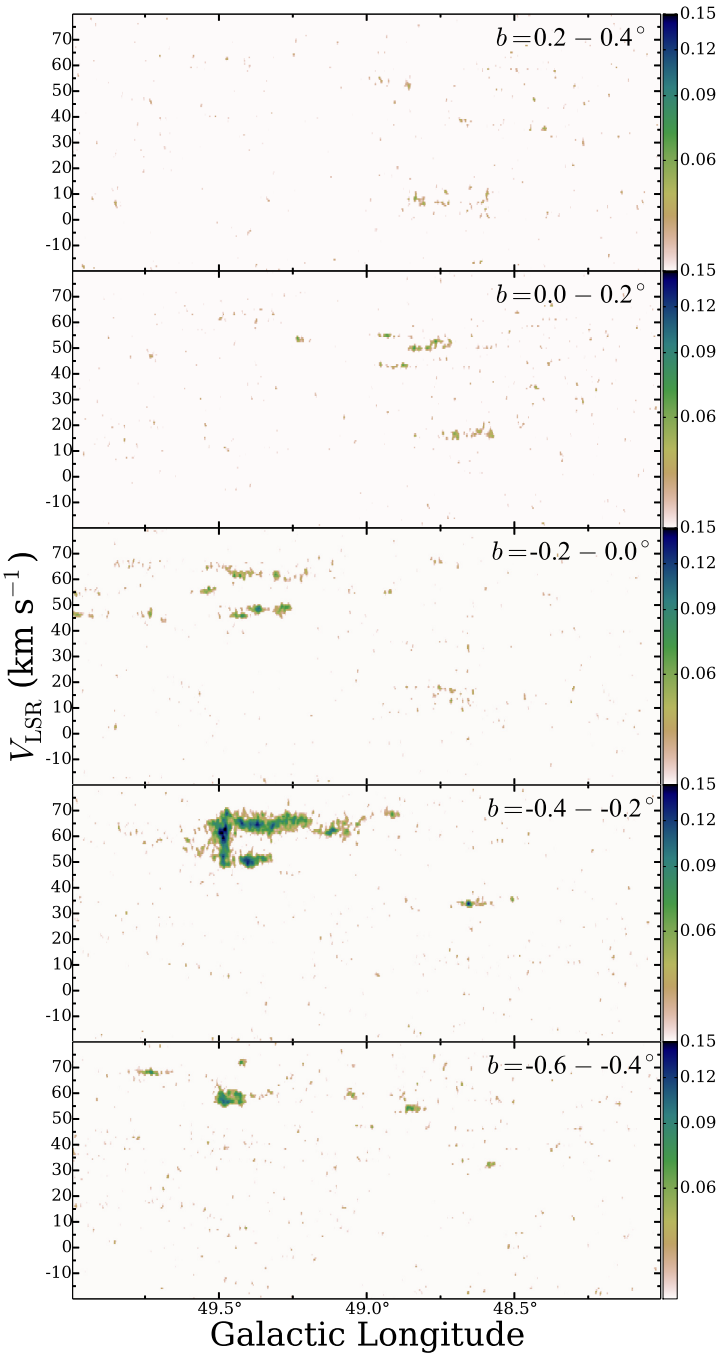

Figure 3.5: Continued.

3.1.4 Intensity ratio map

Figure 3.6 shows intensity ratios of ^{13}CO ($J = 1 - 0$) / ^{12}CO ($J = 1 - 0$) ($\equiv R_{1312}$) and ^{13}CO ($J = 3 - 2$) / ^{13}CO ($J = 1 - 0$) ($\equiv R_{3210}$) overlaid on the ^{13}CO ($J = 1 - 0$) integrated intensity map. The velocity ranges are 45–55 kms^{-1}, 55–65 kms^{-1} and 65–75 kms^{-1} from top. For the top and middle figures, IRS 1 ($\sim$ W51e, $(l, b) = (49.486, -0.380)$) and IRS 2 ($\sim$ W51d, $(l, b) = (49.490, -0.370)$) are strong infrared emission sources (e.g., Wynn-Williams et al. 1974). We can see that the regions near the sources have high R_{1312} (> 0.4) and R_{3210} (> 1.0). In Figure 3.6 (b), there is a cloud (G49.17-0.21) with high R_{1312} (> 1.0). Kang et al. (2010) suggested that this cloud is a star formation site triggered by Cloud-Cloud Collision (CCC), because the Infrared Dark Cloud (IRDC) associated with G49.17-0.21 has kinematics that appears to be consistent with the cloud collision model for massive star formation. Figure 3.6 (c) and (f) show the 68 kms^{-1} cloud (HVS) components. Although both R_{1312} and R_{3210} are high in W51A (about > 0.4 and > 1.0, respectively), R_{1312} is relatively low in W51B (about < 0.3). In particular, R_{3210} is high at the edge of the 68 kms^{-1} cloud. It is thought that the high R_{3210} at the edge is due to the strong radiation field in the W51B.

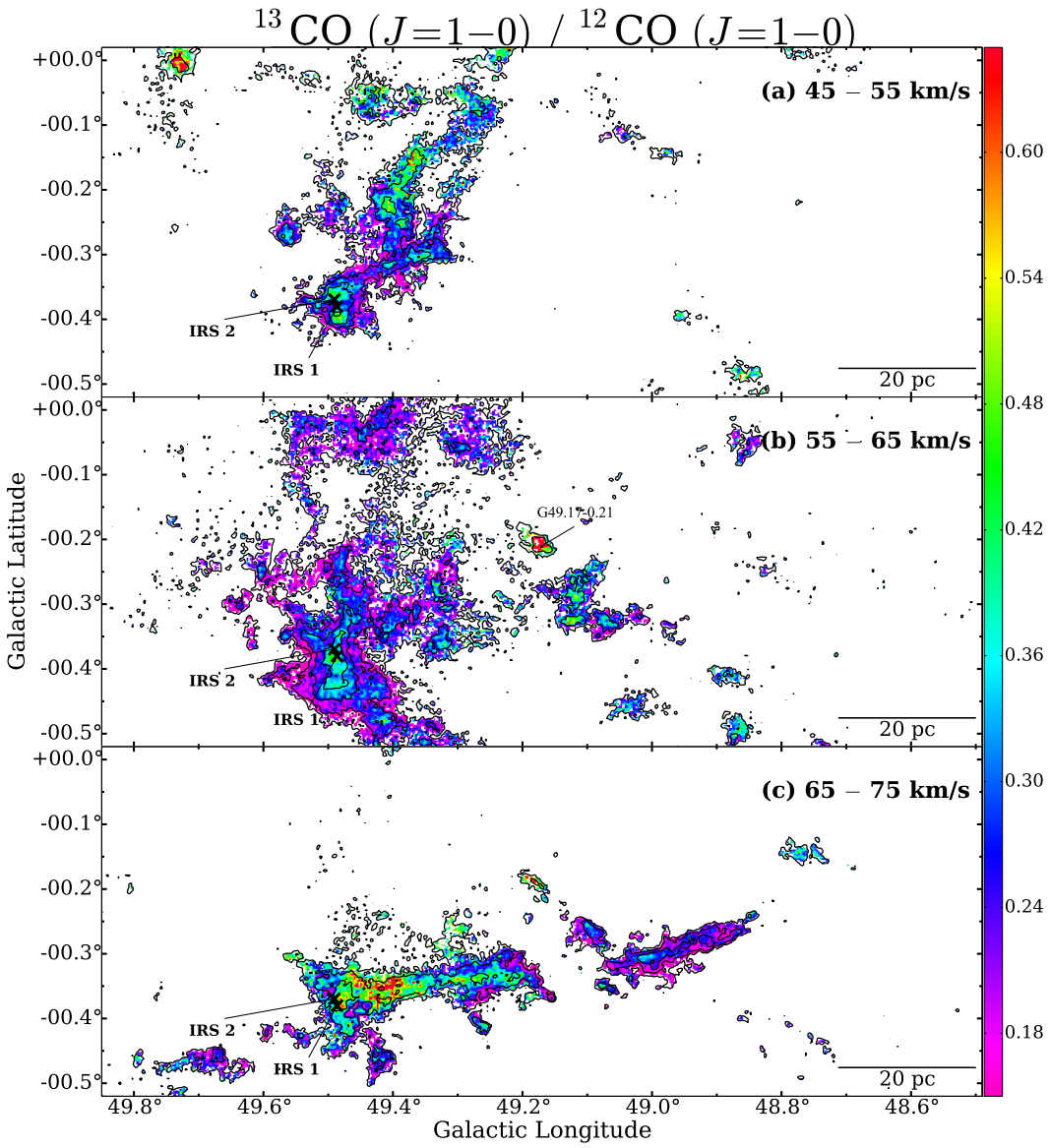

Figure 3.6: Color scale shows that ^{13}CO ($J = 1 - 0$) / ^{12}CO ($J = 1 - 0$) intensity ratio (left figure) and ^{13}CO ($J = 3 - 2$) / ^{13}CO ($J = 1 - 0$) intensity ratio (right figure). Intensity ratio was calculated for only $> 3\sigma$ pixels. Contours show that ^{13}CO ($J = 1 - 0$) integrated intensity. Contour levels are 11.2, 22.4, 44.8, 89.6, and 179.2 K kms^{-1}. Green lines in right side figures indicate the area of JCMT ^{13}CO ($J = 3 - 2$) dataset.

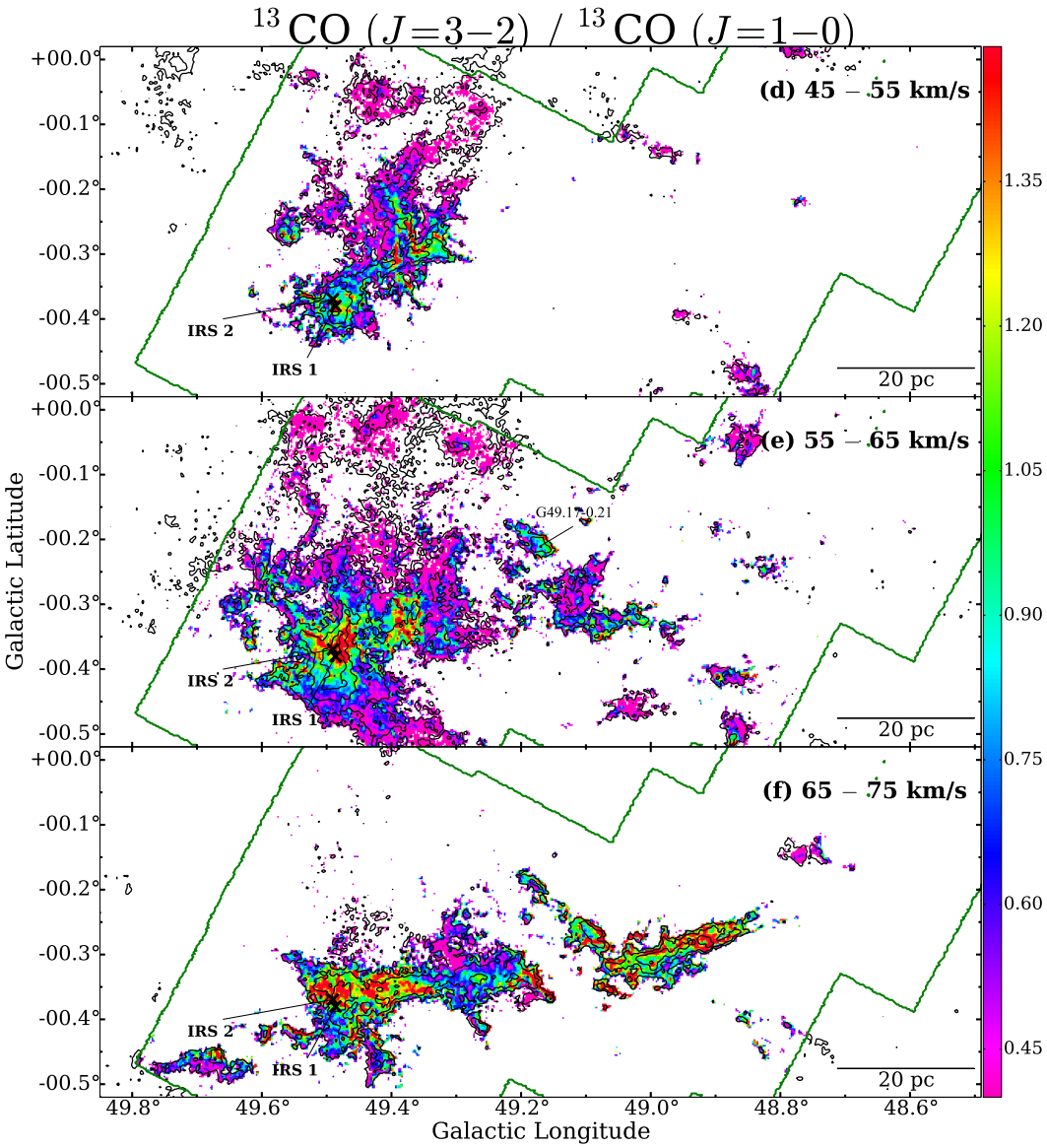

Figure 3.6: Continued.

3.2 Dendrograms

As mentioned above, previous studies have suggested that the active star formation in W51A is due to CCC between the 68 km s^{-1} cloud (HVS) and other clouds. By using FUGIN ^{12}CO ($J = 1 - 0$), ^{13}CO ($J = 1 - 0$) and C^{18}O ($J = 1 - 0$) dataset presented above, we investigate the relations of star forming activity and the components with different velocity within our map. We first discuss the internal structure of the GMC.

3.2.1 Set up of Dendrograms

FUGIN CO dataset covers entire area of the W51 GMC. We will divide the GMC into several clouds in order to discuss the internal structure of the GMC by using Dendrograms algorithm (Rosolowsky et al. 2008).

Dendrograms constructs tree structures that represent the hierarchy of the structures in the dataset. This tree structure is composed of two types of structures, leaves and branches. Leaves are structures that have no sub-structure. Branches are structures which split into multiple sub-structures and can split up into branches and leaves. In particular, branches that have no parent structure are called trunks. This tree structure enables us to distinguish clouds mechanically and quantitatively. We performed Dendrograms to FUGIN ^{13}CO ($J = 1 - 0$) three-dimensional (Position-Position-Velocity) dataset. Spatial grids and a velocity grid are 8.5″ and 0.65 km s^{-1} respectively. We have to set three parameters, "a minimum value", "a minimum height" and "a minimum number of voxels" for Dendrograms. "A minimum values" means the minimum value to consider in the dataset. "A minimum height" means the minimum value for a leaf to be considered an independent entity. The significance is measured from the difference between its peak value and the value at which it is being merged into the tree. "A minimum number of voxels" means the minimum number of voxels needed for a leaf to be considered an independent entity. We set these parameters to 2.1 K (3σ), 1.4 K (2σ) and 32 respectively. As a result, 523 trunks and 1146 leaves were identified.

3.2.2 Selection of parent clouds (PCs) by using Dendrograms

We selected representative trunks or branches from the tree structure. We call these clouds "parent clouds (PCs)". The criteria for the selection are (1) it includes more than 5,000 voxels (e.g., a cloud with radius of 5 pc, and averaged velocity range of 2 km s^{-1} includes ∼5,000 voxels) and (2) not locate in the edge of the map . As a results, 10 PCs are selected (PC 1 – PC 10). However, PC 2 and PC 3 are branch belonging to the same trunk. The minimum intensity of these branches is $\sim$ 2.13 K, which is nearly equal to the minimum intensity of the other trunks (we found that the difference in the integrated intensity resulting from this difference of the minimum intensity is approximately 1% by the calculation of extrapolation). Therefore, we identified these branches as separate PCs.

Basic information of the selected PCs is listed in Table 3.1. ID color is the color used in Figure 3.7. $l_{\rm peak}$, $b_{\rm peak}$, and $v_{\rm peak}$ are the position of peak intensity voxel. $T_{\rm peak}$ is the peak intensity ($T_{\rm mb}$ scale). $v_{\rm rms}$ is the intensity-weighted second moment of velocity. R is geometric mean of the major and minor radii. Major radius was computed from the intensity-weighted second moment in direction of greatest elongation in the Position-Position plane. Minor radius was computed from the intensity-weighted second moment perpendicular to the major axis. $N_{\rm vo,all}$ is the number of voxels included in the parent cloud. We assumed that PC 1 – PC 5 are located at the same distance, 5.4 kpc (Sato et al. 2010), and that PC 7, 9 and 10 are in Perseus arm (distance of 10.8 kpc, Zaung et al. 2013). The distance of PC 6 and 8 are ambiguous. For PC 6, we derived the distance of 2.2 kpc by assuming a flat rotation curve of the Galaxy ($R_0 = 8.5$ kpc, and $V_0 = 254.0$ km s^{-1}). Since the velocity of PC 8 is close to that of PC1 – PC 5, we assumed that PC 8 is located at the same distance as PC 1– PC 5 (5.4 kpc).

Figure 3.7 shows the integrated intensity of each PC overlaid on the *Spitzer* IRAC 8.0 μm map.

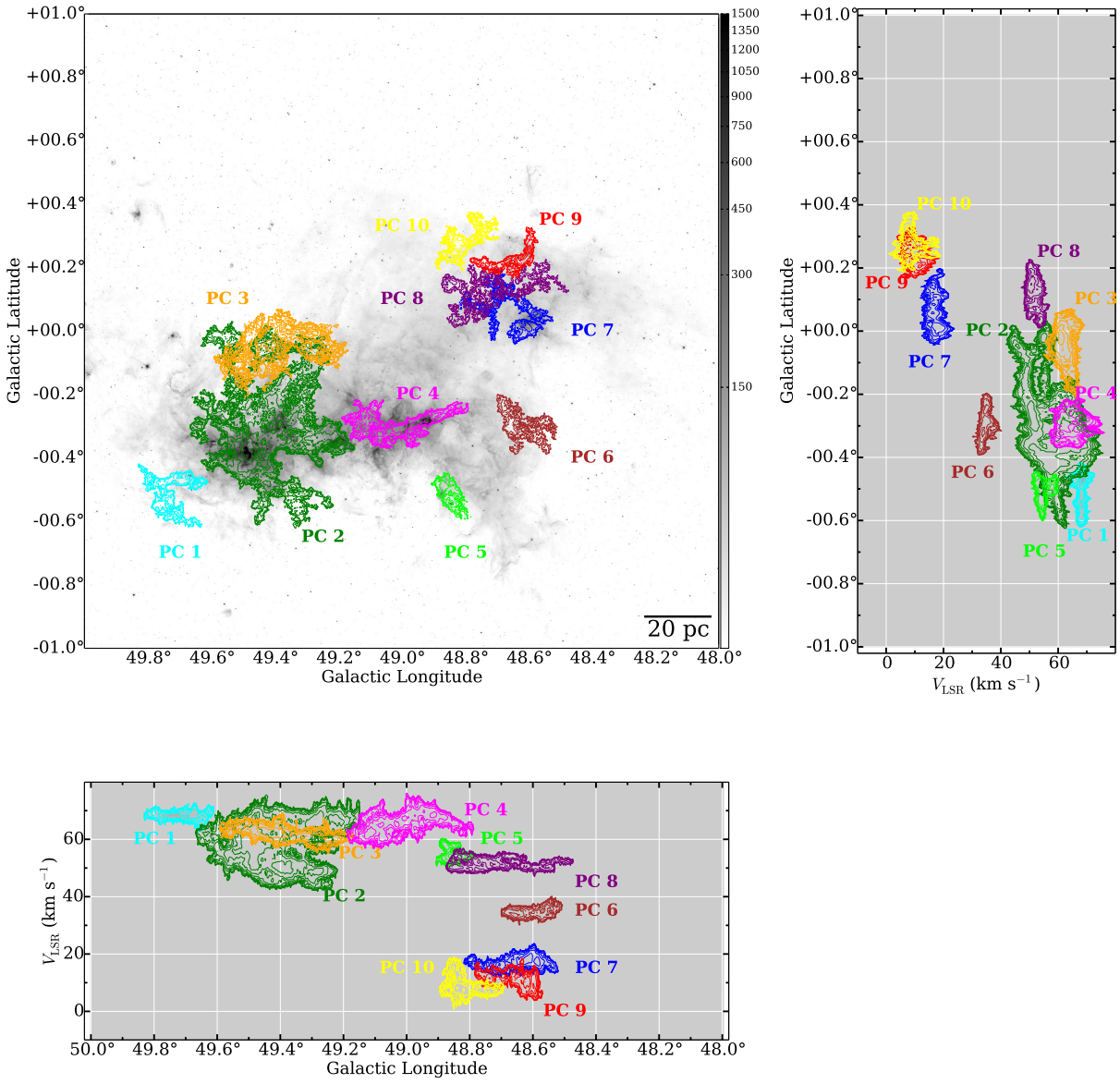

Figure 3.7: The integrated intensity map, $l-v$ map and $v-b$ map of identified 10 PCs. Color contours show that intensity of ^{13}CO ($J = 1-0$). The Contours levels are; [$2.1\times1,\ 2.1\times4,\ 2.1\times16,\ 2.1\times64$ K km s^{-1}], [$0.005\times1,\ 0.005\times2,\ 0.005\times4,\ 0.005\times8,\ 0.005\times16,\ 0.005\times32,\ 0.005\times64,\ 0.005\times128$ K degree] and [$0.005\times1,\ 0.005\times2,\ 0.005\times4,\ 0.005\times8,\ 0.005\times16,\ 0.005\times32,\ 0.005\times64,\ 0.005\times128$ K degree] for the integrated intensity map, $l-v$ map and $v-b$ map respectively. Grayscale show that *Spitzer* IRAC 8.0 μm intensity (MJy sr^{-1}).

3.2.3 Characteristics of parent clouds

We note the characteristics of PCs in this subsection.

Figure 3.8 shows the histograms of R_{1312}, R_{1813}, R_{3210} (for each voxel), the *Spitzer* IRAC 8.0 μm intensity and $N(\mathrm{H_2})$ (column density of hydrogen molecules) (for each pixel), for each PC.

R_{1312}, R_{3210} and R_{1813} in Table 3.2 are the ratio of the integrated intensity over whole region of each PC. We adopted "bijection" scheme (see Rosolowsky et al. 2008) to estimate the integrated intensity. 8.0 μm intensity in Table 3.2 is the median intensities within the area of each PC.

$M_{\mathrm{PC,LTE}}$ is the LTE (Local Thermodynamic Equilibrium) mass of PC. We calculated the excited temperature (T_{ex}) for each pixel with the following equation,

$$T_{\mathrm{ex}} = \frac{T_0}{\ln\{\frac{T_0}{T_{\mathrm{mb}}+J(T_{\mathrm{bg}})}+1\}}, \tag{3.1}$$

where $T_0 = \frac{h\nu}{k}$ and $J(T) = \frac{T_0}{\exp(T_0/T)-1}$, assuming that ^{12}CO ($J = 1-0$) is optically thick. We used the peak main beam temperature of ^{12}CO ($J = 1-0$) in T_{mb} in this formula, and the column density of hydrogen molecules ($N(\mathrm{H_2})$) is given by the next equation (Carpenter & Sanders 1998)

$$N(\mathrm{H_2}) = 3.05 \times 10^{19} T_{\mathrm{ex}} e^{5.29/T_{\mathrm{ex}}} \int T_{\mathrm{mb}} dv \quad [\mathrm{cm^{-2}}]. \tag{3.2}$$

We estimated $M_{\mathrm{PC,LTE}}$ by summing $N(\mathrm{H_2})$ in each PC. M_{VT} is the virial mass of the PC. We calculated M_{VT} by the following equation (Solomon et al. 1987) assuming that $\rho \propto r^{-1}$ and spectral profiles are Gaussian,

$$M_{\mathrm{VT}} = 189 \times (2\sqrt{2ln2}v_{\mathrm{rms}})^2 \times R \quad [M_\odot], \tag{3.3}$$

where v_{rms} is the intensity-weighted second moment of velocity and R is the radius of PC (geometric mean of major radius and minor radius).

Figure 3.9 shows the map of ^{13}CO ($J = 1-0$) moment 0, moment 1, moment 2, the map of 8.0 μm intensity, R_{1312}, R_{3210}, $N(\mathrm{H_2})$, C^{18}O ($J = 1-0$) intensity and C^{18}O ($J = 1-0$) / ^{13}CO ($J = 1-0$) intensity ratio ($\equiv R_{1813}$) of each PC.

YSO candidates listed in Kang et al. (2009) are plotted in the map of 8.0 μm intensity and $C^{18}O$ ($J = 1 - 0$) intensity (Figure 3.9), although it should be noted that the area covered by the catalog is smaller ($l = 48.75 - 50.0°$, $b = -0.7 - 0.3°$) than that of our map. Information of the YSO candidates is given in Table 3.3. Since PC2 and PC3 are overlapped along the line of sight, several YSO candidates in PC 2 and PC 3 are counted for both PCs to get an upper limit of number of associated YSO candidates in the catalog. Furthermore, fluxes in the most luminous area in PC 2 are saturated in the GLIMPSE and MIPSGAL images, hence they are not included in YSOs candidates catalog.

The properties of each PC are summarized as follows.

PC 1 (cyan)

This cloud is a part of HVS (68 km s^{-1} cloud) and located in the eastern side of G49.5-0.4. $v_{\rm rms}$ is relatively small (1.1 km s^{-1}) in comparison to the other PCs. R_{1312} is slightly low (0.30) and 8.0 μm intensity is weak ($\sim$ 30 MJy sr^{-1}), but R_{3210} is high (0.66). The 8.0 μm peak in the northwestern part coincides with the peak of R_{3210} rather than the peak of $N(H_2)$. There are 22 YSO candidates in this PC which are all $\leq 8M_\odot$ and the average mass of the YSO candidates is low ($4.3M_\odot$).

PC 2 (green)

This is the largest and most complicated PC. This cloud contains W51main, the strongest source in this region. Most of the previous studies are concentrated on this area. R_{3210}, 8.0 μm intensity and $N(H_2)$ are all high (0.75, 72 MJy sr^{-1} and 6.6×10^{21} cm^{-2} respectively). Especially R_{1312} is high (> 0.6) in the Northern area. While many YSOs are not identified because of the flux saturation in the center of PC 2, many massive YSO candidates ($\leq 8M_\odot$) are found in this PC and averaged mass is high ($5.8M_\odot$). We discuss about PC2 in 3.2.4 into details.

PC 3 (orange)

This cloud is located in the northern side of W51 main. R_{3210} is low (0.20), and 8.0 μm intensity is weak ($\sim$ 38 MJy sr^{-1}). The map of moment 1 shows an arc-like structure. The

8.0 μm peaks coincide with the R_{3210} peaks and the $N(H_2)$ peaks. While 41 YSO candidates are identified, most of them are low mass objects (the average mass of the YSO candidates is $4.8M_{\odot}$). In addition, three massive YSO candidates are identified in the area overlapped with PC 2, but we consider that at least two of them are not associated with PC 3 from the comparison with our $C^{18}O$ ($J = 1 - 0$) map (see Figure 3.9).

PC 4 (magenta)

This cloud is located in the western side of W51 main. It contains a part of HVS (68 km s^{-1} cloud). R_{1312} is slightly low(0.28), and R_{3210} is high (0.99). This tendency resembles that of PC 1. However, 8.0 μm intensity is very high ($\sim$ 166) and $N(H_2)$ is also high (6.7×10^{21} cm^{-2}). Although R_{3210} is especially high (> 1.3) at the edge of the cloud in the western part, R_{1312} is low (< 0.3). The velocity structure of the western part shows expanding arc structure as discussed in Moon & Park (1998) and Kang et al. (2010). CCCC 1 discussed in 4.1.5 is located in the eastern part of PC 4. 35 YSO candidates are identified, and averaged mass is very high ($7.7M_{\odot}$).

PC 5 (lime)

This cloud is located in the southern side of PC 4. It is compact and R_{1312}, R_{3210} and R_{1813} are relatively high (0.39, 0.52 and 0.14 respectively). There are two 8.0 μm peaks in the northeastern and central regions which coincide with R_{3210} and $N(H_2)$ peaks. On the other hand, R_{1312} is low ($\sim$ 0.3) at the peaks. 10 YSO candidates are identified in this PC, and one of these is a massive YSO candidate. The average mass of the YSO candidates is low ($4.4M_{\odot}$).

PC 6 (brown)

This cloud is located in the western side of PC 4. The velocity range is 30–40 km s^{-1}. It is not certain whether it locates close to PC 4 or not. Kinematic distance is 2.2 or 8.9 kpc. Since the cloud coincides with dark feature in infrared images, we adopted near distance of 2.2 kpc. $v_{\rm rms}$ is relatively small (1.3 km s^{-1}). R_{1312} and R_{1813} are high (0.48 and 0.16), but R_{3210} is low (0.26) and 8.0 μm intensity is weak (43 MJy sr^{-1}). There is a clear velocity gradient from

southeast to northwest. This PC is located in the outside of YSO candidates catalog.

PC 7 (blue)

This cloud is located in W51BW. We adopted the distance of 10.8 kpc (Perseus arm). $T_{\rm peak}$ is high (14.9 K) in W51BW. R_{1312} is relatively low (0.31), but R_{3210} is high (0.65) and 8.0 μm intensity is slightly high (58 MJy sr^{-1}). This PC was discussed as G48.60+0.02 in Nagayama et al. (2011) and Zhang et al. (2013), and *Spitzer* bubble G048.610+00.0593 (Hou et al. 2014) has been identified in this cloud. In the edge of the southwestern area, 8.0 μm intensity and R_{3210} are very high ($>$ 100 MJy sr^{-1} and $>$ 1.3), although R_{1312} is low ($<$ 0.3).

PC 8 (purple)

This cloud is also located in W51BW. A part of this cloud was discussed as IRDC1 in Kang et al. (2010). Since the velocity of this cloud is close to PC 1–5, we adopted the same distance as PC 1 – PC 5. R_{1312} is relatively high (0.38), but R_{3210} low (0.23). Relative to the surrounding, this cloud is dark in 8.0 μm. Therefore we speculate that this cloud is located in front of the surrounding radiation field.

PC 9 (red)

This cloud is also located in W51BW. We assumed that this cloud is in Perseus arm (distance of 10.8 kpc). R_{1312} is high (0.41). R_{3210}, 8.0 μm intensity and $N(\rm H_2)$ are moderate value (0.42, 51 MJy sr^{-1} and 3.4×10^{21} cm^{-2} respectively). This cloud looks like a filamentary cloud and *Spitzer* bubble G048.643+00.2474 (Hou et al. 2014) is associated with this cloud. R_{3210} is slightly high ($\sim$ 0.8) in the central region. This PC is located in the outside of YSO candidates catalog.

PC 10 (yellow)

This cloud is also located in W51BW. We also assumed that this cloud is in Perseus arm (distance of 10.8 kpc). R_{1312} is relatively high (0.38) and 8.0 μm intensity is weak ($\sim$ 34 MJy sr^{-1}). The majority of the area of this cloud is outside JCMT ^{13}CO ($J = 3 - 2$) dataset, therefore we did not calculate R_{3210}. R_{1312} is high ($>$ 0.6) in the northwestern part. At least one massive YSO candidate is associated with this cloud.

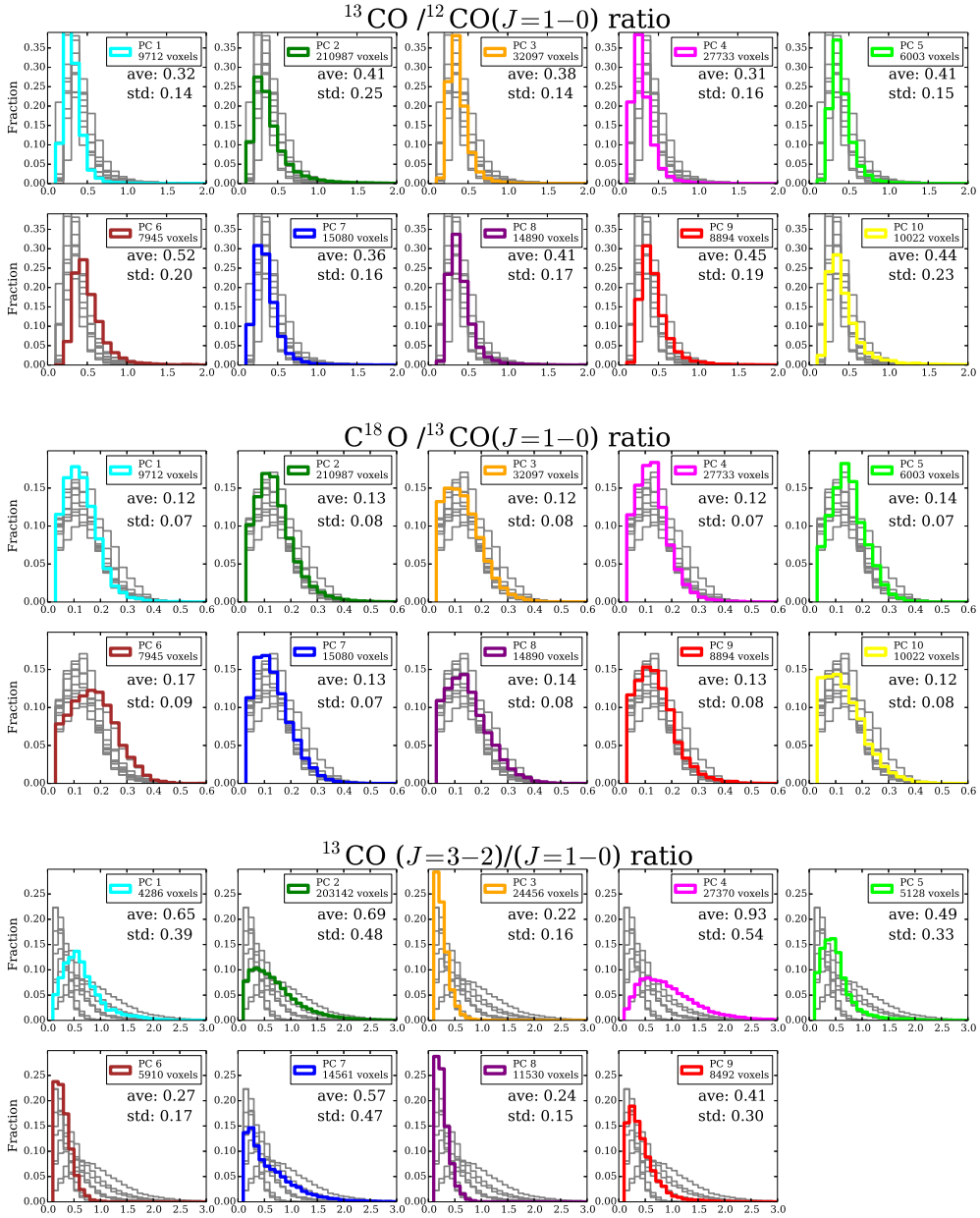

Figure 3.8: ^{13}CO ($J = 1 - 0$) / ^{12}CO ($J = 1 - 0$), C^{18}O ($J = 1 - 0$) / ^{13}CO ($J = 1 - 0$), ^{13}CO ($J = 3 - 2$) / ^{13}CO ($J = 1 - 0$), and 8 μm histograms for each pixel in PC 1–10.

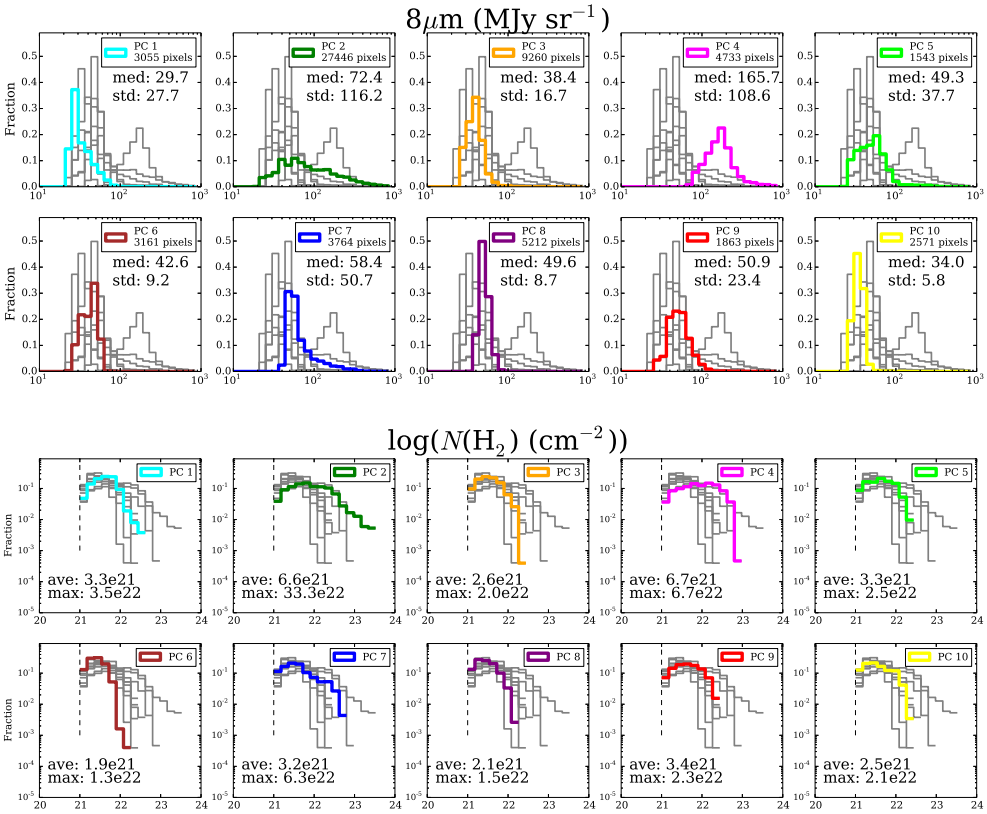

Figure 3.8: Continued.

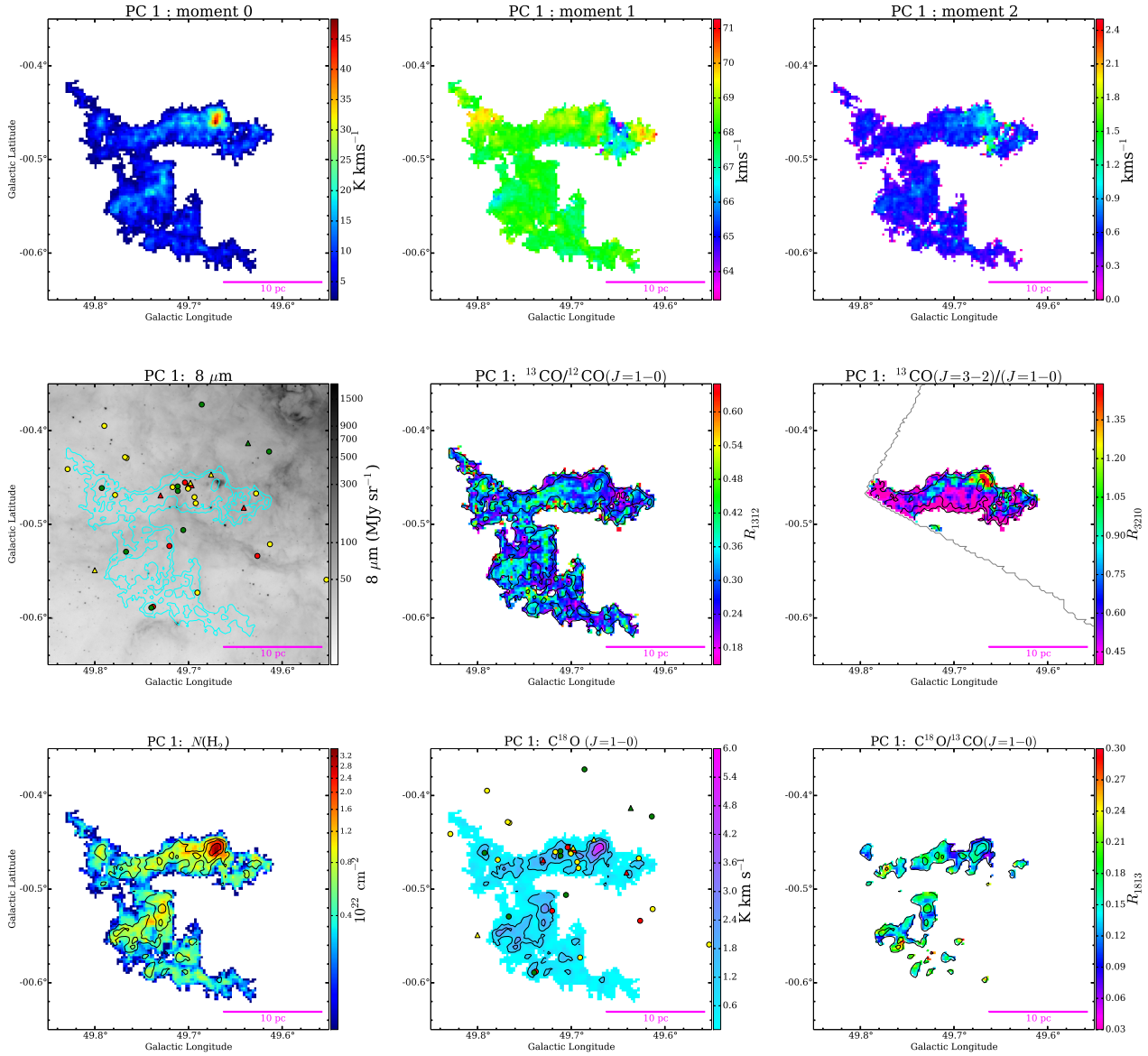

Figure 3.9: ^{13}CO ($J = 1{-}0$) moment 0, moment 1, moment 2, 8.0 μm intensity, R_{1312}, R_{3210}, column density of H_2, $C^{18}O$ ($J = 1 - 0$) integrated intensity and R_{1813} map of PC 1–10 ($R_{1312} \equiv {}^{13}$CO ($J = 1 - 0$) / ^{12}CO ($J = 1 - 0$) intensity ratio, $R_{3210} \equiv {}^{13}$CO ($J = 3 - 2$) / ^{13}CO ($J = 1 - 0$) intensity ratio and $R_{1813} \equiv C^{18}O$ ($J = 1 - 0$) / ^{13}CO ($J = 1 - 0$) intensity ratio). YSO candidates (Kang et al. 2009) are represented in red star for Stage 0/I, yellow star for Stage II, and green star for ambiguous sources. Black crosses represent the radio continuum sources listed by Koo & Moon 1997.

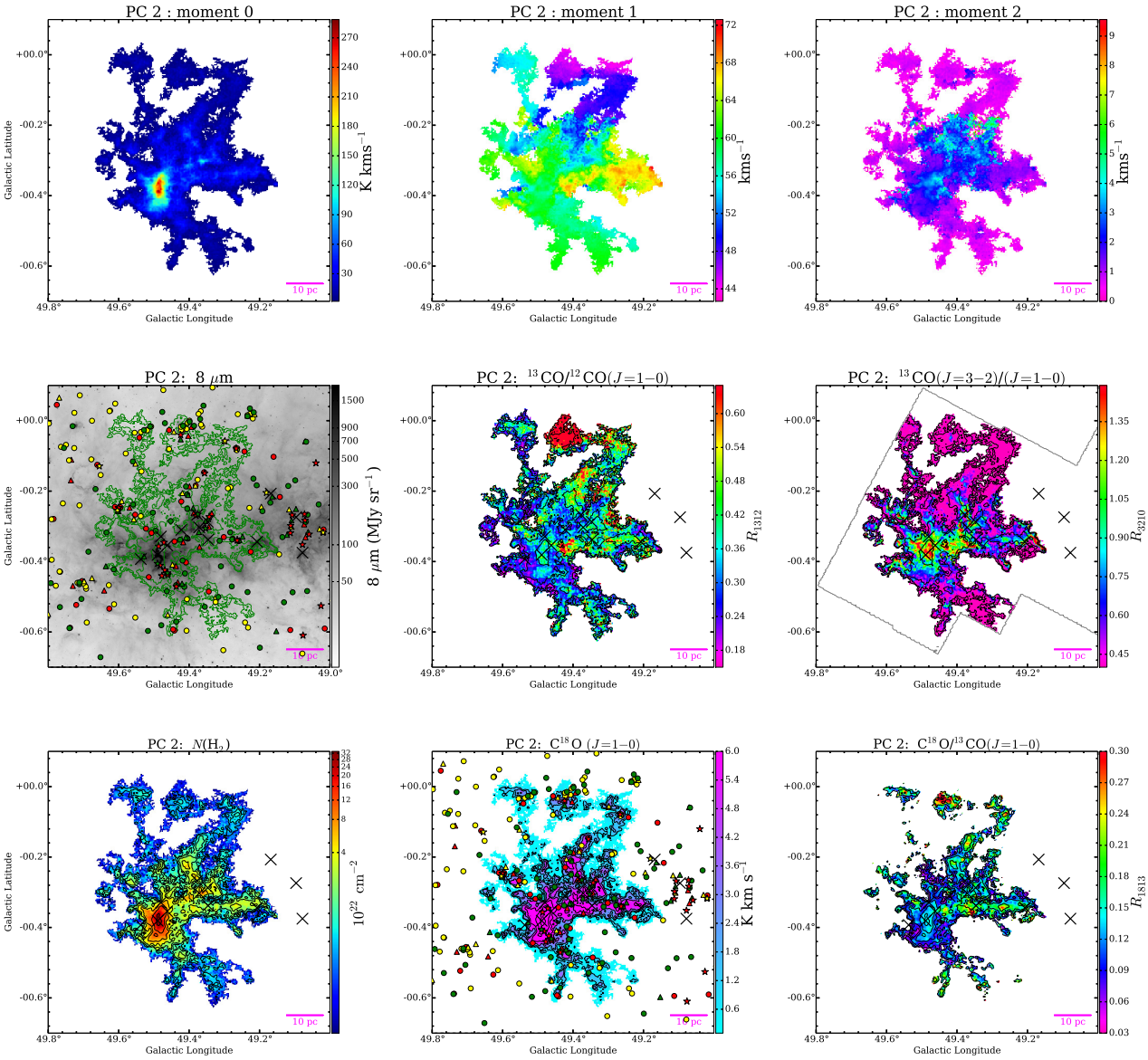

Figure 3.9: Continued.

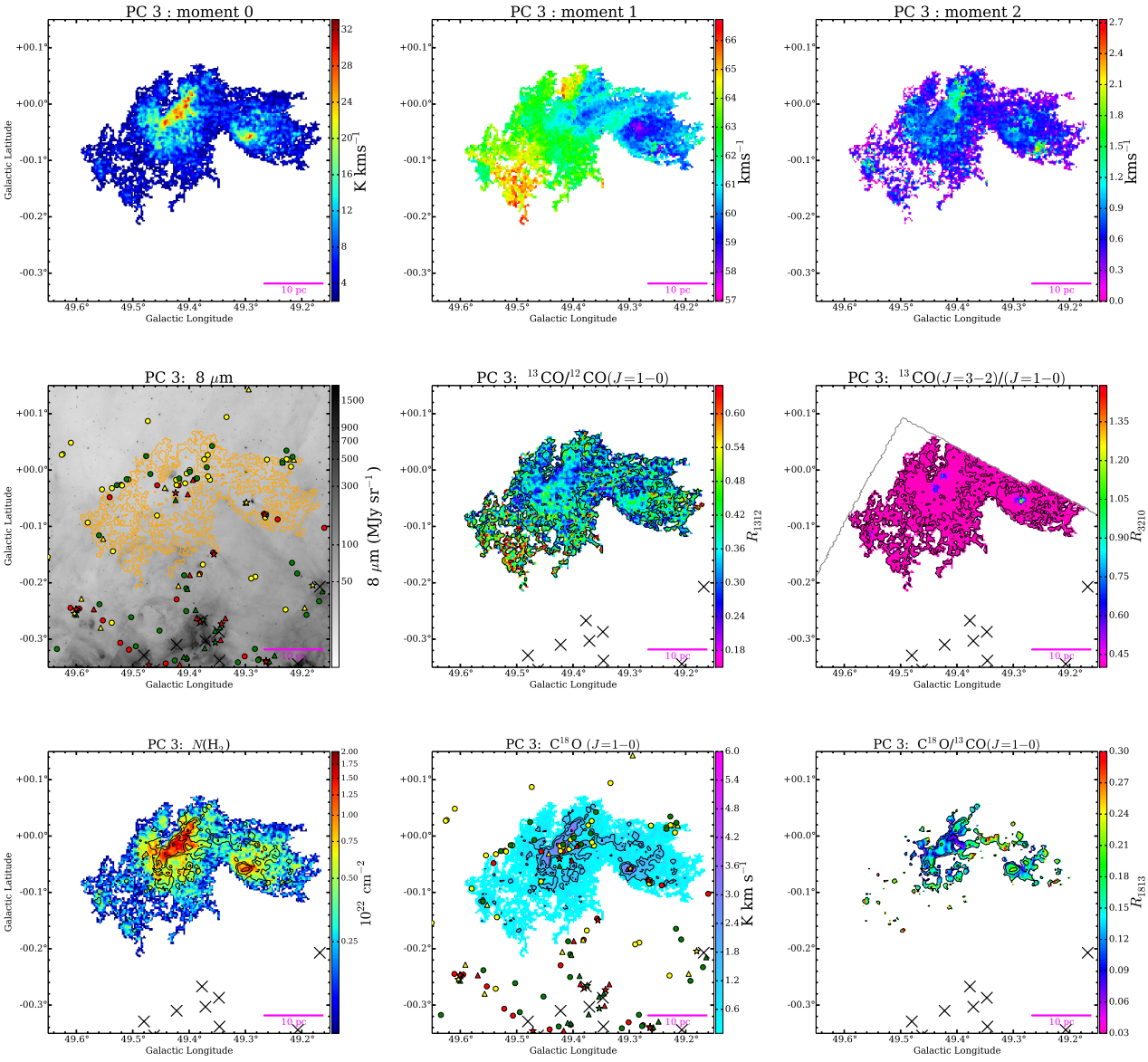

Figure 3.9: Continued.

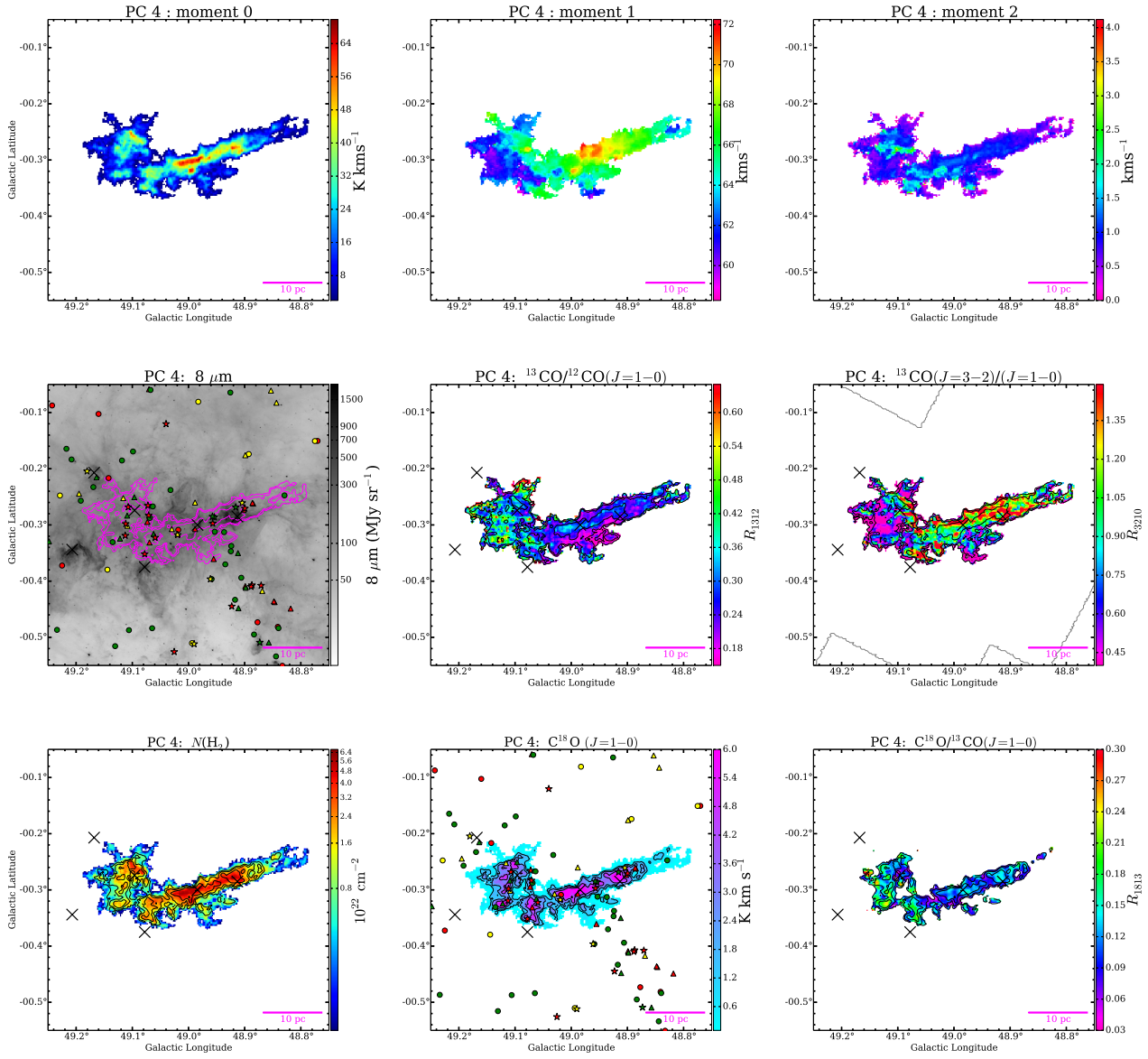

Figure 3.9: Continued.

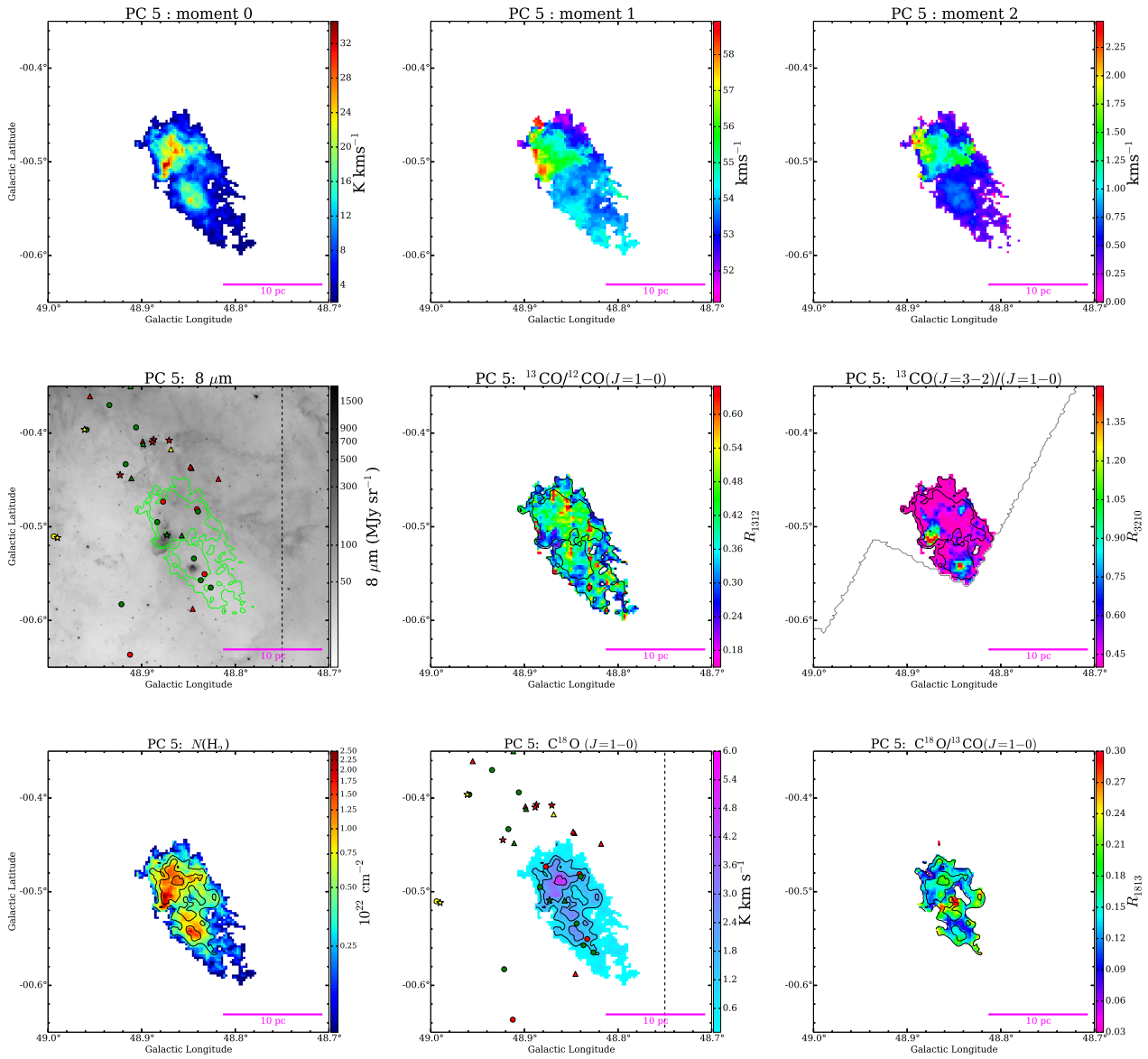

Figure 3.9: Continued.

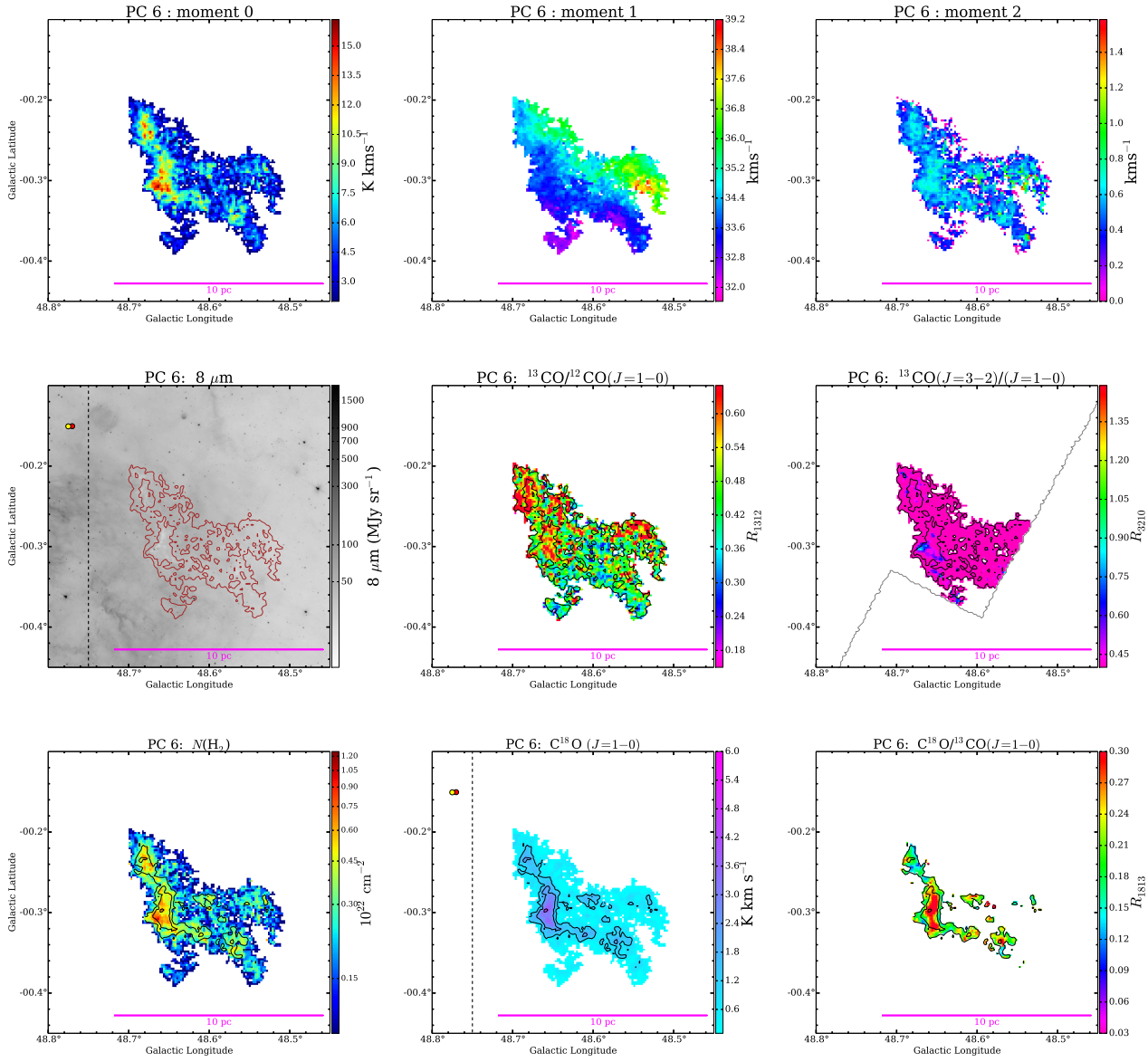

Figure 3.9: Continued.

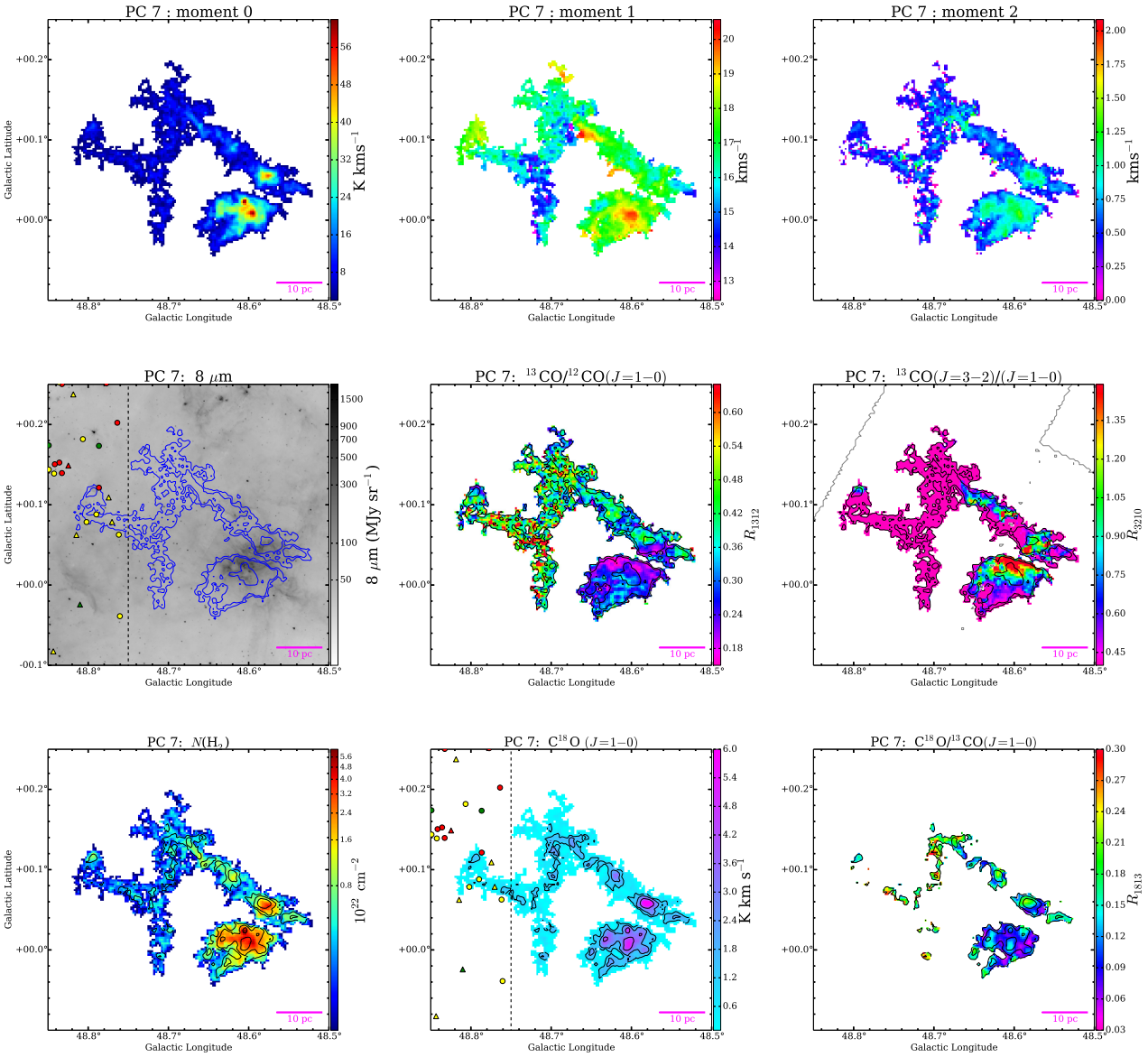

Figure 3.9: Continued.

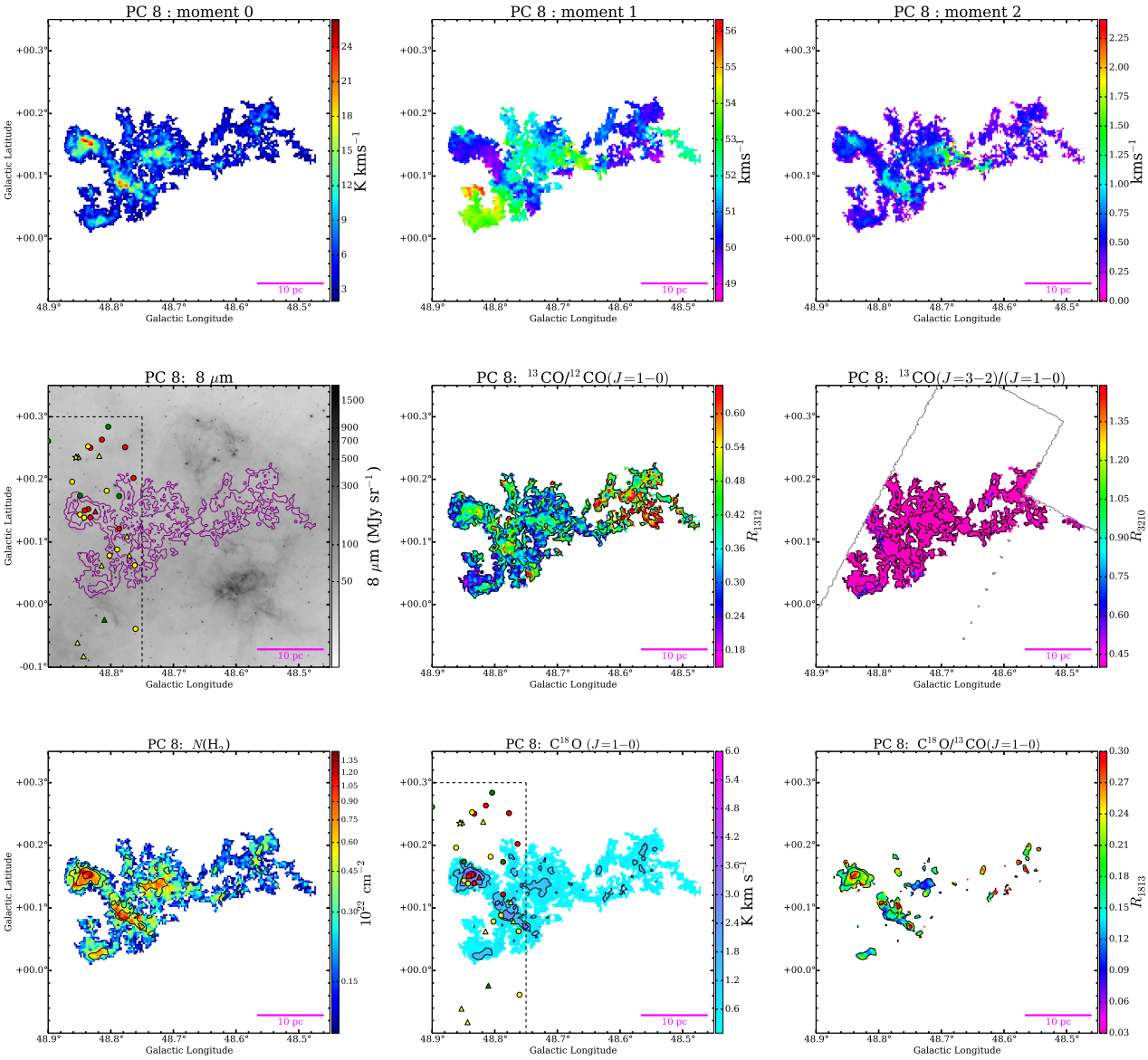

Figure 3.9: Continued.

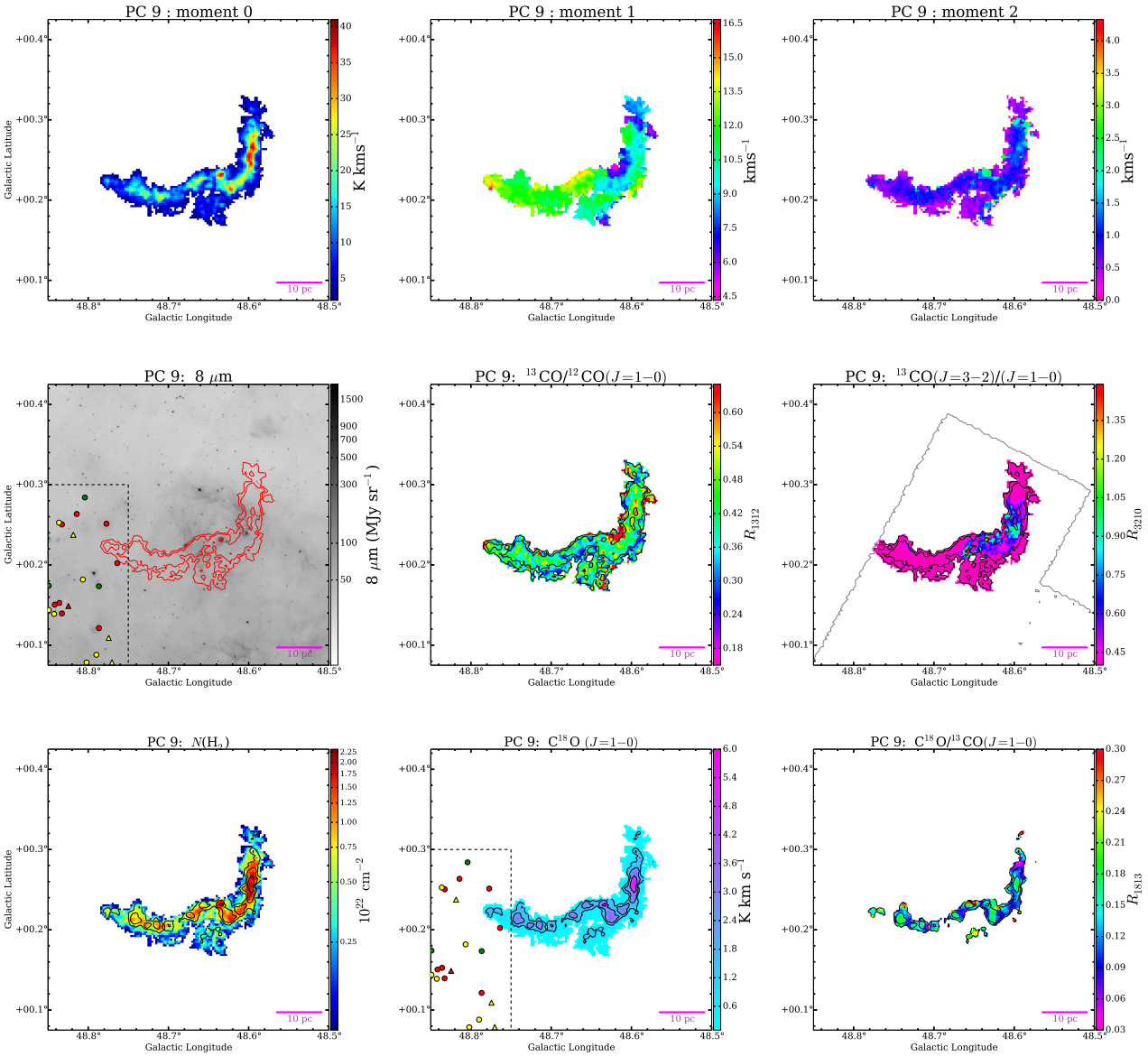

Figure 3.9: Continued.

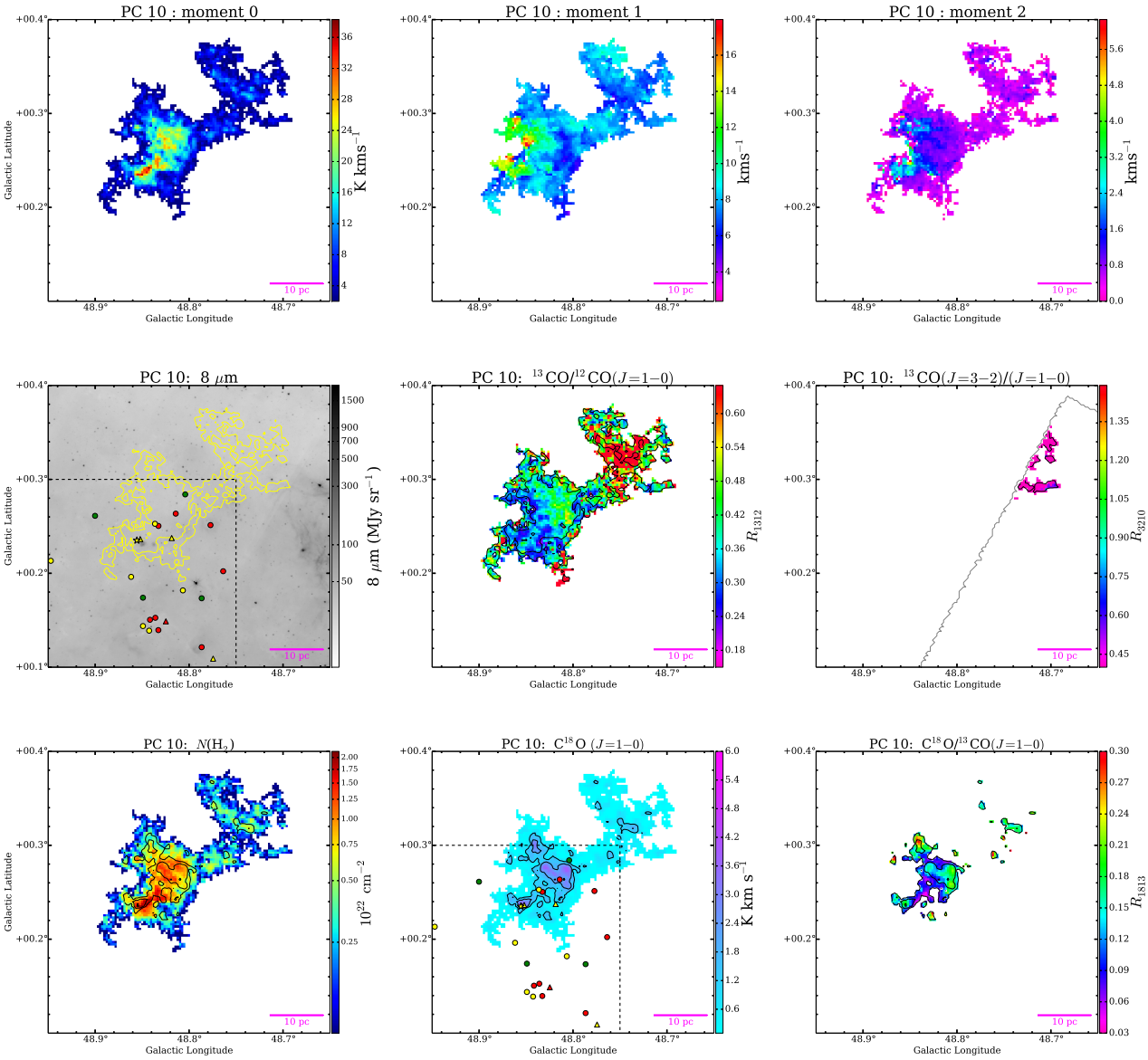

Figure 3.9: Continued.

Table 3.1: Properties of Parent Clouds I

ID name	ID color	$l_{\rm peak}$ [*1] (deg)	$b_{\rm peak}$ [*1] (deg)	$v_{\rm peak}$ [*1] (km s^{-1})	$T_{\rm peak}$ [*2] (K)	$v_{\rm rms}$ [*3] (km s^{-1})	R [*4] (pc)	$N_{\rm vo,all}$ [*5] (10^2)	$n_{\rm le,all}$ [*6]	Distance [*7] (k pc)
PC 1	cyan	49.67	-0.46	69.3	11.1	1.1	4.4	97.1	16	5.4
PC 2	green	49.49	-0.38	61.5	25.3	6.5	9.4	2109.9	205	5.4
PC 3	orange	49.44	-0.04	60.9	10.5	1.9	6.0	321.0	55	5.4
PC 4	magenta	48.92	-0.28	69.3	17.6	3.3	4.6	277.3	30	5.4
PC 5	lime	48.85	-0.54	54.4	10.6	1.9	2.2	60.0	6	5.4
PC 6	brown	48.66	-0.31	33.6	7.9	1.3	(1.6)	79.5	13	(2.2)
PC 7	blue	48.61	0.02	18.6	14.9	1.8	9.5	150.8	16	10.8
PC 8	purple	48.83	0.15	49.8	8.7	1.6	(5.7)	148.9	26	(5.4)
PC 9	red	48.60	0.25	7.6	9.0	2.4	6.9	88.9	14	10.8
PC 10	yellow	48.85	0.23	6.3	6.3	2.7	6.4	100.2	15	10.8

[*1] Peak position of ^{13}CO ($J = 1 - 0$) in the parent cloud.

[*2] Peak intensity of ^{13}CO ($J = 1 - 0$) in the parent cloud.

[*3] Intensity-weighted second moment of velocity.

[*4] Geometric mean of major radius and minor radius. Major radius was computed from the intensity-weighted second moment in direction of greatest elongation in the Position-Position plane. Minor radius was computed from the intensity-weighted second moment perpendicular to the major axis.

[*5] Number of voxels included in the parent cloud.

[*6] Number of leaves included in the parent cloud.

[*7] We assumed PC 1–5 are in about the same distance of 5.4 kpc (Sato et al. 2010) and PC 7, 9 and 10 are 10.8 kpc (Zaung et al. 2013). The distance of PC 6 and 8 are ambiguous.

Table 3.2: Properties of Parent Clouds II

ID name	R_{1312}[*1] ratio	R_{3210}[*2] ratio	8 μm[*3] (MJy sr^{-1})	average $N(H_2)$ ($\times 10^{21}$cm^{-2})	max $N(H_2)$ ($\times 10^{22}$cm^{-2})	R_{1813}[*4] ratio	M_{LTE}[*5] ($10^4 M_\odot$)	M_{VT}[*6] ($10^4 M_\odot$)
PC 1	0.30±0.05	0.66±0.09	29.7	3.3	3.5	0.10±0.01	1.4	0.6
PC 2	0.35±0.06	0.75±0.11	72.4	6.6	33.3	0.12±0.02	43.5	42.0
PC 3	0.36±0.06	0.20±0.03	38.4	2.6	2.0	0.09±0.01	3.5	2.4
PC 4	0.28±0.05	0.99±0.14	165.7	6.7	6.7	0.11±0.02	6.0	5.3
PC 5	0.39±0.07	0.52±0.07	49.3	3.3	2.5	0.14±0.02	0.8	0.8
PC 6	0.48±0.09	0.26±0.04	42.6	1.9	1.3	0.16±0.02	(0.1)	(0.3)
PC 7	0.31±0.06	0.65±0.09	58.4	3.2	6.3	0.11±0.02	9.0	3.0
PC 8	0.38±0.07	0.23±0.03	49.6	2.1	1.5	0.12±0.02	(1.5)	(1.5)
PC 9	0.41±0.07	0.42±0.06	50.9	3.4	2.3	0.11±0.02	3.9	4.2
PC10	0.38±0.07	–	34.0	2.5	2.1	0.09±0.01	4.1	4.9

[*1] ^{13}CO ($J = 1 - 0$) / ^{12}CO ($J = 1 - 0$) integrated intensity ratio.

[*2] ^{13}CO ($J = 3 - 2$) / ^{13}CO ($J = 1 - 0$) integrated intensity ratio. Note that we do not have ^{13}CO ($J = 3 - 2$) data set in entire FUGIN region. Voxels with deficient data were excluded for calculation. In PC 10, few ^{13}CO ($J = 3 - 2$) data exist.

[*3] Median intensity within area of the parent cloud.

[*4] C^{18}O ($J = 1 - 0$) / ^{13}CO ($J = 1 - 0$) integrated intensity ratio. Note that we used convoluted map for this calculation.

[*5] LTE mass of the parent cloud.

[*6] Virial mass of the parent cloud.

Table 3.3: Properties of Parent Clouds III

ID	area[*1] (pc^2)	n_{YSO}[*2]	n_{YSO} / area (pc^{-2})	n_{YSO} (fraction) $< 5\ M_\odot$	n_{YSO} $5-8\ M_\odot$	n_{YSO} $\geq 8\ M_\odot$	$< M_{YSO} >$[*3] ($M_\odot$)	ΣM_{YSO}[*4] ($M_\odot$)	ΣM_{YSO} / $M_{PC,LTE}$
PC 1	152	22	0.14	15 (0.68)	7 (0.32)	0 (0.00)	4.3	95.3	0.7 %
PC 2	1365	123	0.09	68 (0.55)	33 (0.27)	22 (0.18)	5.8	718.2	0.2 %
PC 3	460	41	0.09	30 (0.73)	8 (0.20)	3 (0.07)	4.8	196.7	0.6 %
PC 4	235	35	0.15	6 (0.17)	15 (0.43)	14 (0.40)	7.7	268.7	0.4 %
PC 5	77	10	0.13	8 (0.80)	1 (0.10)	1 (0.10)	4.4	43.6	0.6 %

[*1] The exact area of the parent cloud with assuming 5.4 kpc away.
[*2] Number of YSOs (Kang et al. 2009) included in the parent cloud.
[*3] The averaged mass of YSO in the parent cloud. The errors of each estimated YSO mass are 30 % typically.
[*4] The total mass of YSO in the parent cloud.

3.2.4 Internal structure of PC 2

PC 2 is a considerably active star forming, large, massive and very complicated parent cloud in W51. To investigate the relation between spatial distribution and velocity structure more clearly, we extracted the branches from the tree diagram of Dendrograms by using SCIMES (Colombo et al. 2015, clustering analysis). Figure 3.10 shows the integrated intensity map, $l-v$ and $v-b$ diagrams of the extracted branches. Note that the extracted branches have a different lowest intensity level. IRS 1 ($\sim$ W51e, $(l, b) = (49.486, -0.380)$) and IRS 2 ($\sim$ W51d, $(l, b) = (49.490, -0.370)$) are the strongest sources of near-infrared emission in W51. The center velocity of the recombination lines are $\sim$58 km s^{-1} and $\sim$52 km s^{-1}, respectively (Mehiringer et al. 1994).

We can see that some parts of HVS in PC 2 were extracted (Figure 3.11). However, we could not extract HVS as a single component in the central region (green contor, PC 2-1) due to the complication of the structure. The H I gas distribution of PC 2 is presented in Figure 3.12 and we can see strong absorption features at the position of PC 2-1. We will discuss the internal structure of PC 2 in detail in following section.

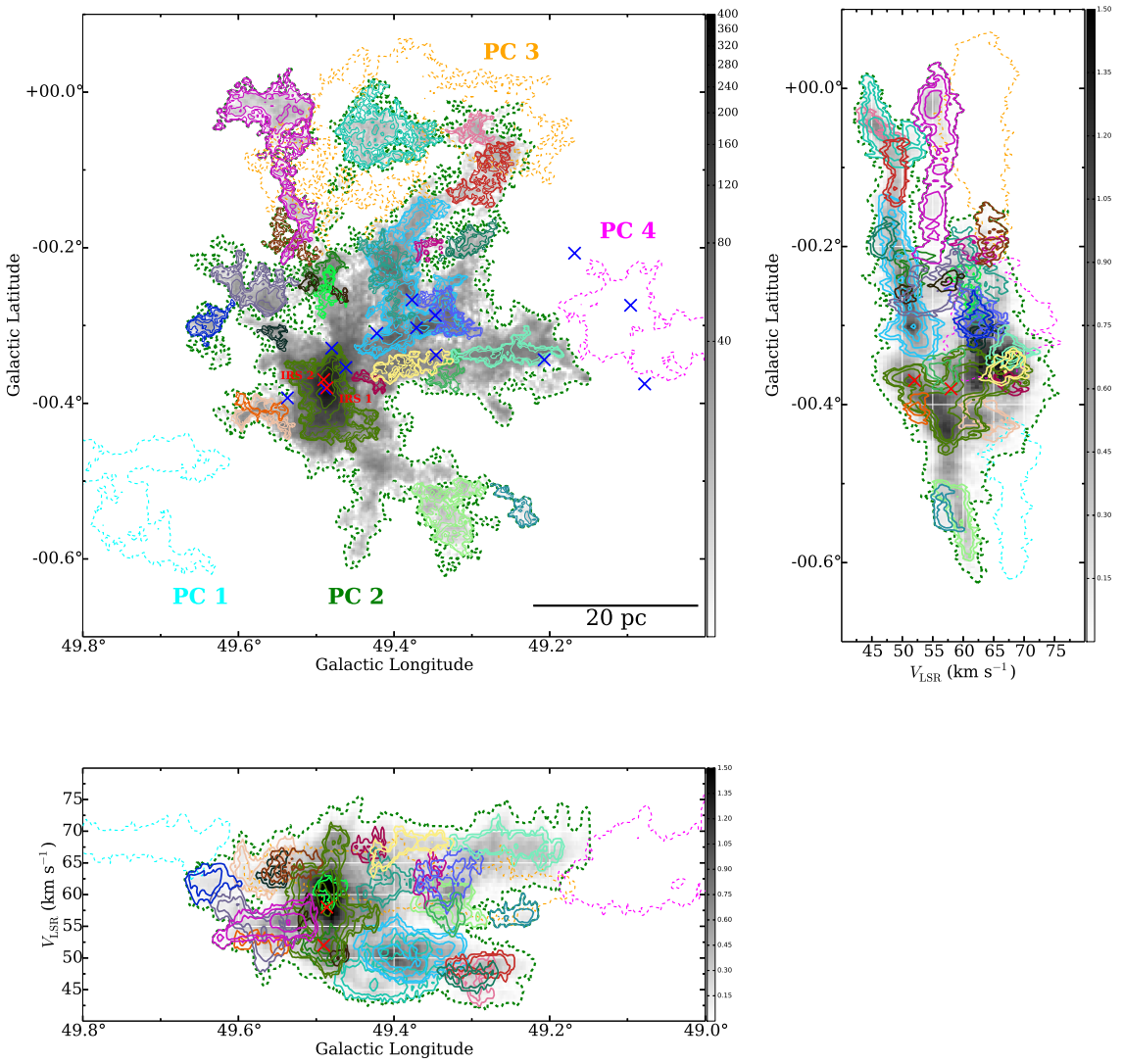

Figure 3.10: The ^{13}CO ($J = 1 - 0$) integrated intensity map, $l - v$ map and $v - b$ map of PC 1, PC 2, PC 3 and PC 4 (dashed lines) and extracted structures (solid lines). Grayscale show that integrated intensities of ^{13}CO ($J = 1 - 0$).

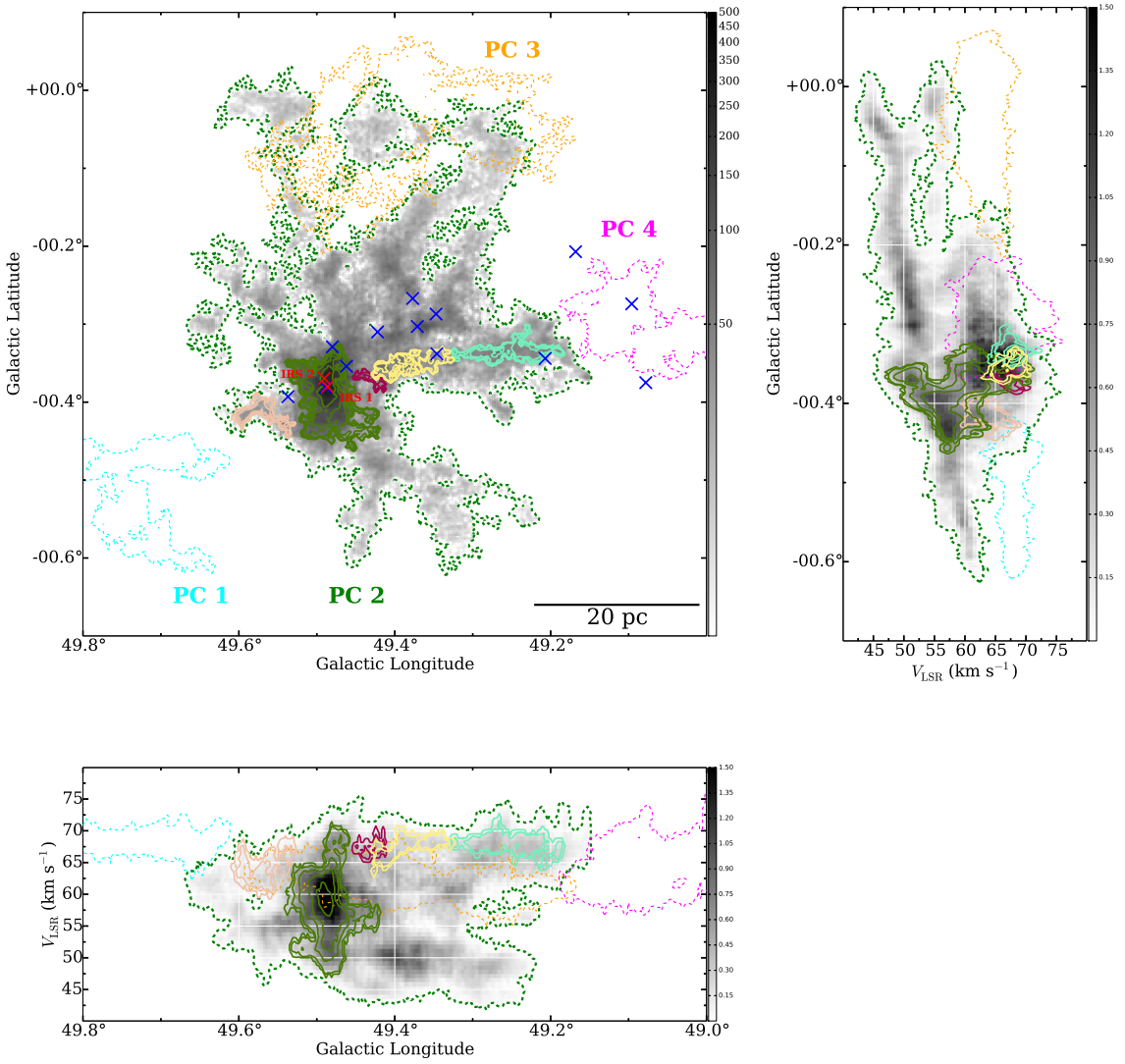

Figure 3.11: The ^{13}CO ($J = 1 - 0$) integrated intensity map, $l - v$ map and $v - b$ map of PC 1, PC 2, PC 3 and PC 4 (dashed lines) and extracted structures (solid lines). Grayscale show that integrated intensities of ^{13}CO ($J = 1 - 0$).

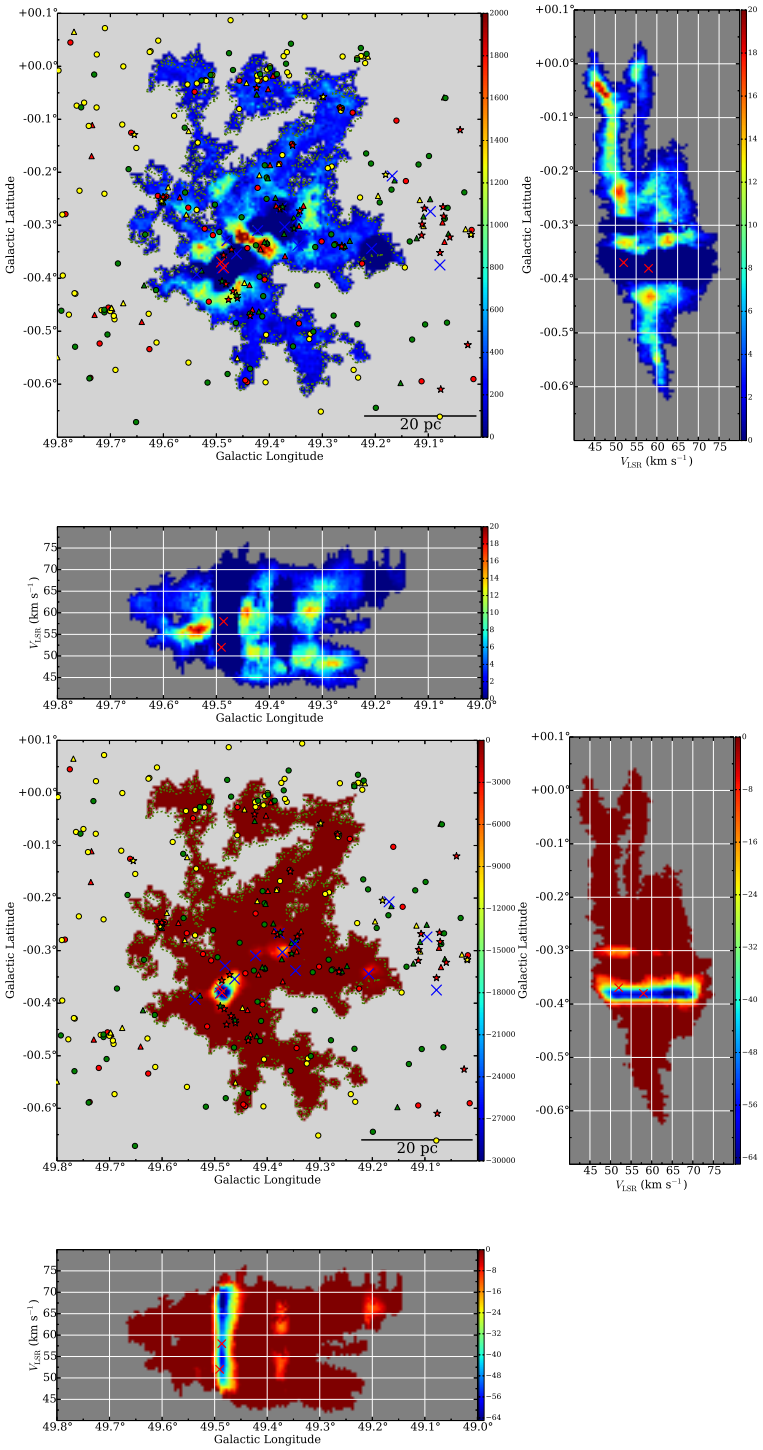

Figure 3.12: The map of H I of PC 2. The units are K km s^{-1}, K degree and K degree, respectively. This data was taken from VGPS archive. Two figures have different color ranges. Markers are same as Figure 3.9. Note that, the spatial resolution of this data is $\sim 1'$.

3.2.5 Internal structure of PC 2-1

Previous studies suggest that PC2-1 is the site of cloud-cloud collision (e.g., Carpenter & Sanders 1998; Okumura et al. 2001). Okumura et al. (2001) observed this region in ^{13}CO ($J = 1 - 0$), and proposed the following things. (1) There are four discrete molecular clouds toward this region. (2) The break (break 1) in the HVS has resulted from a cloud-cloud collision. (3) A "pileup" of three molecular clouds resulted in a burst of massive star formation. We make clear the correspondence between spatial distribution and velocity distribution of the complicated clouds PC 2-1.

Firstly, Figure 3.13 shows the integrated intensity map, $l - v$ and $v - b$ diagrams of ^{13}CO ($J = 1 - 0$) of PC 2-1. The mass of PC 2-1 is $\sim 2.0 \times 10^5\ M_\odot$. Figure 3.14 and Figure 3.15 show C^{18}O ($J = 1 - 0$) and H I map of PC 2-1, respectively. C^{18}O ($J = 1 - 0$) emission lines trace dense gas. From Figure 3.13 and Figure 3.14, it can be seen that PC 2-1 contains mainly four velocity components (51, 56, 62 and 68 km s^{-1}) (in addition to that, there is a $\sim$ 57 km s^{-1} component in the lower half). This is consistent with the result of Okumura et al. (2001).

Figure 3.16 shows the tree diagram of Dendrograms in PC 2-1 and its position. The colors in the tree diagram correspond to the colors in the maps, and the not-filled contours show the branches and filled contours show the leaves. In particular, various velocity components crowd in the upper half of PC 2-1, and the intensity of radio continuum ($\sim$H II region) is also strong. Figure 3.17 shows the components of HVS included in PC 2-1 (red contour) and another component of HVS included in PC 2. It was found that a HVS component (68 km s^{-1}) (red contour in figure 3.16 and 3.17) is located on the upper right of PC 2-1, whereas there is no HVS component on the left side of PC 2-1 (break 1). We will discuss about PC 2-9 in 4.1.2. We were able to clarify the molecular gas structure in PC 2-1.

3.2.6 The intensity of 8 μm and CO emission lines

The 8 μm emission is dominated by radiation from PAH molecules excited by UV from the surrounding stars. On the other hand, R_{3210} is also expected to be enhanced by surrounding UV sources. In Figure 3.9, especially on PC 1, PC 4, PC 5, and PC 7, there is a tendency that R_{3210} is high in the region where the intensity of 8 μm is high. Since the irradiated PAH molecules raise the

temperature of surrounding ISM by photoelectric heating mechanism (e.g., Hollenbach et al. 1999), the molecular gas in the region with intense 8 μm emission and high R_{3210} is thought to be the heated gas by young stars. On the other hand, R_{1312} and R_{1813} tend to be low in the area of PC 1, PC 4, PC 5, and PC 7 where 8 μm is intense and R_{3210} is high. Selective destruction of ^{13}CO and C^{18}O by strong UV radiation is though to be the main cause of low R_{1312} and R_{1813} (e.g., Shimajiri et al. 2014). It is consistent with the above idea that the intense 8 μm emission and high R_{3210} are caused by strong UV radiation.

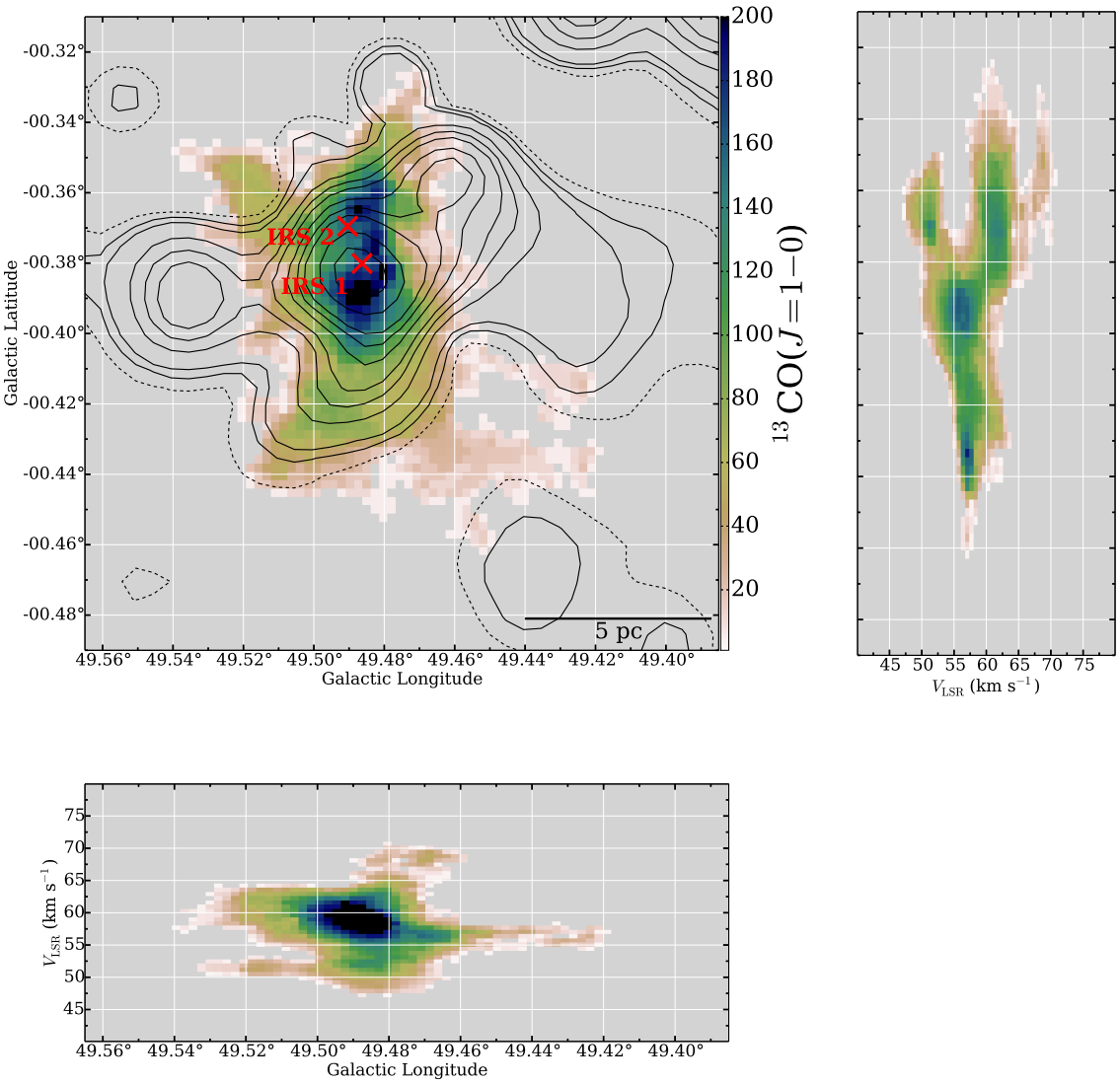

Figure 3.13: The map of ^{13}CO ($J = 1 - 0$) of PC 2-1. The units are K km s^{-1}, K degree and K degree, respectively. The triangle represent compact H II region c_1 (e.g., Mehringer 1994). The black contour shows the 21 cm continuum intensity taken from VGPS data. The contour levels are [50 (broken lines), 75, 100, 200, 300, 400, 600, 800, 1000, 1500, 2000 K].

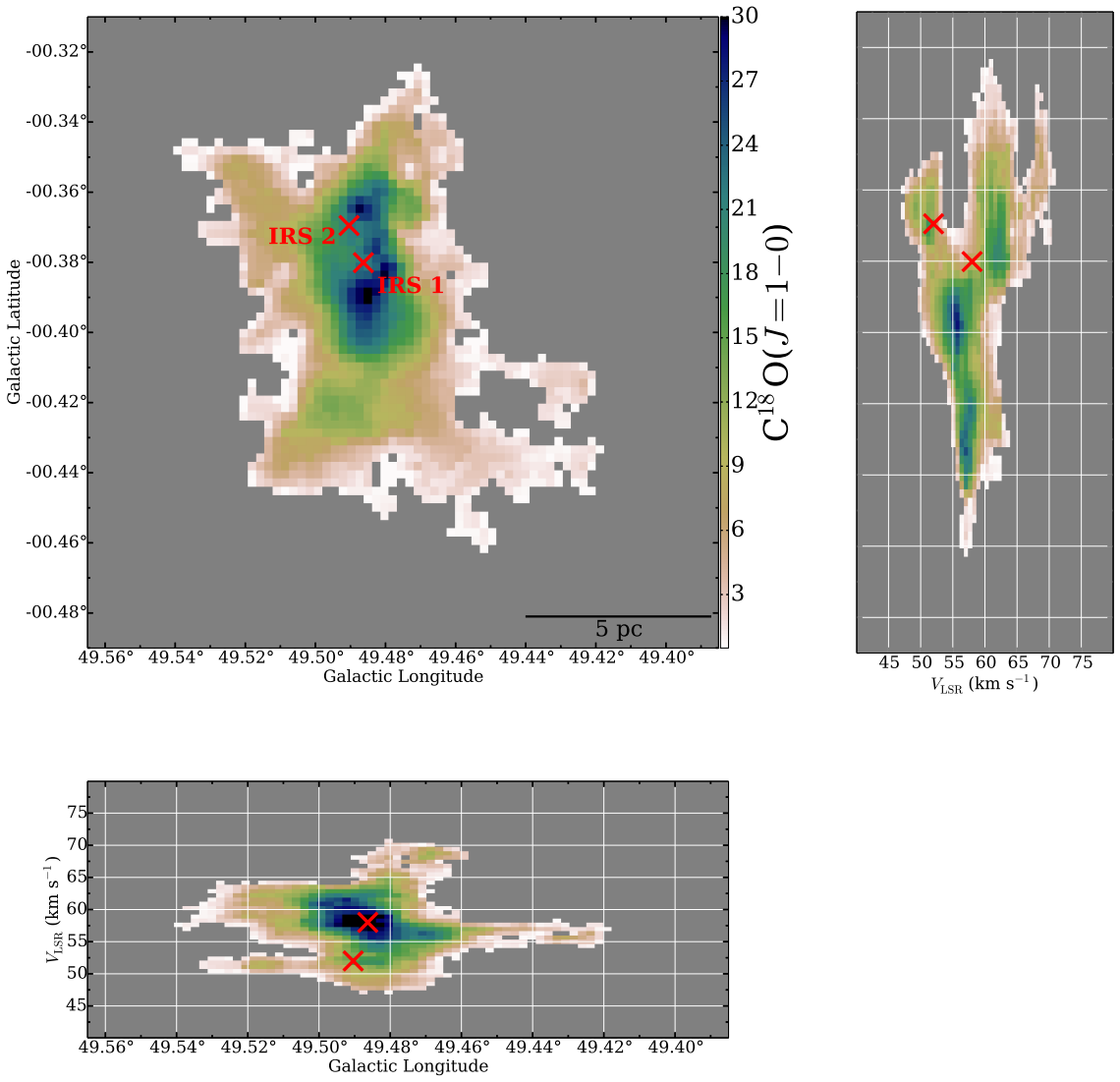

Figure 3.14: The map of $C^{18}O$ ($J = 1 - 0$) of PC 2-1. The units are K km s^{-1}, K degree and K degree, respectively. The triangle represent compact H II region c_1 (e.g., Mehringer 1994).

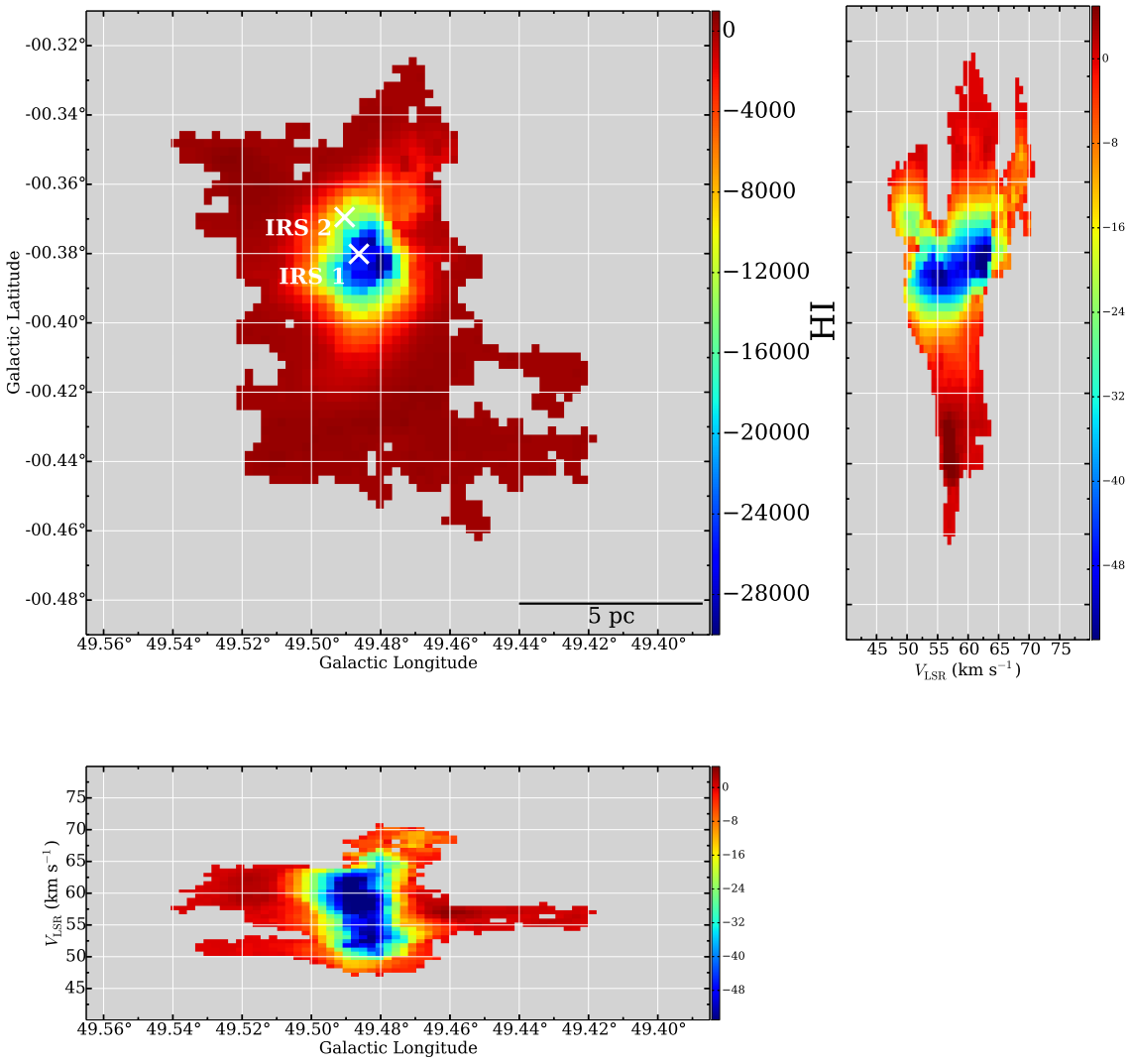

Figure 3.15: The map of H I of PC 2-1. The units are K km s^{-1}, K degree and K degree, respectively. Note that, the spatial resolution of this data is $\sim 1'$.

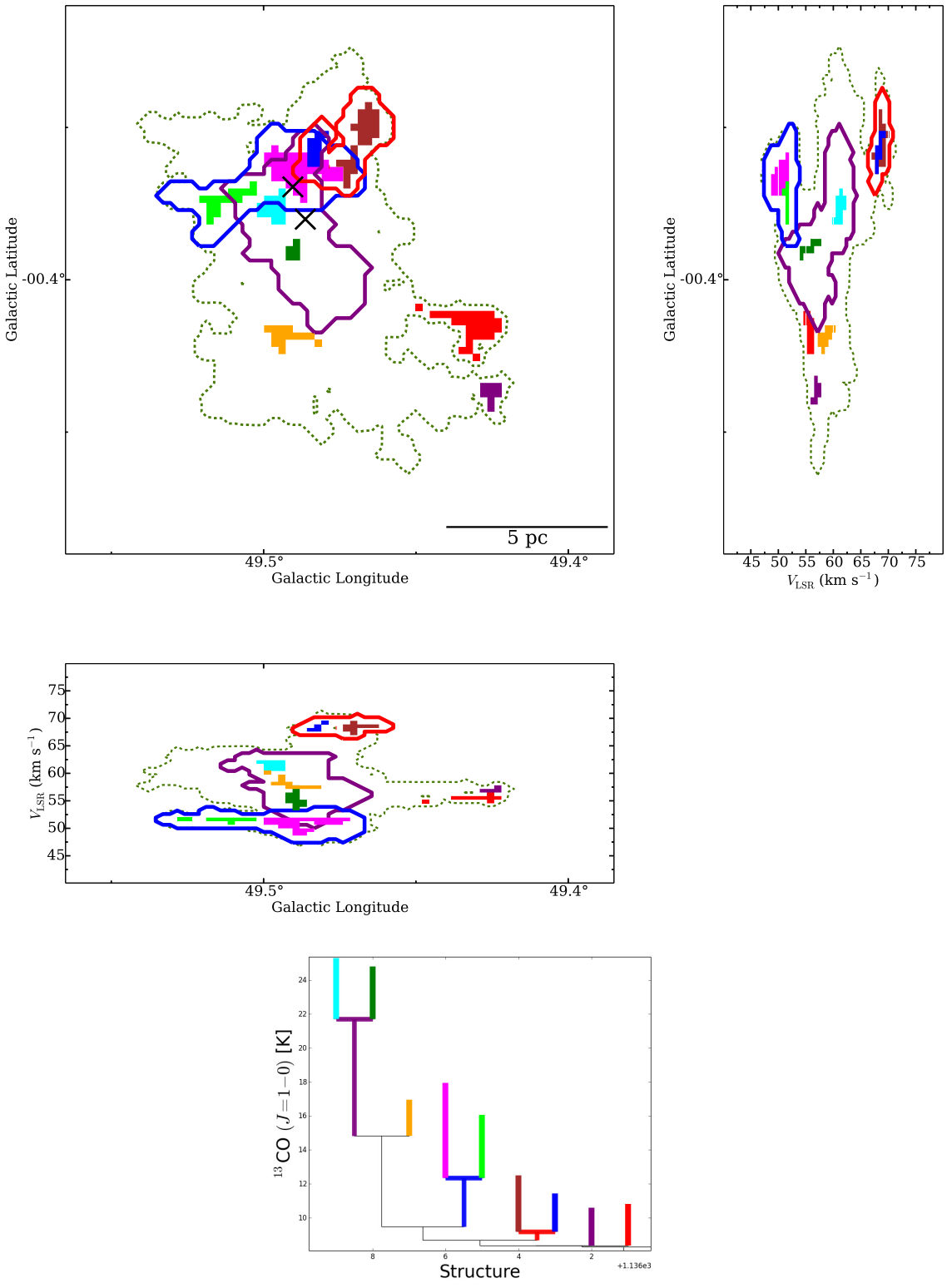

Figure 3.16: The structure map of PC 2-1. The not-filled contours show the branches and filled contours show the leaves in the tree diagram (bottom figure).

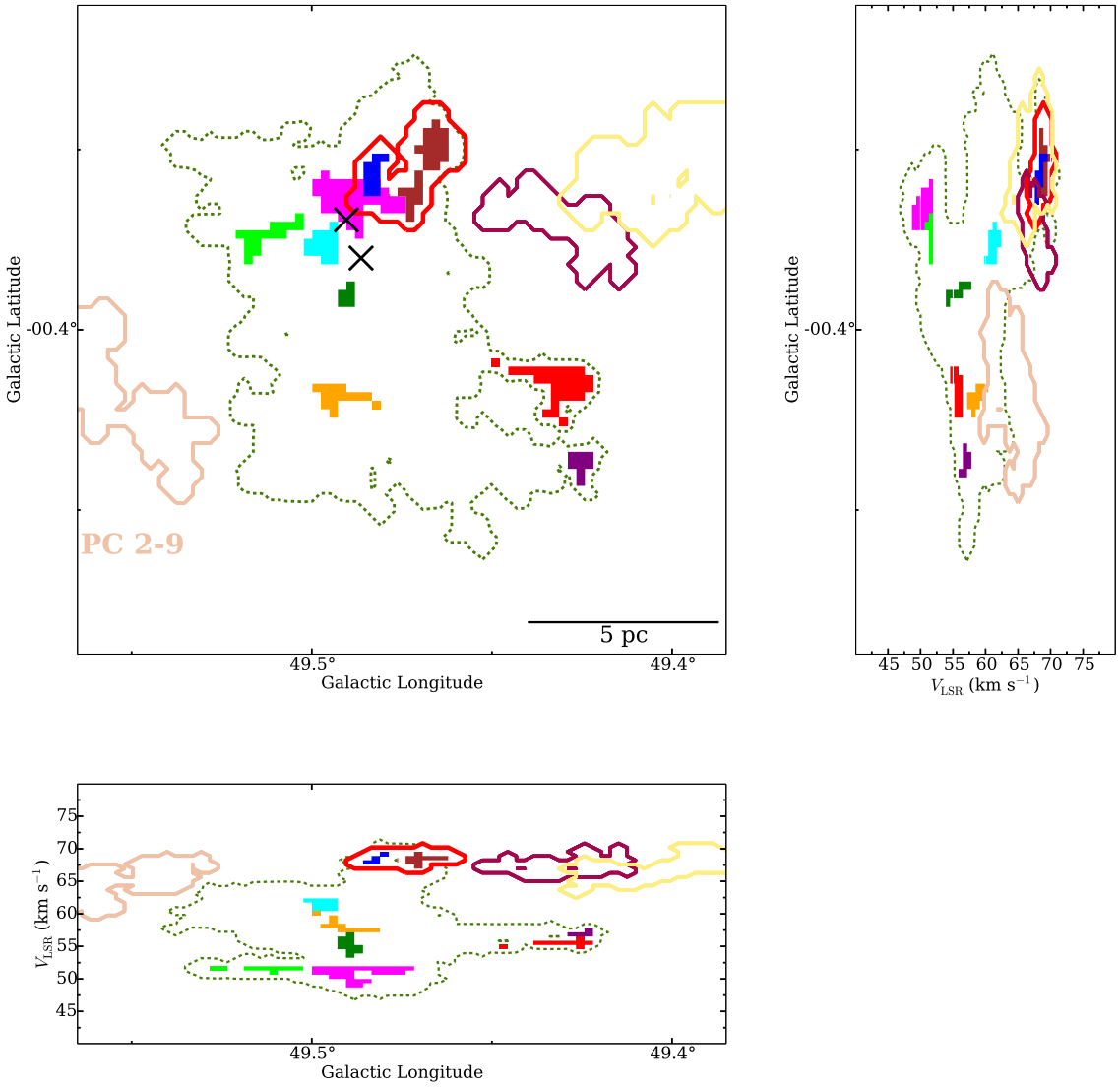

Figure 3.17: The structure map of PC 2-1 with HVS components. The not-filled contours show the branches and filled contours show the leaves. The contours in outside of PC 2-1 show the HVS components in PC 2.

Chapter 4

Discussion

4.1 The internal structure of W51 GMC

To understand the formation mechanism of massive stars is one of the most important task for the astronomy. Many previous studies have found that a lot of massive stars were formed in W51 GMC. We will investigate the internal structure of W51 GMC in detail, and discuss the relationship between GMC and star formation (especially massive stars).

4.1.1 Collisions of internal clouds in PC 2-1

The center of W51 (PC 2-1) is the place where massive star formation is thought to have been triggered by Cloud-Cloud Collisions (CCCs) (e.g., Carpenter & Sanders 1998; Okumura et al. 2001). It has become obvious from observational studies recently that CCC plays very important roles on the massive star formation (e.g., RCW 38 with $\sim$ 20 O stars (Fukui et al. 2016), NGC 3603 with $\sim$ 30 O stars (Fukui et al. 2014), Westerlund 2 with 14 O stars (Furukawa et al. 2009; Ohama et al. 2010), M20 with 1 O star (Torii et al. 2011; Torii et al. 2017)).

First, we investigate whether the molecular cloud in PC 2-1 is interacting with the H II region or not. According to the Large Velocity Gradient (LVG) model (e.g., Goldreich & Kwan 1974), R_{3210} (the intensity ratio ^{13}CO ($J = 3 - 2$)/^{13}CO ($J = 1 - 0$)) of heated molecular clouds is generally high. We compare the 21 cm continuum ($\sim$ H II region) intensity with R_{3210}. Figure 4.1 shows R_{3210} of PC 2-1 and Figure 4.2 (c) also shows R_{3210} of PC 2-1. On the $l - b$ map, R_{3210} is high

at the upper half of the PC 2-1, and also high especially at the velocities of 55 - 65 km s^{-1} on the $l-v$ and $v-b$ diagrams. However, R_{3210} depends on the density also. Therefore, it is necessary to distinguish whether the increases of the ratio are due to high density or high temperature in PC 2-1.

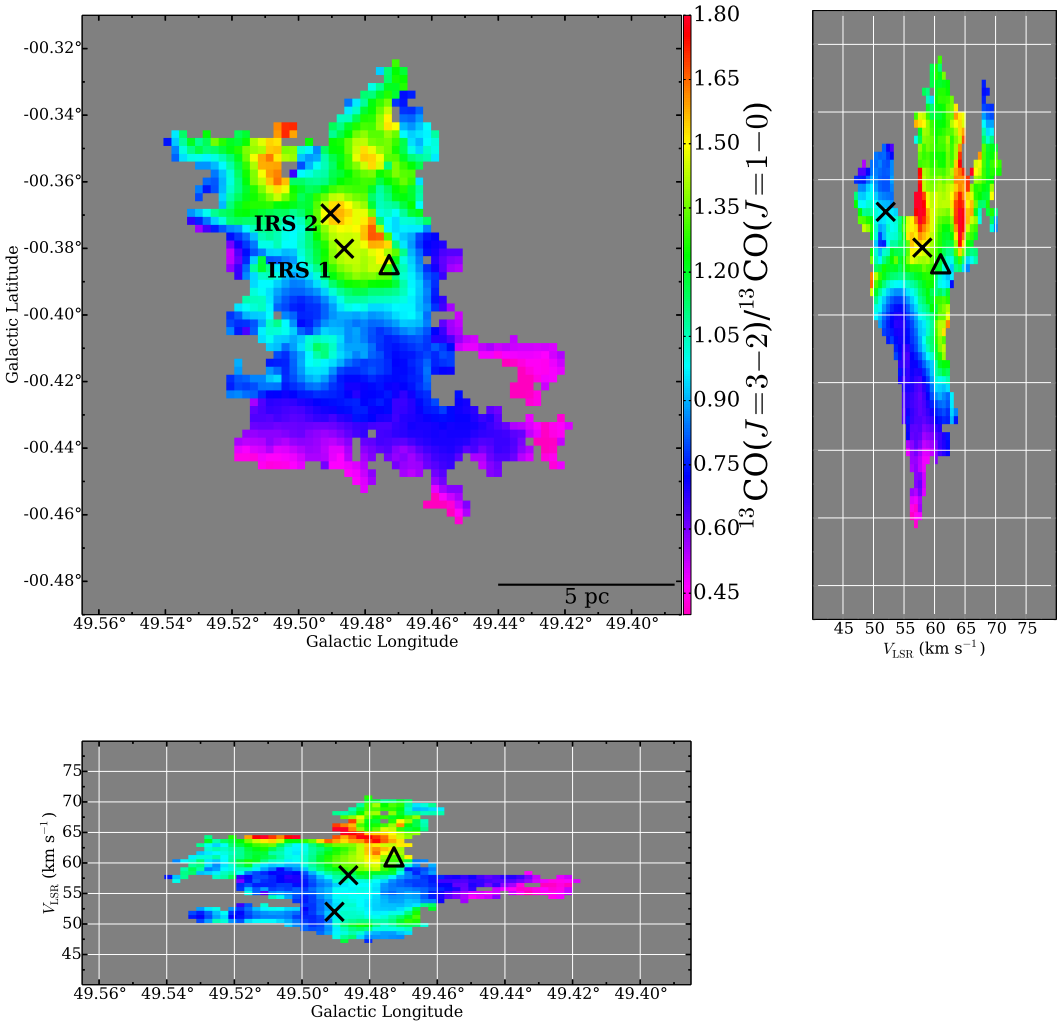

Figure 4.1: The intensity ratio ^{13}CO $(J=3-2)/^{13}$CO $(J=1-0)$ of the integrated intensity of $l-b$ map, $l-v$ map and $v-b$ map of PC 2-1.

Generally, 8 μm emission is radiated mostly from PAH (Polycyclic Aromatic Hydrocarbon) molecules excited by radiation from the surrounding stars. On the other hand, it is known that PAH molecules irradiated by UV heat the surrounding ISM via photoelectric heating mechanism (e.g., Hollenbach et al. 1999). Namely, if there is a good correlation between 8 μm intensity and R_{3210} in a cloud, it implies that the gas is heated by the photoelectric heating. Figure 4.3 is a plot of 8 μm intensity versus R_{3210} for each pixel in the PC 2-1. The color of the plot indicates the difference of b (Galactic Latitude). Overall, 8 μm intensity and R_{3210} are weakly correlated (coefficient 0.38). However, the upper half of PC 2-1 (colored orange – red) appears to be out of the overall trend. R_{3210} of these points are higher than others. This is because the 8 μm emission is extincted by the dust in HVS and the points are shifted to the left in the plot. Except for these points ($b > -0.38$), 8 μm intensity and R_{3210} are in good correlation (coefficient 0.63). In other words, it is thought that molecular clouds in PC 2-1 is heated due to interaction with H II region made by neighborhood massive stars.

In order to confirm the validity of the cloud-cloud collision scenario proposed in Okumura et al. (2001), we will calculate the collision time scale. From the above research, the extent of the region associated with the H II region is ~ 5 pc. The range of the difference of radial velocities of colliding clouds are roughly 5 – 15 km s $^{-1}$. Assuming that the direction of collision is 45° with respect to the line of sight, the collision time scale is calculated as 5 pc/(5-15 km s^{-1} $\times \sqrt{2}$) = 0.2 – 0.7 Myr. The age of H II region inside PC 2-1 is estimated to be 0.4$\pm$0.2 Myr (Okumura et al. (2000)), and the time scale of the massive star formation due to cloud-cloud collision is ~ 0.1 Myr (e.g., Fukui et al. 2015). Therefore, there is no contradiction in the scenario that these H II region are formed by massive stars induced by cloud-cloud collision.

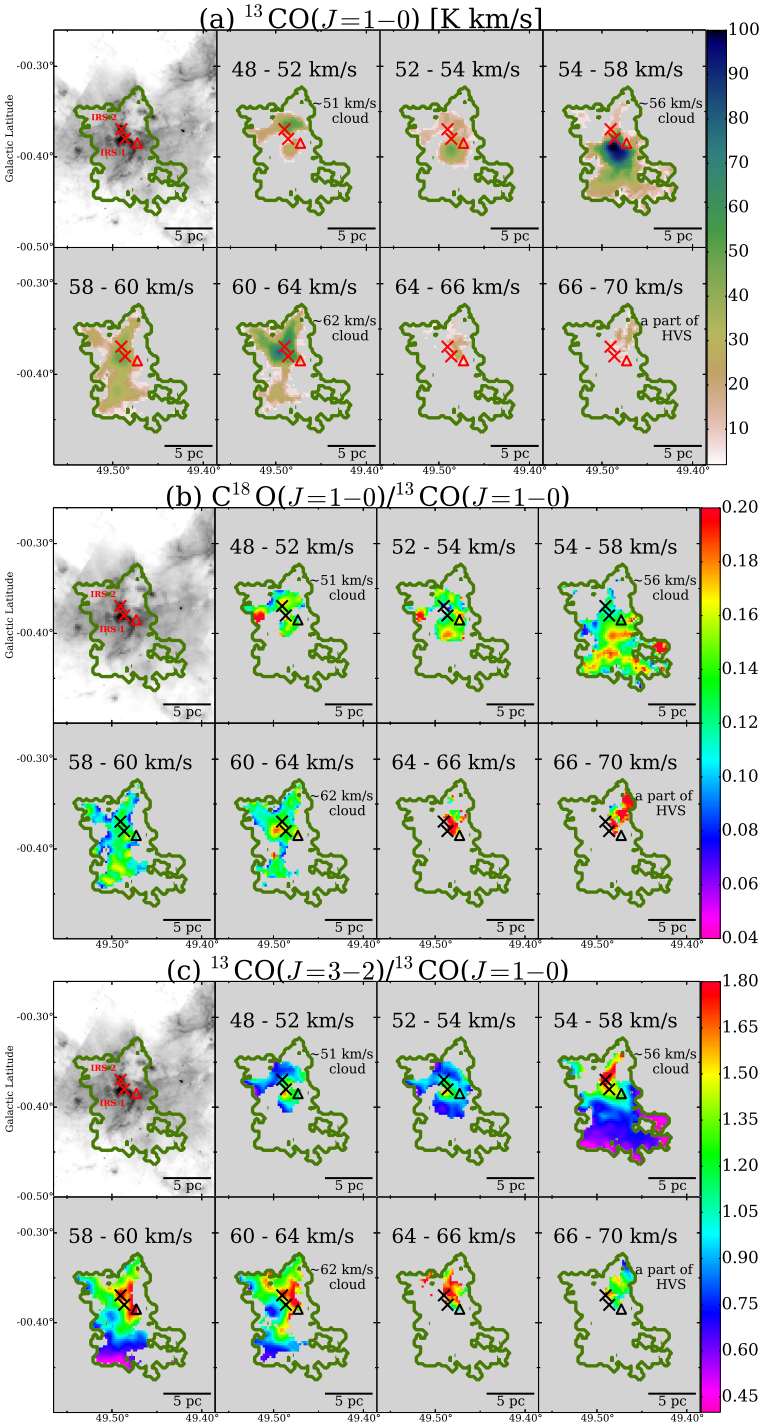

Figure 4.2: (a) The ^{13}CO ($J = 1 - 0$) integrated intensity of PC 2-1. The values printed in the top of each panel denote the velocity range. (b) The integrated intensity ratio of C^{18}O ($J = 1-0$)/^{13}CO ($J = 1 - 0$). (c) The integrated intensity ratio of ^{13}CO ($J = 3 - 2$)/^{13}CO ($J = 1 - 0$). The top left panels shows the intensity of 8 μm. The triangle represent compact H II region c$_1$ (e.g., Mehringer 1994). These maps are convoluted to 2 times resolutions.

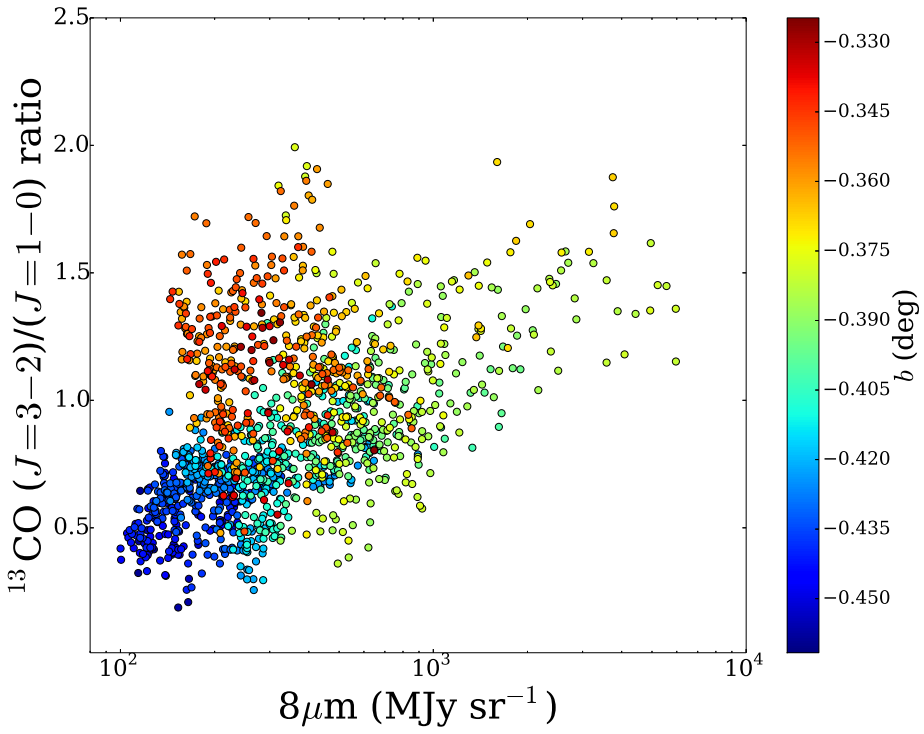

Figure 4.3: The 8 μm intensity versus R_{3210} for each pixel in the PC 2-1. The color of the plot indicates the difference of b (Galactic Latitude).

4.1.2 Collision and the break of HVS

Next we discuss break 1 (left side of PC 2-1). Okumura et al. (2001) suggest that break 1 was formed by collision between HVS (68 km s $^{-1}$) and 62 (60) km s $^{-1}$ cloud. We found that there is a component (PC 2-9) with intermediate velocity of these clouds at the position of break 1 (Figure 3.17 and Figure 4.4). The mass of PC 2-9 is $\sim 6 \times 10^3 M_\odot$. Black contours in Figure 4.4 shows 21 cm continuum intensity, and the age of the H II region distributed at the upper side of PC 2-9 is estimated to be $\sim$ 2 Myr (Okumura et al. 2000). PC 2-9 is located where the radio continuum intensity is weak. This means that, it can be expected that the molecular gas of PC 2-9 has remained while the molecular gas near the massive stars has already dissipated (or PC 2-9 may have been swept by the expansion of the II region).

We calculate the collision time scale. The width of break 1 on the $l-b$ plane is roughly $15-20$ pc, and the difference in radial velocity is $\sim$ 6 km s $^{-1}$. The collision time scale is calculated as 15–20 pc/(6 km s^{-1} $\times \sqrt{2}$) $\simeq$ 1.8 – 2.4 Myr. This value is consistent with the age of the surrounding H II region. Therefore, there is no contradiction in the scenario that break 1 was formed by cloud-cloud collision between HVS (68 km s $^{-1}$) and 62 (60) km s $^{-1}$ cloud.

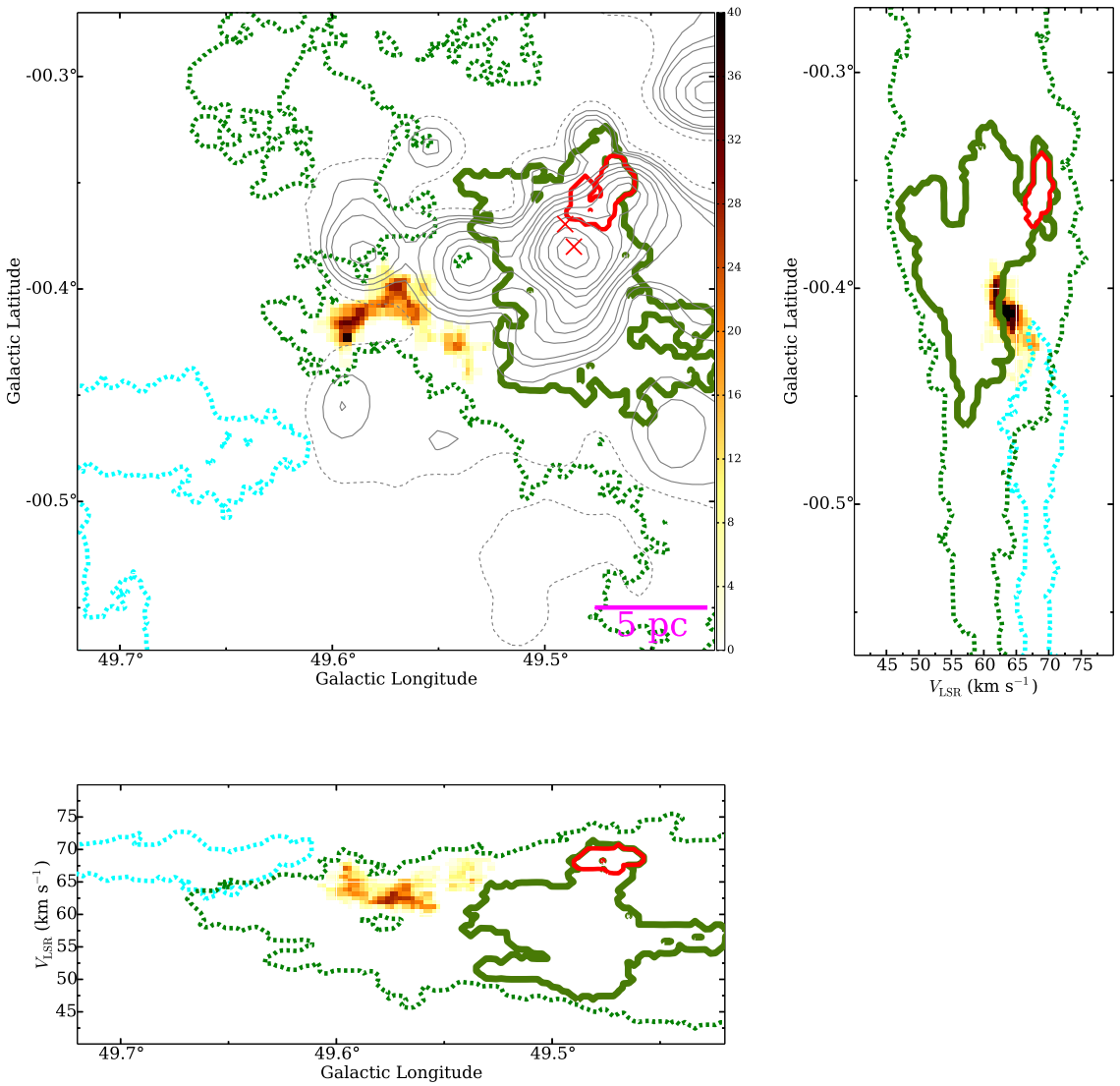

Figure 4.4: The map of around break 1. The colorscale shows PC 2-9. Cyan and green dotted lines shows PC 1 and PC 2, respectively. Green solid line show PC 2-1 and red solid line show HVS component (branch) in PC 2-1. Black contours shows the 21 cm continuum intensity and the contour levels are [25 (broken lines), 50, 75, 100, 200, 300, 400, 600, 800, 1000, 1500, 2000 K].

4.1.3 Massive star formation in the future at PC 2-1

Next we discuss the future massive star formation in PC 2-1. First, the grayscale in Figure 4.6 (top) shows the integrated intensity of ^{13}CO ($J = 1 - 0$) of all data (integrated range is 65 - 75 km s^{-1}) and contours show the integrated intensity of ^{13}CO ($J = 1 - 0$) of PC 2-1 (all velocity range). The upper half of the PC 2-1 overlaps with the HVS. The colorscale in Figure 4.6 (bottom) shows *Spitzer* 8 μm intensities and the contours show the integrated intensity of ^{13}CO ($J = 1 - 0$) of all data (65 – 75 km s^{-1}). The 8 μm intensity is weak in the strong part of ^{13}CO ($J = 1 - 0$), where PC 2-1 overlaps with HVS. Since HVS is located in the front side on the line-of-sight, it is highly probable that the radiation of 8 μm has been extincted. On the other hand, Figure 4.2 (b) and Figure 4.7 shows the map of R_{1813} in PC 2-1. Generally, R_{1813} can be used as a tracer of dense gas. Although R_{1312} is also used as a tracer of dense gas, R_{1813} is more suitable because ^{12}CO ($J = 1 - 0$) is optically thick (it may be causing self-absorption) in this region. From Figure 4.2 (b) and Figure 4.7, we found that R_{1813} is high at the velocities between 62 km s^{-1} cloud and HVS (68 km s^{-1}) at the upper part of the PC 2-1. It is likely that the gas has been compressed and become denser due to the collision between these clouds.

From Figure 3.16, we know that there are multiple clouds (51, 56, 62 km s^{-1}) on the line-of-sight at this site. This means that the HVS component in the PC 2-1 is currently colliding with other components, or will collide in the future. In other words, massive star formation due to cloud-cloud collision in this region is expected to continue.

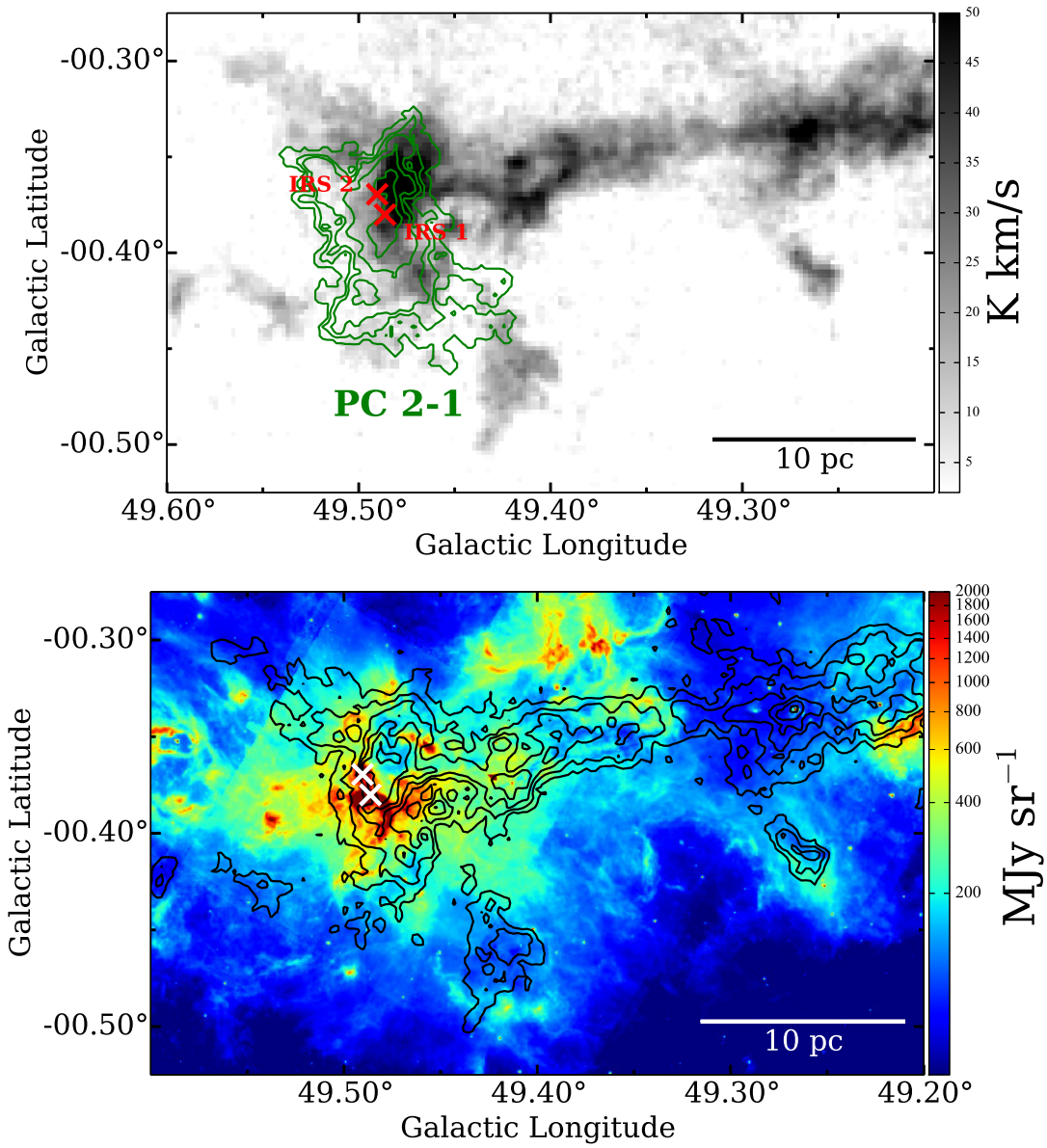

Figure 4.5: (top figure) The grayscale shows the integrated intensity of ^{13}CO ($J = 1 - 0$) of $65 - 75$ km s $^{-1}$ (HVS). The contours shows the integrated intensity of ^{13}CO ($J = 1 - 0$) of all velocity range. The contour levels are [2.1, 21, 42, 84, 168 K]. (bottom figure) The color shows *Spitzer* IRAC 8 μm intensities. The contours shows the integrated intensity of ^{13}CO ($J = 1 - 0$) of $65 - 75$ km s $^{-1}$ (HVS). The contour levels are [10, 20, 30, 40, 50, 60 K km s^{-1}].

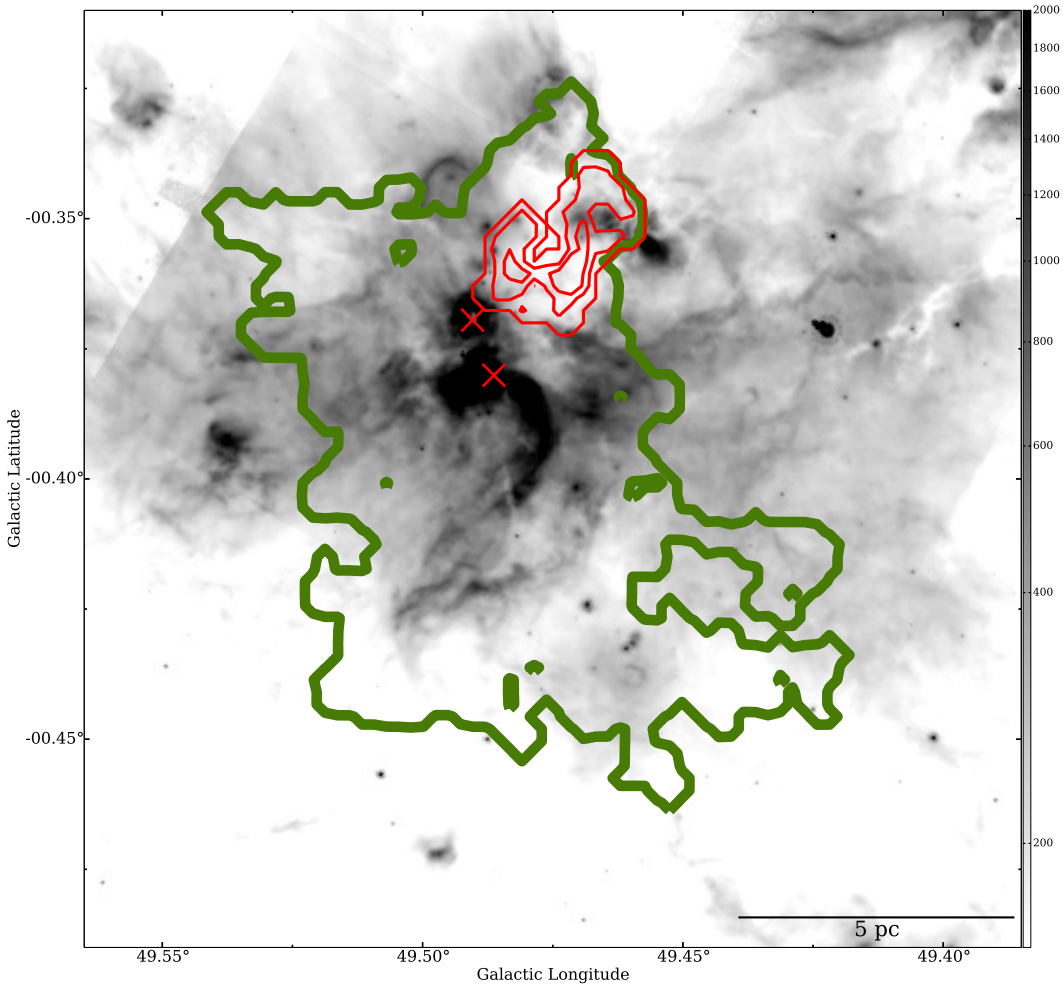

Figure 4.6: The colorscale show *Spitzer* 8 μm intensity. Green and red line shows PC 2-1 and HVS component in PC 2-1, respectively. The crosses represents IRS 1 (upper left) and IRS 2 (lower right), respectively.

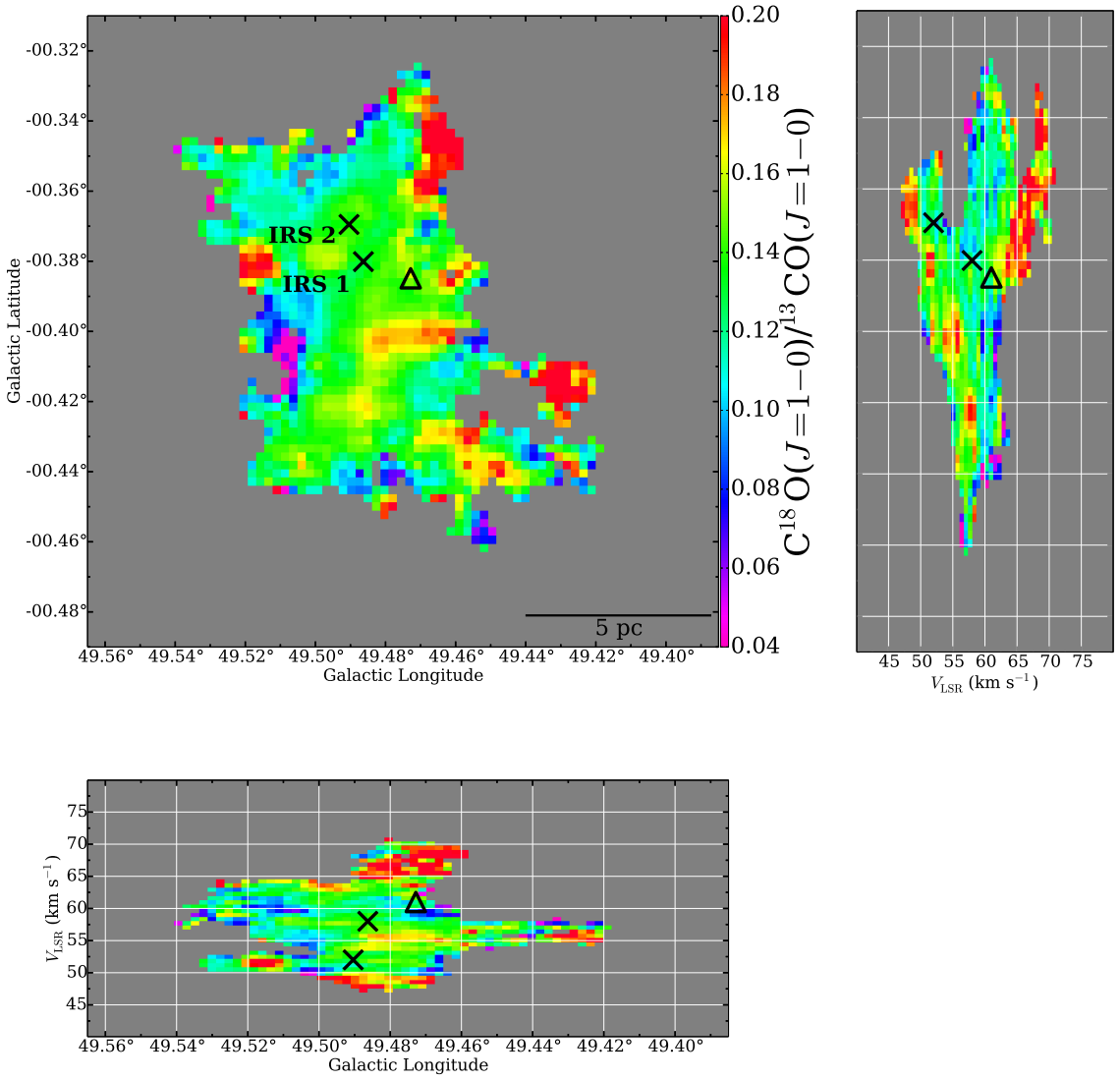

Figure 4.7: The intensity ratio $C^{18}O$ $(J = 1 - 0)/^{13}CO$ $(J = 1 - 0)$ of the integrated intensity of $l - b$ map, $l - v$ map and $v - b$ map of PC 2-1. The triangle represent compact H II region c_1 (e.g., Mehringer 1994).

4.1.4 The velocity structure along HVS

In section 4.1.1 – 4.1.3, cloud-cloud collisions at the center of W51 were discussed. Since HVS has a higher radial velocities than the other molecular clouds in W51, HVS may also cause CCC in other places. We will investigate the velocity structure of W51GMC along HVS.

Figure 4.8 shows the integrated intensity map and the P–V diagrams along the High Velocity Stream (HVS, 68 kms^{-1} cloud). We can see that there are two breaks, that is break1 and break2, in Figure 4.8 (a). The red crosses represent compact radio continuum sources ($\sim$ H II region) listed in Koo (1997) that are roughly located along HVS. Figure 4.8 (b), (c) and (d) are the P–V diagrams of ^{12}CO ($J = 1-0$), ^{13}CO ($J = 1-0$) and C^{18}O ($J = 1-0$) along the red dashed line in Figure 4.8 (a), respectively. In Figure 4.8 (b) and (c), we can see an arc structure at OFFSET= $1200 - 2000$ (arcsec), $v = 64 - 72$ (km s^{-1}). Moon & Park (1998) suggested that the CO ring structure were produced by stellar winds from nearby O-type stars.

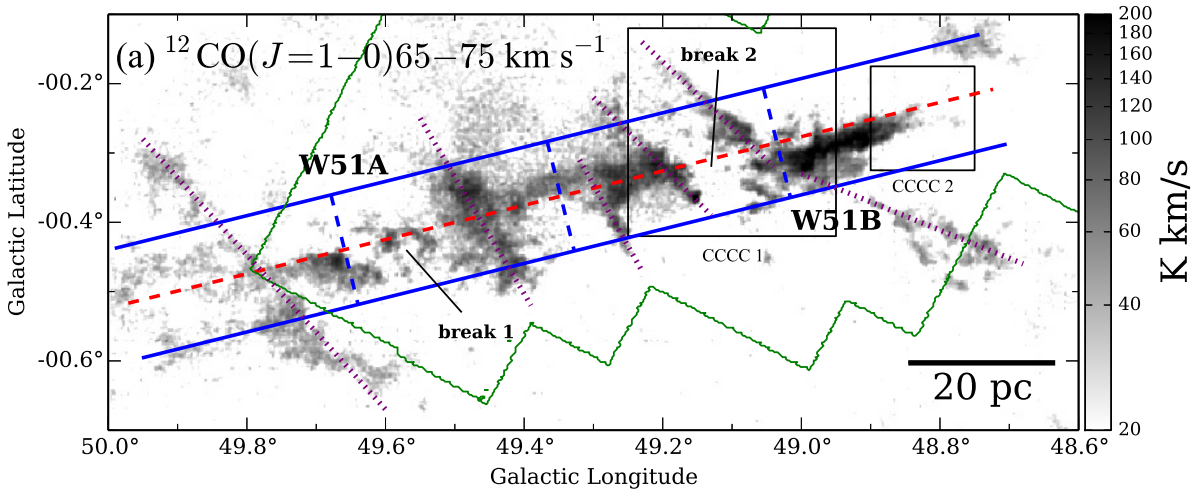

Figure 4.8: (a): Integrated intensity of ^{13}CO ($J = 1 - 0$) (65 – 75 km s^{-1}). The red dashed line and blue lines indicate the range of P–V diagram. The green line indicates the area of *JCMT* data.

Meanwhile, we found the several features crossing HVS (the purple dot line in Figure 4.8 (a)). Its origin and the three-dimensional structures are unclear. We will carry out the follow up observations by other tracers such as SiO molecule emission lines.

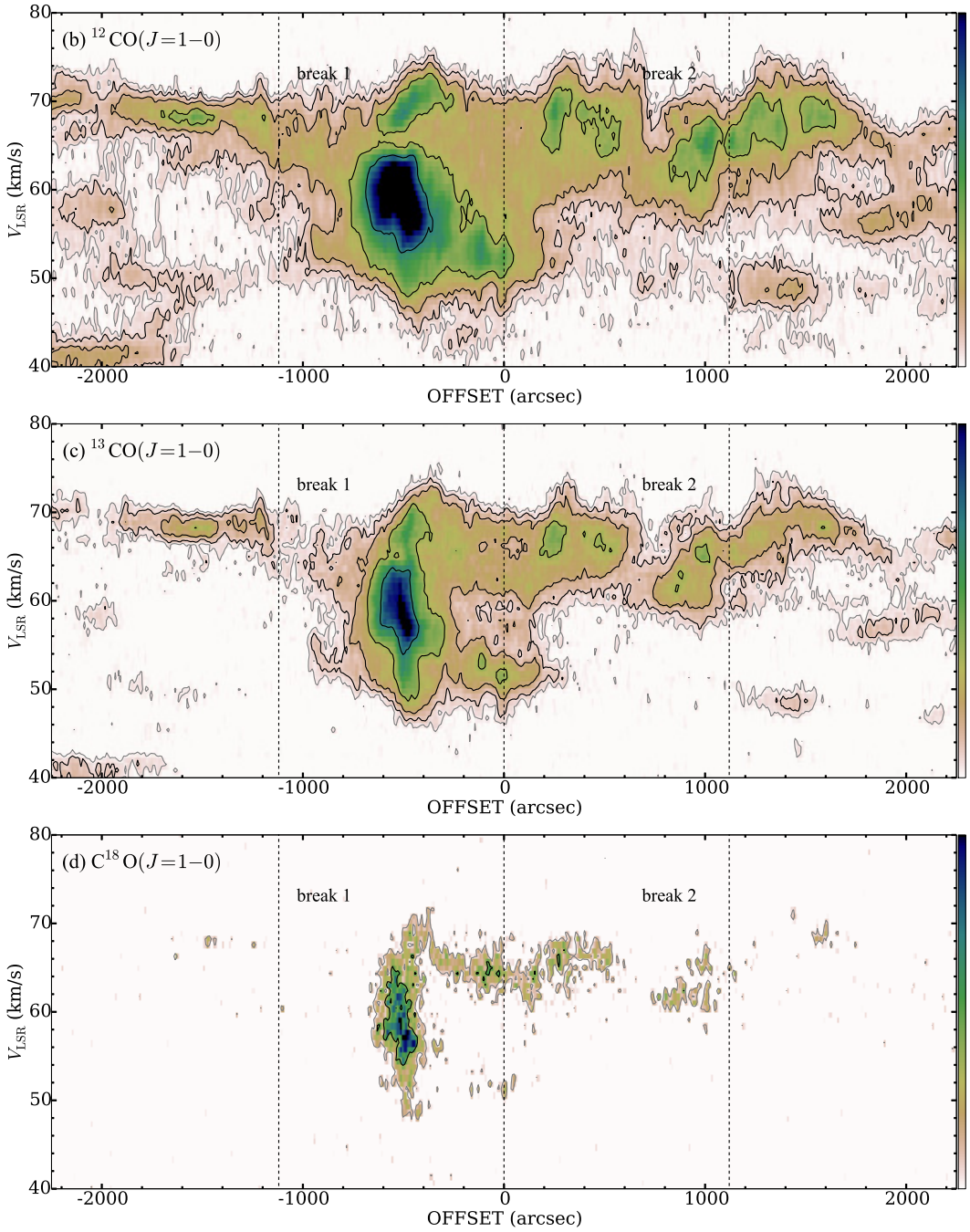

Figure 4.8: (b): P–V diagram of ^{12}CO ($J = 1 - 0$) along HVS (averaged intensity). (c): P–V diagram of ^{13}CO ($J = 1 - 0$) along HVS. (d): P–V diagram of C^{18}O ($J = 1 - 0$) along HVS. The Contour levels are $[0.9 \times 1, 0.9 \times 2, 0.9 \times 4, 0.9 \times 8, 0.9 \times 16$ K], $[0.3 \times 1, 0.3 \times 2, 0.3 \times 4, 0.3 \times 8, 0.3 \times 16$ K], and $[0.3 \times 1, 0.3 \times 2, 0.3 \times 4, 0.3 \times 8, 0.3 \times 16$ K], respectively.

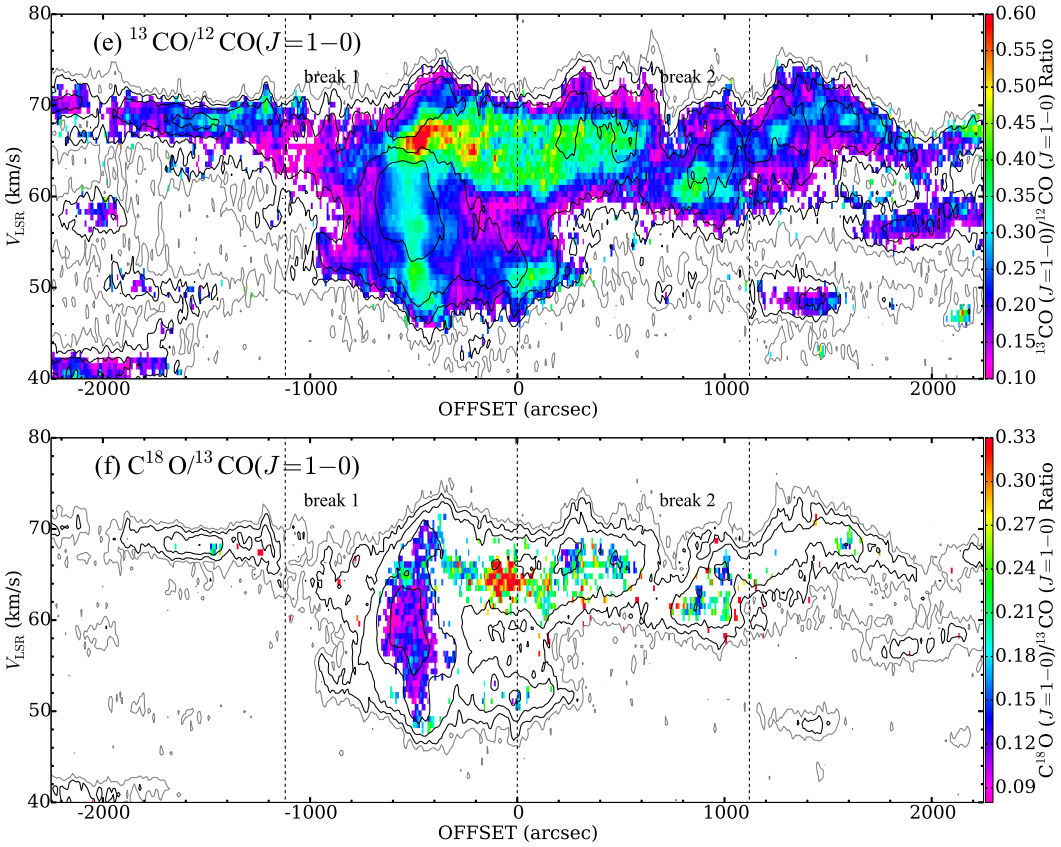

Figure 4.8: [
P – V diagram of HVS (2)](e): P – V diagram of ^{12}CO ($J = 1 - 0$) (contour) and ^{13}CO ($J = 1 - 0$)/^{12}CO ($J = 1 - 0$) intensity ratio (color) along HVS. (f): P – V diagram of ^{13}CO ($J = 1 - 0$) (contour) and C^{18}O ($J = 1 - 0$)/^{13}CO ($J = 1 - 0$) intensity ratio (color) along HVS. The Contour levels are the same as Figure 4.8. (Continue)

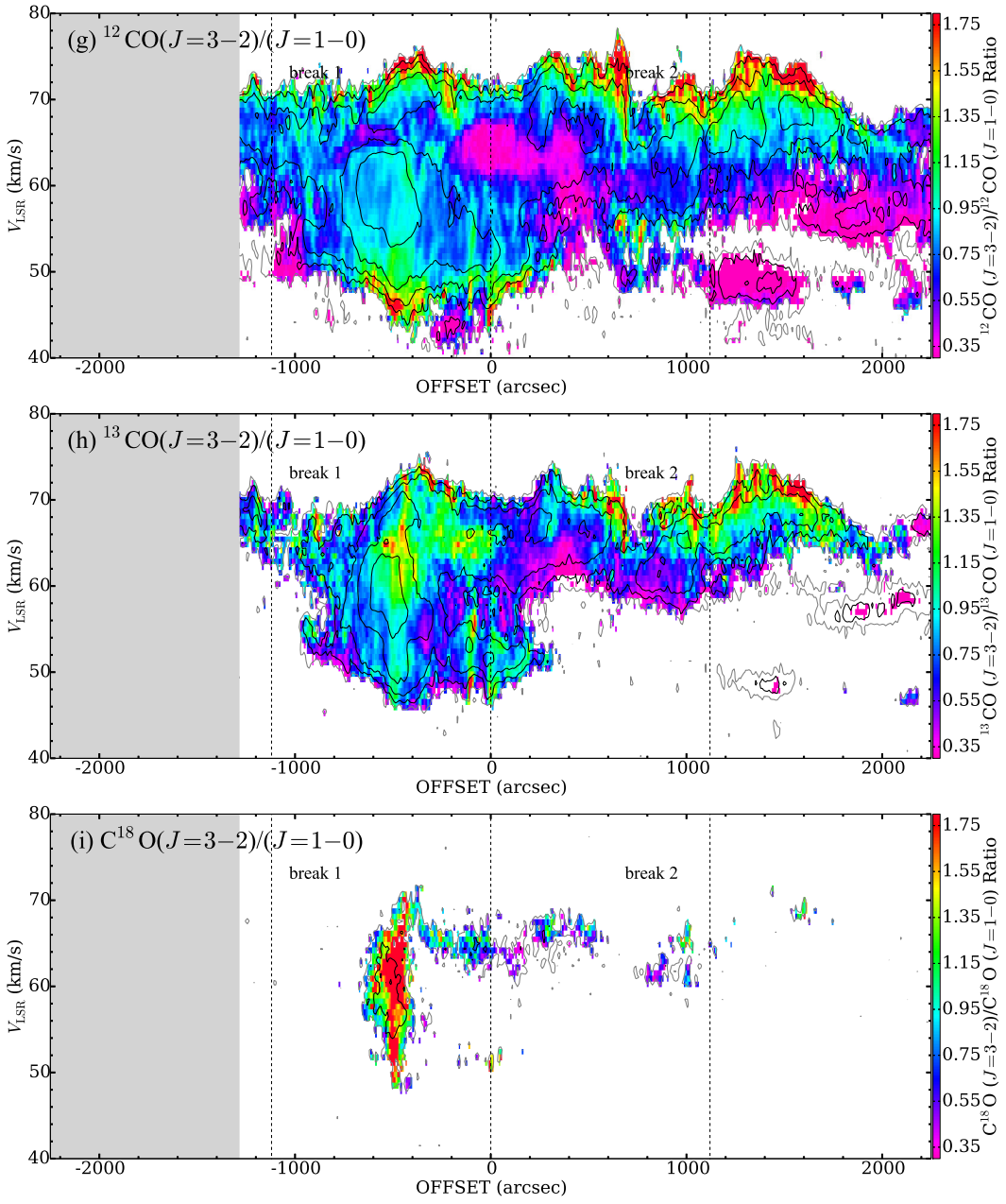

Figure 4.8: Continued. (g): P–V diagram of ^{12}CO ($J = 1-0$) (contour) and ^{12}CO ($J = 3-2$)/^{12}CO ($J = 1-0$) intensity ratio (color) along HVS. (h): P–V diagram of ^{13}CO ($J = 1-0$) (contour) and ^{13}CO ($J = 3-2$)/^{13}CO ($J = 1-0$) intensity ratio (color) along HVS. (i): P–V diagram of C^{18}O ($J = 1-0$) (contour) and C^{18}O ($J = 3-2$)/C^{18}O ($J = 1-0$) intensity ratio (color) along HVS. The intensity ratios are calculated in $> 3\sigma$ pixels. The Contour levels are the same as Figure 4.8.

Figure 4.8 (e) shows ^{12}CO ($J = 1-0$) (contour) and ^{13}O ($J = 1-0$)/^{12}CO ($J = 1-0$) intensity ratio ($\equiv R_{1312}$) (color). Although the velocity structure is complicated, there is an overall trend that R_{1312} is high at the middle of the velocity. It is also high over a wide velocity range, especially at OFFSET = -400 – -600. This area is the place of PC 2-1. Figure 4.8 (f) shows ^{13}CO ($J = 1-0$) (contour) and C^{18}O ($J = 1-0$)/^{13}CO ($J = 1-0$) intensity ratio ($\equiv R_{1813}$) (color). R_{1813} is very high in the place of OFFSET = -100 arcsec, V = 65 km s^{-1}, although R_{1312} is not high in Figure 4.8 (e).

Figure 4.8 (g) shows ^{12}CO ($J = 1-0$) (contour) and ^{12}CO ($J = 3-2$)/^{12}CO ($J = 1-0$) intensity ratio (color). In W51A and near break 2, the ratio is obviously high at the edge of the velocity ($>$ 1.4). In W51B, the ratio is high only at the upper edge of the velocity. The ratio is low in the position where R_{1813} is very high (OFFSET = -100 arcsec, V = 65 km s^{-1}). Figure 4.8 (h) shows ^{13}CO ($J = 1-0$) (contour) and ^{13}CO ($J = 3-2$)/^{13}CO ($J = 1-0$) intensity ratio (color). The ratio is high at OFFSET = -500 arcsec, V = 64 km s^{-1}, while ^{12}CO ($J = 3-2$)/^{12}CO ($J = 1-0$) intensity ratio is low. In W51B, the ratio is also high only at the upper edge of the velocity. Figure 4.8 (i) shows C^{18}O ($J = 1-0$) (contour) and C^{18}O ($J = 3-2$)/C^{18}O ($J = 1-0$) intensity ratio (color). This ratio is very high at PC 2-1 in W51A . The differences between Figure 4.8 (g), (h), and (i) are considered to be due to the difference between optical depth of ^{12}CO ($J = 1-0$), ^{13}CO ($J = 1-0$) and C^{18}O ($J = 1-0$).

4.1.5 Other candidates of collision of internal clouds

We found other candidates of collision of internal clouds (Cloud-Cloud Collision Candidates 1 (CCCC 1) and CCCC 2 in Figure 4.8 (a)) in W51. The common features to the two CCCCs are (1) the blue-shifted and the red-shifted velocity component are nesting distributions, (2) the P–V diagram has a bridging feature, (3) Young Stellar Object (YSO) has been identified at the middle between the blue-shifted and the red-shifted velocity component.

CCCC 1 is located in break 2 and near G49.17-0.21 discussed in Kang et al. (2010). Figure 4.9 shows the integrated intensity map of three velocity ranges of ^{13}CO ($J = 1 - 0$) and $l - v$ diagram of ^{13}CO ($J = 1 - 0$). Many YSO candidates are located along the mid-velocity component (green) of the gas. The difference of the radial velocity is $\sim$ 6km s^{-1} and masses are 1.1×10^4 $M_\odot$ (blue) and 1.0×10^4 $M_\odot$ (red) respectively. This mid-velocity component appears in 8 μm intensity map as a dark feature. It is possible that break 2 was result of this CCC, just like break 1 discussed by Okumura et al. (2001).

CCCC 2 was found at the western part of HVS. Figure 4.10 shows the integrated intensity map of two velocity ranges of ^{13}CO ($J = 1 - 0$) and $l - v$ diagram of ^{13}CO ($J = 1 - 0$). The nesting distribution is clearly seen, and there is a YSO candidate ($4.8\ ^{+1.0}_{-0.9}$ $M_\odot$) at the boundary between blue and red component. The difference of the radial velocity is $\sim$ 3km s^{-1} and masses are 0.7×10^3 $M_\odot$ (blue) and 1.6×10^3 $M_\odot$ (red) respectively. We speculate that the elapsed time of CCC is not so long, since these clouds are not associated with H II regions.

In addition to these, the region of OFFSET = -100 arcsec, V = 65 km in Figure 4.8 (f) may also be a CCC site. Figure 4.11 shows the spectrums of ^{12}CO ($J = 1 - 0$), ^{13}CO ($J = 1 - 0$) and C^{18}O ($J = 1 - 0$) in this position. Clearly the peak velocity of C^{18}O ($J = 1 - 0$) does not correspond to that of ^{12}CO ($J = 1 - 0$). It is considered that this region is very dense, and ^{12}CO ($J = 1 - 0$) emission line is self-absorbed. CCCs may compress the interface of two colliding clouds and trigger star formation. Because the interface will be heated and the other side (fore-side) remain cold, self-absorption of CO emission lines are observed at the CCC interface. Therefore, similar to G49.17-0.21 discussed in Kang et al. (2010) there is a possibility that this region is also a CCC site. However, no definitive evidence has been found yet.

We found that HVS causes many CCCs not only in W51A but also in W51B. The radial velocity of HVS ($\sim$ 68 km s^{-1}) is exceeding the radial velocity explained by Galactic rotation in W51 ($\sim$ 60 km s^{-1}). This high radial velocity is believed to be the streaming motion of the gas (e.g., Burton & Shane 1970). We consider that the velocity difference of molecular cloud is important for active star formation such as W51. However, in order to efficiently induce a large number of CCC, not only one way of the streaming motion but also other molecular cloud acceleration mechanisms are necessary.

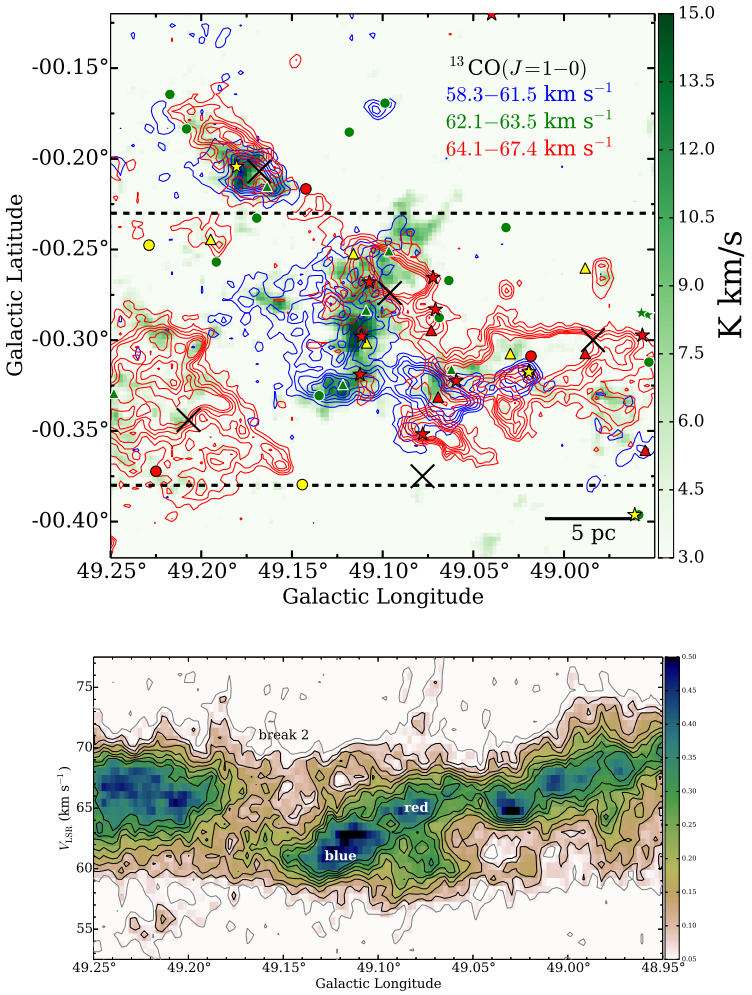

Figure 4.9: (Top figure) The green colorscale blue and red contours shows the ^{13}CO ($J = 1 - 0$) integrated intensity at the around CCCC 1. The values printed in the top left corner denote the respective velocity ranges. YSO candidates (Kang et al. 2009) are represented in circle for ≤ 5 $M_{\odot}$, triangle for $5 - 8$ $M_{\odot}$ and star for ≥ 8 $M_{\odot}$ (red for Stage 0/I, yellow for Stage II, and green for ambiguous sources). Black crosses represent the radio continuum sources listed by Koo & Moon 1997. (Bottom figure) The colorscale and contours shows the intensity of ^{13}CO ($J = 1 - 0$) in $l - v$ diagram. The b (Galactic Latitude) range of this $l - v$ diagram is indicated by black dotted line in the top figure.

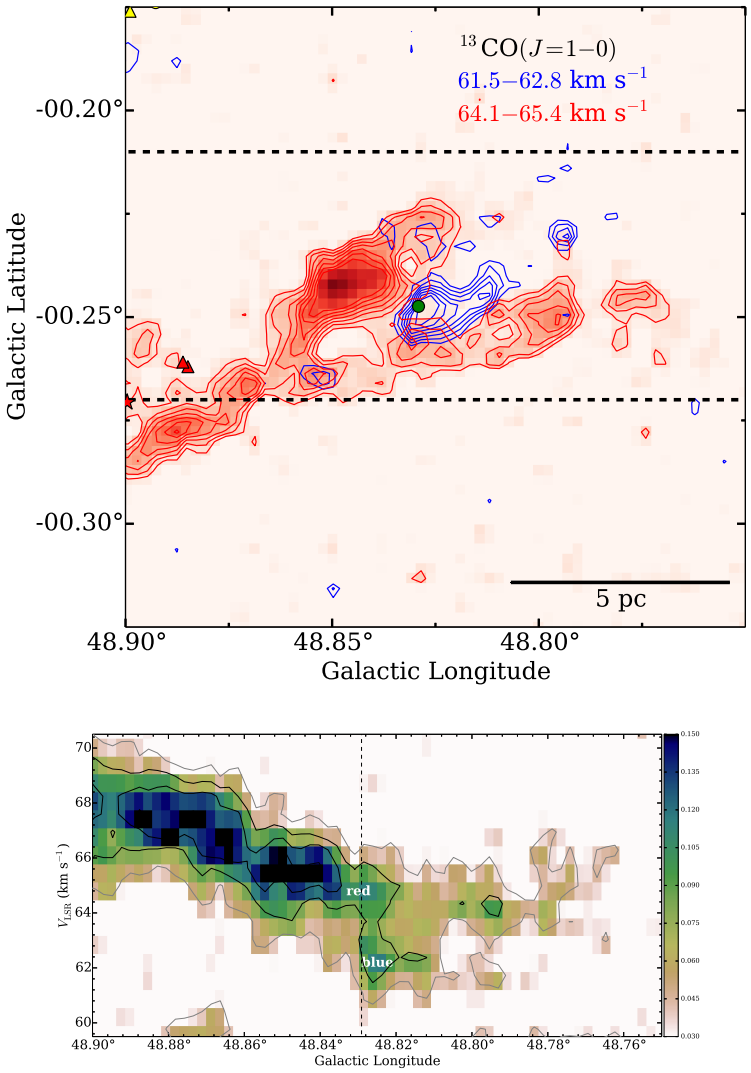

Figure 4.10: (Top figure) The red colorscale and blue contours shows the ^{13}CO ($J = 1-0$) integrated intensity at the around CCCC 2. The values printed in the top left corner denote the respective velocity ranges. YSO candidates (Kang et al. 2009) are represented in circle for $\leq 5\ M_{\odot}$, triangle for $5 - 8\ M_{\odot}$ and star for $\geq 8\ M_{\odot}$ (red for Stage 0/I, yellow for Stage II, and green for ambiguous sources). Black crosses represent the radio continuum sources listed by Koo & Moon 1997. (Bottom figure) The colorscale and contours shows the intensity of ^{13}CO ($J = 1 - 0$) in $l - v$ diagram. The b (Galactic Latitude) range of this $l - v$ diagram is indicated by black dotted line in the top figure. The black dotted line in the bottom figure indicates the position of the YSO candidate located in the center of the top figure.

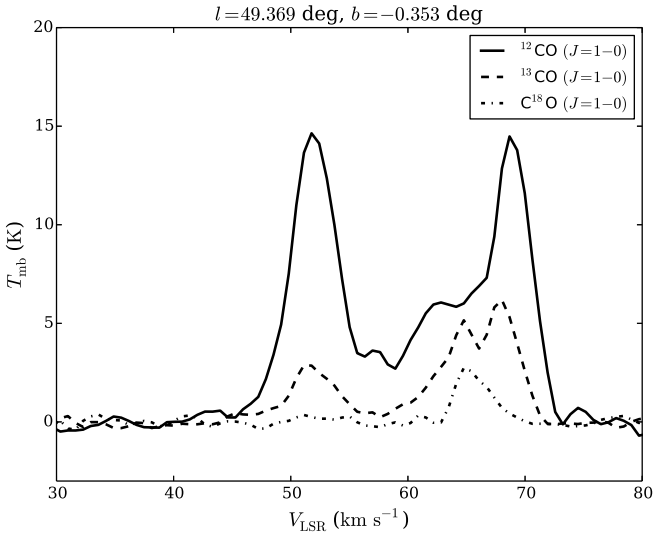

Figure 4.11: The spectra in $(l, b) = (49.369°, -0.353°)$. This data was taken from convoluted maps (convoluted to 2 times resolutions).

4.1.6 An arc structure in W51A

In W51A (PC 2), we found a straight structure extending from the upper left (~ 46 km s^{-1}, $-0.1°$) to the lower right (~ 61 km s^{-1}, $-0.6°$) in the $v - b$ map in Figure 4.12 (black dashed line). In the $l - b$ map in Figure 3.10, this structure is arc-shaped. The model describing this structure is, for example, part of the expanding shell.

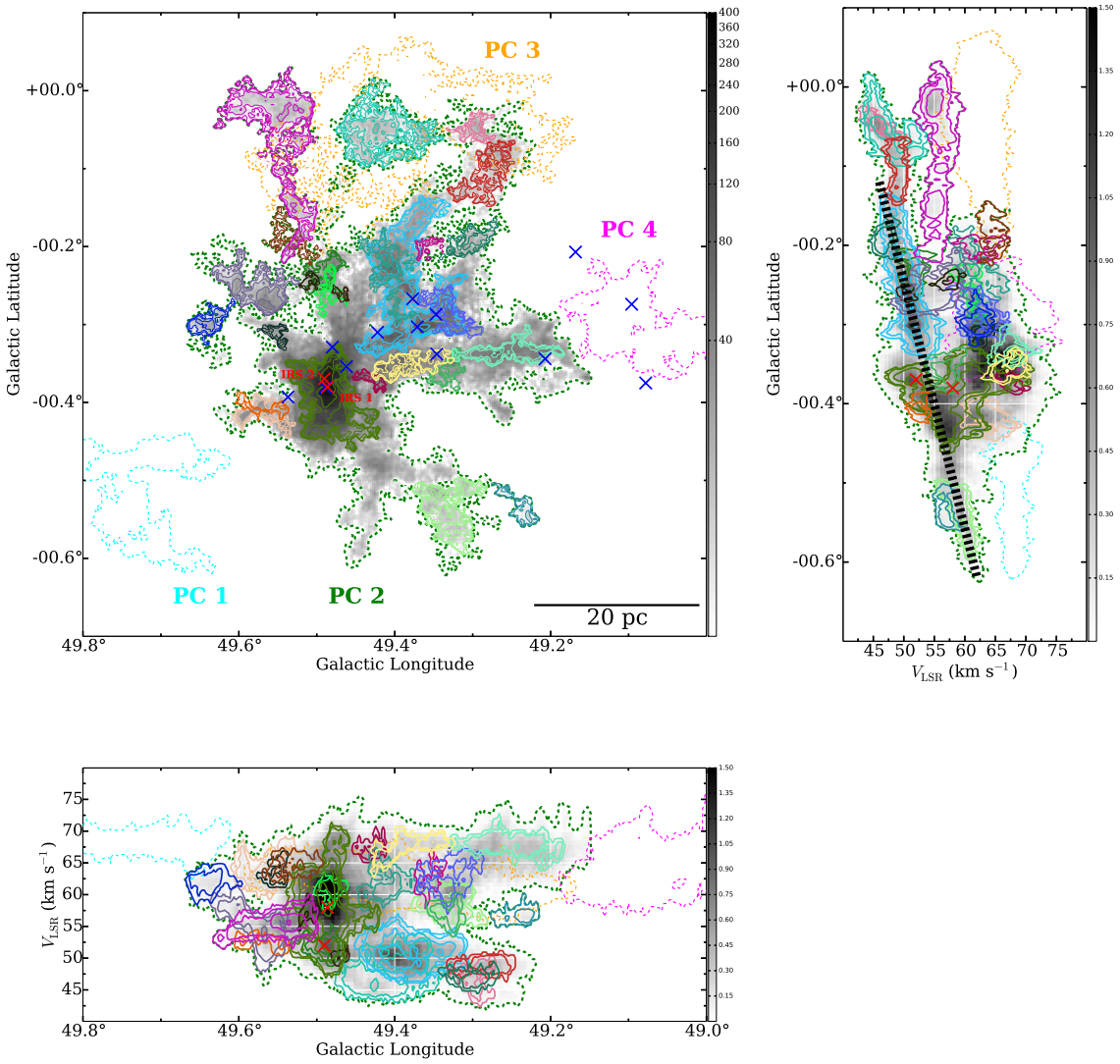

Figure 4.12: The ^{13}CO ($J = 1 - 0$) integrated intensity map, $l - v$ map and $v - b$ map of PC 1, PC 2, PC 3 and PC 4 (dashed lines) and extracted structures (solid lines). Grayscale shows the integrated intensities of ^{13}CO ($J = 1 - 0$).

The arc-shaped feature in the $l - b$ map appears to be along the edge of the *Fermi*-LAT photon

counts map of W51C above 60 MeV presented by Jogler et al. (2016). They found the hadronic explanation of this γ-ray spectrum to be the most convincing model. For example, assuming that the mass of the feature is $1.0 \times 10^5 M_\odot$, the kinetic energy required to accelerate 10 km s^{-1} is $\sim 1.0 \times 10^{50}$ erg. The kinetic energy per supernova explosion is typically $\sim 10^{51}$erg, therefore, we speculate that a supernova explosion formed the shell (arc feature with a radius of $\sim$ 30 pc). However, since the velocities of the molecular clouds are unclear (we can observe the radial velocities only), the uncertainty of this estimation is very large. Further analysis and discussion about PC 2 will be performed in the future.

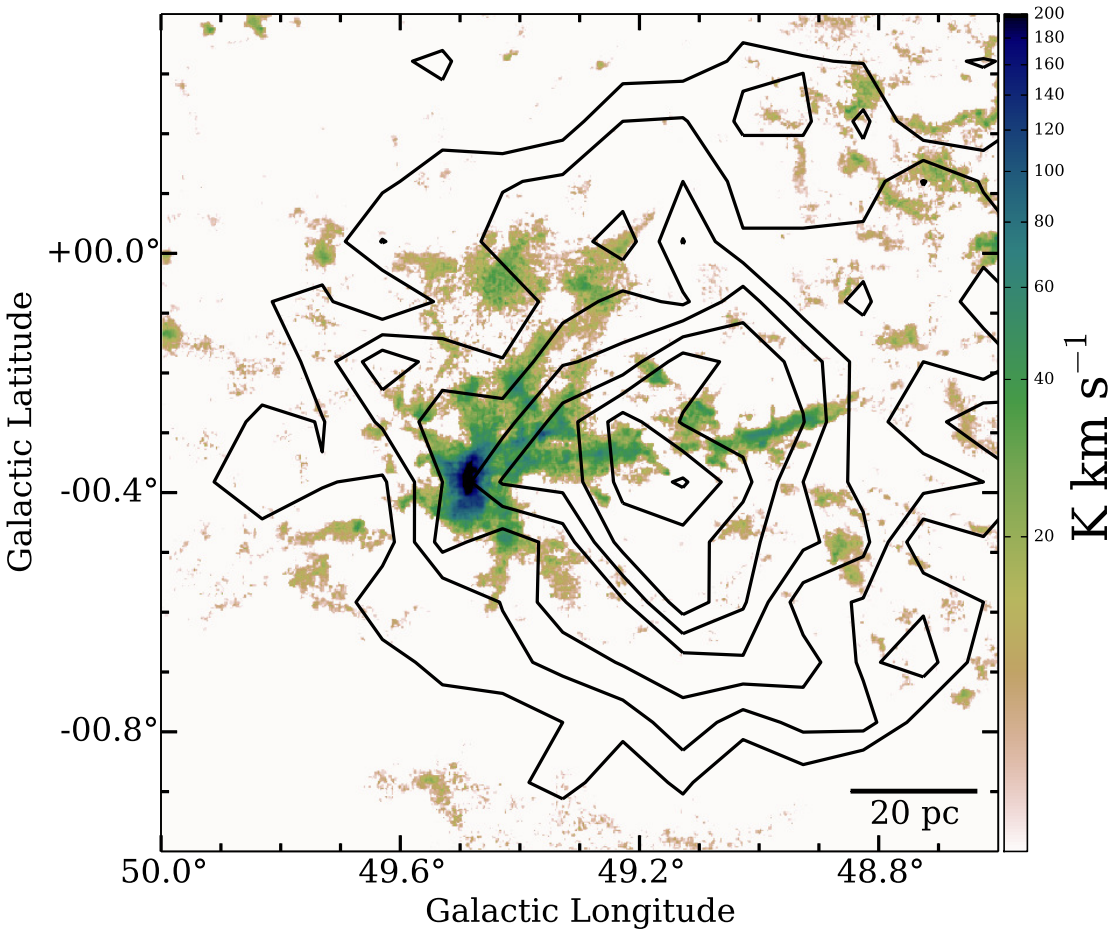

Figure 4.13: The colorscale shows the ^{13}CO ($J = 1-0$) integrated intensity of overall. The contours shows the *Fermi*-LAT photon counts map of W51C above 60 MeV presented by Jogler et al. (2016). The contour levels are [180, 200, 220, ..., 320].

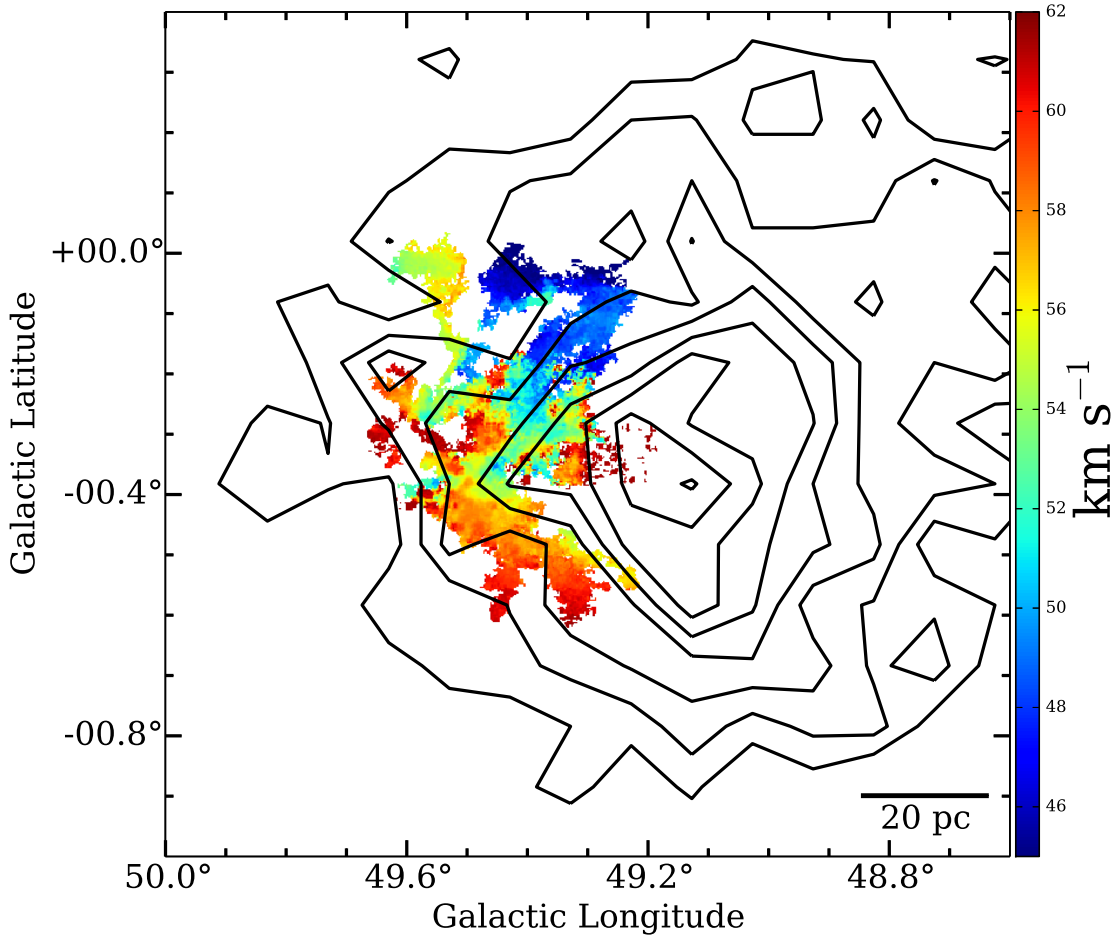

Figure 4.14: The colorscale shows the ^{13}CO ($J = 1 - 0$) moment 1 of PC 2. The velocity range is restricted to 45 - 62 km s^{-1}. The contours shows the *Fermi*-LAT photon counts map of W51C above 60 MeV presented by Jogler et al. (2016). The contour levels are [180, 200, 220, ..., 320].

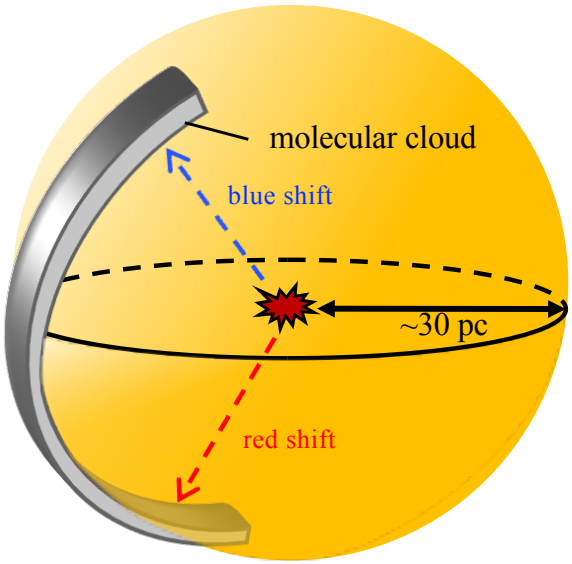

Figure 4.15: The schematic picture of the arc structure in PC 2.

4.2 Massive star formation in W51

In Chapter 3, in order to investigate the difference of the properties of each place in the GMC, we divided W51 GMC into several structures (PCs) and analyzed them. As a result, it was found that PC 2 and PC 4 have high fraction of massive YSO candidate ($\geq 8M_{\odot}$) and high averaged mass of YSO than others (Table 3.3) (Note that for PC 2, it is considered that the number of YSOs and the average mass are larger than the values in Table 3.3, because the *Spitzer* MIPS data is saturated at the center of PC 2.). As shown in Table 2, the averaged column density of PC 2 and PC 4 is high ($> 5 \times 10^{22}$ cm^{-2}). In addition, these PCs are also high in intensities of 8 μm and high in R_{3210} (Incidentally, PC 7 (G48.60+0.02) in Perseus arm also has the same tendencies.). These results are consistent with the scenario that large mass clouds produce massive stars and the radiation of these stars affect surrounding ISMs. However, the issue is, what is the most important for the formation of massive stars in GMC.

In 4.1.1, we concluded that the cloud-cloud collisions (CCCs) occurred and massive stars have been formed in PC 2-1 as proposed in the previous studies (e.g., Okumura et al. 2001). Three or more clouds may collide at the same time in this region. In addition, we also suggested that many other CCCs are occurring (4.1.4). Therefore, we consider that W51 GMC is forming massive stars actively because many CCCs are occuring simultaneously in GMC. Then, what is the main source of the relative velocity that induces CCC ?

In the case of W51, some CCCs are related to HVS. Because W51 is located at the tangential point of a spiral arm, a cloud with a high radial velocity related to streaming motion such as HVS was observed. Perhaps the clouds, that resemble HVS and induce many collisions, may exist universally in the Galaxy. If they exist, it will probably be discovered more frequently by ALMA (Atacama Large Millimeter/submillimeter Array) in nearby galaxies in the future. On the other hand, we have found the possibility that the supernova remnant (SNR) W51C is interacting with the molecular gas in W51A (4.1.6). Since the kinetic energy that a supernova explosion gives to the surrounding ISM is enormous, this should be attached great importance as a major source of the relative velocities.

Chapter 5

Summary

1. To reveal the relationship between a GMC and massive star formation, we carried out the mapping observation of ^{12}CO, ^{13}CO and C^{18}O ($J = 1 - 0$) emission lines toward W51 with high angular resolutions ($\sim 18''$) as a part of the legacy project Nobeyama Space Radio Observatory FOREST Ultra-wide Galactic plane survey In Nobeyama (FUGIN).

2. We detected W51 GMC from diffuse gas to dense gas, and analyzed the data by using the algorithm Dendrograms.

3. We found that molecular clouds with tendency to make YSOs with larger mass have the tendencies as follows. (1) The column density of hydrogen molecules is high and mass is large, (2) ^{13}CO ($J = 3 - 2$)/^{13}CO ($J = 1 - 0$) ratio is high, and (3) 8 μm intensity is high. This result is consistent with the scenario that molecular clouds with high column density of hydrogen molecules and large mass form massive stars, and its surroundings are heated by the radiation.

4. Then, we investigated the internal structure at the most complex molecular cloud in W51 (PC 2-1) where massive stars have been formed very actively. As a result, we found that massive star formation in this region can be explained by the scenario of Cloud-Cloud Collisions (CCCs) suggested in Okumura et al. (2001).

5. Apart from these CCCs, we found many CCC candidates in W51. It is probable that massive

star formation in W51 GMC is deeply related to CCCs (not single CCC) between its internal structures.

6. Furthermore, we also found that molecular clouds having an expanding shell-like structure centered on W51C (radius $\sim$ 30 pc) exist in W51A. This is a new result suggesting the possibility that molecular clouds have been interacted with supernova remnants (SNR) W51C, not only in W51B but also in W51A. Since the kinetic energy that a supernova explosion gives to the surrounding ISM is enormous, this should be attached great importance as a major source of the relative velocities that induce CCCs.

Appendix A

The channel map of other channel

Figure A.1 – A.6 show the channel maps other than presented in Chapter 3.

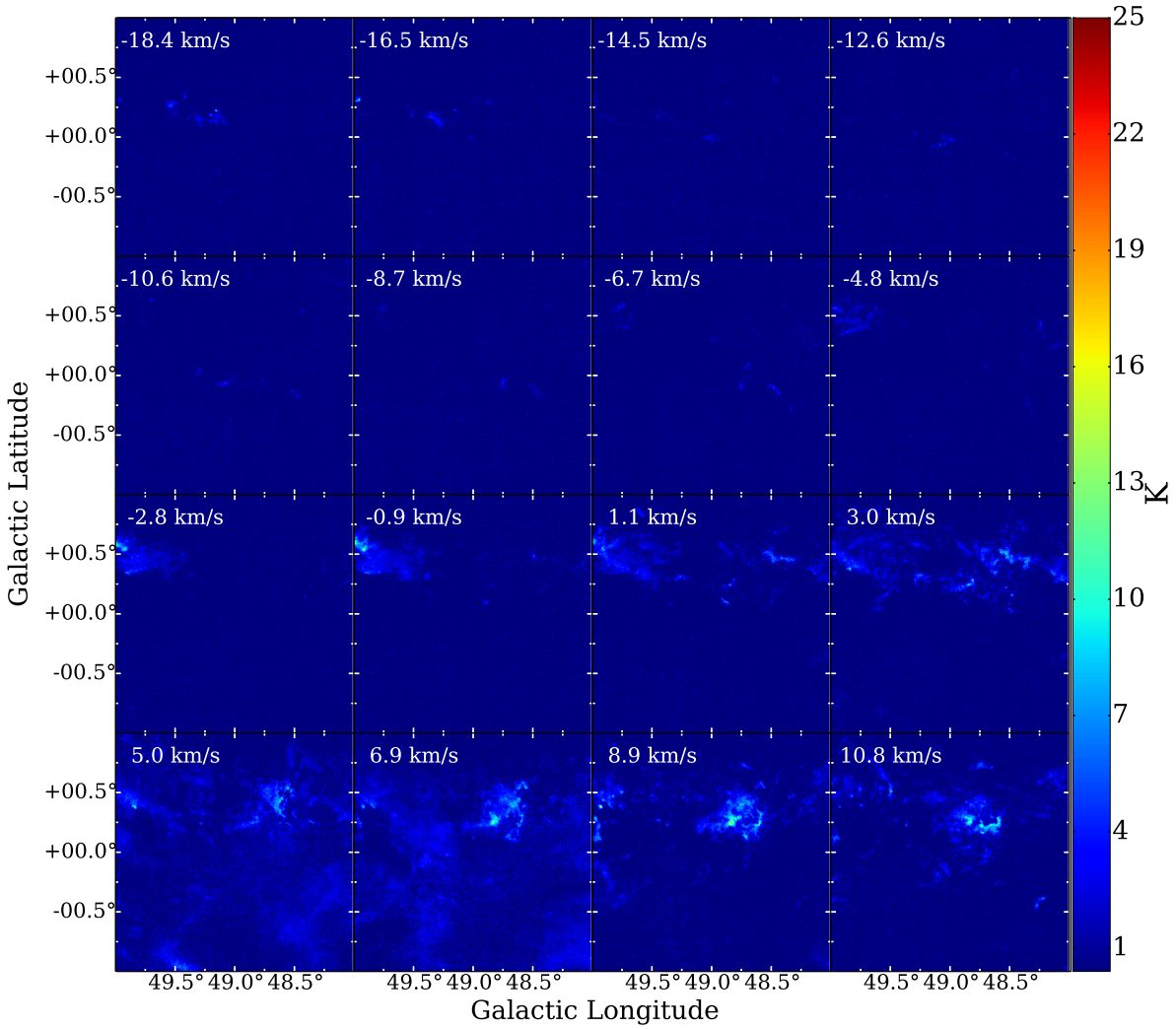

Figure A.1: The channel map of ^{12}CO ($J = 1 - 0$) intensity ($T_{\rm mb}$ scale). The velocity range is -18.4 – 10.8 km $^{-1}$ and the velocity spacings are 3 channels (1.95 km $^{-1}$). This map is spatially convoluted.

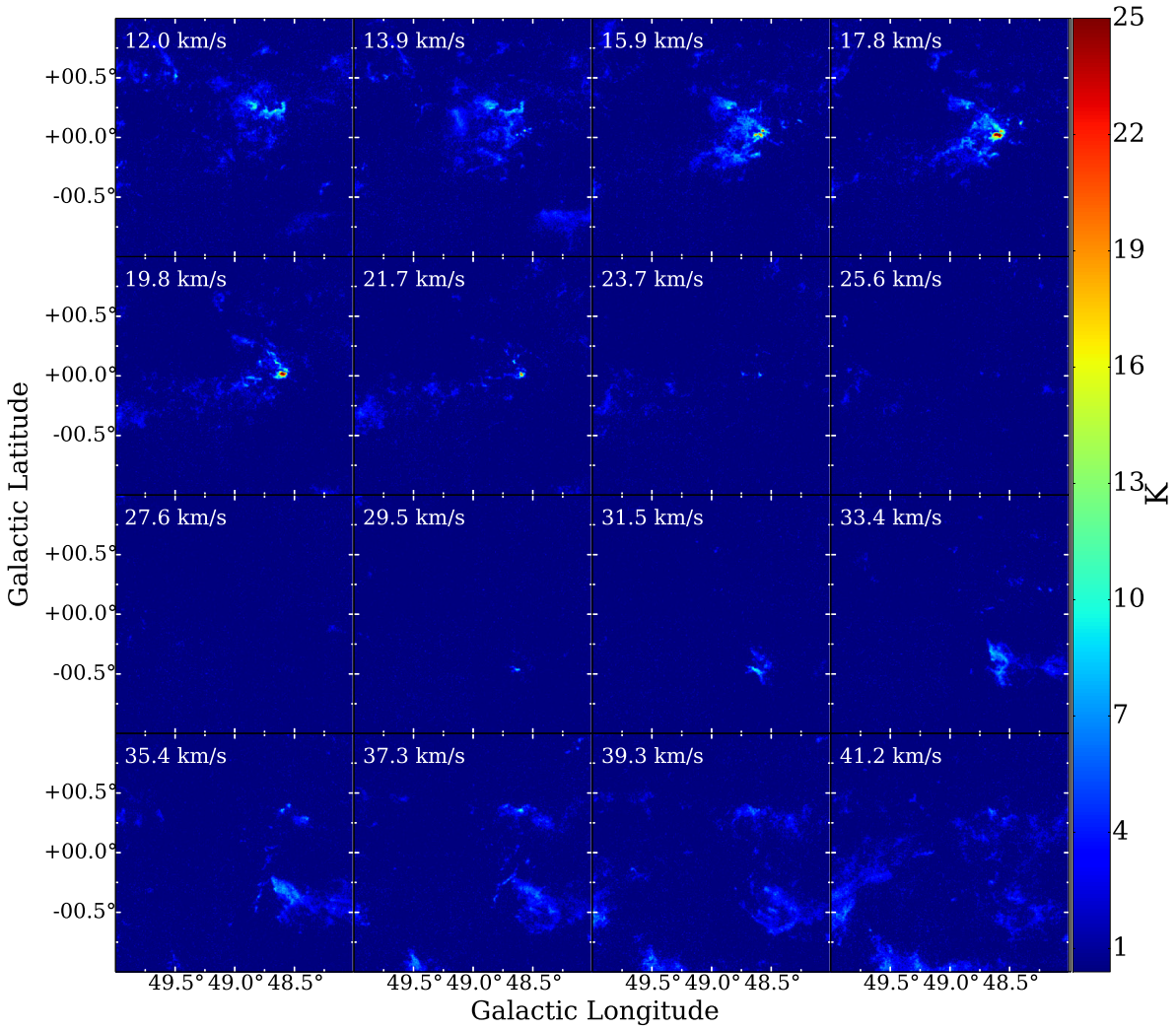

Figure A.2: The channel map of ^{12}CO ($J = 1-0$) intensity ($T_{\rm mb}$ scale). The velocity range is 12.8 – 42.0 km $^{-1}$ and the velocity spacings are 3 channels (1.95 km $^{-1}$). This map is spatially convoluted.

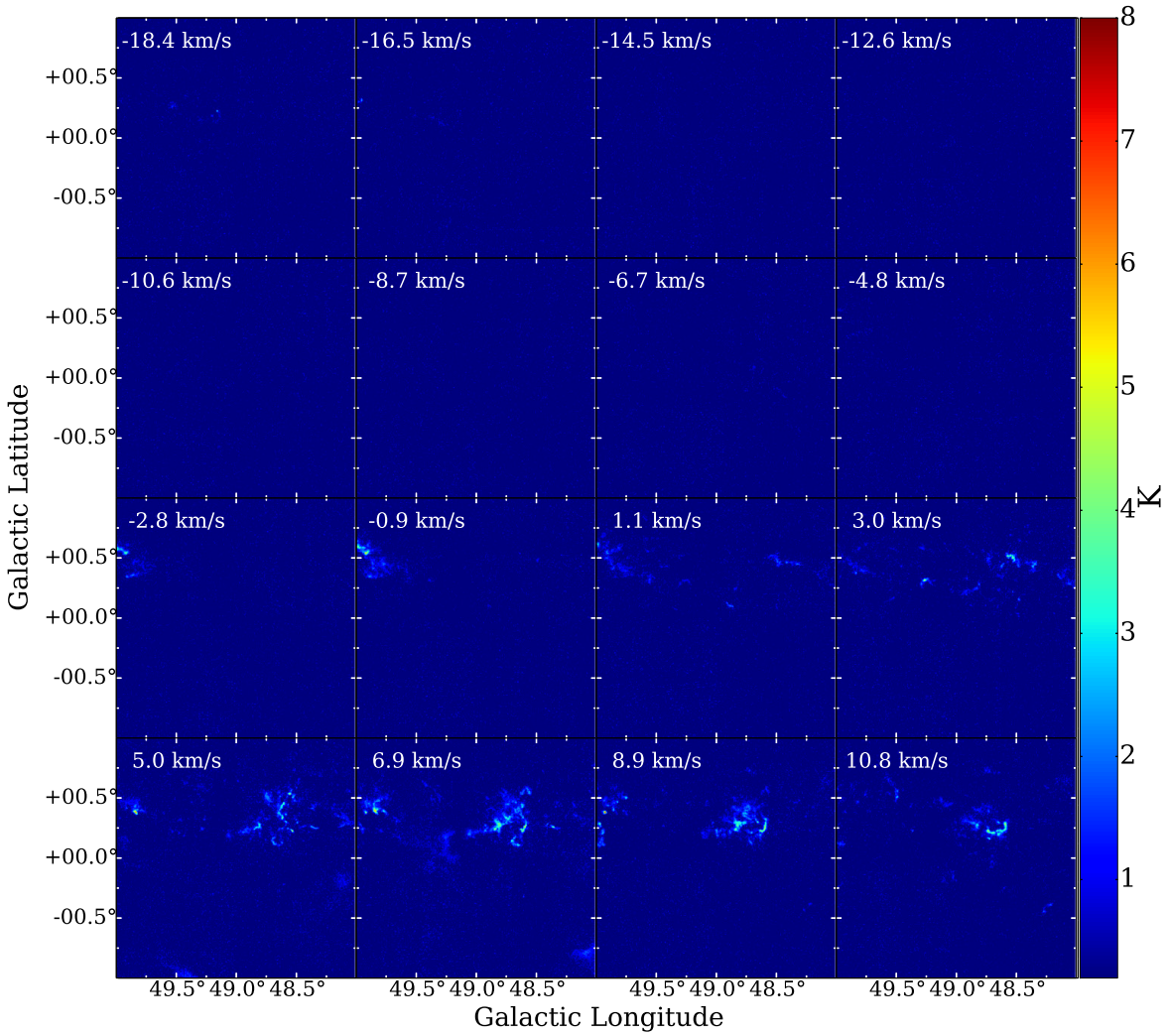

Figure A.3: The channel map of ^{13}CO ($J = 1 - 0$) intensity ($T_{\rm mb}$ scale). The velocity range is -18.4 – 10.8 km $^{-1}$ and the velocity spacings are 3 channels (1.95 km $^{-1}$). This map is spatially convoluted.

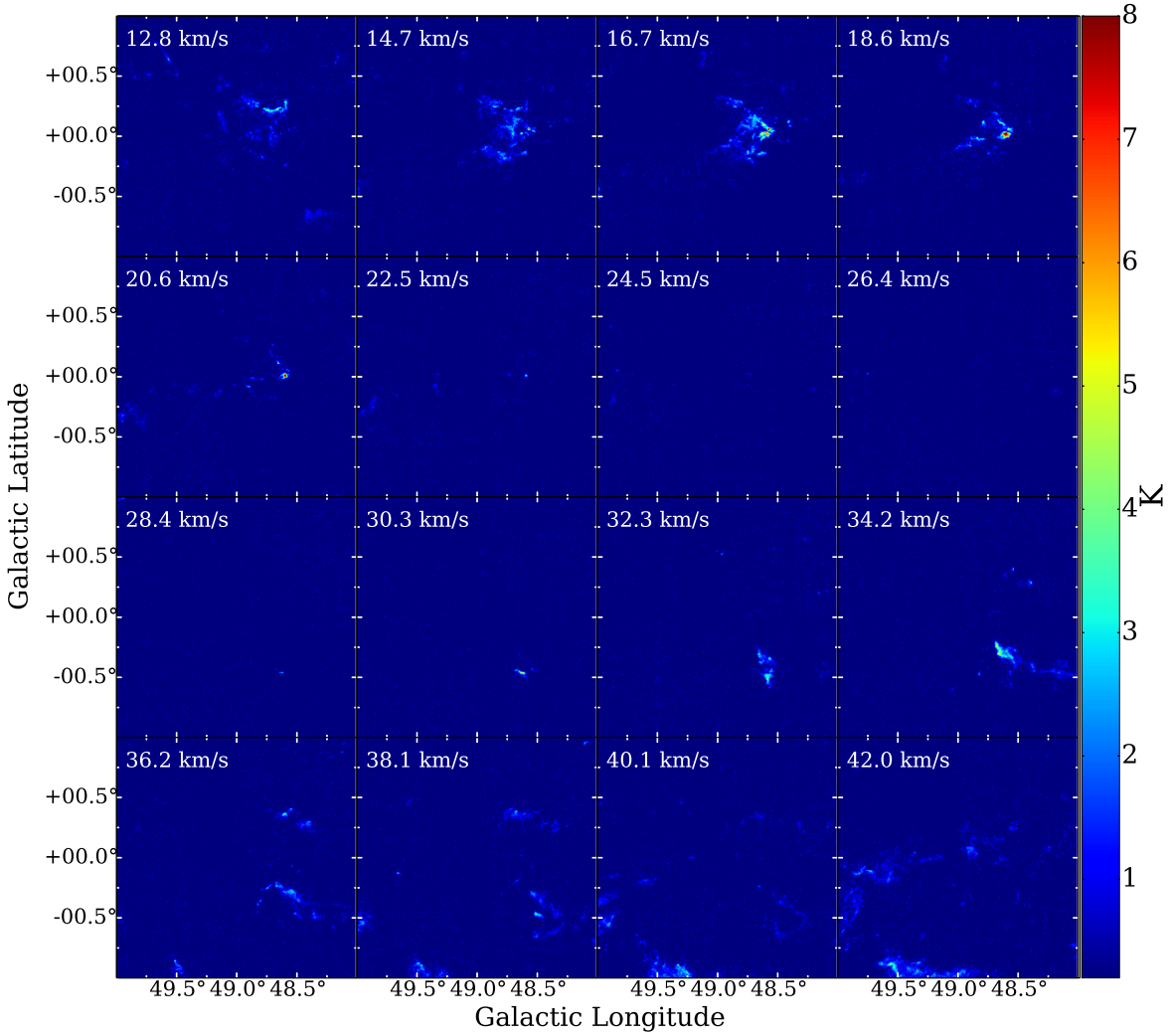

Figure A.4: The channel map of ^{13}CO ($J = 1 - 0$) intensity ($T_{\rm mb}$ scale). The velocity range is 12.8 – 42.0 km $^{-1}$ and the velocity spacings are 3 channels (1.95 km $^{-1}$). This map is spatially convoluted.

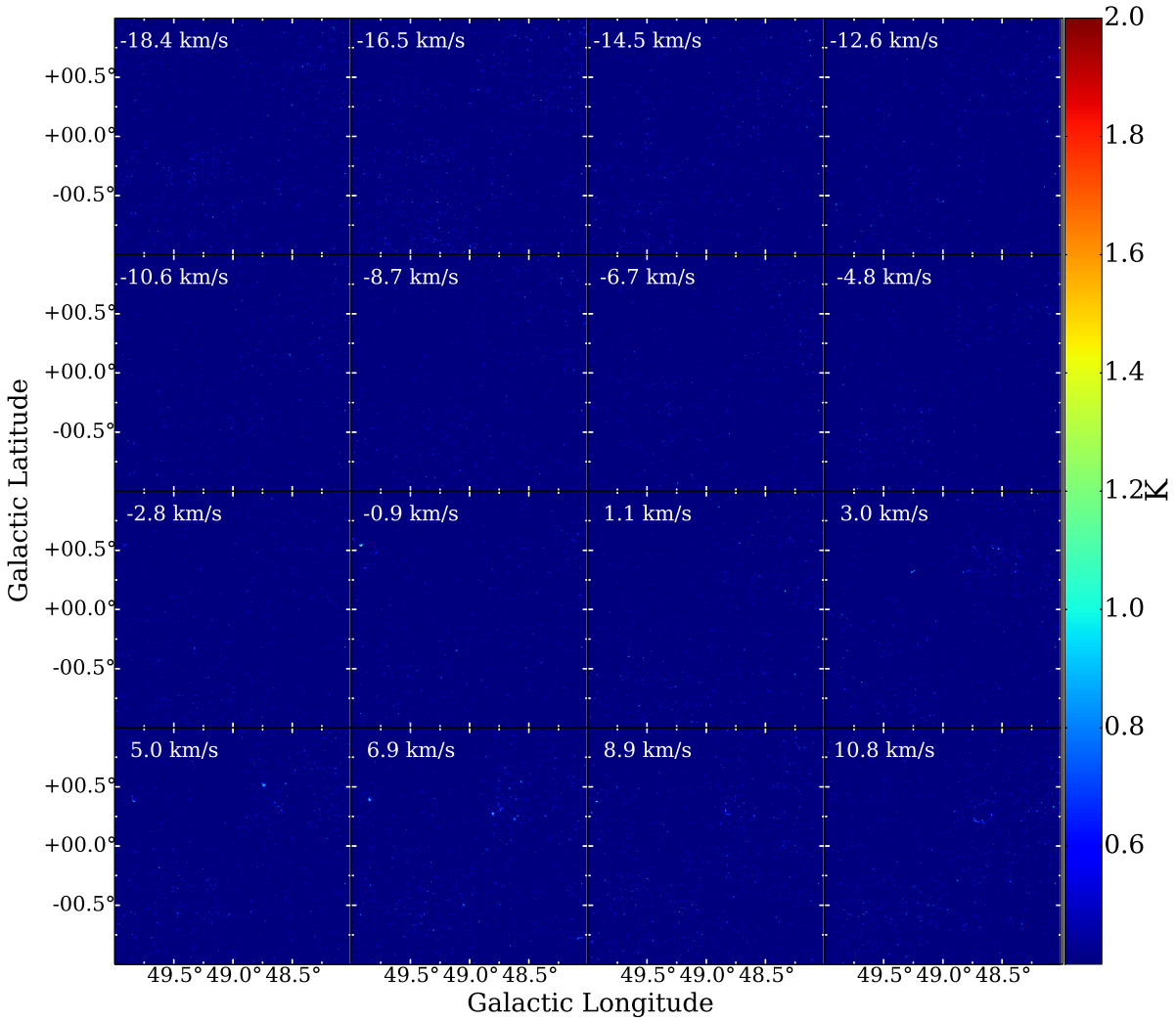

Figure A.5: The channel map of $C^{18}O$ ($J = 1-0$) intensity (T_{mb} scale). The velocity range is 18.4 – 10.8 km $^{-1}$ and the velocity spacings are 3 channels (1.95 km $^{-1}$). This map is spatially convoluted.

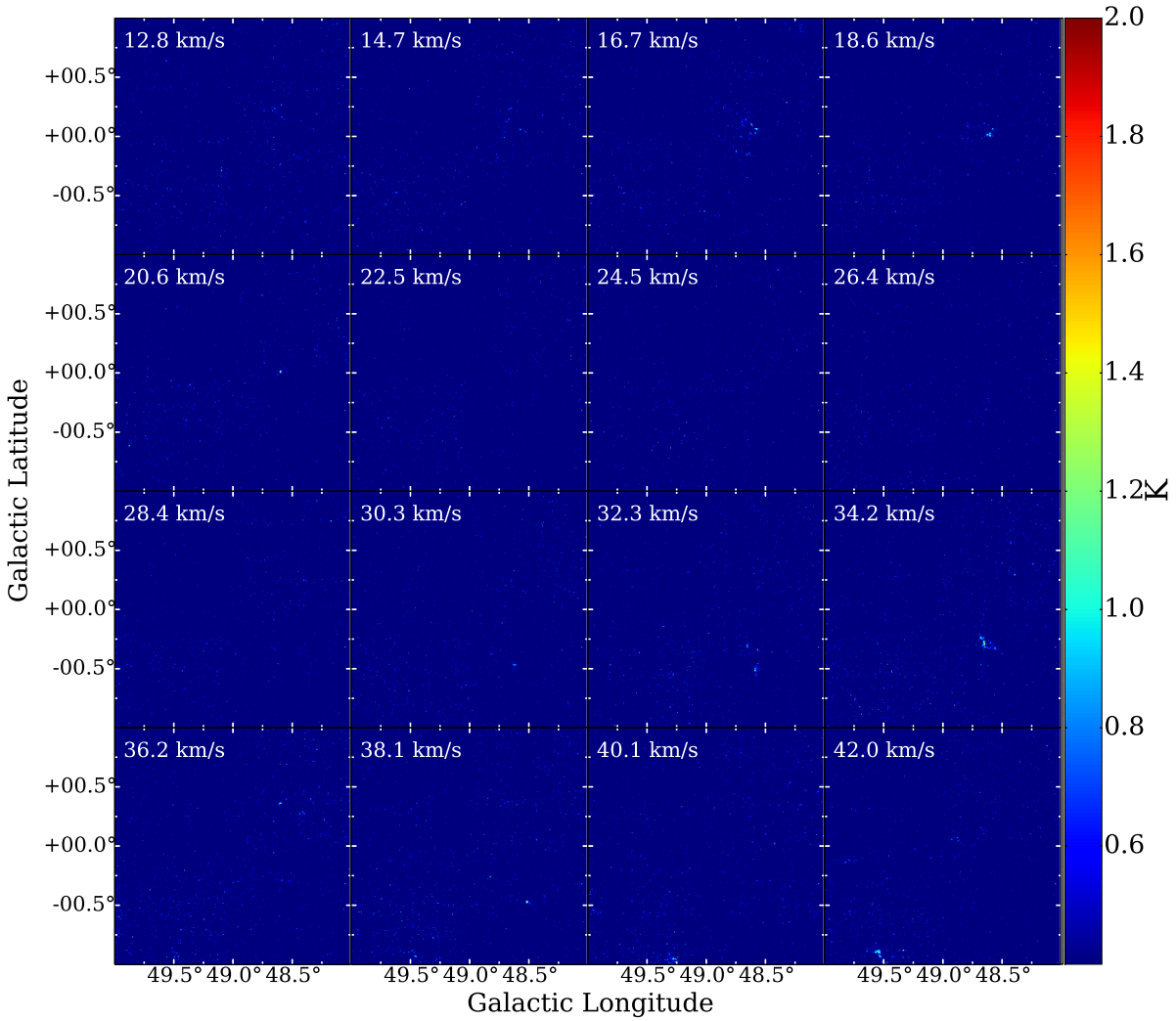

Figure A.6: The channel map of $C^{18}O$ ($J = 1-0$) intensity (T_{mb} scale). The velocity range is 12.8 – 42.0 km $^{-1}$ and the velocity spacings are 3 channels (1.95 km $^{-1}$). This map is spatially convoluted.

Appendix B

The shocked CO gas in W51B

There are shocked molecular clouds in W51B ($>$ 75 km s^{-1}, in break 2) (e.g. Koo & Moon 1997b). Figure B.1 shows the spectrums of the molecular cloud in $(l, b) = (49.108°, -0.328°)$ (discussed as clump 2 in Koo & Moon 1997b). ^{12}CO ($J = 3-2$) emission line was detected and ^{12}CO ($J = 1-0$) emission line was slightly detected, but others (^{13}CO ($J = 1-0$), C^{18}O ($J = 1-0$), ^{13}CO ($J = 3-2$) and C^{18}O ($J = 3-2$)) were not detected significantly. It is an amazing result that ^{12}CO ($J = 1-0$) was detected slightly despite ^{12}CO ($J = 3-2$) was detected considerably ($\sim$ 14 K). Figure B.2 shows the channel map of ^{12}CO ($J = 3-2$) around this molecular clouds, and Figure B.3 shows the integrated intensity of ^{12}CO ($J = 3-2$) and HI. Also, Figure B.4 shows the integrated intensity of ^{13}CO ($J = 1-0$) and ^{12}CO ($J = 3-2$), and Figure B.5 shows the $l-v$ diagram of ^{12}CO ($J = 3-2$).

Perhaps these clouds are the same case as Yamada et al. (2017). We plan to carry out the following observation other molecular emission lines such as SiO, high excitation CO, etc, with high angular resolution and high sensitivity.

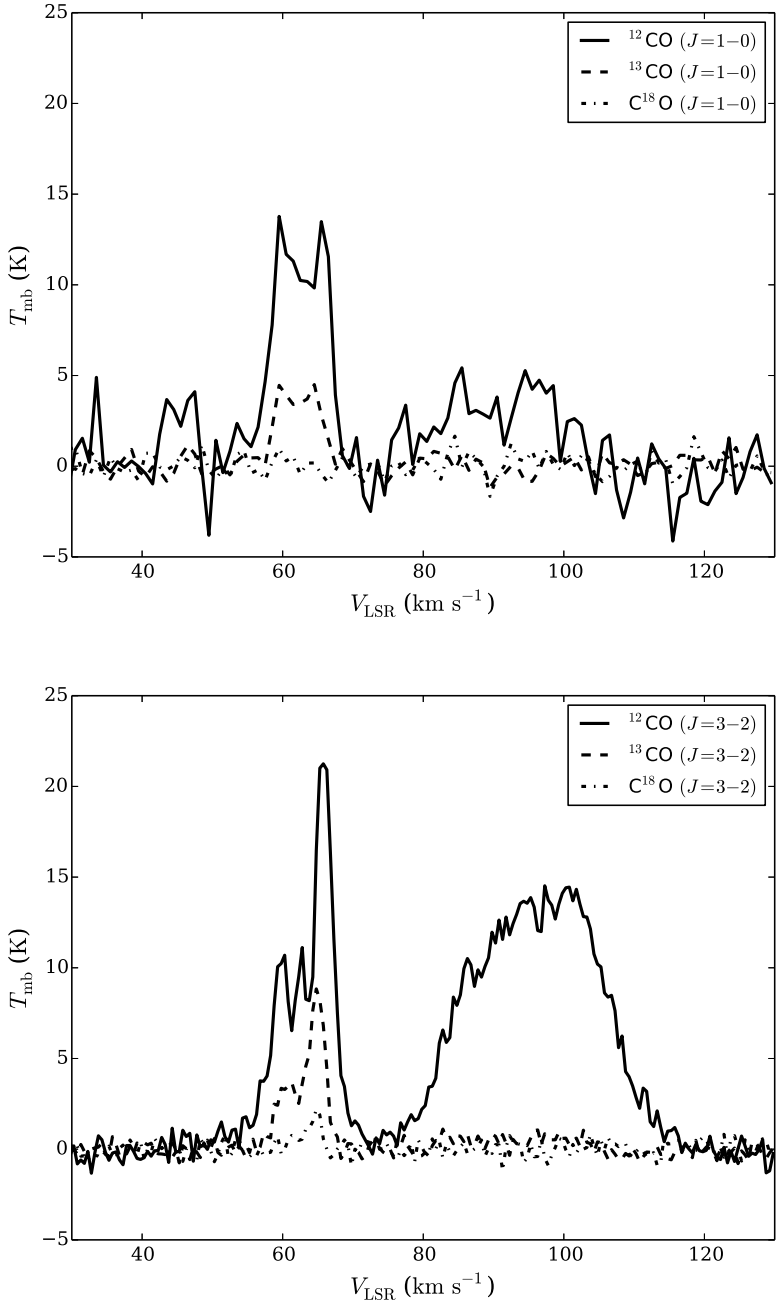

Figure B.1: An example of the spectra of the shocked CO gas ($(l, b) = (49.108°, -0.328°)$). ^{12}CO ($J = 3 - 2$), ^{13}CO ($J = 3 - 2$) and C^{18}O ($J = 3 - 2$) data were taken from *JCMT* data.

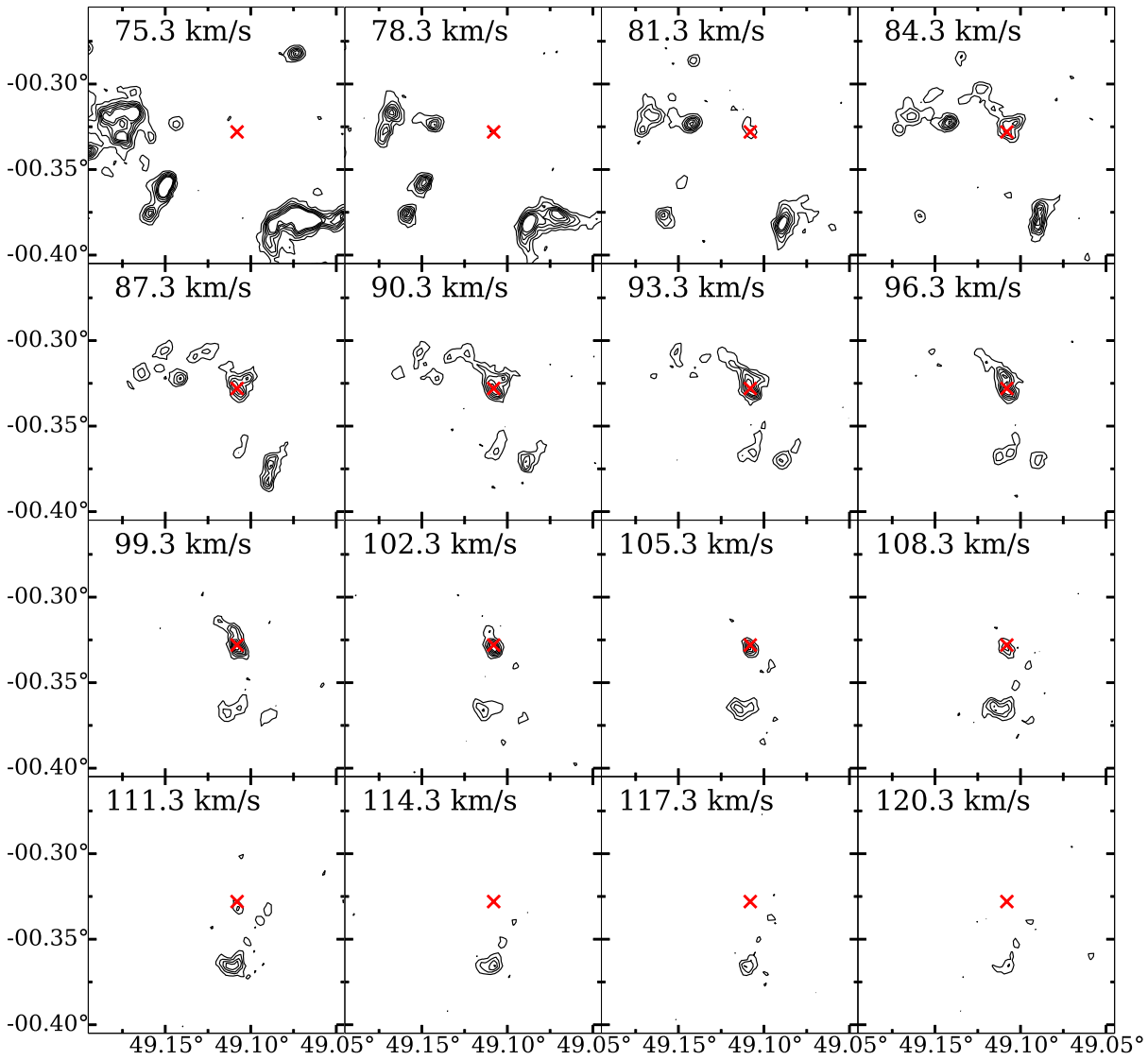

Figure B.2: The channel map of ^{12}CO ($J = 3 - 2$) intensity ($T_{\rm mb}$ scale) taken from *JCMT* data. The velocity range is 75.3 – 120.3 km $^{-1}$ and the velocity spacings are 3.0 km $^{-1}$. The contour levels are [2, 4, 6, 8, 10, 12 K]. The red crosses represent the peak position ($(l, b) = (49.108°, -0.328°)$, Figure B.1).

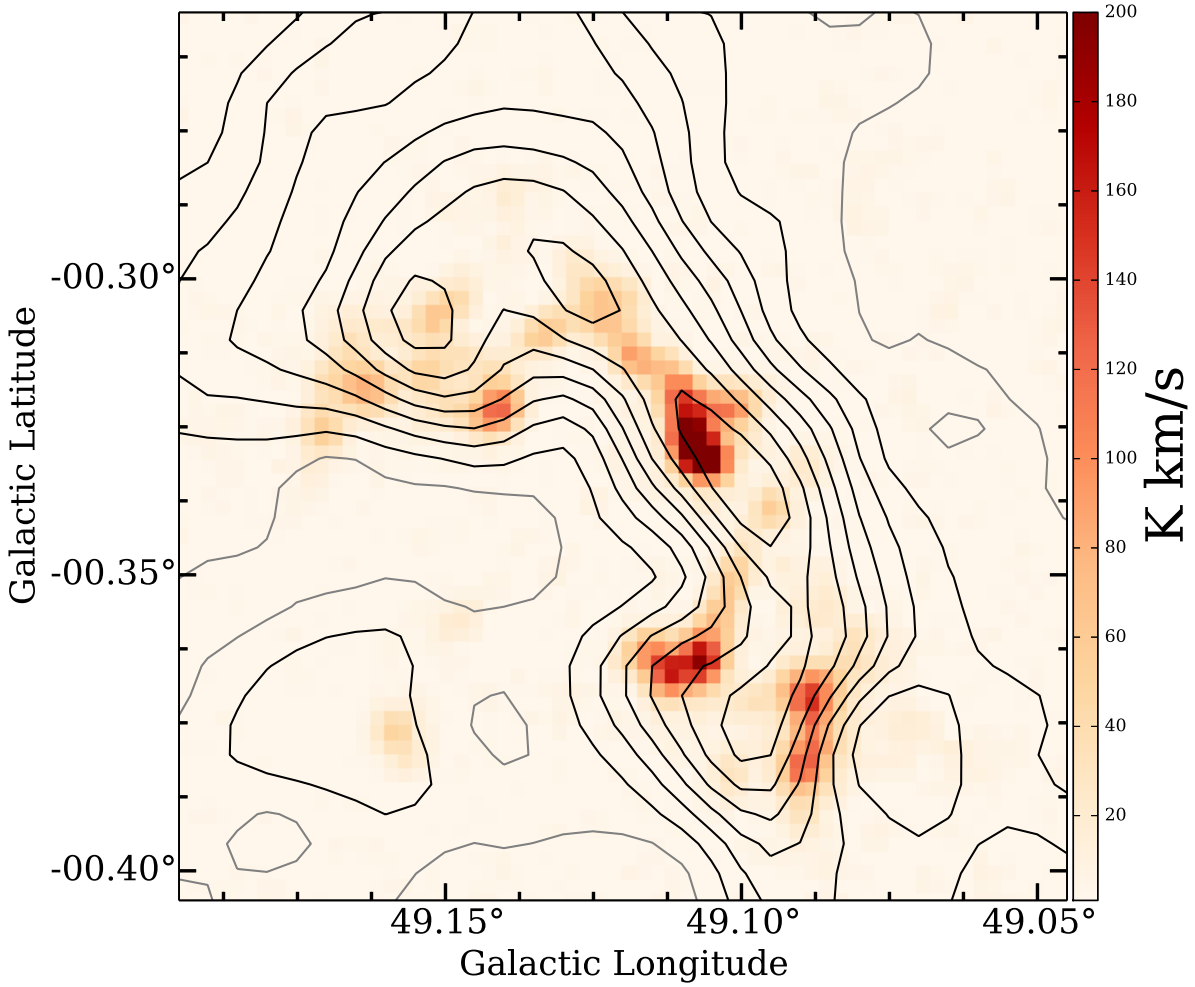

Figure B.3: The integrated intensity of ^{12}CO ($J = 3 - 2$) (colorscale) and HI (contour) of the shocked CO gas in W51B. The integrated velocity range is $80 - 120$ km s^{-1}. The contour levels are [50, 150, 250, ..., 850 K km s^{-1}]. The HI data was taken from VGPS data archive.

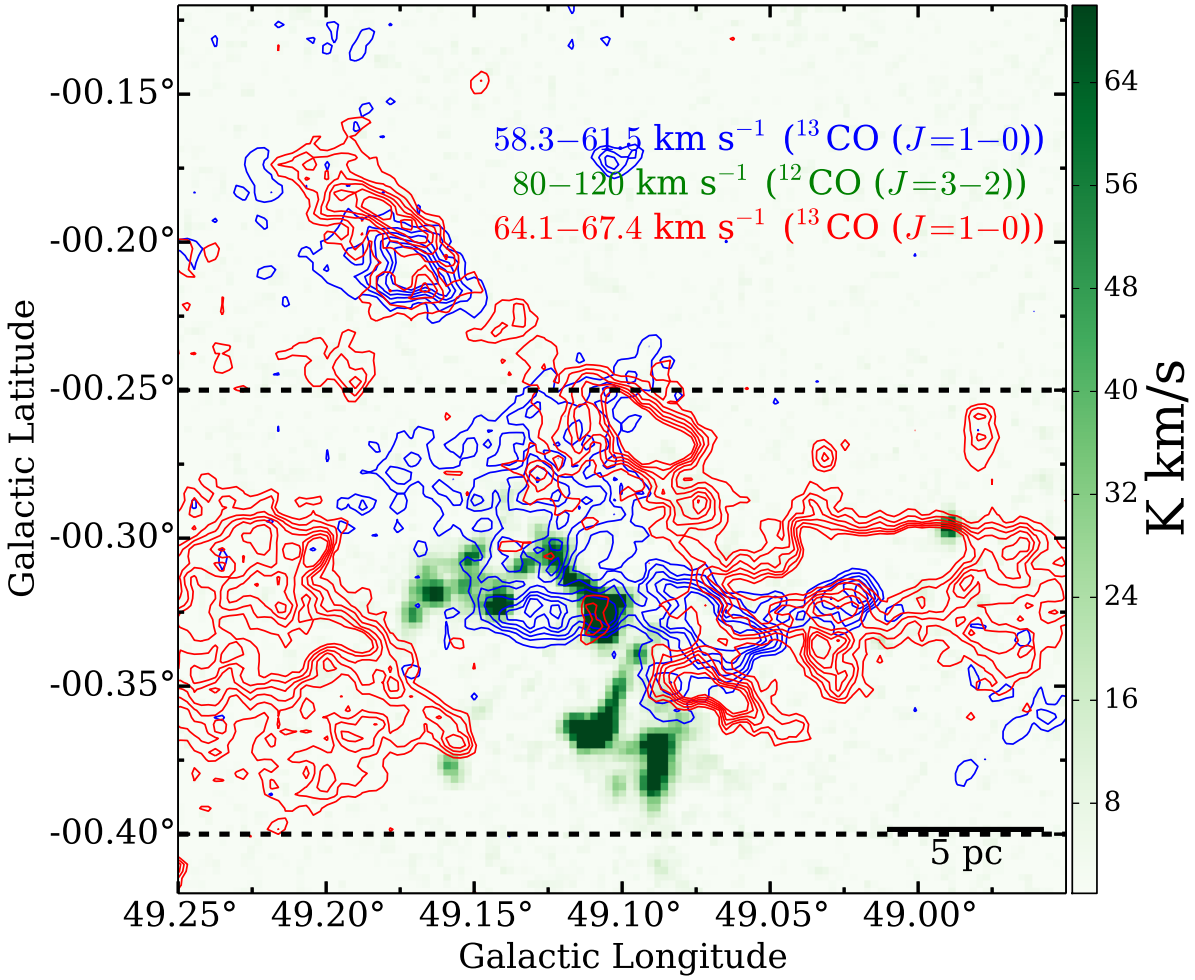

Figure B.4: The integrated intensity map in break 2. The blue and red contours show the integrated intensity of ^{13}CO ($J = 1-0$). The green colorscale shows the integrated intensity of ^{12}CO ($J = 3-2$).

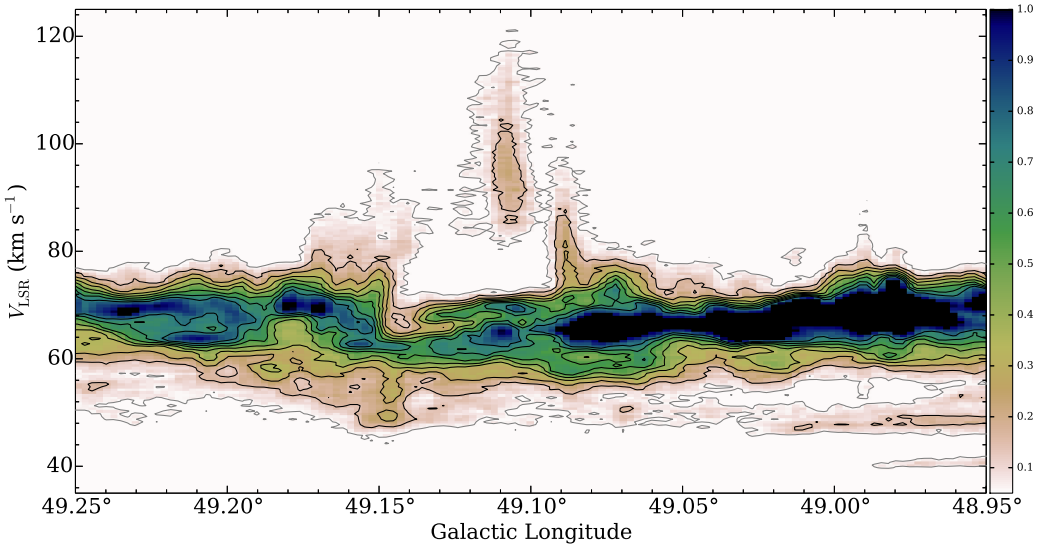

Figure B.5: The ^{12}CO ($J = 3 - 2$) $l - v$ diagram. The range of integrated Galactic Latitude (b) is $-0.40°$ to $-0.25°$ (the black broken lines in Figure B.4).

Appendix C

The structure catalog of the Dendrograms

Table C is the structure catalog of the Dendrograms tree in W51. The parameters of Dendrograms are described in Chapter 3.

ID:

The ID of the structure.

type:

The type of the structure. "T" is a trunk, and among others, "L" is a leaf and "B" is a branch.

ID_a:

The ID of the ancestor of the structure.

ID_p:

The ID of the parent of the structure.

l_{peak}, b_{peak}, v_{peak}**:**

The position of the peak voxel. The units are (deg), (deg) and (km s^{-1}), respectively. Note that the spacial resolution is $\sim 18''$ (= 0.005 deg) and the velocity resolution is 0.65 km s^{-1}.

area:

The exact area of the structure on the sky. The unit is (pix). The pixel size is $8''.5 \times 8''.5$.

$v_{\rm rms}$**:**

The intensity-weighted second moment of the velocity. The unit is (km s^{-1}).

min:

The minimum value of ^{13}CO ($J = 1 - 0$) in the structure. The unit is (K).

max:

The maximum value of ^{13}CO ($J = 1 - 0$) in the structure. The unit is (K).

$I_{\rm F12}$**:**

The sum of all the value of FUGIN ^{12}CO ($J = 1 - 0$) of the voxels in the structure. The unit is (K), but note that the voxel size is $8''.5 \times 8''.5 \times 0.65$ km s^{-1}.

$I_{\rm F13}$**:**

The sum of all the value of FUGIN ^{13}CO ($J = 1 - 0$) of the voxels in the structure. The unit is (K), but note that the voxel size is $8''.5 \times 8''.5 \times 0.65$ km s^{-1}.

$I_{\rm F18}$**:**

The sum of all the value of FUGIN C^{18}O ($J = 1 - 0$) of the voxels in the structure. The unit is (K), but note that the voxel size is $8''.5 \times 8''.5 \times 0.65$ km s^{-1}. Note that only $> 3\sigma$ are listed.

$I_{\rm J13}$**:**

The sum of all the value of JCMT ^{13}CO ($J = 3 - 2$) of the voxels in the structure. The unit is (K), but note that the voxel size is $8''.5 \times 8''.5 \times 0.65$ km s^{-1}.

R_{1312}**:**

$I_{\rm F13}/I_{\rm F12}$ ratio.

R_{3210}**:**

$I_{\rm J13}/I_{\rm F13}$ ratio. Note that we do not have ^{13}CO ($J = 3 - 2$) data set in entire FUGIN region.

R_{1813}**:**

$I_{\mathrm{F18}}/I_{\mathrm{F13}}$ ratio.

8 μm**:**

The median intensity of *Spitzer* IRAC 8 μm within area of the parent cloud. The unit is (MJy sr^{-1}).

Table C.1: The structures catalog of the Dendrograms tree in W51

ID	type	ID_a	ID_p	l_{peak}	b_{peak}	v_{peak}	area	v_{rms}	min	max	I_{F12}	I_{F13}	I_{F18}	I_{J13}	R_{1312}	R_{3210}	R_{1813}	8 μm
0	T	0	-	48.635	0.726	-39.9	28	0.6	2.1	4.2	358.9	165.2	18.5	-	0.46	0.11	-	18.6
1	T	1	-	48.453	0.537	-35.3	19	0.7	2.1	4.0	343.4	136.5	-	-	0.40	-	-	23.2
2	L	3	3	49.419	0.327	-21.7	115	0.8	2.3	7.4	3803.1	1200.4	87.0	-	0.32	0.07	-	32.4
3	T	3	-	49.419	0.327	-21.7	168	0.9	2.1	7.4	4582.5	1450.4	108.6	-	0.32	0.07	-	29.2
4	L	3	3	49.417	0.358	-19.7	39	0.5	2.3	4.9	412.3	151.9	-	-	0.37	-	-	26.9
5	T	5	-	49.159	0.221	-17.8	27	0.7	2.1	5.5	749.3	226.1	-	-	0.30	-	-	36.8
6	T	6	-	49.950	0.308	-16.5	54	0.5	2.1	4.1	892.6	264.7	-	-	0.30	-	-	26.0
7	T	7	-	49.889	0.336	-0.9	114	0.9	2.1	4.1	1139.6	571.6	102.0	-	0.50	0.18	-	24.8
8	T	8	-	49.920	0.537	-0.9	1094	1.1	2.1	8.8	28247.3	10208.8	1248.7	-	0.36	0.12	-	23.0
9	B	8	8	49.920	0.537	-0.9	901	1.1	2.4	8.8	21807.3	8191.6	1084.0	-	0.38	0.13	-	23.3
10	T	10	-	49.910	0.339	-2.8	63	0.6	2.1	3.7	699.4	286.3	-	-	0.41	-	-	24.0
11	B	8	9	49.920	0.537	-0.9	776	1.1	2.6	8.8	18412.1	7074.1	989.1	-	0.38	0.14	-	23.6
12	L	8	11	49.920	0.537	-0.9	260	0.9	2.7	8.8	7447.0	3020.6	523.7	-	0.41	0.17	-	24.4
13	L	8	11	49.995	0.589	-1.5	376	1.2	2.7	6.1	8130.5	3030.7	373.4	-	0.37	0.12	-	24.0
14	T	14	-	49.776	0.443	-0.9	53	0.6	2.1	3.7	236.1	201.2	-	-	0.85	-	-	25.5
15	T	15	-	49.858	0.407	-0.9	43	0.9	2.1	3.8	379.3	251.3	-	-	0.66	-	-	28.2
16	L	8	8	49.941	0.542	-0.9	23	0.4	2.4	4.3	235.0	103.6	16.8	-	0.44	0.16	-	23.1
17	L	8	9	49.995	0.629	-0.2	33	0.4	2.6	4.7	409.5	166.4	-	-	0.41	-	-	23.0
18	L	21	20	48.883	0.093	0.4	23	0.6	2.3	4.4	293.4	123.2	13.9	-	0.42	0.11	-	46.2
19	L	21	20	48.899	0.103	0.4	56	0.4	2.3	3.9	492.7	237.4	-	-	0.48	-	-	46.3
20	B	21	21	48.883	0.093	0.4	86	0.5	2.3	4.4	866.1	391.1	-	-	0.45	-	-	46.3
21	T	21	-	48.866	0.093	1.1	146	0.7	2.1	4.7	1479.9	644.5	39.8	-	0.44	0.06	-	46.5
22	T	22	-	48.366	0.405	4.3	440	1.1	2.1	5.5	4878.2	2200.4	178.6	-	0.45	0.08	-	22.4
23	T	23	-	49.868	0.443	1.1	24	0.4	2.1	3.7	132.7	86.4	-	-	0.65	-	-	24.7
24	L	22	22	48.347	0.452	2.4	128	0.7	2.4	5.2	1333.5	613.4	66.5	-	0.46	0.11	-	21.4
25	T	25	-	48.420	0.459	1.1	67	0.8	2.1	4.8	780.5	353.9	40.3	-	0.45	0.11	-	22.7
26	T	26	-	48.491	0.464	1.1	27	0.9	2.1	4.2	292.4	143.8	-	-	0.49	-	-	26.7
27	L	21	21	48.866	0.093	1.1	30	0.5	2.3	4.7	285.1	124.8	-	-	0.44	-	-	47.8
28	T	28	-	48.479	0.150	3.7	44	0.7	2.1	4.1	392.9	177.3	24.3	-	0.45	0.14	-	58.5
29	T	29	-	48.850	0.233	6.3	2571	2.7	2.1	6.3	76512.2	29249.4	2282.4	-	0.38	0.08	-	34.0
30	T	30	-	49.294	0.275	2.4	72	0.4	2.1	4.4	506.8	277.2	-	-	0.55	-	-	32.0
31	T	31	-	49.265	0.308	3.0	222	0.7	2.1	7.9	2544.2	1499.2	224.1	-	0.59	0.15	-	33.5
32	T	32	-	48.491	0.436	3.0	81	0.7	2.1	4.3	855.6	357.4	53.3	-	0.42	0.15	-	27.9
33	T	33	-	48.479	0.457	1.1	37	0.5	2.1	4.0	358.8	163.8	-	-	0.46	-	-	29.8
34	T	34	-	48.583	0.511	3.0	822	1.7	2.1	6.9	15954.8	6840.5	737.3	-	0.43	0.11	-	26.9
35	L	34	37	48.562	0.525	4.3	107	1.2	3.3	6.6	2306.9	1117.9	150.8	-	0.48	0.13	-	29.0
36	B	34	34	48.583	0.511	3.0	345	1.2	3.0	6.9	6698.4	3187.1	420.4	-	0.48	0.13	-	27.8
37	B	34	36	48.583	0.511	3.0	188	1.3	3.0	6.9	3922.4	1845.3	281.5	-	0.47	0.15	-	30.2

38	B	29	29	48.850	0.233	6.3	2482	2.7	2.1	6.3	74691.5	28595.9	2249.9	-	0.38	0.08	-	33.7
39	T	39	-	48.163	0.355	2.4	28	0.4	2.1	4.2	188.6	118.7	23.7	-	0.63	0.20	-	23.7
40	B	22	22	48.366	0.405	4.3	193	0.8	2.4	5.5	1842.9	915.1	51.5	-	0.50	0.06	-	22.7
41	B	34	36	48.538	0.492	3.7	134	0.8	3.0	6.0	2290.9	1114.3	126.3	-	0.49	0.11	-	26.6
42	L	34	41	48.538	0.492	3.7	80	0.8	3.2	6.0	1508.9	766.9	84.1	-	0.51	0.11	-	26.5
43	L	34	37	48.583	0.511	3.0	54	0.7	3.3	6.9	1011.7	482.6	89.3	-	0.48	0.19	-	34.5
44	T	44	-	48.538	0.216	4.3	100	0.7	2.1	7.1	1377.8	882.2	63.0	-	0.64	0.07	-	54.5
45	B	29	46	48.850	0.233	6.3	1422	2.5	2.3	6.3	51146.5	18919.3	1655.8	-	0.37	0.09	-	35.7
46	B	29	38	48.850	0.233	6.3	1530	2.8	2.2	6.3	57800.0	21017.1	1752.6	-	0.36	0.08	-	35.8
47	T	47	-	48.153	0.343	3.7	26	0.9	2.1	3.7	239.4	126.6	-	-	0.53	-	-	22.6
48	L	62	62	49.830	0.372	4.3	605	1.2	2.3	9.1	12179.8	7272.2	922.7	-	0.60	0.13	-	32.3
49	T	49	-	48.607	0.445	4.3	1067	1.3	2.1	6.3	20352.7	8411.9	647.1	-	0.41	0.08	-	27.9
50	L	22	40	48.366	0.405	4.3	71	0.7	2.7	5.5	664.4	333.2	-	-	0.50	-	-	22.8
51	L	22	40	48.361	0.433	3.0	46	0.6	2.7	4.1	396.8	206.9	29.4	-	0.52	0.14	-	21.8
52	T	52	-	48.755	0.528	5.6	415	1.0	2.1	4.4	3409.0	2009.5	302.6	-	0.59	0.15	-	26.0
53	L	34	41	48.519	0.480	3.0	26	0.5	3.3	4.7	252.9	128.2	18.6	-	0.51	0.15	-	26.1
54	T	54	-	48.656	0.225	4.3	27	0.7	2.1	3.9	131.6	108.8	25.1	40.6	0.83	0.23	0.37	73.1
55	B	29	45	48.850	0.233	6.3	1261	2.5	2.5	6.3	44391.2	16815.3	1505.4	-	0.38	0.09	-	35.7
56	B	29	71	48.850	0.233	6.3	893	1.6	2.7	6.3	29396.8	11619.6	1117.7	-	0.40	0.10	-	34.7
57	T	57	-	49.284	0.242	4.3	47	0.5	2.1	5.1	304.6	144.8	-	-	0.48	-	-	29.7
58	L	29	56	48.850	0.233	6.3	153	1.5	3.1	6.3	4601.1	1785.6	125.3	-	0.39	0.07	-	38.9
59	B	29	56	48.810	0.282	7.6	476	1.4	3.1	6.2	13405.5	5802.0	631.7	-	0.43	0.11	-	33.0
60	T	60	-	48.083	0.287	4.3	28	0.4	2.1	3.9	199.6	125.8	-	-	0.63	-	-	24.0
61	L	49	65	48.619	0.332	5.0	150	1.1	2.4	5.9	2668.0	1288.7	128.3	-	0.48	0.10	-	28.2
62	T	62	-	49.830	0.372	4.3	853	1.4	2.1	9.1	15998.6	9209.5	1083.4	-	0.58	0.12	-	31.4
63	B	49	97	48.607	0.445	4.3	303	1.3	2.5	6.3	6397.6	2759.0	219.4	-	0.43	0.08	-	28.2
64	B	49	65	48.607	0.445	4.3	655	1.2	2.4	6.3	11183.1	4775.8	377.0	-	0.43	0.08	-	27.7
65	B	49	49	48.607	0.445	4.3	811	1.2	2.3	6.3	14721.7	6386.4	510.1	-	0.43	0.08	-	27.8
66	B	49	63	48.607	0.445	4.3	138	1.1	3.1	6.3	2487.1	1145.3	89.0	-	0.46	0.08	-	28.2
67	L	52	52	48.737	0.495	6.3	108	1.0	2.3	3.8	959.5	583.7	66.3	-	0.61	0.11	-	26.6
68	T	68	-	48.687	0.112	6.3	656	1.7	2.1	5.8	8465.0	4707.3	485.5	1520.4	0.56	0.10	0.32	47.4
69	T	69	-	48.623	0.119	5.0	31	0.5	2.1	4.0	92.9	142.1	16.6	42.5	1.53	0.12	0.30	52.4
70	B	68	68	48.687	0.112	6.3	514	1.0	2.4	5.8	5261.8	3397.2	342.2	1070.6	0.65	0.10	0.32	48.1
71	B	29	55	48.850	0.233	6.3	1089	1.6	2.6	6.3	33567.3	13397.8	1266.7	-	0.40	0.09	-	35.6
72	T	72	-	48.111	0.277	6.3	77	0.7	2.1	4.2	370.9	305.7	35.8	-	0.82	0.12	-	25.0
73	B	49	64	48.607	0.445	4.3	612	1.2	2.4	6.3	10631.5	4539.3	374.6	-	0.43	0.08	-	27.6
74	L	49	75	48.649	0.355	4.3	42	0.9	2.8	4.3	411.8	215.7	-	31.7	0.52	-	0.15	27.6
75	B	49	97	48.652	0.369	5.0	160	0.9	2.5	4.5	1967.8	901.2	82.5	-	0.46	0.09	-	27.5
76	L	49	66	48.623	0.428	3.7	32	0.4	3.9	5.5	370.2	201.4	-	-	0.54	-	-	26.9
77	T	77	-	48.574	0.440	5.0	30	0.5	2.1	4.6	212.6	116.3	-	-	0.55	-	-	32.0
78	L	49	66	48.607	0.445	4.3	39	0.4	3.9	6.3	453.0	225.7	23.8	-	0.50	0.11	-	31.9

79	T	79	-	48.640	0.506	5.0	33	0.6	2.1	4.8	300.6	129.1	-	-	0.43	-	-	28.7
80	L	52	52	48.755	0.528	5.6	143	0.6	2.3	4.4	1009.2	653.9	147.5	-	0.65	0.23	-	24.7
81	T	81	-	49.386	-0.967	5.6	46	0.4	2.1	4.0	294.5	161.9	-	-	0.55	-	-	14.8
82	B	68	70	48.687	0.112	6.3	426	0.9	2.5	5.8	4061.1	2788.4	284.3	882.0	0.69	0.10	0.32	47.2
83	T	83	-	48.937	0.209	5.6	177	0.9	2.1	3.9	1496.2	891.5	52.4	-	0.60	0.06	-	36.1
84	T	84	-	48.574	0.242	5.0	30	0.9	2.1	4.5	276.1	162.1	-	79.0	0.59	-	0.49	56.0
85	B	91	94	48.602	0.249	7.6	1513	2.4	2.4	9.0	54314.3	23128.9	2432.2	-	0.43	0.11	-	52.0
86	B	91	132	48.602	0.249	7.6	672	2.5	2.9	9.0	25141.6	11536.6	1282.5	6611.5	0.46	0.11	0.57	60.4
87	T	87	-	48.375	0.254	6.3	247	0.7	2.1	7.9	2014.3	1920.8	307.2	-	0.95	0.16	-	36.5
88	L	87	87	48.375	0.254	6.3	130	0.7	2.7	7.9	1266.1	1261.0	225.7	-	1.00	0.18	-	38.1
89	B	91	91	48.602	0.249	7.6	1774	2.4	2.2	9.0	63364.4	26387.8	2714.2	-	0.42	0.10	-	51.0
90	B	29	59	48.810	0.282	7.6	207	1.2	3.8	6.2	4107.9	1950.6	178.1	-	0.47	0.09	-	32.5
91	T	91	-	48.602	0.249	7.6	1863	2.4	2.1	9.0	68264.5	28108.9	2786.1	-	0.41	0.10	-	50.9
92	B	91	86	48.602	0.249	7.6	489	2.2	3.1	9.0	17747.6	8634.8	954.5	5208.0	0.49	0.11	0.60	58.7
93	L	91	92	48.593	0.296	6.3	18	0.6	3.3	4.7	241.7	120.9	20.3	30.7	0.50	0.17	0.25	33.6
94	B	91	89	48.602	0.249	7.6	1694	2.4	2.3	9.0	60019.4	25197.2	2626.0	-	0.42	0.10	-	51.0
95	B	29	38	48.737	0.315	6.9	714	1.0	2.2	5.6	8702.5	4781.3	314.3	-	0.55	0.07	-	29.7
96	L	49	75	48.652	0.369	5.0	41	0.6	2.8	4.5	468.7	236.5	48.6	-	0.50	0.21	-	26.6
97	B	49	73	48.607	0.445	4.3	483	1.2	2.5	6.3	8602.1	3753.5	307.8	-	0.44	0.08	-	27.9
98	T	98	-	49.768	0.381	6.3	194	0.9	2.1	4.5	1132.1	1049.1	72.8	-	0.93	0.07	-	33.2
99	L	49	63	48.633	0.407	5.0	25	0.6	3.1	4.5	275.5	146.3	-	-	0.53	-	-	26.2
100	T	100	-	49.915	0.421	6.9	63	0.9	2.1	4.1	453.3	305.5	53.7	-	0.67	0.18	-	28.9
101	T	101	-	48.715	0.459	5.6	64	0.7	2.1	4.1	620.4	292.4	-	-	0.47	-	-	27.7
102	T	102	-	48.548	0.551	5.0	31	0.4	2.1	4.0	248.7	116.6	-	-	0.47	-	-	23.3
103	T	103	-	49.429	-0.986	5.6	66	0.3	2.1	3.9	429.0	206.6	28.3	-	0.48	0.14	-	14.4
104	T	104	-	49.405	-0.972	5.6	50	0.3	2.1	4.2	356.5	170.2	-	-	0.48	-	-	15.1
105	T	105	-	49.424	-0.920	5.6	37	0.3	2.1	4.0	248.1	128.9	-	-	0.52	-	-	16.4
106	L	68	70	48.706	0.110	7.6	34	0.8	2.5	4.1	396.5	166.1	23.3	48.3	0.42	0.14	0.29	52.8
107	B	68	82	48.687	0.112	6.3	254	1.0	2.9	5.8	2242.1	1599.1	157.2	530.6	0.71	0.10	0.33	45.3
108	L	68	82	48.661	0.110	6.3	68	0.6	2.9	5.1	435.8	378.7	38.6	107.4	0.87	0.10	0.28	58.3
109	L	68	107	48.687	0.112	6.3	74	0.6	3.1	5.8	347.6	436.0	62.3	156.8	1.25	0.14	0.36	49.9
110	L	68	111	48.713	0.133	7.6	107	1.0	3.2	5.1	1049.6	594.1	48.5	208.1	0.57	0.08	0.35	43.6
111	B	68	107	48.713	0.133	7.6	151	0.9	3.1	5.1	1416.1	893.7	77.3	282.7	0.63	0.09	0.32	44.2
112	L	68	111	48.680	0.169	6.3	41	0.6	3.1	4.7	236.2	234.5	23.7	54.2	0.99	0.10	0.23	45.3
113	L	91	91	48.635	0.173	5.6	24	0.6	2.2	4.6	156.9	106.9	-	33.7	0.68	-	0.32	66.3
114	T	114	-	49.055	0.188	6.3	80	0.7	2.1	4.2	335.6	383.5	29.5	-	1.14	0.08	-	34.6
115	T	115	-	48.888	0.233	5.6	26	0.4	2.1	3.6	116.4	85.3	-	-	0.73	-	-	37.8
116	L	29	29	48.878	0.195	9.5	82	1.0	2.1	4.0	988.4	402.1	32.3	-	0.41	0.08	-	38.3
117	T	117	-	48.904	0.242	5.6	39	1.0	2.1	3.6	191.4	149.5	-	-	0.78	-	-	36.6
118	B	91	92	48.602	0.249	7.6	424	2.1	3.3	9.0	14575.6	7306.8	826.9	4589.5	0.50	0.11	0.63	59.5
119	B	91	118	48.602	0.249	7.6	339	1.7	3.6	9.0	10482.8	5550.5	662.1	3537.0	0.53	0.12	0.64	60.1

120	L	87	87	48.330	0.242	5.6	39	0.3	2.7	4.7	117.8	174.5	18.8	-	1.48	0.11	-	31.1
121	T	121	-	48.423	0.266	6.3	128	0.5	2.1	5.6	458.6	589.4	41.0	-	1.29	0.07	-	35.7
122	L	29	59	48.805	0.256	6.3	34	0.8	3.8	5.3	583.5	332.3	64.7	-	0.57	0.19	-	37.7
123	T	123	-	48.498	0.289	5.0	41	0.4	2.1	6.1	330.4	213.9	-	-	0.65	-	-	31.1
124	B	29	125	48.737	0.315	6.9	298	0.9	2.7	5.6	3162.6	2160.0	152.4	-	0.68	0.07	-	29.7
125	B	29	138	48.737	0.315	6.9	439	1.0	2.4	5.6	5078.2	3131.8	209.5	-	0.62	0.07	-	29.7
126	T	126	-	48.590	0.353	5.6	78	0.4	2.1	5.4	516.4	338.6	36.1	-	0.66	0.11	-	30.8
127	L	49	73	48.649	0.410	6.3	24	0.8	2.5	4.3	304.6	132.5	-	-	0.43	-	-	26.0
128	L	170	170	48.737	0.436	5.0	118	1.2	2.1	4.3	1415.5	612.4	-	-	0.43	-	-	30.3
129	B	62	62	49.818	0.459	8.9	148	1.5	2.3	5.3	1760.5	960.1	70.1	-	0.55	0.07	-	30.7
130	T	130	-	48.600	0.476	5.6	22	0.5	2.1	4.1	196.0	99.6	-	-	0.51	-	-	48.0
131	L	91	119	48.630	0.233	6.9	40	0.5	4.2	6.6	462.3	321.8	49.7	222.7	0.70	0.15	0.69	70.8
132	B	91	85	48.602	0.249	7.6	1061	2.4	2.8	9.0	36486.1	16479.6	1820.2	-	0.45	0.11	-	51.6
133	T	133	-	48.715	0.247	6.3	26	0.5	2.1	4.2	152.0	98.5	-	22.2	0.65	-	0.23	45.3
134	B	91	119	48.602	0.249	7.6	238	1.6	4.2	9.0	6383.6	3547.9	457.4	2374.0	0.56	0.13	0.67	59.0
135	B	91	134	48.602	0.249	7.6	113	1.6	4.6	9.0	2937.6	1731.3	235.9	1311.2	0.59	0.14	0.76	65.3
136	T	136	-	48.928	0.266	6.9	32	0.6	2.1	3.8	266.6	156.6	-	-	0.59	-	-	37.5
137	L	29	90	48.810	0.282	7.6	111	0.8	4.0	6.2	1815.1	913.3	59.9	-	0.50	0.07	-	31.8
138	B	29	95	48.737	0.315	6.9	524	1.0	2.4	5.6	6033.4	3556.1	244.2	-	0.59	0.07	-	29.6
139	L	29	141	48.737	0.315	6.9	75	0.7	3.3	5.6	579.4	506.0	61.0	-	0.87	0.12	-	29.9
140	T	140	-	48.800	0.322	6.3	23	0.5	2.1	4.1	168.6	97.9	-	-	0.58	-	-	38.7
141	B	29	124	48.737	0.315	6.9	188	0.8	2.9	5.6	1736.2	1325.1	119.7	-	0.76	0.09	-	29.8
142	L	29	124	48.727	0.336	6.3	40	0.6	2.9	4.6	426.7	279.7	-	-	0.66	-	-	29.3
143	L	49	64	48.635	0.374	6.9	43	0.6	2.4	4.0	436.1	193.3	-	-	0.44	-	-	28.3
144	T	144	-	49.915	0.372	8.2	143	0.9	2.1	10.9	5736.2	2263.4	281.4	-	0.39	0.12	-	32.6
145	L	49	49	48.678	0.386	7.6	91	0.7	2.3	4.2	979.5	368.7	39.2	-	0.38	0.11	-	28.4
146	T	146	-	49.894	0.424	7.6	121	0.9	2.1	3.9	1287.2	604.6	59.4	-	0.47	0.10	-	27.8
147	L	62	129	49.811	0.469	6.9	69	0.6	2.5	4.7	423.1	344.2	-	-	0.81	-	-	30.3
148	T	148	-	48.611	0.554	7.6	143	0.7	2.1	3.8	1615.5	637.5	65.1	-	0.39	0.10	-	24.7
149	L	34	34	48.564	0.544	6.9	31	0.6	3.0	4.7	292.8	149.1	-	-	0.51	-	-	22.7
150	T	150	-	48.106	-0.795	6.9	62	0.1	2.1	4.2	201.1	169.1	-	-	0.84	-	-	12.6
151	T	151	-	48.097	-0.783	6.9	88	0.2	2.1	3.9	259.9	255.9	67.7	-	0.98	0.26	-	14.6
152	T	152	-	48.019	-0.731	6.3	49	0.1	2.1	4.2	147.6	135.3	-	-	0.92	-	-	16.3
153	L	91	89	48.633	0.192	7.6	19	0.7	2.3	3.9	180.2	105.5	-	22.6	0.59	-	0.21	56.7
154	T	154	-	49.938	0.197	8.9	231	0.6	2.1	4.1	2506.1	1047.7	99.1	-	0.42	0.09	-	27.6
155	L	91	134	48.607	0.228	8.2	55	0.8	4.6	6.7	855.6	525.0	66.6	282.3	0.61	0.13	0.54	56.7
156	L	91	135	48.602	0.249	7.6	63	1.1	4.8	9.0	1656.4	1013.8	145.1	883.9	0.61	0.14	0.87	67.1
157	L	29	71	48.755	0.282	8.2	170	0.8	2.7	5.0	2485.1	1187.2	96.2	-	0.48	0.08	-	37.1
158	L	29	95	48.725	0.292	6.9	65	0.6	2.4	4.9	745.8	310.5	44.3	-	0.42	0.14	-	34.1
159	L	29	141	48.774	0.341	7.6	30	0.6	3.4	4.8	272.4	195.6	-	-	0.72	-	-	29.4
160	L	170	168	48.741	0.386	9.5	120	0.8	2.3	4.4	1690.8	630.3	51.5	-	0.37	0.08	-	28.6

161	T	161	-	48.682	0.454	6.9	53	0.6	2.1	3.9	498.6	257.3	-	-	0.52	-	-	28.5
162	T	162	-	48.994	0.223	8.2	151	0.7	2.1	3.9	1292.4	714.0	91.3	-	0.55	0.13	-	37.4
163	L	162	162	48.994	0.223	8.2	88	0.6	2.2	3.9	729.6	422.9	43.5	-	0.58	0.10	-	38.0
164	L	29	90	48.824	0.263	11.5	56	1.3	4.0	6.0	1208.5	525.5	65.7	-	0.43	0.13	-	34.0
165	T	165	-	49.962	0.280	8.9	184	0.6	2.1	5.9	2812.8	1128.6	150.4	-	0.40	0.13	-	28.8
166	L	91	94	48.602	0.318	8.2	81	0.7	2.4	4.9	1128.0	481.1	41.8	93.1	0.43	0.09	0.19	29.1
167	L	29	138	48.706	0.343	8.2	44	0.6	2.5	4.1	414.9	175.7	-	-	0.42	-	-	28.5
168	B	170	170	48.741	0.386	9.5	263	0.9	2.1	4.4	3036.8	1227.5	88.0	-	0.40	0.07	-	29.0
169	L	170	168	48.734	0.414	8.9	82	0.8	2.3	3.8	628.3	306.3	-	-	0.49	-	-	29.7
170	T	170	-	48.741	0.386	9.5	386	1.2	2.1	4.4	4527.9	1865.1	102.3	-	0.41	0.05	-	29.5
171	L	172	172	49.785	0.485	7.6	88	0.4	2.3	4.2	550.4	327.1	48.5	-	0.59	0.15	-	29.3
172	T	172	-	49.745	0.485	8.2	187	0.5	2.1	5.1	1904.7	976.4	156.6	-	0.51	0.16	-	28.2
173	T	173	-	48.661	0.292	9.5	127	1.0	2.1	6.2	1815.2	1014.8	-	430.2	0.56	-	0.42	53.8
174	L	173	173	48.661	0.292	9.5	70	1.0	2.3	6.2	1137.1	678.6	-	331.7	0.60	-	0.49	68.2
175	T	175	-	48.824	0.386	8.2	47	0.8	2.1	3.8	522.9	253.9	-	-	0.49	-	-	28.8
176	L	172	172	49.745	0.485	8.2	70	0.5	2.3	5.1	1036.1	509.2	89.3	-	0.49	0.18	-	26.5
177	T	177	-	49.962	0.122	9.5	205	0.7	2.1	4.0	2113.0	835.5	64.1	-	0.40	0.08	-	30.4
178	L	162	162	48.999	0.185	8.9	47	0.5	2.2	3.6	378.7	198.0	31.3	-	0.52	0.16	-	35.3
179	B	91	132	48.741	0.223	11.5	379	1.3	2.9	5.8	10068.4	4472.1	494.9	-	0.44	0.11	-	42.2
180	L	173	173	48.678	0.320	9.5	37	0.5	2.3	3.9	335.2	167.2	-	36.9	0.50	-	0.22	35.2
181	L	29	125	48.763	0.367	8.9	28	0.4	2.7	4.4	257.3	130.2	18.0	-	0.51	0.14	-	27.8
182	T	182	-	48.727	0.403	8.9	24	0.4	2.1	4.0	215.6	88.3	-	-	0.41	-	-	28.3
183	L	62	129	49.818	0.459	8.9	31	0.7	2.6	5.3	713.3	263.8	19.1	-	0.37	0.07	-	37.2
184	T	184	-	48.283	-0.447	10.8	51	0.7	2.1	3.7	433.9	171.0	17.8	-	0.39	0.10	-	31.2
185	T	185	-	48.227	-0.391	10.2	42	0.5	2.1	4.7	393.6	183.4	39.5	-	0.47	0.22	-	25.3
186	L	68	68	48.727	0.152	10.8	64	0.8	2.4	5.0	1418.5	468.9	65.4	189.1	0.33	0.14	0.40	45.0
187	B	91	85	48.642	0.185	8.9	138	0.9	2.8	5.4	1963.8	906.1	102.8	164.0	0.46	0.11	0.18	54.4
188	L	91	187	48.642	0.185	8.9	59	0.6	3.2	5.4	693.5	354.5	38.3	64.3	0.51	0.11	0.18	57.1
189	L	91	179	48.711	0.202	10.2	66	1.0	3.6	5.3	1349.0	667.2	76.0	154.4	0.49	0.11	0.23	44.1
190	L	91	179	48.741	0.223	11.5	131	1.0	3.6	5.8	2965.1	1374.7	174.5	356.3	0.46	0.13	0.26	38.9
191	L	29	55	48.852	0.235	16.7	128	1.8	2.6	4.8	3664.2	1135.6	76.5	-	0.31	0.07	-	37.0
192	L	91	135	48.602	0.270	10.8	32	0.8	4.8	6.8	726.1	397.6	54.2	212.3	0.55	0.14	0.53	55.0
193	L	29	45	48.866	0.292	12.1	39	0.9	2.5	4.1	684.7	230.1	29.3	-	0.34	0.13	-	34.4
194	L	91	86	48.659	0.225	12.8	118	1.2	3.1	6.6	3682.7	1498.4	189.8	708.3	0.41	0.13	0.47	74.2
195	T	195	-	48.734	0.244	10.8	33	0.5	2.1	3.7	428.3	135.9	-	47.0	0.32	-	0.35	39.3
196	T	196	-	49.487	0.506	11.5	114	0.5	2.1	6.5	1965.6	678.3	61.2	-	0.35	0.09	-	25.7
197	T	197	-	49.487	0.544	11.5	28	0.4	2.1	3.9	281.9	148.5	29.0	-	0.53	0.20	-	20.3
198	T	198	-	49.568	0.639	12.8	74	0.7	2.1	3.6	764.3	391.5	53.6	-	0.51	0.14	-	18.9
199	L	91	187	48.637	0.197	12.1	22	0.4	3.2	4.9	303.4	141.2	21.6	20.9	0.47	0.15	0.15	50.4
200	L	91	118	48.635	0.235	14.7	21	1.4	3.6	6.7	666.0	241.9	33.4	292.0	0.36	0.14	1.21	88.4
201	T	201	-	48.902	0.263	12.8	34	0.7	2.1	5.9	755.7	283.5	-	-	0.38	-	-	36.6

202	L	205	205	48.772	-0.188	14.7	136	0.9	2.1	4.2	2024.3	813.4	97.7	179.4	0.40	0.12	0.22	51.6
203	B	204	208	48.708	0.008	14.7	309	1.0	2.3	4.9	4679.3	2210.4	206.3	399.7	0.47	0.09	0.18	55.8
204	T	204	-	48.607	0.022	18.6	3764	1.8	2.1	14.9	171854.3	52854.5	5473.2	-	0.31	0.10	-	58.4
205	T	205	-	48.737	-0.190	16.7	215	1.1	2.1	4.3	3068.9	1276.1	119.0	262.8	0.42	0.09	0.21	52.3
206	B	204	208	48.607	0.022	18.6	2826	1.7	2.3	14.9	146171.7	44156.1	4615.3	-	0.30	0.10	-	61.0
207	B	204	211	48.607	0.022	18.6	836	1.6	2.4	14.9	85796.6	22328.1	2110.3	-	0.26	0.09	-	83.7
208	B	204	204	48.607	0.022	18.6	3155	1.7	2.3	14.9	151580.6	46591.2	4847.2	-	0.31	0.10	-	59.6
209	B	204	221	48.720	0.074	14.1	231	1.1	2.5	4.3	2704.5	1421.1	190.4	281.2	0.53	0.13	0.20	54.9
210	L	204	209	48.720	0.074	14.1	103	1.1	2.6	4.3	1222.2	651.6	95.0	138.6	0.53	0.15	0.21	57.6
211	B	204	206	48.607	0.022	18.6	2799	1.7	2.3	14.9	145512.6	43932.0	4591.7	-	0.30	0.10	-	61.2
212	B	204	221	48.578	0.055	16.0	1459	1.3	2.5	12.9	46737.9	16995.8	1964.7	-	0.36	0.12	-	60.2
213	T	213	-	48.975	0.277	13.4	81	0.5	2.1	4.6	779.4	387.2	34.8	-	0.50	0.09	-	40.3
214	L	216	215	48.814	-0.136	14.7	127	0.5	2.5	4.3	1415.3	592.8	-	114.3	0.42	-	0.19	42.9
215	B	216	216	48.831	-0.136	14.7	156	0.5	2.4	5.0	1765.3	738.5	-	142.2	0.42	-	0.19	44.3
216	T	216	-	48.746	-0.143	17.3	378	1.2	2.1	5.0	5929.0	2344.4	196.4	566.5	0.40	0.08	0.24	46.3
217	T	217	-	48.925	-0.093	14.7	61	1.0	2.1	3.8	753.9	357.9	-	59.7	0.47	-	0.17	73.9
218	T	218	-	48.701	-0.072	15.4	48	0.7	2.1	3.9	457.1	232.8	24.4	33.4	0.51	0.10	0.14	39.0
219	L	204	203	48.708	0.008	14.7	57	0.8	2.8	4.9	669.8	338.0	27.1	60.4	0.50	0.08	0.18	53.9
220	L	204	203	48.701	0.022	14.1	18	0.9	2.8	4.5	300.3	137.1	25.1	32.3	0.46	0.18	0.24	51.7
221	B	204	211	48.578	0.055	16.0	1833	1.4	2.4	12.9	53516.3	19806.9	2303.4	-	0.37	0.12	-	56.9
222	B	204	224	48.578	0.055	16.0	321	1.3	3.2	12.9	16307.0	5593.2	697.1	-	0.34	0.12	-	103.0
223	L	204	222	48.578	0.055	16.0	204	1.3	3.4	12.9	12427.6	4310.1	516.5	3706.8	0.35	0.12	0.86	108.7
224	B	204	232	48.578	0.055	16.0	668	1.4	3.0	12.9	27452.2	9920.3	1227.6	-	0.36	0.12	-	77.3
225	L	205	205	48.737	-0.190	16.7	62	0.8	2.1	4.3	865.2	397.7	-	72.1	0.46	-	0.18	51.4
226	T	226	-	48.810	-0.178	15.4	22	0.5	2.1	3.9	236.3	100.8	-	15.8	0.43	-	0.16	43.7
227	T	227	-	48.630	-0.143	16.0	329	0.8	2.1	6.0	7013.1	2409.8	201.5	891.7	0.34	0.08	0.37	37.4
228	L	216	215	48.831	-0.136	14.7	21	0.3	2.6	5.0	234.7	106.6	-	17.9	0.45	-	0.17	51.8
229	T	229	-	48.718	-0.089	16.0	44	1.0	2.1	3.7	585.4	260.0	23.8	16.3	0.44	0.09	0.06	37.6
230	L	204	207	48.635	0.022	15.4	20	0.8	5.5	8.3	1193.4	358.1	24.6	311.3	0.30	0.07	0.87	111.3
231	L	204	222	48.536	0.041	16.0	61	0.8	3.4	5.7	1816.7	676.8	115.8	303.5	0.37	0.17	0.45	84.9
232	B	204	212	48.578	0.055	16.0	932	1.3	2.8	12.9	32919.6	12057.6	1473.2	-	0.37	0.12	-	65.6
233	T	233	-	48.399	0.079	15.4	41	0.8	2.1	4.8	677.6	307.7	-	-	0.45	-	-	48.3
234	L	204	209	48.772	0.074	15.4	105	0.8	2.6	4.3	969.8	533.3	69.5	98.2	0.55	0.13	0.18	52.0
235	L	204	206	48.647	0.140	15.4	21	0.7	2.3	3.8	266.6	113.4	-	11.6	0.43	-	0.10	47.3
236	L	216	216	48.746	-0.143	17.3	128	0.9	2.4	5.0	2336.3	968.4	119.1	274.9	0.41	0.12	0.28	50.3
237	L	227	227	48.630	-0.143	16.0	65	0.7	3.2	6.0	1265.5	478.1	28.6	233.7	0.38	0.06	0.49	35.6
238	T	238	-	48.715	-0.115	16.7	152	0.6	2.1	4.2	1897.2	833.7	66.6	103.5	0.44	0.08	0.12	38.0
239	T	239	-	48.890	-0.093	15.4	22	0.4	2.1	3.6	203.7	100.3	-	16.3	0.49	-	0.16	73.4
240	L	204	212	48.713	0.084	16.0	37	0.5	2.9	4.4	385.9	196.7	28.9	40.0	0.51	0.15	0.20	62.4
241	T	241	-	48.753	0.117	16.0	60	0.7	2.1	4.9	981.3	412.8	33.7	76.2	0.42	0.08	0.18	46.1
242	B	204	224	48.621	0.091	17.3	289	1.2	3.2	8.8	7866.2	3326.0	423.2	2399.3	0.42	0.13	0.72	61.4

243	L	204	232	48.696	0.148	16.7	94	0.7	3.0	5.2	1198.8	569.8	41.0	124.7	0.48	0.07	0.22	45.2
244	T	244	-	48.807	0.280	16.7	74	0.7	2.1	4.1	1181.5	429.3	50.8	-	0.36	0.12	-	33.1
245	L	29	46	48.855	0.284	16.7	54	0.8	2.3	3.8	808.4	278.2	-	-	0.34	-	-	33.0
246	L	227	227	48.656	-0.148	16.0	41	0.4	3.2	4.7	500.6	198.8	30.9	59.6	0.40	0.16	0.30	40.1
247	T	247	-	48.907	-0.079	18.6	95	1.3	2.1	4.4	2049.8	788.2	120.3	160.0	0.38	0.15	0.20	69.4
248	T	248	-	48.680	0.074	16.7	66	0.7	2.1	4.5	1062.8	373.9	48.8	166.1	0.35	0.13	0.44	67.1
249	T	249	-	48.413	0.112	16.7	85	0.6	2.1	5.5	2373.2	604.5	30.8	-	0.25	0.05	-	72.4
250	L	238	238	48.706	-0.126	16.7	28	0.5	2.5	3.9	433.0	183.5	-	27.8	0.42	-	0.15	38.4
251	L	238	238	48.715	-0.115	16.7	26	0.5	2.5	4.2	243.3	153.1	-	15.2	0.63	-	0.10	37.5
252	T	252	-	48.838	-0.022	18.6	323	0.9	2.1	5.1	5317.4	2073.2	227.1	720.1	0.39	0.11	0.35	60.6
253	T	253	-	48.902	-0.037	16.7	61	0.7	2.1	3.5	716.8	251.9	21.3	51.8	0.35	0.08	0.21	71.8
254	T	254	-	48.888	-0.027	18.0	88	0.7	2.1	4.0	1218.7	437.3	49.3	109.2	0.36	0.11	0.25	64.6
255	B	204	207	48.607	0.022	18.6	290	1.3	5.5	14.9	27979.1	8677.5	858.6	-	0.31	0.10	-	128.4
256	L	204	204	48.793	0.117	18.0	151	0.7	2.3	7.3	2999.6	1091.8	134.4	390.2	0.36	0.12	0.36	54.9
257	L	204	242	48.621	0.091	17.3	101	0.7	3.8	8.8	2823.6	1296.2	176.8	993.7	0.46	0.14	0.77	72.3
258	L	204	242	48.656	0.103	19.3	56	1.2	3.8	6.7	1584.0	603.8	71.1	543.9	0.38	0.12	0.90	58.4
259	T	259	-	48.890	0.301	17.3	56	0.8	2.1	3.7	679.5	295.1	-	-	0.43	-	-	34.3
260	L	252	252	48.838	-0.022	18.6	84	0.7	2.7	5.1	1428.1	576.4	64.4	182.9	0.40	0.11	0.32	61.8
261	T	261	-	48.925	-0.067	18.6	21	0.7	2.1	3.5	193.2	83.1	-	8.6	0.43	-	0.10	61.6
262	L	204	255	48.607	0.022	18.6	13	0.6	9.9	14.9	1273.5	421.1	48.7	630.9	0.33	0.12	1.50	277.4
263	L	252	252	48.793	-0.030	19.9	75	0.6	2.7	4.6	969.5	467.9	42.4	202.0	0.48	0.09	0.43	61.7
264	B	204	255	48.611	0.011	19.3	53	0.9	9.8	14.3	3098.7	1239.3	123.6	1186.4	0.40	0.10	0.96	152.5
265	L	204	264	48.611	0.011	19.3	26	0.5	10.4	14.3	1261.2	487.7	44.1	491.8	0.39	0.09	1.01	165.9
266	L	204	264	48.597	0.008	20.6	20	0.5	10.4	13.0	819.7	367.3	41.3	315.7	0.45	0.11	0.86	148.4
267	T	267	-	49.939	0.979	27.7	67	0.4	2.1	4.0	576.7	281.4	24.7	-	0.49	0.09	-	13.6
268	T	268	-	48.633	-0.464	29.7	1088	1.2	2.1	7.5	18456.9	8021.4	1207.1	-	0.43	0.15	-	27.6
269	L	268	268	48.633	-0.464	29.7	146	0.6	3.3	7.5	3381.1	1551.3	243.8	-	0.46	0.16	-	40.8
270	T	270	-	48.678	-0.436	29.7	69	0.7	2.1	5.2	843.3	361.0	59.3	-	0.43	0.16	-	71.4
271	B	291	276	48.661	-0.306	33.6	2868	1.2	2.2	7.9	46089.9	22685.9	3409.4	-	0.49	0.15	-	42.0
272	T	272	-	48.970	0.521	31.6	41	0.5	2.1	4.0	336.0	186.9	45.9	-	0.56	0.25	-	26.5
273	B	268	274	48.583	-0.485	32.3	277	0.5	3.4	6.2	3108.5	1599.6	247.5	-	0.51	0.15	-	25.8
274	B	268	268	48.583	-0.485	32.3	369	0.6	3.3	6.2	4210.1	2179.3	344.7	-	0.52	0.16	-	26.2
275	L	268	273	48.607	-0.495	31.6	78	0.4	3.7	5.9	932.4	453.7	53.4	-	0.49	0.12	-	26.7
276	B	291	291	48.661	-0.306	33.6	2976	1.3	2.1	7.9	48684.3	23715.7	3509.4	-	0.49	0.15	-	41.6
277	B	268	273	48.583	-0.485	32.3	113	0.4	3.7	6.2	1040.0	625.4	109.7	-	0.60	0.18	-	24.6
278	L	268	277	48.590	-0.511	32.3	54	0.4	3.8	5.4	464.9	322.4	63.6	-	0.69	0.20	-	24.0
279	B	291	291	48.654	-0.374	32.9	179	0.5	2.1	4.7	1937.1	768.7	65.5	-	0.40	0.09	-	53.2
280	L	291	279	48.630	-0.358	32.3	46	0.4	2.3	3.7	365.2	165.7	17.5	-	0.45	0.11	-	50.3
281	B	291	284	48.661	-0.306	33.6	1183	0.7	3.1	7.9	16489.5	9389.0	1702.2	-	0.57	0.18	-	42.8
282	B	291	281	48.548	-0.355	33.6	308	0.6	3.2	5.5	3419.7	1797.5	321.5	-	0.53	0.18	-	34.1
283	B	291	285	48.661	-0.306	33.6	1868	0.8	2.7	7.9	27292.3	14420.1	2416.0	-	0.53	0.17	-	43.9

284	B	291	283	48.661	-0.306	33.6	1560	0.8	2.9	7.9	21917.2	11999.4	2082.6	-	0.55	0.17	-	43.5
285	B	291	271	48.661	-0.306	33.6	2250	1.0	2.5	7.9	33076.3	17278.8	2798.0	-	0.52	0.16	-	42.6
286	B	291	282	48.548	-0.355	33.6	167	0.6	3.3	5.5	1816.9	992.6	160.2	-	0.55	0.16	-	32.1
287	L	291	286	48.559	-0.334	33.6	101	0.6	3.4	5.4	1102.4	645.2	112.7	-	0.59	0.17	-	32.5
288	L	268	277	48.583	-0.485	32.3	33	0.2	3.9	6.2	297.2	150.7	19.8	-	0.51	0.13	-	25.5
289	L	268	274	48.564	-0.464	32.9	49	0.4	3.4	5.2	376.8	229.1	35.9	-	0.61	0.16	-	27.7
290	L	291	279	48.654	-0.374	32.9	90	0.3	2.3	4.7	1076.4	419.1	25.4	-	0.39	0.06	-	54.9
291	T	291	-	48.661	-0.306	33.6	3161	1.3	2.1	7.9	50879.0	24568.6	3588.5	-	0.48	0.15	-	42.6
292	B	291	281	48.661	-0.306	33.6	785	0.7	3.2	7.9	11772.5	6966.0	1272.8	2399.0	0.59	0.18	0.34	46.0
293	B	291	292	48.661	-0.306	33.6	294	0.5	4.1	7.9	4217.7	2625.2	625.7	1067.7	0.62	0.24	0.41	41.9
294	T	294	-	48.172	0.202	32.9	51	0.4	2.1	4.0	386.3	197.2	27.0	-	0.51	0.14	-	28.7
295	L	291	286	48.548	-0.355	33.6	35	0.3	3.4	5.5	362.9	179.3	19.9	-	0.49	0.11	-	31.1
296	L	291	282	48.585	-0.322	34.2	114	0.4	3.3	5.4	1158.5	605.1	121.4	126.5	0.52	0.20	0.21	39.0
297	L	291	293	48.661	-0.306	33.6	187	0.4	4.5	7.9	2748.1	1754.7	434.5	754.8	0.64	0.25	0.43	40.8
298	L	291	293	48.659	-0.275	34.2	23	0.4	4.6	6.0	251.2	175.6	40.3	48.3	0.70	0.23	0.28	38.2
299	T	299	-	48.831	-0.473	34.2	47	0.4	2.1	4.7	356.8	181.7	22.6	52.5	0.51	0.12	0.29	71.2
300	T	300	-	48.170	-0.464	34.2	55	0.4	2.1	3.7	464.1	178.7	20.0	-	0.39	0.11	-	20.9
301	T	301	-	48.375	-0.417	34.2	152	0.4	2.1	4.4	628.7	477.5	28.2	-	0.76	0.06	-	24.3
302	L	291	284	48.600	-0.282	34.9	105	0.5	3.1	5.4	1044.5	572.2	94.6	101.1	0.55	0.17	0.18	46.7
303	L	291	292	48.680	-0.254	34.2	184	0.5	4.1	6.9	1880.2	1367.1	206.9	440.5	0.73	0.15	0.32	46.5
304	L	305	305	48.401	0.280	34.9	129	0.7	2.3	5.9	1552.9	846.9	160.4	-	0.55	0.19	-	35.2
305	T	305	-	48.401	0.280	34.9	203	0.8	2.1	5.9	2295.0	1261.2	169.0	-	0.55	0.13	-	34.6
306	T	306	-	48.548	0.398	35.5	119	0.7	2.1	5.2	1696.5	796.8	154.9	-	0.47	0.19	-	28.8
307	L	291	285	48.543	-0.287	35.5	225	0.7	2.7	4.6	1950.5	1196.3	146.3	-	0.61	0.12	-	32.7
308	T	308	-	48.746	-0.259	36.2	103	0.6	2.1	4.6	945.4	464.5	40.0	103.8	0.49	0.09	0.22	69.4
309	L	291	283	48.642	-0.240	35.5	29	0.5	2.9	4.8	208.8	152.2	18.2	20.3	0.73	0.12	0.13	47.7
310	L	305	305	48.423	0.277	36.2	34	0.8	2.3	4.4	244.6	182.2	-	-	0.74	-	-	33.0
311	T	311	-	48.609	0.353	36.8	190	0.9	2.1	7.2	4456.4	1622.1	228.6	-	0.36	0.14	-	27.4
312	T	312	-	49.516	-0.854	36.2	68	0.6	2.1	6.2	948.6	429.8	62.7	-	0.45	0.15	-	19.6
313	T	313	-	48.205	-0.570	35.5	47	0.4	2.1	3.7	199.1	142.1	30.7	-	0.71	0.22	-	19.8
314	T	314	-	48.491	-0.360	36.2	128	1.2	2.1	4.4	1343.5	633.7	58.3	-	0.47	0.09	-	23.8
315	T	315	-	48.800	-0.355	35.5	69	0.4	2.1	4.2	831.7	292.3	43.4	99.8	0.35	0.15	0.34	56.5
316	L	291	276	48.522	-0.327	36.8	44	0.8	2.2	3.7	418.8	202.1	-	-	0.48	-	-	27.5
317	B	320	320	49.549	-0.882	43.3	2164	2.3	2.1	9.1	35768.5	18514.2	2980.7	-	0.52	0.16	-	17.0
318	B	320	326	49.490	-0.929	36.8	497	1.0	2.4	5.1	5903.6	2835.3	452.2	-	0.48	0.16	-	16.2
319	B	320	321	49.471	-0.906	37.5	280	0.8	2.7	4.8	2973.4	1499.6	235.1	-	0.50	0.16	-	16.6
320	T	320	-	49.549	-0.882	43.3	2431	2.3	2.1	9.1	39837.6	20605.6	3300.2	-	0.52	0.16	-	16.8
321	B	320	318	49.490	-0.929	36.8	353	0.8	2.6	5.1	3845.3	1926.0	291.6	-	0.50	0.15	-	16.4
322	T	322	-	48.359	-0.495	36.8	194	0.4	2.1	4.6	1486.5	742.7	78.7	-	0.50	0.11	-	24.4
323	T	323	-	48.829	-0.381	36.2	40	0.5	2.1	4.3	394.6	145.7	20.0	57.1	0.37	0.14	0.39	69.5
324	T	324	-	48.465	0.270	36.8	35	0.5	2.1	4.2	229.9	138.0	-	-	0.60	-	-	30.5

325	T	325	-	49.462	-0.955	36.8	68	0.4	2.1	3.6	484.3	234.3	30.2	-	0.48	0.13	-	14.8
326	B	320	317	49.490	-0.929	36.8	611	1.3	2.2	5.1	7993.4	3789.8	609.5	-	0.47	0.16	-	16.3
327	L	320	321	49.490	-0.929	36.8	49	0.4	2.7	5.1	498.3	241.2	27.0	-	0.48	0.11	-	14.9
328	B	320	319	49.471	-0.906	37.5	125	0.7	2.9	4.8	1229.3	631.4	96.0	-	0.51	0.15	-	16.5
329	L	320	328	49.471	-0.896	38.1	49	0.8	3.1	4.7	483.5	253.1	48.1	-	0.52	0.19	-	16.6
330	L	322	322	48.359	-0.495	36.8	33	0.5	2.5	4.6	271.1	154.0	-	-	0.57	-	-	24.0
331	T	331	-	48.510	-0.473	38.1	303	0.7	2.1	5.1	3829.7	2124.7	392.9	-	0.55	0.18	-	21.4
332	L	322	322	48.359	-0.469	36.8	31	0.3	2.5	4.3	199.4	109.3	-	-	0.55	-	-	24.5
333	T	333	-	48.541	-0.070	36.8	55	0.3	2.1	4.6	412.4	211.7	-	54.4	0.51	-	0.26	33.3
334	T	334	-	48.441	0.268	36.8	51	0.4	2.1	3.8	361.2	194.8	37.2	-	0.54	0.19	-	31.7
335	T	335	-	48.576	0.384	36.8	23	0.4	2.2	4.6	222.6	97.3	-	-	0.44	-	-	36.1
336	T	336	-	48.094	0.948	38.1	88	0.6	2.1	4.7	786.5	409.4	49.7	-	0.52	0.12	-	14.6
337	L	320	328	49.471	-0.906	37.5	42	0.4	3.2	4.8	330.4	197.7	25.4	-	0.60	0.13	-	15.7
338	L	320	319	49.490	-0.891	36.8	46	0.6	3.0	4.4	410.0	218.4	40.6	-	0.53	0.19	-	17.9
339	B	342	342	49.953	-0.556	38.1	279	0.9	2.2	5.4	2987.5	1380.9	165.3	-	0.46	0.12	-	23.9
340	B	342	339	49.953	-0.556	38.1	238	0.7	2.2	5.4	2499.6	1142.0	152.3	-	0.46	0.13	-	23.7
341	L	342	340	49.953	-0.556	38.1	86	0.7	2.5	5.4	733.7	378.8	58.4	-	0.52	0.15	-	22.8
342	T	342	-	49.953	-0.556	38.1	386	0.8	2.1	5.4	4129.0	1864.9	235.1	-	0.45	0.13	-	23.8
343	L	291	271	48.538	-0.308	38.1	33	0.5	2.6	4.2	271.2	140.8	-	-	0.52	-	-	30.3
344	T	344	-	49.660	-0.131	38.1	50	0.4	2.1	4.8	538.6	219.2	-	-	0.41	-	-	42.5
345	T	345	-	48.685	0.372	38.1	133	0.6	2.1	4.5	1336.0	688.4	122.2	-	0.52	0.18	-	26.9
346	T	346	-	48.725	0.398	37.5	115	0.3	2.1	4.5	850.0	375.0	51.1	-	0.44	0.14	-	28.2
347	T	347	-	49.351	-0.986	40.1	63	1.3	2.1	4.5	523.0	329.3	-	-	0.63	-	-	14.8
348	L	354	360	49.445	-0.974	40.1	41	0.9	2.2	3.9	216.4	209.0	18.8	-	0.97	0.09	-	14.6
349	L	350	350	49.313	-0.991	39.4	79	0.9	2.2	3.9	642.5	396.2	73.6	-	0.62	0.19	-	14.8
350	T	350	-	49.329	-0.889	40.7	2137	1.2	2.1	5.8	20211.2	12571.4	1777.1	-	0.62	0.14	-	15.1
351	B	354	364	49.414	-0.967	38.1	82	0.7	2.3	3.9	446.6	370.4	58.8	-	0.83	0.16	-	14.7
352	B	350	367	49.329	-0.889	40.7	1072	1.0	2.4	5.8	8897.5	6073.0	937.1	-	0.68	0.15	-	15.0
353	B	350	350	49.329	-0.889	40.7	1840	1.1	2.2	5.8	16661.2	10641.9	1535.1	-	0.64	0.14	-	15.1
354	T	354	-	49.403	-0.986	38.8	270	1.0	2.1	4.5	1854.0	1345.8	170.7	-	0.73	0.13	-	14.6
355	L	320	318	49.452	-0.929	38.1	32	0.6	2.6	4.4	247.5	129.1	45.4	-	0.52	0.35	-	15.4
356	T	356	-	48.718	0.365	38.1	28	0.4	2.1	3.9	168.8	98.2	-	-	0.58	-	-	28.1
357	L	350	382	49.289	-0.991	39.4	66	0.7	2.4	4.8	365.9	335.0	88.8	-	0.92	0.27	-	15.3
358	B	350	369	49.329	-0.889	40.7	1700	1.1	2.2	5.8	15129.8	9791.2	1427.9	-	0.65	0.15	-	15.0
359	B	350	358	49.329	-0.889	40.7	1529	1.1	2.3	5.8	12979.9	8536.1	1242.6	-	0.66	0.15	-	15.1
360	B	354	354	49.403	-0.986	38.8	227	0.9	2.1	4.5	1473.2	1141.6	154.0	-	0.77	0.13	-	14.6
361	L	409	409	49.537	-0.983	39.4	51	0.8	2.1	4.1	460.1	216.8	-	-	0.47	-	-	13.3
362	L	354	364	49.403	-0.986	38.8	55	0.8	2.3	4.5	373.1	272.1	31.3	-	0.73	0.12	-	14.5
363	L	354	351	49.414	-0.967	38.1	30	0.3	2.4	3.9	161.7	121.4	24.5	-	0.75	0.20	-	14.7
364	B	354	360	49.403	-0.986	38.8	141	0.9	2.2	4.5	854.0	658.1	93.8	-	0.77	0.14	-	14.7
365	B	350	382	49.329	-0.889	40.7	1203	1.0	2.4	5.8	10073.3	6777.8	981.4	-	0.67	0.14	-	15.0

366	L	350	390	49.301	-0.960	40.1	20	1.0	2.8	4.8	169.3	106.8	12.7	-	0.63	0.12	-	15.3
367	B	350	365	49.329	-0.889	40.7	1138	1.0	2.4	5.8	9548.8	6436.7	948.1	-	0.67	0.15	-	15.0
368	B	350	388	49.329	-0.889	40.7	862	0.9	2.5	5.8	6793.8	4822.6	755.1	-	0.71	0.16	-	15.0
369	B	350	353	49.329	-0.889	40.7	1736	1.1	2.2	5.8	15502.8	10001.6	1447.6	-	0.65	0.14	-	15.1
370	L	350	372	49.292	-0.929	40.1	120	0.6	2.9	4.8	940.2	577.2	134.6	-	0.61	0.23	-	15.7
371	B	350	387	49.256	-0.948	40.1	356	0.7	2.7	5.1	3191.1	2052.5	410.6	-	0.64	0.20	-	15.3
372	B	350	390	49.256	-0.948	40.1	268	0.7	2.8	5.1	2414.4	1543.6	300.3	-	0.64	0.19	-	14.9
373	T	373	-	49.521	-0.896	38.1	28	0.3	2.1	3.7	186.0	86.8	-	-	0.47	-	-	17.9
374	L	320	326	49.506	-0.872	40.1	41	0.6	2.4	4.5	333.8	213.1	41.1	-	0.64	0.19	-	18.4
375	T	375	-	48.522	-0.653	38.8	21	0.4	2.1	3.7	155.2	89.8	16.0	-	0.58	0.18	-	30.5
376	L	342	342	49.988	-0.603	38.8	79	0.4	2.2	4.6	707.4	326.3	49.1	-	0.46	0.15	-	22.7
377	L	342	340	49.972	-0.556	38.8	31	0.4	2.5	4.0	249.2	117.0	19.1	-	0.47	0.16	-	25.0
378	L	342	339	49.934	-0.514	39.4	21	0.9	2.2	4.1	170.2	101.9	-	-	0.60	-	-	24.7
379	B	320	320	49.462	-0.991	40.7	167	1.0	2.1	5.1	2054.8	1134.7	217.8	-	0.55	0.19	-	13.8
380	L	350	365	49.256	-0.991	39.4	35	0.6	2.4	4.0	237.3	162.1	21.3	-	0.68	0.13	-	15.4
381	B	350	368	49.216	-0.995	41.4	635	0.9	2.6	5.3	5043.6	3547.3	579.1	-	0.70	0.16	-	14.9
382	B	350	414	49.329	-0.889	40.7	1324	1.1	2.4	5.8	11154.5	7535.6	1135.8	-	0.68	0.15	-	15.0
383	L	354	351	49.443	-0.965	39.4	47	0.6	2.3	3.9	217.1	209.9	31.1	-	0.97	0.15	-	14.8
384	T	384	-	49.374	-0.972	41.4	81	0.9	2.1	3.8	479.2	391.9	28.5	-	0.82	0.07	-	14.7
385	L	350	358	49.327	-0.967	40.1	25	0.9	2.3	3.8	155.6	153.9	15.8	-	0.99	0.10	-	14.7
386	L	350	388	49.268	-0.969	39.4	80	0.6	2.5	5.2	664.0	358.9	42.4	-	0.54	0.12	-	14.8
387	B	350	381	49.256	-0.948	40.1	536	0.9	2.7	5.1	4038.2	2939.2	521.6	-	0.73	0.18	-	14.9
388	B	350	352	49.329	-0.889	40.7	935	0.9	2.5	5.8	7492.0	5199.1	796.5	-	0.69	0.15	-	15.0
389	L	350	372	49.256	-0.948	40.1	123	0.6	2.9	5.1	1111.5	762.5	126.8	-	0.69	0.17	-	14.5
390	B	350	371	49.256	-0.948	40.1	289	0.7	2.8	5.1	2648.6	1684.0	317.0	-	0.64	0.19	-	15.0
391	B	320	317	49.549	-0.882	43.3	1530	1.1	2.2	9.1	26608.2	14183.4	2317.3	-	0.53	0.16	-	17.5
392	L	350	414	49.284	-0.920	39.4	125	0.6	2.4	4.3	872.2	483.7	32.7	-	0.55	0.07	-	16.6
393	L	350	371	49.303	-0.910	39.4	39	0.4	2.8	5.0	217.0	196.9	54.9	-	0.91	0.28	-	16.2
394	T	394	-	49.483	-0.821	41.4	50	0.8	2.1	3.6	355.3	220.9	-	-	0.62	-	-	19.6
395	L	397	396	49.905	-0.570	38.8	146	0.8	2.1	6.2	1799.3	884.5	104.4	-	0.49	0.12	-	21.7
396	B	397	397	49.905	-0.570	38.8	178	0.8	2.1	6.2	2081.9	1025.4	109.0	-	0.49	0.11	-	22.2
397	T	397	-	49.905	-0.570	38.8	328	0.8	2.1	6.2	3601.9	1660.3	170.7	-	0.46	0.10	-	24.4
398	L	409	409	49.549	-0.991	39.4	23	0.9	2.1	3.5	207.0	90.4	-	-	0.44	-	-	13.3
399	L	350	381	49.216	-0.995	41.4	60	0.6	2.7	5.3	571.5	353.4	26.1	-	0.62	0.07	-	14.0
400	T	400	-	49.020	-0.983	41.4	36	0.8	2.1	3.5	364.8	163.0	-	-	0.45	-	-	13.8
401	B	320	391	49.549	-0.882	43.3	1022	1.1	2.4	9.1	17416.6	9983.0	1723.0	-	0.57	0.17	-	18.0
402	L	350	387	49.341	-0.948	42.0	177	0.8	2.7	5.0	811.2	862.2	105.0	-	1.06	0.12	-	14.5
403	B	413	413	49.407	-0.913	41.4	170	1.0	2.1	3.9	832.3	910.4	93.3	-	1.09	0.10	-	16.7
404	L	350	368	49.329	-0.889	40.7	78	0.4	2.6	5.8	484.0	428.5	44.6	-	0.89	0.10	-	15.8
405	L	397	396	49.915	-0.540	40.7	19	0.6	2.2	3.7	167.2	92.4	-	-	0.55	-	-	25.8
406	L	397	397	49.868	-0.497	40.1	146	0.5	2.1	3.9	1481.7	620.2	63.9	-	0.42	0.10	-	27.1

407	L	354	354	49.433	-0.986	40.1	23	0.8	2.2	3.9	136.0	83.0	13.5	-	0.61	0.16	-	14.4
408	L	320	379	49.462	-0.991	40.7	21	0.5	2.5	5.1	174.7	114.9	26.7	-	0.66	0.23	-	14.6
409	T	409	-	49.537	-0.983	39.4	73	0.9	2.1	4.1	681.3	311.4	-	-	0.46	-	-	13.3
410	L	320	379	49.480	-0.983	41.4	102	0.9	2.5	4.1	1064.6	639.7	128.1	-	0.60	0.20	-	13.7
411	B	320	401	49.549	-0.882	43.3	684	1.0	2.8	9.1	11026.8	6706.6	1285.0	-	0.61	0.19	-	19.1
412	L	320	411	49.509	-0.953	41.4	54	0.5	3.3	5.1	577.4	323.5	38.2	-	0.56	0.12	-	14.2
413	T	413	-	49.407	-0.913	41.4	187	1.0	2.1	3.9	1003.7	1027.9	115.2	-	1.02	0.11	-	16.7
414	B	350	359	49.329	-0.889	40.7	1449	1.0	2.4	5.8	12039.1	8026.4	1171.3	-	0.67	0.15	-	15.1
415	L	413	403	49.407	-0.913	41.4	77	0.7	2.4	3.9	287.4	345.1	-	-	1.20	-	-	16.9
416	L	320	411	49.549	-0.882	43.3	415	0.8	3.3	9.1	6341.2	4244.7	940.3	-	0.67	0.22	-	22.6
417	L	350	353	49.294	-0.891	40.7	27	0.4	2.3	4.4	133.7	101.6	12.7	-	0.76	0.13	-	16.7
418	T	418	-	49.610	-0.854	40.7	63	0.5	2.1	4.1	578.0	298.4	39.0	-	0.52	0.13	-	18.1
419	T	419	-	49.499	-0.856	40.7	45	1.3	2.1	3.7	270.5	197.6	23.4	-	0.73	0.12	-	19.7
420	T	420	-	49.662	-0.643	40.7	31	0.5	2.1	4.4	480.5	194.5	-	-	0.40	-	-	22.0
421	L	436	436	49.582	-0.190	40.7	74	0.5	2.1	3.6	492.4	338.2	44.6	33.9	0.69	0.13	0.10	35.4
422	L	436	436	49.565	-0.190	41.4	31	0.6	2.2	3.9	160.5	150.8	18.5	17.7	0.94	0.12	0.12	32.9
423	T	423	-	49.152	-0.981	43.3	800	0.8	2.1	5.3	11919.6	5702.8	726.0	-	0.48	0.13	-	14.3
424	B	426	426	48.999	-0.976	41.4	187	0.9	2.3	4.3	1964.2	907.0	66.6	-	0.46	0.07	-	13.3
425	L	426	424	48.999	-0.976	41.4	23	0.3	2.5	4.3	195.0	105.3	23.3	-	0.54	0.22	-	12.6
426	T	426	-	48.999	-0.976	41.4	387	0.8	2.1	4.3	4532.4	2038.2	137.3	-	0.45	0.07	-	13.5
427	T	427	-	49.499	-0.981	43.3	33	0.6	2.1	4.1	222.9	140.3	34.8	-	0.63	0.25	-	13.2
428	L	350	359	49.199	-0.969	41.4	36	0.4	2.4	3.8	280.5	153.0	25.1	-	0.55	0.16	-	14.7
429	L	426	424	48.982	-0.960	42.0	82	0.7	2.5	4.1	865.3	404.8	-	-	0.47	-	-	13.2
430	L	426	426	48.966	-0.939	42.0	128	0.6	2.3	3.8	1355.5	642.9	-	-	0.47	-	-	13.7
431	L	413	413	49.414	-0.929	41.4	20	0.8	2.2	3.8	107.6	83.7	17.1	-	0.78	0.20	-	16.4
432	L	413	403	49.412	-0.924	42.7	46	0.7	2.4	3.8	170.7	199.6	28.0	-	1.17	0.14	-	16.6
433	L	350	352	49.327	-0.872	42.0	52	0.5	2.5	4.8	382.4	294.2	63.8	-	0.77	0.22	-	15.4
434	T	434	-	49.955	-0.613	41.4	31	0.4	2.1	4.4	280.5	134.5	36.9	-	0.48	0.27	-	22.7
435	T	435	-	49.832	-0.436	41.4	81	0.4	2.1	3.5	570.3	271.7	-	-	0.48	-	-	26.3
436	T	436	-	49.565	-0.190	41.4	113	0.6	2.1	3.9	714.7	525.9	70.0	56.6	0.74	0.13	0.11	34.3
437	T	437	-	49.811	-0.133	42.0	147	0.6	2.1	4.5	684.2	695.8	114.9	-	1.02	0.17	-	34.3
438	L	437	437	49.820	-0.145	41.4	44	0.5	2.7	4.4	145.3	217.0	38.9	-	1.49	0.18	-	36.6
439	L	455	455	48.876	0.070	42.7	85	0.4	2.2	4.0	588.4	338.7	70.2	-	0.58	0.21	-	48.2
440	B	423	423	49.152	-0.981	43.3	554	0.8	2.3	5.3	7955.6	4074.8	535.0	-	0.51	0.13	-	14.1
441	L	423	440	49.053	-0.986	44.0	33	0.8	2.4	4.4	440.4	220.4	23.4	-	0.50	0.11	-	13.4
442	B	423	457	49.152	-0.981	43.3	407	0.7	2.5	5.3	5465.8	2996.8	404.0	-	0.55	0.13	-	14.3
443	L	423	423	49.037	-0.967	44.0	67	0.8	2.3	4.1	715.6	342.3	44.2	-	0.48	0.13	-	14.4
444	L	350	367	49.195	-0.965	43.3	38	0.6	2.5	4.1	312.0	174.7	-	-	0.56	-	-	14.9
445	T	445	-	49.405	-0.948	42.7	26	0.6	2.1	3.8	139.1	96.5	-	-	0.69	-	-	15.9
446	B	320	391	49.629	-0.877	42.7	268	0.9	2.4	4.7	3503.4	1716.1	267.2	-	0.49	0.16	-	17.2
447	L	320	446	49.629	-0.877	42.7	123	0.7	2.6	4.7	1570.4	805.4	156.2	-	0.51	0.19	-	17.1

448	L	437	437	49.811	-0.133	42.0	21	0.4	2.7	4.5	115.7	108.1	24.3	-	0.93	0.22	-	31.4
449	B	451	451	49.726	-0.117	42.7	569	1.7	2.2	5.4	5826.4	3736.5	334.0	-	0.64	0.09	-	32.6
450	L	451	452	49.726	-0.117	42.7	180	1.0	2.5	5.4	1694.1	1167.0	110.2	-	0.69	0.09	-	30.9
451	T	451	-	49.726	-0.117	42.7	682	1.7	2.1	5.4	7125.7	4517.5	390.9	-	0.63	0.09	-	32.8
452	B	451	449	49.726	-0.117	42.7	230	1.3	2.4	5.4	2220.0	1504.3	138.8	-	0.68	0.09	-	30.1
453	L	451	451	49.766	-0.079	42.7	57	0.7	2.2	4.2	440.2	279.4	29.9	-	0.63	0.11	-	32.8
454	T	454	-	49.931	-0.077	43.3	23	0.5	2.1	3.7	276.7	114.4	-	-	0.41	-	-	28.2
455	T	455	-	48.876	0.070	42.7	274	0.4	2.1	4.0	1988.5	1062.7	169.4	-	0.53	0.16	-	48.8
456	L	350	369	49.181	-0.995	44.6	36	0.7	2.3	3.7	314.2	175.5	-	-	0.56	-	-	15.2
457	B	423	440	49.152	-0.981	43.3	456	0.7	2.4	5.3	6383.7	3379.9	458.5	-	0.53	0.14	-	14.2
458	B	423	442	49.152	-0.981	43.3	280	0.6	2.7	5.3	3185.3	1922.9	260.1	-	0.60	0.14	-	14.4
459	L	423	458	49.152	-0.981	43.3	131	0.6	3.1	5.3	1250.8	817.8	97.6	-	0.65	0.12	-	14.8
460	T	460	-	49.377	-0.910	44.0	36	0.7	2.1	4.1	305.0	191.9	-	-	0.63	-	-	17.6
461	T	461	-	49.294	-0.646	43.3	115	0.5	2.1	5.0	1268.9	561.9	100.6	-	0.44	0.18	-	20.5
462	T	462	-	49.679	-0.183	44.0	124	0.7	2.1	4.0	958.7	563.7	73.4	-	0.59	0.13	-	58.1
463	B	486	509	49.492	-0.379	61.5	22282	6.6	2.4	25.3	2195105.5	780626.1	91346.7	-	0.36	0.12	-	83.7
464	B	486	551	49.492	-0.379	61.5	22663	6.6	2.4	25.3	2239687.7	793488.3	92409.8	-	0.35	0.12	-	83.1
465	B	486	482	49.492	-0.379	61.5	23790	6.6	2.3	25.3	2361029.6	828018.3	95231.1	-	0.35	0.12	-	81.1
466	B	486	501	49.492	-0.379	61.5	33025	6.3	2.1	25.3	2860885.6	993668.7	109445.0	-	0.35	0.11	-	61.1
467	B	486	570	49.492	-0.379	61.5	32940	6.3	2.1	25.3	2850265.7	990567.8	109202.7	-	0.35	0.11	-	61.2
468	T	468	-	49.225	-0.030	43.3	70	1.0	2.1	4.1	958.5	473.1	50.7	-	0.49	0.11	-	41.3
469	T	469	-	49.365	0.027	44.6	135	1.0	2.1	6.3	1054.0	1163.2	228.9	-	1.10	0.20	-	29.2
470	L	455	472	48.909	0.046	42.7	65	0.3	2.2	3.7	461.8	237.0	38.1	-	0.51	0.16	-	50.8
471	T	471	-	48.869	0.039	42.7	52	0.4	2.1	3.6	407.3	192.4	28.2	-	0.47	0.15	-	52.9
472	B	455	455	48.909	0.046	42.7	163	0.4	2.2	3.7	1133.5	603.3	81.9	-	0.53	0.14	-	49.0
473	L	455	472	48.925	0.074	42.0	84	0.4	2.2	3.7	559.0	319.6	34.3	-	0.57	0.11	-	48.2
474	L	423	442	49.084	-0.993	43.3	46	0.6	2.7	4.5	574.0	305.5	47.2	-	0.53	0.15	-	14.0
475	L	423	458	49.119	-0.981	43.3	67	0.4	3.1	5.0	684.9	428.0	74.5	-	0.62	0.17	-	13.8
476	L	423	457	49.072	-0.991	43.3	26	0.5	2.5	4.3	261.4	116.5	15.2	-	0.45	0.13	-	13.4
477	L	320	401	49.594	-0.896	44.0	26	0.6	2.8	4.6	212.7	192.9	33.0	-	0.91	0.17	-	17.3
478	L	320	446	49.622	-0.891	42.7	49	0.7	2.6	4.1	536.3	256.5	-	-	0.48	-	-	18.0
479	T	479	-	48.907	-0.636	43.3	24	0.4	2.1	5.0	236.3	101.1	19.4	-	0.43	0.19	-	21.4
480	T	480	-	49.688	-0.171	46.6	106	0.9	2.1	4.2	1011.0	589.7	44.0	-	0.58	0.07	-	40.4
481	B	486	555	49.492	-0.379	61.5	23384	6.6	2.3	25.3	2303048.0	811933.2	93942.4	-	0.35	0.12	-	81.8
482	B	486	513	49.492	-0.379	61.5	23891	6.6	2.2	25.3	2370623.1	830985.7	95457.8	-	0.35	0.11	-	80.9
483	B	486	628	49.492	-0.379	61.5	27184	6.5	2.2	25.3	2540625.5	882235.0	100229.5	-	0.35	0.11	-	72.9
484	B	486	606	49.492	-0.379	61.5	23158	6.6	2.3	25.3	2284798.8	806476.1	93519.0	-	0.35	0.12	-	82.6
485	B	486	569	49.492	-0.379	61.5	21560	6.5	2.5	25.3	2114015.3	756499.7	89327.5	-	0.36	0.12	-	85.1
486	T	486	-	49.492	-0.379	61.5	33566	6.3	2.1	25.3	2886962.3	1001570.9	109898.9	-	0.35	0.11	-	60.5
487	B	486	488	49.492	-0.379	61.5	21870	6.5	2.5	25.3	2145444.4	765857.9	90047.1	-	0.36	0.12	-	84.4
488	B	486	463	49.492	-0.379	61.5	22101	6.5	2.5	25.3	2170784.0	773397.7	90754.6	-	0.36	0.12	-	83.9

489	B	486	502	49.492	-0.379	61.5	18048	6.4	2.8	25.3	1842796.9	666571.5	80126.4	-	0.36	0.12	-	98.6
490	B	486	540	49.492	-0.379	61.5	13112	6.4	3.4	25.3	1442585.9	536851.3	67046.7	473037.0	0.37	0.12	0.88	121.5
491	B	486	528	49.492	-0.379	61.5	12646	6.4	3.5	25.3	1384531.1	518659.9	65119.8	460096.8	0.37	0.13	0.89	123.3
492	L	486	533	49.291	-0.044	45.3	114	1.4	3.8	6.5	1689.6	1106.5	184.7	262.6	0.65	0.17	0.24	39.0
493	B	486	534	49.492	-0.379	61.5	16291	6.4	3.0	25.3	1716057.4	625870.5	75792.5	-	0.36	0.12	-	107.0
494	B	486	596	49.492	-0.379	61.5	16026	6.4	3.0	25.3	1683714.2	615968.4	74885.5	-	0.37	0.12	-	107.4
495	B	486	550	49.492	-0.379	61.5	18725	6.4	2.7	25.3	1933772.8	695106.1	82743.8	-	0.36	0.12	-	97.4
496	B	486	527	49.492	-0.379	61.5	19363	6.4	2.7	25.3	1997945.2	713319.6	84222.0	-	0.36	0.12	-	94.8
497	B	486	545	49.492	-0.379	61.5	22994	6.6	2.4	25.3	2264143.5	800783.6	93052.2	-	0.35	0.12	-	82.8
498	B	486	538	49.492	-0.379	61.5	24077	6.6	2.2	25.3	2393409.5	837302.5	96036.5	-	0.35	0.11	-	80.7
499	B	486	577	49.492	-0.379	61.5	26804	6.5	2.2	25.3	2517184.2	875405.2	99649.6	-	0.35	0.11	-	73.7
500	B	486	464	49.492	-0.379	61.5	22435	6.6	2.4	25.3	2213441.3	785939.3	91774.3	-	0.36	0.12	-	83.4
501	B	486	524	49.492	-0.379	61.5	33189	6.3	2.1	25.3	2866147.1	995320.8	109524.0	-	0.35	0.11	-	60.9
502	B	486	595	49.492	-0.379	61.5	18276	6.4	2.8	25.3	1873118.1	675430.9	80955.1	-	0.36	0.12	-	98.1
503	B	486	496	49.492	-0.379	61.5	18985	6.4	2.7	25.3	1965812.7	704741.8	83487.4	-	0.36	0.12	-	96.8
504	B	486	532	49.492	-0.379	61.5	16219	6.4	3.0	25.3	1706980.1	622889.2	75550.5	-	0.36	0.12	-	106.8
505	B	486	507	49.492	-0.379	61.5	14777	6.4	3.2	25.3	1551213.7	573889.5	70919.1	-	0.37	0.12	-	111.3
506	B	486	590	49.492	-0.379	61.5	18542	6.4	2.8	25.3	1912741.3	688861.0	82200.8	-	0.36	0.12	-	97.3
507	B	486	543	49.492	-0.379	61.5	15058	6.4	3.2	25.3	1587830.2	585185.0	72084.8	-	0.37	0.12	-	110.4
508	B	486	489	49.492	-0.379	61.5	17973	6.4	2.9	25.3	1832958.4	663510.1	79825.3	-	0.36	0.12	-	98.6
509	B	486	500	49.492	-0.379	61.5	22329	6.6	2.4	25.3	2202235.9	782678.4	91525.1	-	0.36	0.12	-	83.7
510	B	486	485	49.492	-0.379	61.5	21145	6.5	2.6	25.3	2070952.6	743754.6	88173.5	-	0.36	0.12	-	86.1
511	B	486	539	49.492	-0.379	61.5	24547	6.6	2.2	25.3	2418220.6	844919.2	96656.8	-	0.35	0.11	-	79.5
512	L	486	465	49.310	-0.022	43.3	43	0.5	2.3	4.2	299.6	172.2	-	22.5	0.57	-	0.13	36.7
513	B	486	514	49.492	-0.379	61.5	23915	6.6	2.2	25.3	2374901.6	832214.7	95565.4	-	0.35	0.11	-	80.9
514	B	486	498	49.492	-0.379	61.5	24042	6.6	2.2	25.3	2388046.3	835714.6	95905.8	-	0.35	0.11	-	80.7
515	T	515	-	48.961	0.166	44.0	58	0.6	2.1	3.5	379.7	227.5	44.6	-	0.60	0.20	-	38.1
516	T	516	-	48.850	-0.617	44.0	54	0.4	2.1	4.9	467.4	227.1	24.6	-	0.49	0.11	-	32.6
517	L	486	555	49.417	-0.244	45.9	26	0.6	2.3	4.2	270.6	172.9	17.6	130.9	0.64	0.10	0.76	78.5
518	T	518	-	49.986	-0.141	46.6	1149	1.2	2.1	10.8	22716.0	12056.3	1580.6	-	0.53	0.13	-	29.7
519	B	518	518	49.986	-0.141	46.6	827	1.1	2.3	10.8	17613.1	9851.1	1356.6	-	0.56	0.14	-	30.3
520	L	451	452	49.754	-0.107	45.9	22	0.9	2.5	4.0	153.3	106.4	13.5	-	0.69	0.13	-	27.8
521	B	486	547	49.492	-0.379	61.5	27446	6.5	2.1	25.3	2568940.1	890258.5	100837.2	-	0.35	0.11	-	72.7
522	B	486	465	49.492	-0.379	61.5	23620	6.6	2.3	25.3	2340459.0	822311.4	94782.3	-	0.35	0.12	-	81.5
523	B	486	499	49.492	-0.379	61.5	26603	6.5	2.2	25.3	2507172.1	872829.7	99399.0	-	0.35	0.11	-	73.7
524	B	486	486	49.492	-0.379	61.5	33317	6.3	2.1	25.3	2875723.9	998045.9	109704.2	-	0.35	0.11	-	60.8
525	L	486	488	49.263	-0.046	44.6	25	0.5	2.5	4.2	286.1	121.7	-	9.8	0.43	-	0.08	40.2
526	B	486	574	49.424	-0.053	45.9	1183	1.9	2.7	8.5	14700.3	12756.6	2300.8	3610.5	0.87	0.18	0.28	38.5
527	B	486	510	49.492	-0.379	61.5	19583	6.4	2.6	25.3	2026682.0	721575.2	84961.0	-	0.36	0.12	-	94.2
528	B	486	490	49.492	-0.379	61.5	12945	6.4	3.4	25.3	1421794.6	530555.6	66411.5	468559.4	0.37	0.13	0.88	122.3
529	B	486	748	49.492	-0.379	61.5	27231	6.5	2.2	25.3	2547311.7	884117.3	100394.1	-	0.35	0.11	-	72.9

530	B	486	526	49.424	-0.053	45.9	1046	1.9	2.8	8.5	12563.4	11316.7	2099.3	3286.5	0.90	0.19	0.29	38.5
531	B	486	530	49.424	-0.053	45.9	958	1.8	2.9	8.5	10958.4	10437.9	2002.4	3082.7	0.95	0.19	0.30	38.3
532	B	486	598	49.492	-0.379	61.5	16232	6.4	3.0	25.3	1709362.5	623617.6	75602.5	-	0.36	0.12	-	106.8
533	B	486	491	49.291	-0.044	45.3	208	1.7	3.6	6.5	3040.6	1968.2	320.1	408.5	0.65	0.16	0.21	39.5
534	B	486	571	49.492	-0.379	61.5	16334	6.4	3.0	25.3	1721191.3	627499.3	75919.4	-	0.36	0.12	-	106.8
535	B	486	612	49.492	-0.379	61.5	17835	6.4	2.9	25.3	1817088.8	658704.2	79434.1	-	0.36	0.12	-	99.1
536	B	486	510	49.424	-0.053	45.9	1365	2.3	2.6	8.5	19373.2	14973.6	2545.8	4315.2	0.77	0.17	0.29	38.7
537	L	486	599	49.424	-0.053	45.9	654	1.0	3.1	8.5	6154.5	7290.5	1550.3	2263.6	1.18	0.21	0.31	36.3
538	B	486	553	49.492	-0.379	61.5	24147	6.6	2.2	25.3	2399370.1	838984.6	96148.9	-	0.35	0.11	-	80.5
539	B	486	546	49.492	-0.379	61.5	24619	6.6	2.2	25.3	2422037.0	846015.9	96747.4	-	0.35	0.11	-	79.5
540	B	486	803	49.492	-0.379	61.5	13271	6.4	3.3	25.3	1467745.4	544509.9	67883.8	478850.5	0.37	0.12	0.88	120.9
541	B	486	497	49.492	-0.379	61.5	22903	6.6	2.4	25.3	2260140.1	799570.2	92949.2	-	0.35	0.12	-	83.0
542	B	486	579	49.492	-0.379	61.5	17310	6.3	2.9	25.3	1789037.7	649054.5	78403.6	-	0.36	0.12	-	101.7
543	B	486	580	49.492	-0.379	61.5	15546	6.4	3.1	25.3	1628733.4	598976.0	73376.5	-	0.37	0.12	-	107.9
544	B	486	602	49.492	-0.379	61.5	15912	6.4	3.0	25.3	1666962.6	610543.9	74371.1	-	0.37	0.12	-	107.7
545	B	486	484	49.492	-0.379	61.5	23020	6.6	2.4	25.3	2266229.7	801421.6	93097.6	-	0.35	0.12	-	82.8
546	B	486	523	49.492	-0.379	61.5	24703	6.6	2.2	25.3	2434790.7	849629.0	97008.6	-	0.35	0.11	-	79.3
547	B	486	467	49.492	-0.379	61.5	32892	6.3	2.1	25.3	2848266.0	989975.2	109170.1	-	0.35	0.11	-	61.2
548	B	486	505	49.492	-0.379	61.5	13626	6.4	3.3	25.3	1493330.3	553494.9	68808.5	484029.8	0.37	0.12	0.87	119.2
549	T	549	-	49.367	-0.025	44.6	30	0.6	2.1	3.9	186.9	147.9	-	1.6	0.79	-	0.01	38.7
550	B	486	591	49.492	-0.379	61.5	18768	6.4	2.7	25.3	1939134.7	696548.6	82845.1	-	0.36	0.12	-	97.5
551	B	486	541	49.492	-0.379	61.5	22752	6.6	2.4	25.3	2248593.8	796201.4	92631.7	-	0.35	0.12	-	83.0
552	B	486	506	49.492	-0.379	61.5	18483	6.4	2.8	25.3	1899426.0	683109.1	81635.9	-	0.36	0.12	-	97.5
553	B	486	511	49.492	-0.379	61.5	24159	6.6	2.2	25.3	2402203.0	839797.4	96225.9	-	0.35	0.11	-	80.5
554	T	554	-	49.499	-0.046	47.9	250	1.0	2.1	4.4	1568.2	1203.5	101.7	301.8	0.77	0.08	0.25	29.5
555	B	486	522	49.492	-0.379	61.5	23423	6.6	2.3	25.3	2310173.5	814056.4	94117.7	-	0.35	0.12	-	81.8
556	B	486	521	49.492	-0.379	61.5	27323	6.5	2.1	25.3	2553220.3	885887.5	100549.9	-	0.35	0.11	-	72.8
557	T	557	-	48.767	0.018	45.3	120	0.6	2.1	4.7	1175.2	579.4	47.1	130.6	0.49	0.08	0.23	58.0
558	L	486	536	49.414	0.006	44.6	77	0.5	2.7	4.2	299.2	366.8	39.0	99.9	1.23	0.11	0.27	35.8
559	T	559	-	49.969	0.060	44.6	126	0.5	2.1	4.0	935.8	664.8	86.8	-	0.71	0.13	-	29.0
560	T	560	-	49.917	0.055	44.6	246	0.5	2.1	4.8	1777.0	1381.2	136.8	-	0.78	0.10	-	28.8
561	T	561	-	48.966	0.148	43.3	25	0.5	2.1	3.7	194.2	124.8	-	-	0.64	-	-	39.4
562	T	562	-	48.857	0.197	45.3	272	0.9	2.1	4.7	3793.1	1928.5	179.9	-	0.51	0.09	-	40.9
563	L	562	562	48.838	0.155	45.3	74	0.7	2.2	4.1	953.4	435.6	-	-	0.46	-	-	45.0
564	L	562	562	48.857	0.197	45.3	169	0.9	2.2	4.7	2345.3	1292.0	136.5	-	0.55	0.11	-	39.6
565	T	565	-	48.914	0.256	45.3	411	1.0	2.1	5.1	7135.3	3460.5	223.7	-	0.48	0.06	-	37.1
566	T	566	-	49.112	-0.913	45.3	56	0.6	2.1	3.5	512.2	237.0	21.5	-	0.46	0.09	-	14.6
567	T	567	-	49.232	-0.528	44.6	45	0.4	2.1	3.8	511.0	185.9	27.6	-	0.36	0.15	-	33.0
568	L	451	449	49.726	-0.117	45.3	42	1.0	2.4	4.4	471.0	283.9	50.0	-	0.60	0.18	-	32.8
569	B	486	487	49.492	-0.379	61.5	21622	6.5	2.5	25.3	2121423.8	758613.5	89470.4	-	0.36	0.12	-	85.0
570	B	486	466	49.492	-0.379	61.5	32968	6.3	2.1	25.3	2852801.8	991417.9	109273.1	-	0.35	0.11	-	61.2

571	B	486	581	49.492	-0.379	61.5	17140	6.3	2.9	25.3	1774891.9	644599.1	77957.3	-	0.36	0.12	-	102.4
572	B	486	575	49.424	-0.053	45.9	785	1.8	3.0	8.5	9214.9	8922.4	1756.5	2784.2	0.97	0.20	0.31	37.3
573	B	486	544	49.492	-0.379	61.5	15783	6.4	3.1	25.3	1652387.8	606068.0	73912.6	-	0.37	0.12	-	108.2
574	B	486	536	49.424	-0.053	45.9	1266	2.3	2.7	8.5	18601.3	14326.5	2478.0	4145.1	0.77	0.17	0.29	39.0
575	B	486	531	49.424	-0.053	45.9	856	1.8	3.0	8.5	9917.7	9526.0	1835.0	2892.7	0.96	0.19	0.30	37.9
576	L	486	575	49.376	-0.041	45.3	55	0.6	3.1	5.8	375.5	369.9	45.2	51.5	0.99	0.12	0.14	44.7
577	B	486	483	49.492	-0.379	61.5	27073	6.5	2.2	25.3	2525327.4	878043.4	99904.6	-	0.35	0.11	-	73.0
578	B	486	504	49.492	-0.379	61.5	16063	6.4	3.0	25.3	1689686.1	617842.8	75051.1	-	0.37	0.12	-	107.3
579	B	486	535	49.492	-0.379	61.5	17394	6.3	2.9	25.3	1792125.3	650041.6	78456.8	-	0.36	0.12	-	101.4
580	B	486	573	49.492	-0.379	61.5	15672	6.4	3.1	25.3	1640817.3	602557.6	73680.9	-	0.37	0.12	-	107.3
581	B	486	542	49.492	-0.379	61.5	17164	6.3	2.9	25.3	1777862.9	645462.8	78035.4	-	0.36	0.12	-	102.4
582	L	554	554	49.509	-0.032	45.9	30	0.7	2.3	4.1	109.2	145.9	27.5	28.8	1.34	0.19	0.20	28.3
583	T	583	-	49.055	-0.060	46.6	589	0.8	2.1	4.6	8828.4	3702.5	335.0	-	0.42	0.09	-	53.1
584	B	554	554	49.499	-0.046	47.9	154	1.0	2.3	4.4	975.2	698.2	49.5	196.4	0.72	0.07	0.28	29.6
585	L	486	526	49.443	-0.011	44.6	26	0.4	2.9	4.3	97.9	133.2	20.3	33.8	1.36	0.15	0.25	35.9
586	L	588	588	48.706	0.058	45.9	94	1.0	2.1	4.2	981.1	513.4	59.3	94.3	0.52	0.12	0.18	60.6
587	L	588	588	48.682	0.072	46.6	135	0.9	2.1	4.0	1240.3	574.6	54.0	74.8	0.46	0.09	0.13	65.0
588	T	588	-	48.706	0.058	45.9	239	1.0	2.1	4.2	2324.6	1133.9	117.4	171.7	0.49	0.10	0.15	62.5
589	T	589	-	48.734	0.091	44.6	21	0.6	2.1	3.7	164.0	97.3	-	14.7	0.59	-	0.15	50.6
590	B	486	495	49.492	-0.379	61.5	18617	6.4	2.7	25.3	1918788.4	690648.6	82337.8	-	0.36	0.12	-	97.5
591	B	486	503	49.492	-0.379	61.5	18851	6.4	2.7	25.3	1946419.7	699074.6	83067.5	-	0.36	0.12	-	97.2
592	B	486	535	49.291	-0.188	46.6	309	0.8	2.9	6.2	5771.7	2807.1	404.4	697.6	0.49	0.14	0.25	61.0
593	L	518	519	49.986	-0.141	46.6	331	0.9	3.2	10.8	8451.7	5300.6	802.5	-	0.63	0.15	-	38.8
594	T	594	-	49.879	-0.133	45.3	39	0.6	2.1	3.9	258.6	146.2	-	-	0.57	-	-	31.8
595	B	486	600	49.492	-0.379	61.5	18364	6.4	2.8	25.3	1882422.6	678124.9	81201.8	-	0.36	0.12	-	97.8
596	B	486	578	49.492	-0.379	61.5	16033	6.4	3.0	25.3	1685086.7	616470.3	74935.5	-	0.37	0.12	-	107.4
597	T	597	-	49.726	-0.011	48.5	1204	1.3	2.1	10.6	25668.3	14897.2	2093.8	-	0.58	0.14	-	32.7
598	B	486	493	49.492	-0.379	61.5	16251	6.4	3.0	25.3	1713171.9	624787.9	75741.8	-	0.36	0.12	-	106.8
599	B	486	572	49.424	-0.053	45.9	751	1.8	3.1	8.5	8245.6	8233.3	1673.0	2625.4	1.00	0.20	0.32	37.2
600	B	486	552	49.492	-0.379	61.5	18387	6.4	2.8	25.3	1883394.5	678373.2	81219.5	-	0.36	0.12	-	97.7
601	L	554	584	49.525	-0.030	45.9	60	0.5	2.3	4.3	175.9	256.5	28.2	78.7	1.46	0.11	0.31	28.3
602	B	486	494	49.492	-0.379	61.5	15926	6.4	3.0	25.3	1669348.6	611433.8	74422.2	-	0.37	0.12	-	107.7
603	B	597	605	49.726	-0.011	48.5	694	1.0	2.8	10.6	12990.3	9204.0	1517.0	-	0.71	0.16	-	33.0
604	B	597	652	49.726	-0.011	48.5	578	1.0	2.9	10.6	10813.9	7976.2	1367.5	-	0.74	0.17	-	33.0
605	B	597	597	49.726	-0.011	48.5	1080	1.2	2.2	10.6	22905.0	13683.7	1963.3	-	0.60	0.14	-	32.6
606	B	486	481	49.492	-0.379	61.5	23160	6.6	2.3	25.3	2286501.3	806986.1	93583.6	-	0.35	0.12	-	82.6
607	L	565	565	48.914	0.256	45.3	72	0.7	3.1	5.1	917.2	516.9	43.1	-	0.56	0.08	-	36.6
608	T	608	-	48.975	0.282	45.9	57	0.7	2.1	4.7	1069.8	419.4	-	-	0.39	-	-	40.5
609	L	658	633	48.985	-0.509	47.2	309	0.5	2.1	4.8	2678.4	1708.7	421.3	429.7	0.64	0.25	0.25	42.1
610	T	610	-	48.772	-0.221	47.2	111	0.6	2.1	6.0	2124.2	927.7	142.9	529.1	0.44	0.15	0.57	74.9
611	L	486	592	49.291	-0.188	46.6	185	0.7	3.2	6.2	3644.5	1788.7	274.2	458.6	0.49	0.15	0.26	59.8

612	B	486	508	49.492	-0.379	61.5	17895	6.4	2.9	25.3	1819225.6	659384.7	79483.7	-	0.36	0.12	-	98.9
613	L	518	519	49.924	-0.152	47.9	95	1.2	3.2	5.1	1084.7	565.5	110.6	-	0.52	0.20	-	28.6
614	L	486	570	49.414	-0.155	46.6	37	0.7	2.1	4.2	437.5	241.3	-	192.0	0.55	-	0.80	89.2
615	B	486	618	49.492	-0.379	61.5	11230	6.3	3.7	25.3	1258458.7	475489.0	60540.5	430263.6	0.38	0.13	0.90	127.1
616	B	486	647	49.492	-0.379	61.5	9625	6.2	4.1	25.3	1114786.3	428410.9	55182.8	396108.0	0.38	0.13	0.92	143.0
617	B	486	669	49.492	-0.379	61.5	9340	6.2	4.3	25.3	1070032.4	414188.1	53526.2	384193.0	0.39	0.13	0.93	144.7
618	B	486	641	49.492	-0.379	61.5	11608	6.3	3.6	25.3	1297882.5	488071.0	61841.5	439639.1	0.38	0.13	0.90	126.9
619	B	486	643	49.492	-0.379	61.5	11754	6.3	3.6	25.3	1312942.4	493006.0	62357.3	443814.1	0.38	0.13	0.90	127.2
620	B	486	637	49.492	-0.379	61.5	10115	6.2	3.9	25.3	1178060.5	448409.5	57474.7	412162.1	0.38	0.13	0.92	138.8
621	T	621	-	49.039	-0.096	47.2	280	0.6	2.1	4.8	3362.7	1348.1	123.5	-	0.40	0.09	-	64.2
622	L	621	624	49.044	-0.117	46.6	35	0.5	2.5	4.6	434.1	214.3	-	-	0.49	-	-	63.2
623	L	621	624	49.032	-0.117	45.9	66	0.5	2.5	4.3	900.9	363.7	36.1	66.6	0.40	0.10	0.18	63.5
624	B	621	621	49.044	-0.117	46.6	121	0.5	2.4	4.6	1588.7	679.0	60.7	-	0.43	0.09	-	63.8
625	L	486	572	49.424	-0.084	46.6	21	0.7	3.2	5.2	154.1	125.2	-	16.0	0.81	-	0.13	40.9
626	T	626	-	49.716	-0.065	48.5	79	1.2	2.1	3.7	668.2	402.7	-	-	0.60	-	-	32.0
627	B	486	548	49.492	-0.379	61.5	13458	6.4	3.3	25.3	1477212.9	547863.2	68246.0	480626.6	0.37	0.12	0.88	120.5
628	B	486	529	49.492	-0.379	61.5	27186	6.5	2.2	25.3	2541782.5	882590.2	100252.5	-	0.35	0.11	-	72.9
629	L	597	605	49.773	0.065	46.6	96	0.6	2.8	5.5	1506.6	644.9	81.5	-	0.43	0.13	-	25.5
630	T	630	-	48.630	0.100	45.9	45	0.4	2.1	3.7	349.4	204.2	19.3	27.3	0.58	0.09	0.13	67.1
631	T	631	-	48.449	0.225	46.6	82	0.6	2.1	4.2	616.4	393.6	58.7	-	0.64	0.15	-	37.5
632	L	565	565	48.888	0.261	46.6	43	0.5	3.1	4.6	311.1	234.8	-	-	0.75	-	-	37.9
633	B	658	658	49.055	-0.556	47.2	444	0.8	2.1	4.9	3792.1	2439.7	542.0	-	0.64	0.22	-	38.9
634	B	486	636	49.492	-0.379	61.5	12158	6.3	3.6	25.3	1351134.9	504838.8	63408.5	453297.9	0.37	0.13	0.90	126.7
635	B	486	649	49.492	-0.379	61.5	8709	6.2	4.6	25.3	990444.7	387216.1	50353.6	361477.1	0.39	0.13	0.93	149.4
636	B	486	491	49.492	-0.379	61.5	12339	6.3	3.5	25.3	1371212.3	513335.6	64416.7	457509.8	0.37	0.13	0.89	125.6
637	B	486	615	49.492	-0.379	61.5	10840	6.3	3.9	25.3	1211054.3	460759.3	59015.7	418803.3	0.38	0.13	0.91	130.0
638	L	486	592	49.327	-0.192	47.9	46	0.6	3.2	4.8	444.9	255.1	32.2	58.2	0.57	0.13	0.23	65.8
639	B	486	619	49.492	-0.379	61.5	11712	6.3	3.6	25.3	1306560.4	490834.0	62138.0	442105.2	0.38	0.13	0.90	127.4
640	L	518	518	49.879	-0.169	47.9	181	0.5	2.3	4.8	2232.8	942.8	115.5	-	0.42	0.12	-	28.2
641	B	486	639	49.492	-0.379	61.5	11704	6.3	3.6	25.3	1304550.9	489989.7	62038.1	441591.0	0.38	0.13	0.90	127.4
642	T	642	-	48.982	-0.145	49.2	284	1.3	2.1	6.4	5936.8	2342.3	144.9	702.4	0.39	0.06	0.30	61.9
643	B	486	634	49.492	-0.379	61.5	12038	6.3	3.6	25.3	1333533.0	499234.5	62888.5	449367.4	0.37	0.13	0.90	127.5
644	L	642	642	48.982	-0.145	49.2	183	1.2	2.3	6.4	4117.5	1721.9	102.4	518.1	0.42	0.06	0.30	59.8
645	B	486	620	49.492	-0.379	61.5	9927	6.2	4.0	25.3	1154476.8	441021.3	56670.2	406420.5	0.38	0.13	0.92	140.2
646	B	486	616	49.492	-0.379	61.5	9491	6.2	4.2	25.3	1091731.5	421029.0	54387.9	389913.3	0.39	0.13	0.93	143.9
647	B	486	645	49.492	-0.379	61.5	9835	6.2	4.0	25.3	1148943.6	439125.2	56465.1	405211.5	0.38	0.13	0.92	141.3
648	B	486	617	49.492	-0.379	61.5	8986	6.2	4.4	25.3	1023151.1	398646.3	51752.7	371359.9	0.39	0.13	0.93	147.2
649	B	486	648	49.492	-0.379	61.5	8889	6.2	4.5	25.3	1011519.4	394684.6	51261.5	368074.7	0.39	0.13	0.93	148.0
650	L	621	621	49.039	-0.096	47.2	40	0.5	2.4	4.8	346.3	150.3	-	-	0.43	-	-	65.6
651	L	486	531	49.386	-0.065	47.2	48	0.4	3.0	5.0	250.0	245.9	30.4	45.2	0.98	0.12	0.18	41.2
652	B	597	603	49.726	-0.011	48.5	661	1.0	2.8	10.6	12284.1	8867.0	1493.8	-	0.72	0.17	-	33.1

653	L	597	654	49.726	-0.011	48.5	264	1.0	3.4	10.6	4759.9	4499.6	911.2	-	0.95	0.20	-	37.3
654	B	597	604	49.726	-0.011	48.5	417	0.9	3.3	10.6	7064.2	5908.4	1088.0	-	0.84	0.18	-	33.6
655	L	658	656	49.055	-0.556	47.2	66	0.6	2.4	4.9	492.6	349.7	37.4	52.1	0.71	0.11	0.15	28.3
656	B	658	633	49.055	-0.556	47.2	131	0.8	2.1	4.9	1056.0	704.9	114.1	-	0.67	0.16	-	29.6
657	L	658	656	49.046	-0.549	47.9	17	0.7	2.4	4.5	158.4	108.9	36.6	25.8	0.69	0.34	0.24	37.5
658	T	658	-	49.055	-0.556	47.2	552	0.9	2.1	4.9	4440.5	2862.9	595.5	-	0.64	0.21	-	36.3
659	B	486	739	49.492	-0.379	61.5	5814	5.4	4.8	25.3	757525.5	298420.0	38462.0	288160.9	0.39	0.13	0.97	174.1
660	B	486	665	49.492	-0.379	61.5	5108	5.4	5.2	25.3	687324.6	273032.6	35647.5	265766.2	0.40	0.13	0.97	183.5
661	B	486	683	49.492	-0.379	61.5	4521	5.3	5.6	25.3	614812.0	247423.9	32706.2	242456.4	0.40	0.13	0.98	193.0
662	B	486	801	49.492	-0.379	61.5	5906	5.4	4.8	25.3	768701.2	302530.5	39001.6	292139.2	0.39	0.13	0.97	173.1
663	B	486	664	49.492	-0.379	61.5	5353	5.4	5.0	25.3	720979.3	285011.2	36971.6	276819.9	0.40	0.13	0.97	181.3
664	B	486	695	49.492	-0.379	61.5	5420	5.4	4.9	25.3	730775.4	288385.8	37322.7	279773.3	0.39	0.13	0.97	180.9
665	B	486	663	49.492	-0.379	61.5	5186	5.4	5.1	25.3	696103.8	276216.1	36036.3	268702.4	0.40	0.13	0.97	182.0
666	B	486	667	49.360	-0.303	51.1	2256	1.7	4.9	20.8	157881.1	62962.4	8865.1	51511.8	0.40	0.14	0.82	101.7
667	B	486	801	49.360	-0.303	51.1	2339	1.7	4.8	20.8	163018.4	64675.8	9065.7	52628.4	0.40	0.14	0.81	99.9
668	B	486	666	49.376	-0.169	47.2	137	0.6	6.8	9.9	3184.7	2178.6	481.4	1207.2	0.68	0.22	0.55	59.8
669	B	486	646	49.492	-0.379	61.5	9371	6.2	4.3	25.3	1072950.1	415033.4	53633.0	384842.6	0.39	0.13	0.93	144.4
670	L	486	668	49.376	-0.169	47.2	67	0.6	7.5	9.9	1306.0	915.5	217.9	480.8	0.70	0.24	0.53	63.5
671	B	486	637	49.270	-0.117	49.8	570	0.7	3.9	6.4	11398.3	5523.9	782.9	1254.8	0.48	0.14	0.23	55.3
672	B	486	671	49.270	-0.117	49.8	442	0.7	4.1	6.4	8392.6	4161.7	631.3	969.0	0.50	0.15	0.23	54.4
673	T	673	-	49.584	-0.060	47.9	25	0.5	2.1	3.6	147.0	102.1	-	-	0.69	-	-	36.6
674	L	554	675	49.520	-0.051	47.2	20	0.5	2.5	4.2	165.7	105.9	-	20.7	0.64	-	0.20	34.4
675	B	554	584	49.499	-0.046	47.9	82	0.5	2.3	4.4	717.6	388.9	-	104.7	0.54	-	0.27	29.9
676	L	554	675	49.499	-0.046	47.9	45	0.5	2.5	4.4	439.4	218.0	23.1	69.1	0.50	0.11	0.32	29.6
677	L	597	654	49.714	0.044	47.2	128	0.8	3.4	6.1	1856.8	1156.5	156.0	-	0.62	0.13	-	30.0
678	L	597	604	49.742	0.041	47.2	47	0.5	3.3	5.3	541.8	319.2	39.4	-	0.59	0.12	-	30.8
679	L	597	603	49.757	0.053	47.9	23	0.5	2.8	4.4	312.8	131.6	-	-	0.42	-	-	29.7
680	T	680	-	48.446	0.119	47.2	23	0.4	2.1	3.6	264.7	100.1	-	-	0.38	-	-	52.7
681	T	681	-	49.084	-0.646	49.2	94	0.9	2.1	5.0	538.9	443.1	81.2	-	0.82	0.18	-	25.0
682	L	658	658	49.058	-0.573	47.9	104	0.5	2.1	4.2	598.6	393.6	46.8	-	0.66	0.12	-	26.7
683	B	486	690	49.492	-0.379	61.5	4585	5.3	5.5	25.3	621816.3	249945.0	32988.2	244555.8	0.40	0.13	0.98	191.0
684	B	486	661	49.492	-0.379	61.5	4364	5.3	5.7	25.3	594190.0	240185.0	31793.0	236096.2	0.40	0.13	0.98	196.3
685	B	486	686	49.492	-0.379	61.5	3586	5.3	6.2	25.3	512452.1	209553.4	27935.5	208212.3	0.41	0.13	0.99	211.6
686	B	486	697	49.492	-0.379	61.5	3714	5.3	6.1	25.3	527921.6	215373.2	28656.2	213429.2	0.41	0.13	0.99	209.4
687	B	486	685	49.492	-0.379	61.5	2885	4.9	6.4	25.3	461593.8	186226.7	24672.2	187603.1	0.40	0.13	1.01	234.4
688	B	486	694	49.492	-0.379	61.5	1689	4.3	7.4	25.3	350184.0	141380.9	18986.8	146829.4	0.40	0.13	1.04	277.5
689	B	486	887	49.492	-0.379	61.5	1990	4.5	6.8	25.3	408881.4	161803.2	21353.2	166317.4	0.40	0.13	1.03	264.0
690	B	486	701	49.492	-0.379	61.5	4729	5.4	5.4	25.3	638835.3	256007.2	33716.4	250379.1	0.40	0.13	0.98	189.6
691	B	486	740	49.492	-0.379	61.5	1289	4.1	8.4	25.3	275497.5	113885.2	15486.4	120263.3	0.41	0.14	1.06	309.7
692	B	486	722	49.492	-0.379	61.5	2268	4.6	6.7	25.3	421632.8	168148.4	22254.0	171004.7	0.40	0.13	1.02	251.6
693	B	486	691	49.492	-0.379	61.5	1178	3.7	8.7	25.3	253761.8	104976.9	14328.3	110794.3	0.41	0.14	1.06	323.8

694	B	486	689	49.492	-0.379	61.5	1771	4.4	7.2	25.3	362341.2	145542.1	19446.6	150936.4	0.40	0.13	1.04	273.8
695	B	486	743	49.492	-0.379	61.5	5500	5.4	4.9	25.3	738661.8	291132.7	37638.0	282190.3	0.39	0.13	0.97	180.9
696	B	486	688	49.492	-0.379	61.5	1400	4.1	8.3	25.3	283424.3	117043.0	15911.0	122769.6	0.41	0.14	1.05	295.5
697	B	486	698	49.492	-0.379	61.5	3857	5.3	5.9	25.3	547311.3	222403.5	29545.4	219963.9	0.41	0.13	0.99	207.4
698	B	486	699	49.492	-0.379	61.5	4010	5.3	5.9	25.3	555854.7	225713.0	30034.7	222472.4	0.41	0.13	0.99	201.2
699	B	486	767	49.492	-0.379	61.5	4202	5.3	5.8	25.3	579612.6	234565.4	31074.1	230850.7	0.40	0.13	0.98	198.7
700	B	486	687	49.492	-0.379	61.5	2716	4.9	6.6	25.3	441600.9	178762.9	23796.1	180769.0	0.40	0.13	1.01	241.0
701	B	486	660	49.492	-0.379	61.5	4846	5.4	5.4	25.3	652901.0	260995.5	34228.7	254913.6	0.40	0.13	0.98	188.1
702	B	486	666	49.360	-0.303	51.1	1126	1.4	6.8	20.8	78625.2	33784.1	4955.5	30083.6	0.43	0.15	0.89	135.5
703	L	486	702	49.360	-0.303	51.1	350	1.0	7.1	20.8	27985.3	11525.1	1562.3	11131.3	0.41	0.14	0.97	153.1
704	T	704	-	48.980	-0.211	47.9	30	0.5	2.1	3.7	314.9	158.3	-	33.0	0.50	-	0.21	85.2
705	B	486	726	49.386	-0.256	49.8	533	0.9	7.2	16.8	30441.9	14780.0	2491.1	11748.0	0.49	0.17	0.79	81.1
706	L	486	705	49.407	-0.228	50.5	203	0.9	8.5	14.4	9891.6	5631.3	1112.3	3849.8	0.57	0.20	0.68	73.4
707	L	486	668	49.384	-0.183	47.2	18	0.7	7.5	9.0	348.7	256.7	44.1	176.4	0.74	0.17	0.69	58.2
708	T	708	-	49.216	-0.145	47.9	47	0.5	2.1	3.8	838.4	245.1	-	50.3	0.29	-	0.21	62.3
709	T	709	-	49.431	-0.136	48.5	28	0.5	2.1	3.6	209.7	119.6	-	16.7	0.57	-	0.14	75.5
710	B	486	711	49.270	-0.117	49.8	138	0.5	4.6	6.4	2352.2	1114.1	123.6	262.6	0.47	0.11	0.24	60.6
711	B	486	672	49.270	-0.117	49.8	221	0.6	4.5	6.4	3824.2	1819.9	213.9	417.7	0.48	0.12	0.23	59.8
712	L	486	481	49.461	-0.117	49.8	99	0.9	2.3	4.2	1393.0	597.1	51.4	145.8	0.43	0.09	0.24	42.1
713	L	486	672	49.265	-0.079	48.5	68	0.8	4.5	6.1	1070.1	676.3	157.3	180.5	0.63	0.23	0.27	43.6
714	L	486	533	49.291	-0.060	48.5	35	0.7	3.8	5.7	379.0	290.7	44.9	41.3	0.77	0.15	0.14	44.1
715	L	597	652	49.752	0.022	48.5	34	0.6	2.9	5.2	222.7	233.5	30.3	-	1.05	0.13	-	33.7
716	T	716	-	48.512	0.119	49.2	174	0.7	2.1	3.9	1454.5	789.6	62.8	98.3	0.54	0.08	0.12	58.5
717	B	763	734	48.831	0.150	49.8	5001	1.6	2.1	8.7	116534.7	43787.4	4946.5	-	0.38	0.11	-	49.4
718	B	763	761	48.831	0.150	49.8	3716	1.6	2.2	8.7	93663.1	34475.7	3979.9	-	0.37	0.12	-	49.4
719	T	719	-	49.771	0.445	48.5	43	0.4	2.1	4.3	660.8	189.7	27.3	-	0.29	0.14	-	25.4
720	T	720	-	49.036	-0.575	49.8	20	0.7	2.1	3.6	41.0	87.5	-	6.4	2.13	-	0.07	31.8
721	B	486	693	49.492	-0.365	51.1	182	1.2	9.5	17.9	18056.5	8740.2	1289.4	7931.0	0.48	0.15	0.91	429.8
722	B	486	700	49.492	-0.379	61.5	2316	4.6	6.6	25.3	428958.0	170773.3	22558.7	173571.7	0.40	0.13	1.02	251.0
723	L	486	721	49.492	-0.365	51.1	65	0.9	12.4	17.9	4168.8	2360.5	340.1	2066.5	0.57	0.14	0.88	417.3
724	B	486	571	49.603	-0.254	57.6	715	2.4	3.0	9.6	41802.6	13577.7	1654.4	10591.9	0.32	0.12	0.78	55.4
725	B	486	724	49.603	-0.254	57.6	667	2.3	3.0	9.6	40084.9	13017.8	1613.2	10248.9	0.32	0.12	0.79	55.7
726	B	486	702	49.386	-0.256	49.8	702	1.5	7.1	16.8	45030.4	20154.6	3117.5	17205.8	0.45	0.15	0.85	123.2
727	L	486	502	49.513	-0.192	48.5	49	0.6	2.9	4.5	711.4	310.7	32.8	54.6	0.44	0.11	0.18	43.3
728	L	486	710	49.313	-0.133	48.5	22	0.4	4.8	6.3	383.6	203.3	14.8	46.7	0.53	0.07	0.23	55.7
729	L	486	671	49.282	-0.138	48.5	37	0.4	4.1	5.7	460.9	237.7	-	40.3	0.52	-	0.17	62.5
730	L	486	710	49.270	-0.117	49.8	59	0.5	4.8	6.4	961.4	442.8	44.7	103.4	0.46	0.10	0.23	62.3
731	L	486	711	49.284	-0.100	49.8	45	0.6	4.6	6.1	629.3	332.9	46.1	70.7	0.53	0.14	0.21	50.7
732	B	763	717	48.831	0.150	49.8	4630	1.6	2.2	8.7	107102.4	40738.8	4706.9	-	0.38	0.12	-	49.3
733	L	763	718	48.593	0.140	48.5	69	0.7	2.4	3.8	675.1	400.2	40.2	-	0.59	0.10	-	55.6
734	B	763	763	48.831	0.150	49.8	5057	1.6	2.1	8.7	117470.4	44151.9	4961.2	-	0.38	0.11	-	49.4

735	T	735	-	48.460	0.155	48.5	63	0.4	2.1	4.5	440.3	246.2	35.4	-	0.56	0.14	-	54.9
736	T	736	-	49.594	0.384	49.2	145	0.5	2.1	4.0	2045.4	631.3	55.7	-	0.31	0.09	-	24.1
737	T	737	-	49.077	-0.613	50.5	25	0.6	2.1	3.7	88.4	127.1	-	-	1.44	-	-	35.4
738	L	486	541	49.568	-0.381	52.4	78	1.1	2.4	6.5	2166.8	643.9	67.8	361.2	0.30	0.11	0.56	276.1
739	B	486	662	49.492	-0.379	61.5	5831	5.4	4.8	25.3	761246.1	299867.5	38691.8	289727.8	0.39	0.13	0.97	173.9
740	B	486	696	49.492	-0.379	61.5	1313	4.1	8.4	25.3	276464.2	114317.9	15539.3	120486.3	0.41	0.14	1.05	303.9
741	L	486	484	49.405	-0.365	50.5	55	2.0	2.4	4.2	2148.7	469.1	-	252.6	0.22	-	0.54	305.8
742	L	486	688	49.473	-0.348	49.2	36	0.7	8.3	10.3	1202.2	718.1	128.6	411.3	0.60	0.18	0.57	204.7
743	B	486	659	49.492	-0.379	61.5	5690	5.4	4.9	25.3	742797.7	293220.8	37816.6	283394.5	0.39	0.13	0.97	175.8
744	B	486	725	49.603	-0.254	57.6	495	2.3	3.5	9.6	29898.5	10094.0	1334.5	8202.4	0.34	0.13	0.81	56.2
745	L	486	598	49.490	-0.270	49.8	25	0.7	3.0	4.4	505.6	166.6	-	67.2	0.33	-	0.40	82.1
746	L	486	705	49.386	-0.256	49.8	141	0.7	8.5	16.8	9221.1	3973.5	574.5	4084.4	0.43	0.14	1.03	216.2
747	L	486	544	49.492	-0.195	49.8	24	0.4	3.1	4.6	377.4	160.1	23.7	34.0	0.42	0.15	0.21	53.6
748	B	486	556	49.492	-0.379	61.5	27256	6.5	2.2	25.3	2547826.7	884293.5	100422.6	-	0.35	0.11	-	72.8
749	L	486	574	49.367	-0.060	51.8	127	0.7	2.7	6.5	3252.8	1182.0	112.8	442.0	0.36	0.10	0.37	42.6
750	T	750	-	48.789	0.015	49.8	247	0.7	2.1	6.4	4042.8	2046.3	283.6	894.0	0.51	0.14	0.44	60.0
751	B	763	718	48.831	0.150	49.8	3232	1.6	2.4	8.7	80566.2	30195.9	3621.4	-	0.37	0.12	-	48.6
752	B	763	785	48.831	0.150	49.8	2710	1.5	2.5	8.7	67303.5	25719.1	3228.2	-	0.38	0.13	-	48.1
753	B	763	754	48.831	0.150	49.8	1085	1.2	2.8	8.7	27500.4	11501.2	1835.8	-	0.42	0.16	-	48.6
754	B	763	787	48.831	0.150	49.8	1635	1.3	2.8	8.7	41131.2	16770.1	2281.9	-	0.41	0.14	-	47.0
755	B	763	752	48.831	0.150	49.8	2199	1.4	2.6	8.7	52703.4	21007.6	2754.3	-	0.40	0.13	-	47.1
756	B	763	755	48.831	0.150	49.8	1970	1.3	2.7	8.7	47262.0	19147.0	2559.0	-	0.41	0.13	-	46.7
757	B	763	784	48.774	0.084	49.2	174	1.3	3.6	6.9	3086.6	1523.7	200.2	479.0	0.49	0.13	0.31	51.0
758	B	763	756	48.831	0.150	49.8	1895	1.3	2.7	8.7	45788.2	18649.3	2501.2	-	0.41	0.13	-	46.6
759	B	763	753	48.831	0.150	49.8	462	0.6	3.4	8.7	12057.6	5292.9	1021.8	-	0.44	0.19	-	44.9
760	L	763	759	48.796	0.100	49.2	63	0.3	4.3	7.2	1076.9	508.6	90.3	264.0	0.47	0.18	0.52	50.4
761	B	763	732	48.831	0.150	49.8	4438	1.6	2.2	8.7	102759.5	39130.3	4562.1	-	0.38	0.12	-	49.2
762	L	763	732	48.536	0.136	50.5	92	0.8	2.2	3.7	659.2	462.9	31.2	64.9	0.70	0.07	0.14	52.8
763	T	763	-	48.831	0.150	49.8	5212	1.6	2.1	8.7	119041.2	44851.2	5004.4	-	0.38	0.11	-	49.6
764	B	763	789	48.555	0.204	49.8	662	0.7	2.3	5.9	8156.4	4229.7	538.3	-	0.52	0.13	-	48.0
765	T	765	-	49.145	0.556	49.2	33	0.3	2.1	3.5	310.9	127.2	-	-	0.41	-	-	22.9
766	T	766	-	48.961	-0.391	52.4	509	0.7	2.1	5.8	8116.5	3956.7	587.5	1057.3	0.49	0.15	0.27	57.1
767	B	486	684	49.492	-0.379	61.5	4216	5.3	5.7	25.3	581827.5	235674.5	31216.5	232118.3	0.41	0.13	0.98	198.8
768	L	486	551	49.528	-0.334	51.1	22	0.7	2.4	4.1	340.2	111.3	15.1	46.1	0.33	0.14	0.41	237.2
769	B	486	744	49.570	-0.273	51.1	235	1.6	4.4	9.4	15223.1	5213.4	689.3	4740.0	0.34	0.13	0.91	63.6
770	L	486	769	49.570	-0.273	51.1	149	1.3	5.2	9.4	8905.9	3247.5	480.4	3131.8	0.36	0.15	0.96	61.2
771	L	486	800	49.473	-0.256	49.8	21	0.4	3.7	5.9	396.8	167.1	-	56.3	0.42	-	0.34	56.6
772	B	486	548	49.490	-0.249	51.8	268	0.9	3.3	6.5	8159.0	3219.4	319.8	1669.4	0.39	0.10	0.52	54.3
773	L	486	772	49.490	-0.249	51.8	191	0.7	3.8	6.5	4308.5	1821.7	174.8	1019.3	0.42	0.10	0.56	53.2
774	L	486	772	49.478	-0.209	51.8	13	1.5	3.8	5.5	485.6	230.1	31.3	50.6	0.47	0.14	0.22	55.9
775	L	486	748	49.452	-0.181	49.8	33	0.5	2.2	4.6	422.5	156.8	23.5	40.5	0.37	0.15	0.26	61.1

776	L	486	485	49.480	-0.162	49.8	91	0.5	2.6	4.8	1385.4	571.8	84.8	104.8	0.41	0.15	0.18	44.5
777	L	642	642	48.928	-0.162	49.8	55	0.7	2.3	3.9	717.3	250.2	-	77.7	0.35	-	0.31	65.3
778	T	778	-	49.487	-0.105	49.8	22	0.4	2.1	3.6	226.9	96.2	-	15.7	0.42	-	0.16	38.6
779	L	486	780	49.433	-0.086	50.5	64	0.5	3.4	6.5	1049.8	479.9	69.6	192.2	0.46	0.15	0.40	39.8
780	B	486	599	49.433	-0.086	50.5	108	0.9	3.1	6.5	2037.5	889.0	117.7	346.8	0.44	0.13	0.39	40.7
781	T	781	-	49.150	-0.074	50.5	48	0.6	2.1	3.9	807.1	260.4	-	-	0.32	-	-	51.3
782	L	597	597	49.702	0.013	49.2	18	0.4	2.2	3.9	227.8	93.7	-	-	0.41	-	-	32.4
783	L	763	757	48.774	0.084	49.2	44	0.4	3.7	6.9	640.2	296.5	41.1	112.3	0.46	0.14	0.38	51.3
784	B	763	753	48.774	0.084	49.2	298	1.2	3.4	6.9	4979.2	2365.5	317.2	702.4	0.48	0.13	0.30	51.6
785	B	763	751	48.831	0.150	49.8	2797	1.5	2.5	8.7	68931.2	26377.5	3308.2	-	0.38	0.13	-	48.3
786	L	763	785	48.630	0.119	49.8	82	1.3	2.5	4.5	1449.6	603.0	76.1	97.0	0.42	0.13	0.16	52.4
787	B	763	758	48.831	0.150	49.8	1678	1.3	2.8	8.7	41993.6	17130.9	2328.0	-	0.41	0.14	-	47.0
788	L	763	759	48.831	0.150	49.8	229	0.5	4.3	8.7	5975.3	2854.1	638.2	-	0.48	0.22	-	43.3
789	B	763	761	48.555	0.204	49.8	720	0.7	2.2	5.9	9004.4	4623.2	576.9	-	0.51	0.12	-	48.2
790	T	790	-	48.611	0.159	49.8	23	0.4	2.1	3.9	181.6	98.6	-	9.9	0.54	-	0.10	54.8
791	B	763	764	48.555	0.204	49.8	406	0.7	2.6	5.9	4825.7	2511.1	271.6	-	0.52	0.11	-	46.6
792	L	763	791	48.555	0.204	49.8	294	0.7	2.7	5.9	3777.7	1993.6	230.6	-	0.53	0.12	-	45.4
793	B	819	819	48.852	0.379	52.4	1242	0.9	2.3	6.0	23029.8	8919.5	876.9	-	0.39	0.10	-	30.4
794	T	794	-	48.895	0.521	49.8	143	0.6	2.1	6.1	2086.9	1034.0	202.0	-	0.50	0.20	-	22.8
795	B	486	693	49.492	-0.379	61.5	914	3.0	9.5	25.3	194144.7	81114.1	11190.4	87593.7	0.42	0.14	1.08	340.5
796	L	486	504	49.369	-0.370	51.1	18	0.5	3.0	5.0	443.4	120.0	-	82.0	0.27	-	0.68	164.3
797	L	486	726	49.395	-0.313	52.4	134	1.0	7.2	15.8	12226.1	4498.8	508.8	4758.2	0.37	0.11	1.06	345.7
798	L	486	606	49.296	-0.303	51.8	46	0.6	2.4	4.6	1019.2	320.4	41.1	251.6	0.31	0.13	0.79	79.0
799	L	486	800	49.461	-0.263	49.8	22	0.5	3.7	5.3	415.3	168.6	20.1	63.0	0.41	0.12	0.37	60.9
800	B	486	634	49.473	-0.256	49.8	48	0.6	3.6	5.9	926.8	375.9	28.3	130.2	0.41	0.08	0.35	59.2
801	B	486	635	49.492	-0.379	61.5	8176	6.1	4.8	25.3	931786.2	367230.1	48069.0	344785.1	0.39	0.13	0.94	154.8
802	L	486	620	49.454	-0.247	51.1	44	0.4	4.0	5.6	809.2	322.7	24.0	112.0	0.40	0.07	0.35	79.0
803	B	486	627	49.492	-0.379	61.5	13301	6.4	3.3	25.3	1468367.7	544714.7	67919.6	478917.4	0.37	0.12	0.88	120.5
804	T	804	-	48.489	-0.209	50.5	30	0.3	2.1	4.2	330.4	117.1	-	-	0.35	-	-	27.9
805	T	805	-	49.440	-0.053	51.1	33	0.5	2.1	4.2	498.1	181.5	-	65.7	0.36	-	0.36	36.1
806	T	806	-	49.216	0.027	53.1	1136	1.0	2.1	7.2	26465.4	11749.5	1594.9	-	0.44	0.14	-	36.6
807	L	806	806	49.280	-0.030	50.5	99	0.4	2.3	4.4	1216.1	500.2	41.9	-	0.41	0.08	-	37.2
808	B	806	806	49.216	0.027	53.1	932	1.0	2.3	7.2	22207.0	10200.6	1464.8	-	0.46	0.14	-	36.2
809	L	763	784	48.727	0.077	50.5	64	0.3	3.6	5.4	766.6	352.9	31.9	91.8	0.46	0.09	0.26	57.2
810	B	763	754	48.722	0.136	51.1	529	1.0	2.8	6.2	12558.6	4909.5	402.3	1087.4	0.39	0.08	0.22	45.4
811	L	763	764	48.633	0.162	51.1	76	0.5	2.6	4.9	744.5	439.9	86.8	145.6	0.59	0.20	0.33	54.0
812	B	763	810	48.722	0.136	51.1	312	0.8	3.3	6.2	6994.7	2894.0	263.2	671.4	0.41	0.09	0.23	45.1
813	L	763	812	48.711	0.155	50.5	88	0.6	3.4	5.3	1441.6	599.2	44.6	125.4	0.42	0.07	0.21	45.4
814	L	763	791	48.614	0.185	51.1	59	0.4	2.7	4.2	478.5	264.9	21.2	47.5	0.55	0.08	0.18	53.8
815	B	763	734	48.524	0.169	53.1	48	0.7	2.1	3.8	628.9	267.2	-	-	0.42	-	-	45.4
816	L	867	867	48.944	0.214	51.8	29	0.5	2.2	4.3	339.5	157.5	-	-	0.46	-	-	34.6

817	T	817	-	48.855	0.235	50.5	30	0.4	2.1	3.8	378.0	135.5	-	-	0.36	-	-	38.5
818	L	819	819	48.895	0.303	50.5	161	0.5	2.3	4.1	1782.2	775.3	44.1	-	0.44	0.06	-	32.8
819	T	819	-	48.852	0.379	52.4	1613	1.0	2.1	6.0	30440.9	11468.4	1054.8	-	0.38	0.09	-	31.1
820	B	819	821	48.852	0.379	52.4	999	0.9	2.5	6.0	18379.4	7305.0	791.7	-	0.40	0.11	-	29.9
821	B	819	793	48.852	0.379	52.4	1045	0.9	2.4	6.0	19405.2	7670.9	813.5	-	0.40	0.11	-	29.9
822	L	819	847	48.888	0.346	51.1	61	0.5	2.8	4.5	706.3	321.6	-	-	0.46	-	-	33.4
823	B	819	847	48.852	0.379	52.4	404	0.8	2.8	6.0	7956.2	3298.0	421.1	-	0.41	0.13	-	28.9
824	T	824	-	48.666	-0.587	53.7	40	1.0	2.1	4.3	919.1	302.3	-	-	0.33	-	-	43.1
825	L	909	909	48.694	-0.587	52.4	79	0.7	2.1	5.8	1669.6	651.1	73.2	-	0.39	0.11	-	52.3
826	B	827	827	48.850	-0.544	54.4	1388	1.8	2.3	10.6	48507.6	19349.5	2644.4	-	0.40	0.14	-	50.7
827	T	827	-	48.850	-0.544	54.4	1543	1.9	2.1	10.6	54340.0	21145.0	2795.7	-	0.39	0.13	-	49.3
828	L	486	829	49.546	-0.405	51.8	61	0.6	2.8	6.1	1560.5	505.2	46.7	279.2	0.32	0.09	0.55	200.5
829	B	486	590	49.546	-0.405	51.8	147	0.7	2.8	6.1	3698.6	1073.2	74.7	517.6	0.29	0.07	0.48	166.8
830	B	486	795	49.492	-0.379	61.5	246	3.0	14.8	25.3	55689.4	26715.8	3971.6	30147.8	0.48	0.15	1.13	682.7
831	L	766	766	48.961	-0.391	52.4	100	0.5	3.2	5.8	1253.6	846.5	184.7	318.3	0.68	0.22	0.38	54.0
832	L	486	721	49.511	-0.372	51.1	37	0.4	12.3	16.1	1818.9	911.0	150.4	755.4	0.50	0.17	0.83	441.3
833	L	486	647	49.376	-0.348	51.1	20	0.6	4.2	6.0	680.7	170.9	-	172.1	0.25	-	1.01	159.1
834	L	486	667	49.428	-0.280	50.5	26	0.4	4.9	6.6	707.7	221.7	19.2	106.1	0.31	0.09	0.48	93.9
835	T	835	-	49.041	-0.119	54.4	303	0.9	2.1	8.1	6844.9	2282.4	219.8	-	0.33	0.10	-	64.8
836	T	836	-	49.129	-0.079	51.8	41	0.4	2.1	4.3	520.1	177.9	-	-	0.34	-	-	56.1
837	L	486	780	49.398	-0.082	51.8	27	0.7	3.4	5.6	533.1	242.8	25.0	94.9	0.46	0.10	0.39	42.8
838	T	838	-	48.699	-0.011	52.4	37	0.6	2.1	4.0	433.2	168.1	25.2	18.5	0.39	0.15	0.11	44.9
839	B	806	808	49.216	0.027	53.1	427	0.8	3.4	7.2	8683.6	4673.7	864.4	-	0.54	0.18	-	37.1
840	T	840	-	49.452	-0.004	53.1	302	0.7	2.1	5.2	4899.4	1815.3	118.0	465.9	0.37	0.07	0.26	29.2
841	L	763	812	48.722	0.136	51.1	177	0.8	3.4	6.2	4461.2	1870.4	195.3	448.3	0.42	0.10	0.24	45.0
842	L	763	755	48.661	0.126	53.7	127	1.0	2.7	5.3	2017.8	723.0	100.4	174.3	0.36	0.14	0.24	49.5
843	L	763	758	48.774	0.176	51.8	127	0.6	2.8	4.7	1815.7	823.0	111.5	-	0.45	0.14	-	42.6
844	L	763	815	48.538	0.173	52.4	18	0.7	2.2	3.8	179.7	86.7	-	-	0.48	-	-	45.4
845	L	763	789	48.616	0.204	51.1	23	0.4	2.3	3.9	228.7	105.0	-	19.0	0.46	-	0.18	51.6
846	L	819	821	48.869	0.341	51.1	18	0.4	2.5	4.4	245.4	106.8	-	-	0.44	-	-	33.6
847	B	819	820	48.852	0.379	52.4	529	0.8	2.7	6.0	9912.1	4069.8	474.3	-	0.41	0.12	-	29.1
848	L	819	823	48.852	0.379	52.4	131	0.6	3.5	6.0	2156.7	956.2	143.5	-	0.44	0.15	-	28.7
849	L	819	823	48.892	0.391	51.8	57	0.6	3.5	5.5	945.7	451.1	76.2	-	0.48	0.17	-	28.2
850	T	850	-	49.440	0.393	51.1	70	0.7	2.1	3.8	1438.5	370.9	-	-	0.26	-	-	29.0
851	B	909	909	48.720	-0.617	54.4	308	1.2	2.1	5.0	5079.1	1840.0	144.0	-	0.36	0.08	-	42.8
852	B	827	826	48.850	-0.544	54.4	1169	1.8	2.7	10.6	39892.7	16519.7	2318.6	-	0.41	0.14	-	52.6
853	L	486	569	49.525	-0.412	51.8	24	0.4	2.6	4.4	523.5	150.3	-	127.8	0.29	-	0.85	159.8
854	T	854	-	48.831	-0.436	52.4	55	0.5	2.1	5.5	545.4	276.3	-	75.3	0.51	-	0.27	73.9
855	L	486	595	49.291	-0.285	51.8	40	0.3	2.8	4.8	675.8	219.0	21.1	155.3	0.32	0.10	0.71	74.9
856	T	856	-	49.294	-0.244	53.1	42	0.7	2.1	4.0	1217.4	262.4	-	85.9	0.22	-	0.33	83.5
857	T	857	-	48.590	-0.141	51.8	30	0.4	2.1	3.8	251.9	114.9	17.1	40.7	0.46	0.15	0.35	39.1

858	L	486	530	49.379	-0.079	52.4	17	0.6	2.9	4.5	440.4	128.2	-	44.8	0.29	-	0.35	44.5
859	T	859	-	48.727	0.018	51.8	101	0.7	2.1	4.1	1477.1	516.9	39.2	68.8	0.35	0.08	0.13	58.6
860	L	859	859	48.727	0.018	51.8	20	0.6	2.4	4.1	395.9	130.9	19.9	11.2	0.33	0.15	0.09	59.1
861	T	861	-	49.402	0.053	52.4	58	0.5	2.1	4.0	951.6	292.8	44.3	-	0.31	0.15	-	28.4
862	L	763	757	48.784	0.084	51.8	72	0.6	3.7	6.4	1247.2	724.4	96.1	228.3	0.58	0.13	0.32	50.4
863	T	863	-	49.393	0.100	51.8	113	0.6	2.1	4.2	1762.8	565.6	-	-	0.32	-	-	27.5
864	L	763	865	48.491	0.136	52.4	51	0.4	2.3	3.9	500.2	227.6	-	-	0.46	-	-	58.4
865	B	763	763	48.508	0.150	52.4	150	0.5	2.1	4.1	1418.4	648.9	36.0	-	0.46	0.06	-	55.0
866	L	763	865	48.508	0.150	52.4	37	0.5	2.3	4.1	314.0	178.9	-	-	0.57	-	-	53.5
867	T	867	-	48.937	0.131	55.0	1401	1.1	2.1	7.6	32098.4	10992.0	1351.0	-	0.34	0.12	-	39.1
868	B	867	869	48.984	0.223	51.8	354	1.1	2.4	6.6	6488.0	2712.2	325.3	-	0.42	0.12	-	37.4
869	B	867	867	48.937	0.131	55.0	1290	1.0	2.2	7.6	28859.4	9986.1	1247.7	-	0.35	0.12	-	39.0
870	L	867	868	48.984	0.223	51.8	35	0.4	3.5	6.6	590.7	270.7	43.4	-	0.46	0.16	-	34.3
871	L	819	820	48.923	0.386	53.1	210	0.7	2.7	4.8	2932.3	1282.1	156.8	-	0.44	0.12	-	31.1
872	T	872	-	48.791	0.395	51.8	43	0.4	2.1	3.9	481.8	181.7	-	-	0.38	-	-	29.7
873	T	873	-	49.499	0.407	52.4	89	0.8	2.1	4.5	2327.5	590.9	35.3	-	0.25	0.06	-	27.9
874	T	874	-	49.518	0.457	51.8	47	0.3	2.2	4.7	733.9	246.4	23.7	-	0.34	0.10	-	25.0
875	B	961	961	48.614	-0.688	55.0	236	0.8	2.1	6.4	5089.5	1790.1	213.1	-	0.35	0.12	-	44.2
876	L	909	878	48.687	-0.629	52.4	33	0.5	2.4	3.9	395.9	201.1	24.3	-	0.51	0.12	-	41.8
877	L	909	878	48.687	-0.603	53.7	95	0.9	2.4	3.9	1688.7	569.4	-	-	0.34	-	-	45.4
878	B	909	851	48.687	-0.629	52.4	133	1.0	2.3	3.9	2259.0	834.0	55.2	-	0.37	0.07	-	44.8
879	T	879	-	49.103	-0.570	53.1	34	0.5	2.1	4.1	302.2	186.8	-	-	0.62	-	-	28.2
880	B	827	852	48.850	-0.544	54.4	747	0.7	3.5	10.6	18644.3	8672.5	1406.8	-	0.47	0.16	-	54.4
881	L	854	854	48.831	-0.436	52.4	23	0.4	2.2	5.5	207.3	114.4	-	28.1	0.55	-	0.25	71.7
882	L	766	883	48.907	-0.417	52.4	54	0.3	3.3	4.8	570.5	281.8	27.5	54.5	0.49	0.10	0.19	59.9
883	B	766	766	48.907	-0.417	52.4	150	0.4	3.2	4.8	1629.7	787.7	89.3	167.8	0.48	0.11	0.21	61.1
884	L	486	829	49.596	-0.398	52.4	78	0.6	2.8	5.0	1925.0	515.4	28.6	210.8	0.27	0.06	0.41	150.3
885	T	885	-	49.369	-0.398	53.1	32	0.6	2.1	3.6	591.3	163.7	-	76.1	0.28	-	0.46	130.4
886	L	766	883	48.895	-0.398	52.4	68	0.4	3.3	4.8	736.7	361.1	42.6	80.9	0.49	0.12	0.22	61.4
887	B	486	692	49.492	-0.379	61.5	2081	4.6	6.8	25.3	410539.4	163435.2	21624.7	168017.2	0.40	0.13	1.03	269.6
888	T	888	-	49.738	-0.256	53.7	262	0.8	2.1	5.4	4257.5	1657.9	179.6	-	0.39	0.11	-	44.1
889	B	486	916	49.528	-0.155	54.4	556	1.0	2.3	8.0	19183.9	5696.7	529.7	2980.1	0.30	0.09	0.52	40.7
890	B	486	523	49.518	-0.027	55.0	1990	1.2	2.2	8.2	68351.5	22102.1	2301.5	-	0.32	0.10	-	30.6
891	L	486	890	49.624	-0.044	53.1	34	0.4	2.2	4.5	481.0	158.2	17.8	-	0.33	0.11	-	34.4
892	B	486	916	49.518	-0.027	55.0	1350	1.2	2.3	8.2	45931.5	15585.2	1708.8	-	0.34	0.11	-	26.5
893	L	806	839	49.216	0.027	53.1	83	0.5	4.8	7.2	1342.6	851.3	209.2	-	0.63	0.25	-	42.1
894	L	859	859	48.715	0.029	53.1	52	0.5	2.4	3.8	529.4	207.0	-	30.8	0.39	-	0.15	58.3
895	T	895	-	48.517	0.041	53.1	87	0.4	2.1	5.0	1075.8	419.8	47.5	149.8	0.39	0.11	0.36	50.2
896	L	763	756	48.772	0.046	53.1	39	0.5	2.7	4.4	485.7	169.5	18.4	31.5	0.35	0.11	0.19	59.9
897	T	897	-	48.493	0.063	53.1	29	0.4	2.1	4.0	353.4	120.8	23.1	47.0	0.34	0.19	0.39	48.2
898	T	898	-	48.822	0.093	52.4	48	0.4	2.1	3.7	584.3	212.0	-	41.4	0.36	-	0.20	53.7

899	L	763	787	48.850	0.169	52.4	32	0.6	2.8	4.8	523.2	225.9	39.0	-	0.43	0.17	-	45.0
900	L	763	815	48.524	0.169	53.1	30	0.4	2.2	3.8	344.9	143.6	-	-	0.42	-	-	45.2
901	L	763	717	48.781	0.204	51.8	22	0.4	2.2	3.7	236.7	81.7	-	-	0.35	-	-	41.5
902	T	902	-	49.015	0.506	54.4	330	0.5	2.1	5.3	4777.1	1888.5	295.6	-	0.40	0.16	-	26.7
903	T	903	-	49.471	0.542	52.4	315	1.0	2.1	5.3	5075.7	1860.0	208.3	-	0.37	0.11	-	19.2
904	L	903	903	49.471	0.542	52.4	41	0.4	2.8	5.3	598.2	249.7	34.3	-	0.42	0.14	-	20.3
905	T	905	-	49.513	0.537	52.4	50	0.4	2.1	4.3	563.2	194.4	22.2	-	0.35	0.11	-	20.7
906	T	906	-	49.065	0.981	53.1	87	0.5	2.1	5.3	1432.2	575.9	70.8	-	0.40	0.12	-	18.1
907	T	907	-	48.031	-0.750	55.7	399	1.7	2.1	4.8	7407.8	3588.4	308.3	-	0.48	0.09	-	16.1
908	L	961	875	48.595	-0.665	53.1	43	0.3	3.5	6.1	713.6	279.9	29.1	-	0.39	0.10	-	47.6
909	T	909	-	48.694	-0.587	52.4	386	1.3	2.1	5.8	6756.7	2493.2	217.4	-	0.37	0.09	-	44.1
910	L	827	880	48.850	-0.544	54.4	210	0.6	4.8	10.6	5497.3	2411.2	399.7	1686.6	0.44	0.17	0.70	47.2
911	B	827	880	48.850	-0.483	53.1	90	0.7	4.8	7.2	1698.8	1043.0	193.4	512.9	0.61	0.19	0.49	61.0
912	L	827	911	48.850	-0.483	53.1	35	0.4	5.3	7.2	632.6	343.3	53.4	194.1	0.54	0.16	0.57	62.6
913	L	854	854	48.845	-0.433	53.1	21	0.4	2.2	4.1	206.3	111.5	15.0	33.2	0.54	0.13	0.30	76.0
914	T	914	-	49.615	-0.362	55.0	109	0.8	2.1	8.3	5130.2	1397.9	163.5	1391.9	0.27	0.12	1.00	173.8
915	B	486	889	49.528	-0.155	54.4	324	0.8	2.8	8.0	10644.5	3443.5	363.6	1940.9	0.32	0.11	0.56	42.6
916	B	486	890	49.518	-0.027	55.0	1936	1.1	2.2	8.2	66791.1	21678.0	2260.2	-	0.32	0.10	-	30.4
917	L	835	835	49.041	-0.119	54.4	128	0.8	2.6	8.1	3173.6	1155.1	121.3	-	0.36	0.11	-	63.4
918	T	918	-	49.896	-0.086	53.1	30	0.5	2.1	4.2	474.1	167.8	21.4	-	0.35	0.13	-	26.0
919	T	919	-	48.715	-0.011	53.7	18	0.5	2.1	3.7	204.5	90.3	-	5.0	0.44	-	0.06	50.6
920	L	806	808	49.294	-0.004	53.1	25	0.6	3.4	5.2	303.2	147.5	18.7	-	0.49	0.13	-	32.9
921	L	806	839	49.235	0.003	53.7	23	0.5	4.8	6.5	341.4	216.6	50.4	-	0.63	0.23	-	38.3
922	L	763	752	48.822	0.027	53.7	321	0.5	2.6	7.4	7975.1	2577.8	280.4	904.8	0.32	0.11	0.35	63.1
923	T	923	-	49.509	0.034	54.4	28	0.6	2.1	4.1	526.0	143.5	-	32.3	0.27	-	0.23	26.5
924	L	763	751	48.829	0.072	53.1	46	1.0	2.5	4.4	874.4	303.1	-	54.8	0.35	-	0.18	58.2
925	T	925	-	49.825	0.124	53.1	40	0.4	2.1	3.6	287.6	181.2	24.2	-	0.63	0.13	-	29.2
926	L	763	810	48.706	0.133	53.7	39	0.5	3.3	5.1	477.9	227.6	19.3	55.3	0.48	0.08	0.24	43.3
927	T	927	-	48.517	0.145	53.1	35	0.4	2.1	3.6	313.7	144.8	-	-	0.46	-	-	55.4
928	B	867	869	48.937	0.131	55.0	739	0.6	2.4	7.6	17793.6	5897.8	756.8	-	0.33	0.13	-	41.5
929	T	929	-	48.848	0.223	53.1	132	0.4	2.1	4.4	1329.9	624.3	81.2	-	0.47	0.13	-	39.1
930	L	929	929	48.855	0.207	53.1	50	0.4	2.4	3.8	541.3	260.1	46.9	-	0.48	0.18	-	38.1
931	L	929	929	48.848	0.223	53.1	46	0.4	2.4	4.4	402.5	202.7	21.4	-	0.50	0.11	-	40.0
932	L	867	868	48.987	0.233	53.7	95	0.5	3.5	6.1	1202.6	640.9	93.3	-	0.53	0.15	-	36.9
933	L	819	793	48.944	0.332	53.1	37	0.4	2.5	4.1	354.3	145.5	-	-	0.41	-	-	32.8
934	T	934	-	49.452	0.464	53.1	84	0.6	2.1	4.8	1229.3	408.4	34.9	-	0.33	0.09	-	27.9
935	T	935	-	49.384	0.502	53.1	23	0.4	2.1	3.8	261.1	109.3	-	-	0.42	-	-	20.8
936	T	936	-	48.885	0.495	53.7	85	0.5	2.1	4.1	938.2	364.7	-	-	0.39	-	-	23.4
937	L	903	903	49.447	0.513	54.4	120	0.7	2.8	5.2	1809.4	720.3	77.8	-	0.40	0.11	-	19.0
938	T	938	-	49.492	-0.894	53.7	36	0.5	2.1	3.7	210.6	158.0	21.0	-	0.75	0.13	-	16.7
939	L	961	962	48.614	-0.648	55.0	61	0.9	2.2	4.3	842.8	301.9	25.8	-	0.36	0.09	-	36.3

940	L	909	851	48.720	-0.617	54.4	91	0.5	2.3	5.0	1361.0	534.8	43.0	-	0.39	0.08	-	37.1
941	T	941	-	48.753	-0.613	57.0	240	1.0	2.1	6.3	5441.0	1981.2	283.1	-	0.36	0.14	-	40.2
942	L	827	826	48.796	-0.566	53.7	25	0.3	2.7	4.4	268.0	116.7	21.9	-	0.44	0.19	-	31.6
943	L	486	509	49.424	-0.518	55.0	28	0.5	2.4	4.8	286.1	122.3	-	21.1	0.43	-	0.17	84.4
944	L	827	911	48.857	-0.492	53.7	30	0.4	5.3	7.1	429.4	343.2	71.0	146.8	0.80	0.21	0.43	55.0
945	L	486	830	49.490	-0.388	56.3	13	1.6	21.7	24.8	1993.1	1059.0	161.3	1220.1	0.53	0.15	1.15	777.9
946	T	946	-	49.868	-0.303	54.4	37	1.4	2.1	3.8	436.6	175.8	25.2	-	0.40	0.14	-	32.0
947	L	486	553	49.395	-0.254	54.4	53	0.4	2.2	4.7	841.9	250.2	34.1	101.8	0.30	0.14	0.41	94.6
948	L	486	725	49.546	-0.230	53.7	20	0.4	3.5	5.2	477.1	152.4	13.2	116.2	0.32	0.09	0.76	52.1
949	T	949	-	49.223	-0.230	54.4	102	0.8	2.1	4.8	2015.9	705.2	61.2	342.4	0.35	0.09	0.49	73.8
950	T	950	-	49.981	-0.098	53.7	56	0.5	2.1	5.8	1083.4	336.5	34.0	-	0.31	0.10	-	40.5
951	B	486	892	49.518	-0.027	55.0	863	0.9	2.8	8.2	28560.9	10684.3	1353.4	-	0.37	0.13	-	25.5
952	L	486	951	49.605	-0.027	53.7	26	0.5	4.0	6.4	541.0	229.6	-	-	0.42	-	-	27.4
953	T	953	-	49.995	-0.004	54.4	130	0.7	2.1	8.9	5048.6	1596.2	149.8	-	0.32	0.09	-	40.9
954	T	954	-	48.855	0.051	54.4	82	0.3	2.1	3.8	1357.4	312.9	-	-	0.23	-	-	51.0
955	B	867	928	48.937	0.131	55.0	434	0.5	3.2	7.6	9934.2	3617.1	496.4	-	0.36	0.14	-	41.0
956	T	956	-	48.904	0.214	53.7	62	0.4	2.1	3.8	621.5	209.2	25.5	-	0.34	0.12	-	38.2
957	T	957	-	48.921	0.242	53.7	23	0.4	2.1	3.6	234.3	84.7	-	-	0.36	-	-	36.3
958	T	958	-	48.840	0.343	55.7	266	0.6	2.1	5.1	3516.3	1540.2	179.2	-	0.44	0.12	-	32.2
959	T	959	-	49.034	0.447	53.7	63	0.4	2.1	3.7	581.9	260.3	-	-	0.45	-	-	30.6
960	L	961	875	48.614	-0.688	55.0	75	0.5	3.5	6.4	1172.7	478.2	62.3	-	0.41	0.13	-	42.5
961	T	961	-	48.614	-0.688	55.0	316	1.8	2.1	6.4	6843.8	2458.5	301.5	-	0.36	0.12	-	39.8
962	B	961	1093	48.614	-0.648	55.0	82	2.1	2.1	4.3	1338.6	511.5	69.0	-	0.38	0.13	-	35.8
963	T	963	-	48.758	-0.582	54.4	55	0.4	2.1	3.6	688.5	237.5	25.2	-	0.34	0.11	-	35.4
964	L	486	645	49.343	-0.485	55.7	69	1.0	4.0	7.1	1858.2	757.0	84.3	299.2	0.41	0.11	0.40	45.8
965	T	965	-	49.301	-0.367	54.4	17	0.5	2.1	4.6	330.7	99.7	-	45.8	0.30	-	0.46	87.9
966	L	486	690	49.565	-0.351	55.7	63	0.9	5.5	11.4	3212.2	1188.2	174.1	1232.0	0.37	0.15	1.04	142.0
967	B	486	573	49.341	-0.362	56.3	240	1.2	3.1	8.1	9236.3	2814.5	151.5	1842.3	0.30	0.05	0.65	140.9
968	L	486	967	49.329	-0.362	55.7	70	1.3	3.8	7.0	3475.8	1041.2	54.5	676.9	0.30	0.05	0.65	126.1
969	T	969	-	49.953	-0.174	54.4	38	0.3	2.1	3.6	373.9	140.1	24.0	-	0.37	0.17	-	30.4
970	L	486	915	49.518	-0.174	55.0	59	0.7	3.3	5.7	1258.8	419.0	-	244.7	0.33	-	0.58	40.9
971	T	971	-	49.983	-0.162	54.4	54	0.4	2.1	4.9	807.1	278.0	49.2	-	0.34	0.18	-	30.0
972	L	486	915	49.528	-0.155	54.4	164	0.7	3.3	8.0	5672.2	1981.8	249.1	1088.3	0.35	0.13	0.55	42.9
973	T	973	-	49.993	-0.136	54.4	56	0.4	2.1	3.9	810.6	228.1	-	-	0.28	-	-	51.3
974	T	974	-	49.506	-0.110	55.7	63	0.6	2.1	4.7	1343.0	375.3	-	116.1	0.28	-	0.31	36.6
975	T	975	-	48.942	-0.074	55.0	338	0.6	2.1	4.4	4741.8	2104.3	361.2	-	0.44	0.17	-	69.5
976	T	976	-	49.480	-0.065	57.0	118	0.9	2.1	4.1	2164.1	650.8	-	101.0	0.30	-	0.16	30.7
977	L	976	976	49.480	-0.065	57.0	34	0.8	2.5	4.1	637.2	216.4	-	34.4	0.34	-	0.16	30.6
978	T	978	-	49.995	-0.051	54.4	17	0.5	2.1	4.1	319.8	109.0	-	-	0.34	-	-	33.8
979	L	486	951	49.518	-0.027	55.0	508	0.7	4.0	8.2	13421.3	5845.8	904.5	-	0.44	0.15	-	24.8
980	T	980	-	48.576	0.084	54.4	23	0.3	2.1	4.1	265.4	89.3	-	15.7	0.34	-	0.18	57.0

981	B	867	955	48.937	0.131	55.0	281	0.5	3.9	7.6	5921.4	2313.3	311.8	-	0.39	0.13	-	39.1
982	L	867	981	48.937	0.131	55.0	128	0.4	4.7	7.6	2519.2	1060.6	149.8	-	0.42	0.14	-	38.0
983	T	983	-	49.034	0.204	54.4	62	0.4	2.1	3.8	659.6	240.3	37.4	-	0.36	0.16	-	34.9
984	T	984	-	48.763	0.329	54.4	33	0.5	2.1	4.5	229.6	120.8	-	-	0.53	-	-	29.4
985	T	985	-	49.015	0.388	55.0	37	0.5	2.1	4.0	305.4	141.0	26.4	-	0.46	0.19	-	30.5
986	T	986	-	48.859	0.490	55.0	56	0.5	2.1	3.8	559.5	220.1	24.3	-	0.39	0.11	-	23.8
987	T	987	-	48.722	-0.702	55.7	61	0.4	2.1	3.8	474.6	202.2	38.3	-	0.43	0.19	-	39.8
988	T	988	-	48.460	-0.677	57.0	162	0.7	2.1	4.1	2429.5	853.0	74.8	-	0.35	0.09	-	28.2
989	B	1016	1016	48.326	-0.625	58.3	1339	1.2	2.1	5.3	26159.5	10232.1	928.2	-	0.39	0.09	-	20.6
990	T	990	-	48.517	-0.639	56.3	186	1.2	2.1	7.9	6440.6	2242.8	236.3	-	0.35	0.11	-	32.1
991	T	991	-	48.791	-0.620	55.0	36	0.4	2.1	3.6	296.7	131.4	-	-	0.44	-	-	27.2
992	T	992	-	48.175	-0.608	56.3	559	0.9	2.1	4.1	6116.8	2776.4	336.3	-	0.45	0.12	-	19.3
993	T	993	-	49.480	-0.556	55.7	325	0.4	2.1	7.5	3052.7	1665.4	108.1	433.2	0.55	0.06	0.26	40.5
994	L	993	993	49.433	-0.547	55.7	178	0.4	2.6	5.7	1219.6	816.4	54.4	229.3	0.67	0.07	0.28	40.6
995	L	993	993	49.480	-0.556	55.7	48	0.4	2.6	7.5	597.4	279.9	-	57.8	0.47	-	0.21	41.3
996	T	996	-	49.360	-0.457	55.7	42	1.1	2.1	4.0	452.5	170.9	-	51.5	0.38	-	0.30	88.5
997	T	997	-	49.376	-0.433	55.7	24	0.7	2.1	3.6	416.5	129.1	-	45.9	0.31	-	0.36	113.6
998	L	486	696	49.424	-0.414	55.7	55	0.5	8.4	10.8	1970.2	863.0	152.1	388.1	0.44	0.18	0.45	275.2
999	B	1196	1102	49.924	-0.294	57.6	114	1.3	2.1	4.1	1311.1	620.8	-	-	0.47	-	-	28.0
1000	L	486	769	49.594	-0.268	57.0	34	0.8	5.2	6.9	1063.7	337.2	29.2	214.2	0.32	0.09	0.64	69.1
1001	B	486	580	49.511	-0.254	56.3	73	0.9	3.1	5.0	2294.3	542.6	30.9	269.1	0.24	0.06	0.50	53.8
1002	L	835	835	49.055	-0.141	55.0	62	0.5	2.6	4.1	927.6	328.6	38.5	68.7	0.35	0.12	0.21	64.2
1003	T	1003	-	49.452	-0.162	57.6	98	1.2	2.1	4.6	1610.7	577.1	58.5	186.5	0.36	0.10	0.32	58.3
1004	L	486	889	49.546	-0.105	56.3	56	0.6	2.8	5.3	1530.3	492.8	46.7	214.4	0.32	0.09	0.44	35.9
1005	L	486	892	49.511	-0.065	57.6	130	1.0	2.8	5.6	3211.3	1091.2	82.1	365.9	0.34	0.08	0.34	31.3
1006	L	867	928	48.923	0.053	54.4	50	0.3	3.2	5.7	993.6	330.3	56.0	-	0.33	0.17	-	49.5
1007	L	867	955	48.914	0.077	55.0	33	0.3	3.9	6.2	584.6	200.4	33.5	-	0.34	0.17	-	48.5
1008	L	867	981	48.923	0.105	55.0	40	0.3	4.7	6.3	600.6	232.9	27.5	-	0.39	0.12	-	44.8
1009	T	1009	-	48.113	-0.806	58.9	284	1.0	2.1	4.2	3044.2	1630.3	236.9	-	0.54	0.15	-	13.0
1010	L	1014	1050	48.755	-0.702	57.6	154	0.7	2.3	4.8	2881.7	1039.9	115.3	-	0.36	0.11	-	26.1
1011	L	1016	989	48.356	-0.684	56.3	76	0.5	2.3	4.2	833.7	340.6	56.5	-	0.41	0.17	-	17.8
1012	L	1016	1017	48.328	-0.660	57.0	163	1.0	2.6	4.7	2793.8	1130.2	83.9	-	0.40	0.07	-	19.8
1013	T	1013	-	48.385	-0.669	57.0	54	0.9	2.1	3.6	1163.6	380.1	-	-	0.33	-	-	21.9
1014	T	1014	-	48.796	-0.658	57.6	584	0.8	2.1	8.3	12590.2	3950.6	430.8	-	0.31	0.11	-	27.1
1015	B	1014	1014	48.796	-0.658	57.6	292	0.7	2.2	8.3	7158.2	2169.6	258.3	-	0.30	0.12	-	30.6
1016	T	1016	-	48.326	-0.625	58.3	1398	1.2	2.1	5.3	27453.0	10686.2	979.8	-	0.39	0.09	-	20.5
1017	B	1016	1052	48.286	-0.672	57.6	587	1.0	2.3	4.9	9581.1	3941.1	335.5	-	0.41	0.09	-	19.0
1018	T	1018	-	48.550	-0.561	57.6	197	0.9	2.1	5.3	3716.8	1413.8	153.5	-	0.38	0.11	-	37.6
1019	L	1018	1018	48.555	-0.599	57.6	106	0.8	2.4	5.2	2019.6	820.7	88.6	-	0.41	0.11	-	36.7
1020	L	992	1022	48.205	-0.599	55.7	138	0.6	2.4	4.0	1625.0	750.9	66.3	-	0.46	0.09	-	19.0
1021	B	992	992	48.175	-0.608	56.3	353	0.8	2.2	4.1	3903.3	1775.1	197.0	-	0.45	0.11	-	19.2

1022	B	992	1021	48.175	-0.608	56.3	206	0.6	2.3	4.1	2237.3	1022.1	92.2	-	0.46	0.09	-	18.9
1023	T	1023	-	48.123	-0.596	55.7	23	0.3	2.1	3.6	168.3	83.1	-	-	0.49	-	-	17.1
1024	L	1016	1025	48.326	-0.625	58.3	351	1.0	2.3	5.3	8146.5	3299.7	337.5	-	0.41	0.10	-	23.6
1025	B	1016	1051	48.326	-0.625	58.3	465	1.0	2.3	5.3	9809.9	3954.7	396.3	-	0.40	0.10	-	23.1
1026	L	992	992	48.165	-0.573	56.3	49	0.6	2.2	4.0	378.6	196.8	32.4	-	0.52	0.16	-	19.5
1027	L	486	1057	49.230	-0.540	56.3	165	0.7	2.2	5.9	4062.5	1450.4	168.4	-	0.36	0.12	-	27.2
1028	L	486	1057	49.256	-0.518	55.7	61	0.6	2.2	5.7	1134.8	374.6	-	124.9	0.33	-	0.33	35.5
1029	B	486	505	49.310	-0.504	56.3	842	1.3	3.3	9.3	21803.8	9200.9	1026.1	-	0.42	0.11	-	30.1
1030	L	486	494	49.398	-0.457	55.7	21	0.6	3.0	4.8	413.2	142.6	20.9	64.7	0.35	0.15	0.45	129.7
1031	T	1031	-	48.661	-0.266	56.3	94	0.7	2.1	3.9	1123.3	426.5	62.5	42.2	0.38	0.15	0.10	46.6
1032	L	486	744	49.603	-0.254	57.6	91	0.9	4.4	9.6	3694.2	1573.2	229.4	1001.6	0.43	0.15	0.64	53.7
1033	L	1035	1035	48.907	-0.181	56.3	74	0.5	2.3	4.8	831.3	360.3	43.9	78.0	0.43	0.12	0.22	64.9
1034	T	1034	-	48.602	-0.188	56.3	130	0.6	2.1	5.7	1948.4	829.5	153.4	208.0	0.43	0.18	0.25	33.4
1035	T	1035	-	48.907	-0.181	56.3	212	0.6	2.1	4.8	2393.6	1070.4	110.7	185.1	0.45	0.10	0.17	60.3
1036	B	486	1118	49.445	-0.037	60.9	8220	1.9	2.2	10.5	243278.9	88298.9	7620.4	-	0.36	0.09	-	38.0
1037	B	486	1121	49.445	-0.037	60.9	9080	1.9	2.1	10.5	267777.9	96202.1	8137.5	-	0.36	0.08	-	38.4
1038	T	1038	-	49.457	-0.065	57.6	41	0.8	2.1	3.6	596.4	199.0	-	38.6	0.33	-	0.19	36.8
1039	T	1039	-	48.866	-0.072	60.9	562	1.9	2.1	7.2	16748.7	5389.5	317.9	-	0.32	0.06	-	65.4
1040	B	1039	1039	48.866	-0.072	60.9	385	1.7	2.5	7.2	10813.3	3697.0	206.5	1614.6	0.34	0.06	0.44	64.9
1041	B	1039	1040	48.866	-0.072	60.9	326	1.7	2.5	7.2	9463.8	3286.9	186.3	1455.7	0.35	0.06	0.44	66.2
1042	T	1042	-	49.627	0.032	55.7	73	0.5	2.1	5.1	1173.4	382.0	50.4	-	0.33	0.13	-	28.3
1043	T	1043	-	48.404	0.072	56.3	39	0.5	2.1	4.0	498.8	166.5	-	25.6	0.33	-	0.15	45.3
1044	T	1044	-	48.970	0.093	55.7	44	0.4	2.1	4.7	744.5	218.0	-	-	0.29	-	-	46.8
1045	T	1045	-	48.168	-0.844	57.6	49	0.6	2.1	3.9	461.6	237.5	-	-	0.51	-	-	13.5
1046	T	1046	-	48.066	-0.839	58.3	215	0.9	2.1	3.9	2042.7	1189.6	111.1	-	0.58	0.09	-	14.2
1047	T	1047	-	48.019	-0.818	58.9	99	1.6	2.1	4.6	956.0	550.8	38.4	-	0.58	0.07	-	15.5
1048	T	1048	-	48.170	-0.787	57.6	93	0.7	2.1	4.0	728.3	408.1	41.8	-	0.56	0.10	-	13.8
1049	L	1014	1050	48.763	-0.679	56.3	47	0.5	2.3	3.8	586.7	183.5	-	-	0.31	-	-	26.3
1050	B	1014	1014	48.755	-0.702	57.6	203	0.9	2.2	4.8	3585.8	1259.8	135.1	-	0.35	0.11	-	26.3
1051	B	1016	989	48.326	-0.625	58.3	1097	1.1	2.3	5.3	20574.6	8300.2	745.1	-	0.40	0.09	-	20.9
1052	B	1016	1051	48.286	-0.672	57.6	620	1.1	2.3	4.9	10299.9	4187.4	328.1	-	0.41	0.08	-	19.2
1053	B	1016	1017	48.286	-0.672	57.6	249	0.8	2.6	4.9	3583.6	1603.5	158.6	-	0.45	0.10	-	18.4
1054	L	992	1022	48.175	-0.608	56.3	44	0.3	2.4	4.1	352.6	159.7	-	-	0.45	-	-	19.0
1055	L	992	1021	48.217	-0.587	57.0	67	0.7	2.3	4.1	828.0	380.3	57.0	-	0.46	0.15	-	21.5
1056	T	1056	-	48.281	-0.568	57.0	51	0.6	2.1	4.2	613.6	263.7	41.0	-	0.43	0.16	-	24.5
1057	B	486	577	49.230	-0.540	56.3	234	0.7	2.2	5.9	5364.4	1871.4	187.0	-	0.35	0.10	-	30.0
1058	L	827	852	48.876	-0.504	58.3	198	0.8	3.5	10.1	6430.9	2433.4	308.3	2271.0	0.38	0.13	0.93	63.5
1059	L	486	1029	49.310	-0.504	56.3	77	0.6	3.9	9.3	1953.1	765.9	57.9	296.3	0.39	0.08	0.39	38.7
1060	L	486	692	49.414	-0.473	57.0	165	0.8	6.8	10.8	6350.2	3067.9	436.9	1436.5	0.48	0.14	0.47	118.6
1061	B	1101	1062	49.055	-0.466	57.6	570	0.9	2.5	7.2	14956.4	5814.8	761.8	2218.1	0.39	0.13	0.38	41.6
1062	B	1101	1100	49.055	-0.466	57.6	760	0.9	2.2	7.2	19937.0	7468.6	903.3	2694.7	0.37	0.12	0.36	41.3

1063	L	486	740	49.424	-0.438	56.3	22	0.6	8.4	10.6	710.4	340.6	40.9	130.1	0.48	0.12	0.38	186.9
1064	L	486	967	49.341	-0.362	56.3	60	0.7	3.8	8.1	1923.4	673.7	54.0	505.2	0.35	0.08	0.75	154.9
1065	T	1065	-	48.453	-0.275	57.0	103	0.5	2.1	4.0	1151.5	487.6	64.6	-	0.42	0.13	-	25.5
1066	T	1066	-	48.604	-0.273	56.3	24	0.4	2.1	3.6	221.9	86.9	-	8.7	0.39	-	0.10	48.6
1067	L	486	1001	49.511	-0.254	56.3	24	0.5	3.2	5.0	689.2	172.2	-	91.5	0.25	-	0.53	69.4
1068	L	486	1001	49.499	-0.242	57.6	32	0.7	3.3	4.9	1019.5	237.9	-	120.4	0.23	-	0.51	51.5
1069	T	1069	-	48.659	-0.249	57.0	67	0.5	2.1	3.8	692.7	280.3	31.2	26.9	0.40	0.11	0.10	48.3
1070	T	1070	-	49.707	-0.252	58.3	222	1.1	2.1	4.4	3431.9	1187.8	132.7	-	0.35	0.11	-	50.2
1071	L	486	532	49.499	-0.226	57.6	13	0.9	3.0	4.9	444.3	118.8	-	38.8	0.27	-	0.33	48.3
1072	L	1035	1035	48.850	-0.209	57.0	101	0.5	2.4	4.4	931.5	455.2	43.7	66.2	0.49	0.10	0.15	58.5
1073	B	486	1113	49.445	-0.037	60.9	8693	1.9	2.2	10.5	254624.7	92072.5	7833.9	-	0.36	0.09	-	38.2
1074	B	486	1117	49.445	-0.037	60.9	6505	1.8	2.4	10.5	200441.0	72972.4	6622.0	-	0.36	0.09	-	37.7
1075	L	1039	1076	48.866	-0.072	60.9	186	1.7	2.9	7.2	5355.6	1999.9	151.0	921.2	0.37	0.08	0.46	66.9
1076	B	1039	1041	48.866	-0.072	60.9	239	1.7	2.9	7.2	6467.9	2339.7	163.2	1092.7	0.36	0.07	0.47	67.3
1077	B	486	1168	49.445	-0.037	60.9	7275	1.8	2.3	10.5	221674.0	80347.8	7149.6	-	0.36	0.09	-	37.5
1078	B	486	1120	49.445	-0.037	60.9	5169	1.7	2.7	10.5	147063.2	55790.9	5327.4	-	0.38	0.10	-	37.4
1079	T	1079	-	48.418	0.020	56.3	25	0.5	2.1	4.0	273.0	123.8	-	12.3	0.45	-	0.10	38.2
1080	T	1080	-	48.413	0.055	56.3	33	0.4	2.1	4.2	248.9	114.9	-	23.4	0.46	-	0.20	40.9
1081	T	1081	-	49.499	0.081	56.3	106	0.6	2.1	4.0	1052.9	454.3	63.2	-	0.43	0.14	-	23.8
1082	L	1081	1081	49.499	0.081	56.3	34	0.5	2.4	4.0	349.2	146.7	19.4	-	0.42	0.13	-	23.4
1083	T	1083	-	49.549	0.093	57.0	171	0.4	2.1	4.9	1572.1	695.1	81.0	-	0.44	0.12	-	24.3
1084	T	1084	-	48.082	-0.898	57.6	37	0.5	2.1	3.8	174.2	127.8	-	-	0.73	-	-	15.0
1085	T	1085	-	48.210	-0.844	58.3	449	0.7	2.1	4.4	3201.1	2089.4	354.3	-	0.65	0.17	-	14.7
1086	B	1085	1085	48.210	-0.844	58.3	242	0.5	2.3	4.4	1697.1	1151.6	216.8	-	0.68	0.19	-	14.5
1087	T	1087	-	48.208	-0.733	58.3	29	0.7	2.1	4.2	286.5	139.2	-	-	0.49	-	-	15.3
1088	T	1088	-	48.243	-0.700	57.6	75	0.6	2.1	4.3	810.5	402.3	51.7	-	0.50	0.13	-	15.0
1089	L	1016	1053	48.286	-0.672	57.6	123	0.8	2.7	4.9	1776.4	820.6	78.6	-	0.46	0.10	-	18.5
1090	L	1016	1053	48.319	-0.681	57.6	53	0.4	2.7	4.1	507.3	244.2	32.6	-	0.48	0.13	-	17.6
1091	L	1014	1015	48.796	-0.658	57.6	192	0.6	2.6	8.3	5049.6	1612.5	211.2	-	0.32	0.13	-	32.3
1092	L	961	962	48.611	-0.662	58.3	22	0.9	2.2	4.0	394.7	179.6	39.0	-	0.46	0.22	-	33.8
1093	B	961	961	48.614	-0.648	55.0	114	2.2	2.1	4.3	1714.2	655.4	87.0	-	0.38	0.13	-	36.8
1094	L	486	486	49.244	-0.570	59.6	173	0.9	2.1	9.1	3489.9	1326.0	-	-	0.38	-	-	22.5
1095	T	1095	-	48.222	-0.525	57.6	213	0.6	2.1	4.2	2615.6	1058.0	63.2	-	0.40	0.06	-	23.4
1096	L	486	617	49.358	-0.495	57.0	33	0.3	4.5	6.3	523.8	242.0	26.7	70.6	0.46	0.11	0.29	62.7
1097	L	486	684	49.398	-0.485	57.0	37	0.6	5.8	7.7	975.4	394.4	46.9	189.7	0.40	0.12	0.48	131.5
1098	L	827	827	48.831	-0.485	57.6	27	0.5	2.3	4.1	277.4	100.7	-	17.2	0.36	-	0.17	62.9
1099	B	1101	1061	49.055	-0.466	57.6	503	0.9	2.7	7.2	12886.8	5115.5	701.9	1966.0	0.40	0.14	0.38	41.8
1100	B	1101	1101	49.055	-0.466	57.6	791	0.9	2.2	7.2	20621.3	7691.4	912.1	2750.4	0.37	0.12	0.36	40.9
1101	T	1101	-	49.055	-0.466	57.6	935	1.3	2.1	7.2	23736.3	8757.4	1055.3	3070.2	0.37	0.12	0.35	41.8
1102	B	1196	1196	49.924	-0.294	57.6	155	2.3	2.1	4.1	2004.1	985.0	43.4	-	0.49	0.04	-	27.9
1103	L	1196	999	49.924	-0.320	58.9	21	0.9	2.3	3.9	306.2	121.8	-	-	0.40	-	-	27.6

1104	T	1104	-	48.562	-0.308	57.6	46	0.5	2.1	3.7	484.0	192.2	-	-	0.40	-	-	32.2
1105	L	486	600	49.528	-0.273	57.6	19	0.7	2.8	4.5	486.1	111.8	-	76.0	0.23	-	0.68	67.2
1106	T	1106	-	48.774	-0.259	58.9	390	0.7	2.1	4.6	5248.3	2171.7	264.9	314.6	0.41	0.12	0.14	68.6
1107	L	1108	1108	49.764	-0.254	58.3	77	0.7	2.4	3.9	1061.6	386.6	46.3	-	0.36	0.12	-	38.8
1108	T	1108	-	49.764	-0.268	58.3	132	0.8	2.1	4.3	2100.6	722.6	69.1	-	0.34	0.10	-	39.0
1109	T	1109	-	48.555	-0.228	58.3	160	0.5	2.1	4.1	1666.9	705.1	118.6	105.7	0.42	0.17	0.15	33.0
1110	L	486	508	49.313	-0.235	59.6	146	1.3	2.9	5.6	4010.7	1292.3	69.4	428.3	0.32	0.05	0.33	66.7
1111	T	1111	-	48.718	-0.226	57.0	20	0.4	2.1	4.6	215.8	80.5	-	10.3	0.37	-	0.13	64.9
1112	T	1112	-	49.322	-0.117	59.6	144	1.1	2.1	4.5	1649.4	886.1	-	298.7	0.54	-	0.34	47.9
1113	B	486	1037	49.445	-0.037	60.9	8949	1.9	2.2	10.5	264687.1	95187.6	8054.7	-	0.36	0.08	-	38.3
1114	B	486	1073	49.445	-0.037	60.9	8449	1.9	2.2	10.5	248543.2	90091.2	7746.4	-	0.36	0.09	-	38.1
1115	B	486	1160	49.445	-0.037	60.9	5934	1.7	2.5	10.5	176417.5	65398.1	6062.7	-	0.37	0.09	-	37.5
1116	L	976	976	49.487	-0.070	56.3	42	0.5	2.5	3.9	513.5	165.9	-	24.2	0.32	-	0.15	30.9
1117	B	486	1172	49.445	-0.037	60.9	6923	1.8	2.3	10.5	212780.1	77116.4	6885.8	-	0.36	0.09	-	37.4
1118	B	486	1114	49.445	-0.037	60.9	8293	1.9	2.2	10.5	244143.8	88661.3	7653.7	-	0.36	0.09	-	38.1
1119	B	486	1257	49.445	-0.037	60.9	5547	1.7	2.6	10.5	163197.7	61080.3	5726.9	-	0.37	0.09	-	37.4
1120	B	486	1119	49.445	-0.037	60.9	5448	1.7	2.6	10.5	159678.2	59859.7	5648.0	-	0.37	0.09	-	37.5
1121	B	486	1159	49.445	-0.037	60.9	9185	1.9	2.1	10.5	271191.2	97285.3	8178.3	-	0.36	0.08	-	38.3
1122	T	1122	-	49.452	-0.046	58.3	30	0.6	2.1	3.5	421.7	141.8	-	13.4	0.34	-	0.09	31.7
1123	L	1039	1040	48.845	-0.025	56.3	33	0.3	2.5	4.2	378.3	131.9	-	47.2	0.35	-	0.36	62.8
1124	B	486	1078	49.445	-0.037	60.9	4603	1.7	2.9	10.5	127585.3	49225.1	4822.4	-	0.39	0.10	-	37.2
1125	B	486	1074	49.445	-0.037	60.9	6330	1.8	2.4	10.5	191950.9	70312.2	6398.4	-	0.37	0.09	-	37.5
1126	L	1081	1081	49.516	0.105	57.6	44	0.5	2.5	3.9	361.3	174.2	21.7	-	0.48	0.12	-	24.0
1127	T	1127	-	49.244	0.202	57.0	50	0.3	2.1	4.8	431.3	167.8	-	-	0.39	-	-	28.7
1128	L	1085	1086	48.210	-0.844	58.3	102	0.5	2.4	4.4	799.6	561.9	109.3	-	0.70	0.19	-	14.4
1129	T	1129	-	48.064	-0.806	58.3	36	0.9	2.1	3.5	256.5	174.1	-	-	0.68	-	-	13.9
1130	T	1130	-	48.321	-0.754	57.6	55	0.7	2.1	4.0	404.1	200.5	-	-	0.50	-	-	15.8
1131	T	1131	-	48.219	-0.750	58.9	90	0.8	2.1	4.0	736.4	461.1	52.6	-	0.63	0.11	-	15.1
1132	L	1130	1130	48.321	-0.754	57.6	25	0.4	2.2	4.0	149.0	85.4	-	-	0.57	-	-	16.4
1133	T	1133	-	48.208	-0.719	58.3	43	0.6	2.1	4.2	362.7	187.6	-	-	0.52	-	-	14.5
1134	L	1016	1016	48.297	-0.691	57.6	24	0.5	2.1	3.7	186.5	82.9	-	-	0.44	-	-	16.9
1135	L	1016	1025	48.264	-0.636	58.9	103	0.7	2.3	4.3	1211.1	503.2	42.9	-	0.42	0.09	-	21.4
1136	T	1136	-	48.831	-0.617	58.3	20	0.4	2.1	6.4	263.7	97.5	-	-	0.37	-	-	31.9
1137	L	1018	1018	48.550	-0.561	57.6	51	0.4	2.4	5.3	766.4	292.1	35.9	-	0.38	0.12	-	39.3
1138	B	486	1029	49.358	-0.532	58.9	575	0.9	3.9	8.5	11510.4	5455.8	700.3	-	0.47	0.13	-	27.9
1139	L	1101	1100	48.942	-0.483	57.6	23	0.4	2.2	3.9	235.9	94.0	-	21.2	0.40	-	0.23	25.5
1140	T	1140	-	49.129	-0.485	58.3	34	0.5	2.1	4.0	560.8	179.2	40.8	83.9	0.32	0.23	0.47	35.2
1141	B	1101	1099	49.055	-0.466	57.6	282	0.8	3.3	7.2	7287.8	3041.3	487.0	1277.0	0.42	0.16	0.42	44.4
1142	B	1101	1141	49.055	-0.466	57.6	214	0.6	3.7	7.2	5107.4	2213.9	372.7	1008.0	0.43	0.17	0.46	47.8
1143	L	486	694	49.499	-0.457	57.0	22	0.3	7.4	9.4	628.4	257.7	17.9	151.0	0.41	0.07	0.59	109.2
1144	L	1101	1142	49.055	-0.466	57.6	43	0.4	4.6	7.2	873.5	379.3	69.3	212.1	0.43	0.18	0.56	46.0

1145	L	1101	1062	49.074	-0.457	57.6	40	0.8	2.5	4.1	551.1	238.5	28.4	72.6	0.43	0.12	0.30	46.3
1146	L	1186	1186	48.774	-0.433	58.9	52	0.8	2.1	4.9	521.3	215.4	-	-	0.41	-	-	56.9
1147	L	486	795	49.492	-0.419	58.3	31	1.0	14.8	17.0	2192.1	1000.2	183.0	719.3	0.46	0.18	0.72	484.0
1148	B	1189	1150	48.923	-0.277	69.3	4392	3.3	2.3	17.6	403187.1	114343.9	12054.1	114294.8	0.28	0.11	1.00	169.0
1149	B	1189	1152	48.923	-0.277	69.3	3946	3.3	2.6	17.6	363525.0	105252.6	11356.3	106471.7	0.29	0.11	1.01	172.3
1150	B	1189	1189	48.923	-0.277	69.3	4698	3.3	2.1	17.6	427391.3	119817.6	12523.2	118833.0	0.28	0.10	0.99	166.1
1151	B	1189	1148	48.923	-0.277	69.3	4240	3.3	2.4	17.6	387729.8	110714.5	11775.6	111147.5	0.29	0.11	1.00	169.9
1152	B	1189	1151	48.923	-0.277	69.3	4110	3.3	2.5	17.6	380047.5	108964.0	11658.7	109656.2	0.29	0.11	1.01	171.1
1153	L	1196	999	49.924	-0.294	57.6	39	1.2	2.3	4.1	376.9	197.2	28.8	-	0.52	0.15	-	27.7
1154	L	1196	1196	49.905	-0.303	58.3	24	0.7	2.1	3.8	280.1	118.2	-	-	0.42	-	-	29.3
1155	L	1106	1106	48.774	-0.259	58.9	187	0.5	2.6	4.6	2262.9	1009.2	164.0	163.3	0.45	0.16	0.16	67.6
1156	L	1106	1106	48.812	-0.266	57.6	48	0.5	2.6	4.3	501.4	223.4	-	27.5	0.45	-	0.12	79.9
1157	B	486	636	49.332	-0.273	60.2	454	1.9	3.6	7.6	11412.4	5774.9	713.0	2229.7	0.51	0.12	0.39	102.5
1158	L	1112	1112	49.322	-0.117	59.6	32	1.0	2.5	4.5	292.3	225.4	-	68.5	0.77	-	0.30	48.0
1159	B	486	1162	49.445	-0.037	60.9	9252	1.9	2.1	10.5	272828.9	97845.4	8231.8	-	0.36	0.08	-	38.4
1160	B	486	1125	49.445	-0.037	60.9	6159	1.8	2.5	10.5	184519.5	68024.0	6231.8	-	0.37	0.09	-	37.5
1161	B	486	1339	49.445	-0.037	60.9	3590	1.5	3.1	10.5	93627.3	37200.4	3779.0	-	0.40	0.10	-	37.3
1162	B	486	547	49.445	-0.037	60.9	9260	1.9	2.1	10.5	274315.7	98337.9	8254.5	-	0.36	0.08	-	38.4
1163	B	486	1209	49.445	-0.037	60.9	3044	1.4	3.3	10.5	78538.2	31548.1	3240.1	-	0.40	0.10	-	37.2
1164	B	486	1166	49.445	-0.037	60.9	2697	1.5	3.4	10.5	70416.3	28467.0	2939.5	-	0.40	0.10	-	37.5
1165	B	486	1167	49.445	-0.037	60.9	4116	1.5	3.0	10.5	111353.8	43293.9	4319.0	-	0.39	0.10	-	37.2
1166	B	486	1208	49.445	-0.037	60.9	2792	1.5	3.3	10.5	73720.1	29685.6	3058.7	-	0.40	0.10	-	37.6
1167	B	486	1124	49.445	-0.037	60.9	4271	1.6	3.0	10.5	116412.2	45315.4	4530.9	-	0.39	0.10	-	37.0
1168	B	486	1036	49.445	-0.037	60.9	7365	1.8	2.3	10.5	223574.4	81084.9	7199.4	-	0.36	0.09	-	37.4
1169	B	486	1300	49.445	-0.037	60.9	2075	1.4	3.6	10.5	54968.6	22557.2	2371.9	-	0.41	0.11	-	36.7
1170	B	486	1164	49.445	-0.037	60.9	2409	1.4	3.5	10.5	62013.2	25343.5	2644.9	-	0.41	0.10	-	37.2
1171	L	1039	1041	48.869	-0.034	60.9	36	1.3	2.9	4.4	599.5	226.9	-	63.1	0.38	-	0.28	59.5
1172	B	486	1077	49.445	-0.037	60.9	7077	1.8	2.3	10.5	215776.3	78199.0	6927.2	-	0.36	0.09	-	37.3
1173	L	1085	1086	48.224	-0.816	57.6	58	0.3	2.5	3.9	353.9	237.4	34.3	-	0.67	0.14	-	14.8
1174	L	1085	1085	48.219	-0.804	57.6	36	0.4	2.3	3.7	132.9	126.9	31.5	-	0.95	0.25	-	14.9
1175	L	1130	1130	48.328	-0.773	58.3	22	0.4	2.2	3.7	190.9	84.3	-	-	0.44	-	-	15.4
1176	L	961	1093	48.593	-0.667	58.3	33	0.6	2.1	3.6	364.5	139.7	19.0	-	0.38	0.14	-	46.4
1177	L	1016	1052	48.340	-0.653	59.6	56	0.7	2.3	3.8	643.5	218.7	-	-	0.34	-	-	21.9
1178	B	486	1138	49.358	-0.532	58.9	396	0.7	4.3	8.5	7122.6	3471.2	436.7	-	0.49	0.13	-	26.5
1179	L	486	1138	49.367	-0.514	58.9	54	0.6	4.3	7.2	755.8	490.8	59.7	121.9	0.65	0.12	0.25	38.0
1180	T	1180	-	48.767	-0.495	58.9	73	0.6	2.1	4.1	792.8	398.5	39.3	-	0.50	0.10	-	69.6
1181	L	1101	1061	49.079	-0.481	58.3	20	0.5	2.7	4.4	318.5	130.5	-	58.6	0.41	-	0.45	41.9
1182	L	1101	1142	49.029	-0.476	58.3	61	0.4	4.6	7.2	1020.4	502.6	84.8	222.2	0.49	0.17	0.44	46.6
1183	L	1101	1099	49.001	-0.466	58.9	73	0.4	3.3	5.7	995.0	457.0	54.6	155.9	0.46	0.12	0.34	40.9
1184	B	1186	1186	48.895	-0.412	61.5	680	1.2	2.1	8.8	14975.8	6149.9	904.0	-	0.41	0.15	-	67.0
1185	B	1186	1184	48.793	-0.450	58.3	248	0.7	2.2	5.3	3247.9	1312.8	89.5	-	0.40	0.07	-	63.7

1186	T	1186	-	48.895	-0.412	61.5	736	1.2	2.1	8.8	15625.0	6403.7	915.7	-	0.41	0.14	-	65.4
1187	L	486	615	49.549	-0.431	59.6	35	0.7	3.9	6.2	1381.4	344.4	-	266.6	0.25	-	0.77	117.0
1188	L	1186	1185	48.829	-0.424	59.6	22	0.7	2.6	4.1	298.3	119.5	-	29.9	0.40	-	0.25	68.3
1189	T	1189	-	48.923	-0.277	69.3	4733	3.3	2.1	17.6	430962.1	120609.1	12583.6	119526.7	0.28	0.10	0.99	166.0
1190	T	1190	-	49.983	-0.341	58.9	19	0.7	2.1	3.8	186.8	89.9	-	-	0.48	-	-	26.4
1191	B	1189	1192	48.923	-0.277	69.3	3236	3.2	3.1	17.6	290000.3	86659.5	9631.1	88101.5	0.30	0.11	1.02	175.5
1192	B	1189	1281	48.923	-0.277	69.3	3286	3.3	3.1	17.6	299216.4	88974.8	9811.1	90874.1	0.30	0.11	1.02	175.2
1193	B	1189	1237	49.095	-0.263	64.8	1257	2.1	3.7	13.1	63081.6	25370.0	3425.9	18127.8	0.40	0.14	0.71	161.1
1194	B	1189	1191	48.923	-0.277	69.3	2915	3.2	3.3	17.6	266374.7	81190.2	9144.7	83339.0	0.30	0.11	1.03	178.1
1195	T	1195	-	49.804	-0.308	59.6	113	0.8	2.1	4.1	1406.0	621.7	99.0	-	0.44	0.16	-	41.8
1196	T	1196	-	49.924	-0.294	57.6	179	2.3	2.1	4.1	2300.3	1109.5	57.7	-	0.48	0.05	-	28.1
1197	T	1197	-	49.794	-0.287	58.3	48	0.5	2.1	3.6	432.4	189.2	25.5	-	0.44	0.13	-	45.6
1198	L	1108	1108	49.764	-0.268	58.3	22	0.8	2.4	4.3	258.4	103.1	-	-	0.40	-	-	42.1
1199	B	486	1292	49.480	-0.254	60.2	115	1.0	4.9	7.6	2821.3	1410.4	95.6	729.6	0.50	0.07	0.52	62.9
1200	L	486	724	49.596	-0.209	58.9	34	0.5	3.0	5.7	669.7	267.5	-	153.9	0.40	-	0.58	41.4
1201	B	486	506	49.414	-0.207	60.2	591	1.7	2.8	7.0	8064.9	4221.8	422.4	1429.8	0.52	0.10	0.34	77.7
1202	L	486	1457	49.358	-0.192	59.6	69	1.4	2.3	4.0	836.5	373.2	36.1	55.0	0.45	0.10	0.15	71.0
1203	T	1203	-	49.643	-0.190	58.3	16	0.8	2.1	3.9	228.6	102.6	-	20.2	0.45	-	0.20	40.2
1204	B	486	1205	49.414	-0.207	60.2	323	0.8	2.9	7.0	4643.6	2410.6	218.3	996.0	0.52	0.09	0.41	72.4
1205	B	486	1249	49.414	-0.207	60.2	338	1.2	2.9	7.0	5296.0	2711.7	231.6	1052.3	0.51	0.09	0.39	72.4
1206	T	1206	-	49.745	-0.174	58.9	75	0.6	2.1	5.5	1214.1	569.5	79.1	-	0.47	0.14	-	41.4
1207	B	486	1161	49.445	-0.037	60.9	3355	1.5	3.2	10.5	87064.1	34745.4	3546.9	-	0.40	0.10	-	37.5
1208	B	486	1163	49.445	-0.037	60.9	2888	1.5	3.3	10.5	75666.8	30427.0	3117.8	-	0.40	0.10	-	37.4
1209	B	486	1207	49.445	-0.037	60.9	3105	1.5	3.3	10.5	80282.7	32222.4	3319.4	-	0.40	0.10	-	37.3
1210	B	486	1169	49.445	-0.037	60.9	1898	1.4	3.6	10.5	49896.6	20619.4	2232.8	-	0.41	0.11	-	36.5
1211	L	486	1212	49.294	-0.058	60.2	236	0.9	4.1	7.7	5816.3	2643.1	377.6	1078.8	0.45	0.14	0.41	40.8
1212	B	486	1213	49.294	-0.058	60.2	451	1.0	3.8	7.7	10059.6	4456.5	571.9	1534.6	0.44	0.13	0.34	40.0
1213	B	486	1215	49.445	-0.037	60.9	1412	1.3	3.8	10.5	38980.8	16258.7	1832.3	5503.5	0.42	0.11	0.34	35.9
1214	B	486	1210	49.445	-0.037	60.9	1641	1.4	3.7	10.5	43747.4	18211.2	2012.6	-	0.42	0.11	-	36.6
1215	B	486	1214	49.445	-0.037	60.9	1527	1.4	3.8	10.5	41559.9	17314.2	1907.8	5723.2	0.42	0.11	0.33	36.4
1216	T	1216	-	48.715	0.025	59.6	52	0.7	2.1	4.7	1156.0	357.0	-	202.7	0.31	-	0.57	57.8
1217	T	1217	-	49.124	0.353	58.3	43	0.4	2.1	3.8	237.4	175.9	30.8	-	0.74	0.18	-	33.6
1218	T	1218	-	48.026	-0.993	60.2	15	0.8	2.1	4.1	147.5	90.4	-	-	0.61	-	-	14.9
1219	T	1219	-	48.248	-0.669	58.9	18	0.8	2.1	3.8	167.6	81.8	-	-	0.49	-	-	17.8
1220	L	1014	1015	48.836	-0.660	58.9	28	0.3	2.6	4.2	409.4	130.5	26.8	-	0.32	0.21	-	27.2
1221	T	1221	-	48.774	-0.599	58.3	30	0.5	2.1	4.0	414.5	123.1	-	-	0.30	-	-	32.5
1222	T	1222	-	48.205	-0.606	60.2	52	0.6	2.1	4.1	539.6	204.3	-	-	0.38	-	-	18.9
1223	T	1223	-	49.173	-0.573	60.2	116	0.6	2.1	4.6	1562.3	646.9	62.4	-	0.41	0.10	-	26.1
1224	T	1224	-	49.055	-0.580	59.6	41	1.0	2.1	3.9	429.5	196.5	29.1	-	0.46	0.15	-	26.2
1225	T	1225	-	48.944	-0.582	60.2	110	0.7	2.1	5.0	1905.6	740.6	60.6	-	0.39	0.08	-	26.6
1226	L	486	497	49.273	-0.554	60.2	45	0.6	2.4	6.2	660.9	246.3	34.2	20.7	0.37	0.14	0.08	26.3

1227	L	486	1178	49.358	-0.532	58.9	58	0.4	4.9	8.5	846.7	496.7	59.3	133.0	0.59	0.12	0.27	32.1
1228	L	486	698	49.436	-0.530	59.6	124	0.4	5.9	12.1	3856.8	1590.6	290.3	978.4	0.41	0.18	0.62	63.9
1229	L	486	803	49.398	-0.507	58.9	29	0.5	3.4	5.9	571.5	191.5	34.5	56.9	0.34	0.18	0.30	89.9
1230	L	486	490	49.466	-0.478	59.6	24	0.6	3.5	5.6	650.6	167.4	-	55.7	0.26	-	0.33	105.4
1231	T	1231	-	49.898	-0.464	58.9	24	0.5	2.1	3.9	266.9	103.4	-	-	0.39	-	-	31.0
1232	L	1186	1233	48.793	-0.450	58.3	77	0.4	2.7	5.3	937.3	375.1	24.4	109.0	0.40	0.07	0.29	57.7
1233	B	1186	1185	48.793	-0.450	58.3	133	0.6	2.6	5.3	1527.8	670.2	39.5	191.7	0.44	0.06	0.29	61.9
1234	L	1186	1233	48.831	-0.438	58.9	48	0.6	2.7	4.3	443.1	239.1	-	70.2	0.54	-	0.29	69.8
1235	L	1186	1184	48.895	-0.412	61.5	400	0.9	2.2	8.8	11012.2	4599.0	792.5	3252.5	0.42	0.17	0.71	72.4
1236	L	1189	1237	49.081	-0.348	59.6	25	0.8	3.7	5.4	488.0	184.0	27.2	108.2	0.38	0.15	0.59	146.4
1237	B	1189	1194	49.095	-0.263	64.8	1305	2.1	3.6	13.1	65394.2	26144.2	3525.0	18602.1	0.40	0.13	0.71	160.8
1238	T	1238	-	49.953	-0.344	59.6	16	0.6	2.2	3.7	166.1	83.2	12.8	-	0.50	0.15	-	27.2
1239	B	1189	1149	48.923	-0.277	69.3	3460	3.3	3.0	17.6	311085.6	92399.8	10183.8	93719.8	0.30	0.11	1.01	172.9
1240	L	486	687	49.471	-0.303	58.3	37	0.9	6.6	8.5	1330.3	560.7	65.3	405.9	0.42	0.12	0.72	82.6
1241	B	486	496	49.634	-0.303	61.5	292	1.1	2.7	8.2	14792.5	3722.8	389.2	2320.7	0.25	0.10	0.62	68.2
1242	L	486	1243	49.332	-0.273	60.2	136	1.0	4.1	7.6	3491.6	1672.8	193.1	672.1	0.48	0.12	0.40	108.8
1243	B	486	1157	49.332	-0.273	60.2	324	1.7	3.9	7.6	7405.7	3876.9	497.6	1502.3	0.52	0.13	0.39	102.5
1244	L	486	1199	49.480	-0.235	58.9	19	1.0	5.4	7.0	514.4	234.1	18.6	115.3	0.46	0.08	0.49	62.6
1245	T	1245	-	48.869	-0.242	59.6	24	0.6	2.1	5.2	256.7	146.9	18.4	123.2	0.57	0.13	0.84	79.3
1246	T	1246	-	49.171	-0.211	60.9	605	2.2	2.1	13.0	21047.0	13232.7	1599.5	11333.7	0.63	0.12	0.86	98.1
1247	B	1246	1246	49.171	-0.211	60.9	482	2.1	2.5	13.0	16466.9	11307.6	1436.6	9838.8	0.69	0.13	0.87	97.6
1248	L	486	500	49.301	-0.207	59.6	25	0.6	2.4	3.9	190.4	91.9	-	35.3	0.48	-	0.38	60.1
1249	B	486	1251	49.414	-0.207	60.2	386	1.6	2.9	7.0	5858.5	3022.5	279.2	1097.9	0.52	0.09	0.36	73.4
1250	L	486	1204	49.435	-0.204	59.6	28	0.6	3.2	4.8	273.6	177.1	21.5	41.1	0.65	0.12	0.23	59.2
1251	B	486	1201	49.414	-0.207	60.2	506	1.6	2.8	7.0	6951.5	3650.0	354.5	1248.1	0.53	0.10	0.34	77.2
1252	L	486	513	49.395	-0.190	59.6	25	0.5	2.3	3.8	225.9	107.8	-	17.9	0.48	-	0.17	64.1
1253	T	1253	-	49.100	-0.174	60.9	49	0.9	2.1	5.1	969.9	400.4	-	436.1	0.41	-	1.09	71.3
1254	T	1254	-	49.426	-0.152	59.6	29	0.5	2.1	3.5	313.8	172.6	25.6	35.9	0.55	0.15	0.21	77.7
1255	L	1112	1112	49.339	-0.124	58.9	52	0.5	2.5	4.2	462.2	227.0	-	97.3	0.49	-	0.43	47.0
1256	T	1256	-	48.715	-0.105	60.2	44	0.5	2.1	3.6	276.9	184.4	21.5	14.5	0.67	0.12	0.08	38.9
1257	B	486	1115	49.445	-0.037	60.9	5625	1.7	2.6	10.5	164718.0	61627.9	5769.7	-	0.37	0.09	-	37.4
1258	L	486	1210	49.251	-0.020	60.9	66	0.9	3.7	5.4	845.8	386.3	49.3	-	0.46	0.13	-	37.2
1259	T	1259	-	48.737	-0.030	59.6	85	0.5	2.1	4.9	1077.5	406.7	37.3	102.8	0.38	0.09	0.25	45.7
1260	T	1260	-	48.699	-0.032	58.9	21	0.7	2.1	3.9	201.6	89.3	-	14.6	0.44	-	0.16	47.6
1261	B	486	1305	49.445	-0.037	60.9	591	1.0	4.1	10.5	20832.9	8473.6	994.5	3177.5	0.41	0.12	0.37	30.9
1262	B	486	1308	49.445	-0.037	60.9	807	1.0	3.9	10.5	26221.7	10618.7	1145.6	3708.8	0.40	0.11	0.35	31.5
1263	L	486	1308	49.388	-0.006	60.2	61	0.6	3.9	5.8	927.7	416.5	50.9	105.5	0.45	0.12	0.25	31.9
1264	L	1266	1266	49.317	0.060	58.9	101	0.9	2.1	4.0	1271.8	432.7	-	-	0.34	-	-	32.1
1265	L	1266	1266	49.294	0.065	59.6	16	0.9	2.1	4.0	238.0	100.1	19.9	-	0.42	0.20	-	34.0
1266	T	1266	-	49.317	0.060	58.9	147	0.9	2.1	4.0	1886.5	645.8	36.0	-	0.34	0.06	-	32.1
1267	T	1267	-	48.257	-0.660	60.2	23	0.6	2.1	3.5	190.8	84.0	-	-	0.44	-	-	18.6

1268	T	1268	-	48.234	-0.636	60.2	41	0.4	2.1	3.8	412.9	143.2	20.4	-	0.35	0.14	-	20.0
1269	T	1269	-	49.199	-0.632	60.2	183	0.6	2.1	5.9	2995.6	1053.8	-	-	0.35	-	-	22.6
1270	L	1269	1269	49.199	-0.632	60.2	73	0.5	2.7	5.9	1180.9	468.5	-	-	0.40	-	-	22.8
1271	T	1271	-	48.555	-0.617	62.2	127	0.9	2.1	4.1	1856.1	620.8	60.1	-	0.33	0.10	-	34.0
1272	L	1269	1269	49.171	-0.617	59.6	25	0.4	2.7	5.1	306.3	116.0	-	-	0.38	-	-	22.5
1273	T	1273	-	49.036	-0.592	58.9	26	0.5	2.1	3.6	314.1	112.2	19.3	-	0.36	0.17	-	30.3
1274	T	1274	-	49.395	-0.613	60.9	183	0.6	2.1	5.8	2245.4	880.5	74.3	-	0.39	0.08	-	30.1
1275	T	1275	-	49.072	-0.580	59.6	29	0.6	2.1	3.7	330.4	121.9	-	-	0.37	-	-	39.2
1276	T	1276	-	49.159	-0.580	60.2	46	0.5	2.1	5.1	585.7	253.3	25.0	-	0.43	0.10	-	25.6
1277	L	486	1278	49.317	-0.561	60.2	107	0.5	5.2	7.9	1547.7	804.6	108.1	212.7	0.52	0.13	0.26	26.1
1278	B	486	1178	49.313	-0.570	60.9	182	0.6	4.9	8.2	2783.1	1439.6	186.7	-	0.52	0.13	-	25.6
1279	L	1101	1141	49.027	-0.457	60.2	32	0.5	3.7	5.4	408.1	170.0	25.3	36.1	0.42	0.15	0.21	38.1
1280	L	486	528	49.313	-0.360	60.9	59	0.8	3.5	5.9	666.6	494.5	76.0	277.3	0.74	0.15	0.56	121.8
1281	B	1189	1326	48.923	-0.277	69.3	3330	3.3	3.0	17.6	302944.8	89921.3	9887.8	91665.9	0.30	0.11	1.02	174.6
1282	L	486	499	49.624	-0.341	60.2	121	1.0	2.2	5.7	3506.9	758.9	93.3	578.8	0.22	0.12	0.76	102.5
1283	B	1189	1193	49.095	-0.263	64.8	912	2.2	4.4	13.1	44694.5	18759.7	2617.4	13877.2	0.42	0.14	0.74	166.3
1284	L	1189	1283	49.067	-0.334	60.9	162	0.9	4.6	10.7	6829.6	3427.8	526.5	2423.2	0.50	0.15	0.71	170.0
1285	L	1189	1326	49.020	-0.320	60.2	68	0.7	3.0	8.4	2577.2	836.2	129.3	719.5	0.32	0.15	0.86	173.0
1286	L	1196	1102	49.927	-0.311	62.2	76	1.5	2.1	4.0	631.5	340.8	25.4	-	0.54	0.07	-	27.2
1287	T	1287	-	49.971	-0.311	61.5	43	1.2	2.1	4.2	425.9	221.0	-	-	0.52	-	-	29.6
1288	B	486	1241	49.634	-0.303	61.5	227	1.1	2.8	8.2	12708.8	3258.7	350.0	2075.9	0.26	0.11	0.64	69.9
1289	B	1189	1283	49.095	-0.263	64.8	693	2.1	4.6	13.1	34069.8	13977.4	1925.6	10567.6	0.41	0.14	0.76	163.9
1290	B	1189	1289	49.121	-0.325	60.9	268	1.0	5.5	10.1	8296.9	4508.9	788.1	2505.3	0.54	0.17	0.56	144.3
1291	L	486	1333	49.405	-0.235	60.9	85	0.7	3.3	5.6	1287.1	636.8	58.2	307.6	0.49	0.09	0.48	75.3
1292	B	486	743	49.480	-0.254	60.2	189	1.0	4.9	7.6	3840.9	1995.2	166.9	1126.0	0.52	0.08	0.56	68.4
1293	L	486	464	49.332	-0.209	59.6	18	0.9	2.4	4.0	216.1	107.3	-	14.5	0.50	-	0.14	63.9
1294	T	1294	-	49.247	-0.202	59.6	28	0.4	2.1	3.7	263.1	109.1	15.9	48.8	0.41	0.15	0.45	74.0
1295	L	486	1333	49.414	-0.207	60.2	128	0.6	3.3	7.0	1441.8	867.7	80.9	373.6	0.60	0.09	0.43	71.7
1296	T	1296	-	49.216	-0.181	60.9	29	0.7	2.1	3.9	265.5	123.2	-	58.6	0.46	-	0.48	88.9
1297	L	486	487	49.426	-0.171	60.9	30	0.5	2.5	4.6	319.6	150.6	-	18.8	0.47	-	0.12	60.3
1298	L	486	1115	49.237	-0.082	60.9	15	1.0	2.6	5.3	283.8	110.7	13.7	9.8	0.39	0.12	0.09	46.0
1299	L	486	1120	49.209	-0.093	59.6	43	0.4	2.7	4.3	501.8	195.7	-	26.8	0.39	-	0.14	47.2
1300	B	486	1170	49.445	-0.037	60.9	2142	1.4	3.5	10.5	55829.9	22954.2	2400.7	-	0.41	0.10	-	36.9
1301	T	1301	-	49.745	-0.063	59.6	26	0.3	2.1	3.9	193.7	86.6	-	-	0.45	-	-	34.5
1302	L	1039	1076	48.885	-0.048	59.6	25	0.5	3.0	5.0	539.4	148.6	-	97.8	0.28	-	0.66	76.4
1303	L	486	1169	49.235	-0.041	60.2	22	0.4	3.6	5.4	285.7	139.0	-	24.9	0.49	-	0.18	43.3
1304	T	1304	-	49.688	-0.046	60.2	148	0.8	2.1	4.9	1619.0	744.4	-	-	0.46	-	-	33.4
1305	B	486	1262	49.445	-0.037	60.9	738	1.0	3.9	10.5	24456.7	9938.8	1097.5	3547.5	0.41	0.11	0.36	31.7
1306	B	486	1213	49.445	-0.037	60.9	958	1.1	3.8	10.5	28725.6	11733.2	1261.2	3950.3	0.41	0.11	0.34	31.8
1307	T	1307	-	48.715	-0.018	59.6	25	0.6	2.2	3.8	226.0	103.8	-	44.7	0.46	-	0.43	48.6
1308	B	486	1306	49.445	-0.037	60.9	898	1.1	3.8	10.5	27889.7	11330.1	1222.2	3880.4	0.41	0.11	0.34	31.5

1309	B	486	1261	49.445	-0.037	60.9	447	0.9	4.5	10.5	15848.0	6590.5	811.7	2662.9	0.42	0.12	0.40	30.4
1310	T	1310	-	49.728	0.207	59.6	32	0.4	2.2	5.4	367.7	161.9	44.3	-	0.44	0.27	-	22.2
1311	T	1311	-	49.471	0.440	60.9	196	0.7	2.1	4.6	2207.7	1117.8	194.1	-	0.51	0.17	-	25.3
1312	T	1312	-	49.261	-0.651	60.9	44	0.6	2.1	4.2	435.4	197.3	24.4	-	0.45	0.12	-	21.6
1313	T	1313	-	49.159	-0.599	60.2	19	0.5	2.1	4.4	276.2	101.4	18.8	-	0.37	0.19	-	25.4
1314	L	486	612	49.329	-0.594	60.9	37	0.5	2.9	5.1	606.5	229.4	18.5	-	0.38	0.08	-	22.8
1315	L	486	683	49.464	-0.551	59.6	38	0.4	5.6	7.1	757.0	330.3	58.2	131.9	0.44	0.18	0.40	38.8
1316	T	1316	-	49.225	-0.476	60.2	22	0.4	2.2	4.7	256.8	98.6	-	42.5	0.38	-	0.43	31.1
1317	B	486	643	49.572	-0.398	62.2	303	1.9	3.6	8.1	17933.8	5371.6	443.0	4864.7	0.30	0.08	0.91	132.7
1318	B	486	1317	49.572	-0.398	62.2	215	1.6	3.8	8.1	14406.7	4206.1	349.9	3837.0	0.29	0.08	0.91	134.7
1319	L	486	540	49.546	-0.398	61.5	15	0.9	3.4	5.8	704.0	134.7	-	137.7	0.19	-	1.02	279.0
1320	L	486	830	49.492	-0.379	61.5	25	0.7	21.8	25.3	2575.7	1656.3	273.0	1780.7	0.64	0.16	1.08	1083.7
1321	T	1321	-	48.985	-0.377	60.2	34	0.5	2.1	4.4	549.2	170.2	-	60.0	0.31	-	0.35	85.3
1322	T	1322	-	49.764	-0.386	64.1	246	1.7	2.1	4.5	3187.7	1447.2	132.8	-	0.45	0.09	-	37.6
1323	L	486	649	49.386	-0.325	60.9	121	0.5	4.6	7.6	1568.4	1083.4	199.3	1147.7	0.69	0.18	1.06	244.9
1324	L	1189	1367	49.121	-0.325	60.9	79	0.7	6.1	10.1	2653.4	1665.8	360.0	1004.4	0.63	0.22	0.60	122.5
1325	L	486	514	49.622	-0.322	61.5	22	1.0	2.3	4.2	542.6	112.4	-	68.2	0.21	-	0.61	59.4
1326	B	1189	1239	48.923	-0.277	69.3	3341	3.3	3.0	17.6	305829.7	90824.2	10018.6	92457.9	0.30	0.11	1.02	174.6
1327	L	486	1402	49.329	-0.303	61.5	53	0.6	4.1	5.9	859.3	419.7	34.4	199.7	0.49	0.08	0.48	107.8
1328	L	486	686	49.443	-0.287	60.9	36	0.6	6.2	9.0	1248.2	605.5	78.9	338.4	0.49	0.13	0.56	80.5
1329	L	486	1288	49.634	-0.303	61.5	57	0.8	4.6	8.2	2369.6	771.1	113.0	478.8	0.33	0.15	0.62	71.3
1330	T	1330	-	49.188	-0.287	60.2	18	0.6	2.1	4.9	202.0	106.5	-	73.9	0.53	-	0.69	141.1
1331	L	1189	1290	49.124	-0.285	60.2	31	0.7	5.9	8.7	576.9	350.4	49.5	154.4	0.61	0.14	0.44	137.9
1332	L	1189	1239	49.157	-0.280	63.5	88	1.1	3.0	7.0	2387.4	876.2	77.3	664.1	0.37	0.09	0.76	120.8
1333	B	486	1204	49.414	-0.207	60.2	225	0.7	3.2	7.0	2925.5	1595.2	144.4	716.4	0.55	0.09	0.45	72.9
1334	T	1334	-	49.549	-0.226	61.5	51	0.7	2.1	3.9	631.2	222.9	-	41.8	0.35	-	0.19	47.5
1335	L	1246	1247	49.171	-0.211	60.9	138	1.2	4.8	13.0	3547.5	3786.2	664.0	3159.8	1.07	0.18	0.83	158.4
1336	L	486	538	49.631	-0.197	59.6	32	0.7	2.2	3.8	402.1	156.4	-	4.7	0.39	-	0.03	39.5
1337	T	1337	-	49.273	-0.124	60.2	44	0.7	2.1	4.1	402.2	208.5	-	29.6	0.52	-	0.14	66.8
1338	L	486	524	49.216	-0.126	60.2	35	0.4	2.1	3.8	288.9	112.5	-	5.3	0.39	-	0.05	60.9
1339	B	486	1165	49.445	-0.037	60.9	3683	1.5	3.1	10.5	95638.3	37950.1	3813.1	-	0.40	0.10	-	37.1
1340	L	486	1212	49.322	-0.039	60.9	42	0.4	4.1	6.5	720.6	319.9	-	57.0	0.44	-	0.18	39.6
1341	L	486	1164	49.221	-0.046	60.2	27	0.4	3.5	5.3	350.7	162.4	22.1	-	0.46	0.14	-	45.2
1342	L	486	1300	49.384	-0.037	60.2	60	0.5	3.6	5.2	667.9	324.4	20.4	42.5	0.49	0.06	0.13	42.9
1343	L	486	1309	49.424	-0.022	60.9	64	0.5	6.7	9.4	1919.3	880.3	155.0	425.0	0.46	0.18	0.48	30.8
1344	L	486	1163	49.294	-0.020	61.5	121	0.5	3.3	5.1	1506.8	635.5	80.0	-	0.42	0.13	-	34.9
1345	L	486	1165	49.223	-0.004	60.2	56	0.5	3.1	4.8	708.6	275.5	24.8	-	0.39	0.09	-	37.5
1346	L	486	1208	49.346	0.013	61.5	55	0.6	3.3	5.2	755.3	312.5	-	-	0.41	-	-	31.6
1347	L	486	1348	49.360	0.027	60.2	16	0.6	3.3	5.4	267.5	128.0	-	-	0.48	-	-	28.1
1348	B	486	1161	49.360	0.027	60.2	99	0.7	3.2	5.4	1467.9	656.8	66.4	-	0.45	0.10	-	29.4
1349	L	486	1348	49.365	0.051	60.9	55	0.6	3.3	4.9	783.5	361.6	33.8	-	0.46	0.09	-	29.8

1350	T	1350	-	48.227	0.044	60.9	26	0.5	2.1	3.7	233.8	116.5	-	-	0.50	-	-	32.2
1351	T	1351	-	49.775	0.093	60.9	53	0.5	2.1	3.7	565.1	188.4	-	-	0.33	-	-	26.0
1352	T	1352	-	49.738	0.093	59.6	43	0.5	2.1	3.8	552.1	182.6	-	-	0.33	-	-	29.4
1353	T	1353	-	49.282	0.129	64.1	298	1.3	2.1	4.8	5942.3	1922.9	193.4	-	0.32	0.10	-	31.5
1354	T	1354	-	49.131	0.185	60.9	52	0.6	2.1	3.9	540.9	199.7	-	-	0.37	-	-	33.0
1355	T	1355	-	49.133	-0.674	61.5	47	0.7	2.1	4.0	513.2	211.3	26.4	-	0.41	0.12	-	20.8
1356	T	1356	-	49.299	-0.639	60.9	56	0.6	2.1	4.1	720.2	258.1	24.5	-	0.36	0.09	-	20.6
1357	T	1357	-	48.812	-0.601	61.5	46	0.6	2.1	4.6	527.3	170.2	17.4	-	0.32	0.10	-	29.1
1358	T	1358	-	49.131	-0.599	60.9	29	0.4	2.1	4.0	243.0	102.1	-	-	0.42	-	-	24.8
1359	L	486	661	49.443	-0.570	60.9	55	0.4	5.7	9.9	1120.5	566.0	118.8	238.9	0.51	0.21	0.42	37.2
1360	L	486	1278	49.313	-0.570	60.9	35	0.3	5.2	8.2	492.5	280.0	28.0	-	0.57	0.10	-	24.4
1361	T	1361	-	49.792	-0.537	62.2	151	0.8	2.1	6.1	3402.1	1030.1	56.8	-	0.30	0.06	-	34.2
1362	T	1362	-	48.737	-0.521	62.8	189	0.9	2.1	8.0	6356.3	1997.5	195.4	-	0.31	0.10	-	73.8
1363	L	486	664	49.417	-0.490	61.5	22	0.5	5.0	7.0	758.9	203.2	-	171.9	0.27	-	0.85	214.4
1364	L	1101	1101	49.003	-0.433	61.5	122	0.5	2.2	5.2	1852.7	666.0	104.0	219.3	0.36	0.16	0.33	45.5
1365	L	486	578	49.433	-0.419	62.2	46	1.2	3.0	5.1	1224.6	339.6	-	206.7	0.28	-	0.61	265.7
1366	T	1366	-	49.726	-0.337	60.9	32	0.5	2.2	4.4	474.2	150.2	-	-	0.32	-	-	46.4
1367	B	1189	1290	49.121	-0.325	60.9	177	0.9	5.9	10.1	5684.1	3176.9	582.2	1850.2	0.56	0.18	0.58	141.0
1368	T	1368	-	49.953	-0.322	62.2	28	1.0	2.1	4.1	215.0	124.7	-	-	0.58	-	-	28.2
1369	T	1369	-	49.990	-0.296	61.5	34	0.6	2.1	3.6	266.2	131.9	18.3	-	0.50	0.14	-	29.8
1370	L	486	579	49.587	-0.292	61.5	74	1.3	2.9	5.7	2125.6	682.3	-	433.7	0.32	-	0.64	89.6
1371	L	1189	1367	49.112	-0.296	63.5	84	0.7	6.1	9.0	2443.5	1222.1	180.2	691.1	0.50	0.15	0.57	145.3
1372	L	486	534	49.299	-0.285	62.2	22	0.7	3.0	4.4	213.5	144.8	-	54.4	0.68	-	0.38	75.4
1373	L	486	648	49.443	-0.266	60.9	24	0.6	4.5	6.3	355.0	190.0	15.0	77.2	0.54	0.08	0.41	94.9
1374	L	486	1199	49.480	-0.254	60.2	53	0.4	5.3	7.6	849.7	498.1	22.0	282.2	0.59	0.04	0.57	66.5
1375	L	486	1201	49.376	-0.211	60.9	39	0.5	2.9	4.3	257.7	170.6	19.0	66.2	0.66	0.11	0.39	78.7
1376	L	486	552	49.608	-0.200	60.9	26	0.7	2.8	4.3	355.0	144.6	16.0	11.4	0.41	0.11	0.08	39.9
1377	L	486	1457	49.348	-0.192	62.2	53	1.6	2.3	4.1	414.0	279.0	-	122.9	0.67	-	0.44	60.6
1378	T	1378	-	49.369	-0.136	62.2	24	0.6	2.1	3.7	310.5	118.5	-	14.9	0.38	-	0.13	56.0
1379	T	1379	-	49.251	-0.136	61.5	64	0.6	2.1	3.9	461.9	266.0	35.1	53.1	0.58	0.13	0.20	56.9
1380	L	486	1077	49.558	-0.117	61.5	136	0.6	2.3	6.2	1761.5	882.3	108.1	190.0	0.50	0.12	0.22	39.1
1381	T	1381	-	49.726	-0.077	63.5	252	1.0	2.1	4.0	2628.0	1258.0	53.5	-	0.48	0.04	-	31.4
1382	L	486	1309	49.445	-0.037	60.9	47	0.5	6.7	10.5	1191.3	649.3	93.4	337.2	0.55	0.14	0.52	31.7
1383	L	486	1257	49.303	0.015	61.5	67	0.6	2.6	4.4	960.8	364.6	37.7	-	0.38	0.10	-	36.3
1384	L	1351	1351	49.785	0.084	60.2	25	0.3	2.1	3.6	249.9	87.0	-	-	0.35	-	-	25.4
1385	L	1351	1351	49.775	0.093	60.9	27	0.4	2.1	3.7	279.5	90.9	-	-	0.33	-	-	26.4
1386	T	1386	-	49.110	0.103	61.5	54	0.8	2.1	3.6	692.4	237.6	-	-	0.34	-	-	34.1
1387	T	1387	-	48.276	0.117	61.5	55	0.8	2.1	4.4	821.5	327.9	-	-	0.40	-	-	37.0
1388	T	1388	-	49.400	0.365	60.9	104	0.8	2.1	4.7	1377.0	601.9	-	-	0.44	-	-	24.4
1389	T	1389	-	49.322	0.417	60.9	41	0.4	2.1	4.0	358.1	140.5	-	-	0.39	-	-	23.3
1390	L	1433	1433	48.661	-0.738	64.8	335	1.1	2.2	10.3	11770.9	3967.4	391.6	-	0.34	0.10	-	34.2

1391	L	1435	1435	48.585	-0.617	61.5	43	0.5	2.2	4.3	478.2	189.4	21.7	-	0.40	0.11	-	34.5
1392	L	1361	1361	49.792	-0.537	62.2	74	0.6	2.9	6.1	1365.3	445.2	30.2	-	0.33	0.07	-	33.5
1393	T	1393	-	48.701	-0.492	62.2	24	0.7	2.1	3.7	380.5	123.6	-	-	0.32	-	-	61.3
1394	L	486	522	49.461	-0.457	61.5	24	0.9	2.3	4.4	552.3	129.5	-	52.9	0.23	-	0.41	135.1
1395	T	1395	-	49.041	-0.410	62.2	66	0.5	2.1	5.6	957.4	364.1	30.2	161.4	0.38	0.08	0.44	79.9
1396	L	486	1318	49.572	-0.398	62.2	42	0.7	5.9	8.1	1394.7	518.1	52.5	480.2	0.37	0.10	0.93	160.9
1397	L	1442	1442	48.715	-0.379	62.8	106	0.6	2.2	6.4	2173.7	693.2	58.7	-	0.32	0.08	-	73.6
1398	L	486	493	49.343	-0.381	62.2	66	0.9	3.0	4.8	636.0	443.3	25.1	229.0	0.70	0.06	0.52	153.3
1399	L	1189	1281	48.982	-0.353	62.2	28	0.4	3.1	5.2	408.0	166.0	-	50.1	0.41	-	0.30	111.7
1400	L	1189	1189	49.157	-0.334	63.5	20	0.8	2.1	3.6	362.6	111.7	-	106.2	0.31	-	0.95	126.6
1401	L	486	1402	49.320	-0.287	64.1	101	1.0	4.1	6.5	1451.9	954.9	162.5	284.5	0.66	0.17	0.30	72.7
1402	B	486	1243	49.320	-0.287	64.1	151	1.5	4.1	6.5	2346.7	1391.3	197.9	492.9	0.59	0.14	0.35	83.7
1403	L	486	1292	49.490	-0.275	61.5	47	0.3	4.9	6.9	494.2	304.7	53.5	232.4	0.62	0.18	0.76	80.1
1404	L	486	1251	49.386	-0.292	62.2	102	0.7	2.9	5.5	758.6	475.3	52.8	117.8	0.63	0.11	0.25	280.2
1405	L	486	659	49.483	-0.273	62.2	38	0.5	4.9	6.5	482.1	308.3	29.1	218.2	0.64	0.09	0.71	57.6
1406	L	486	1241	49.613	-0.277	62.2	25	0.4	2.8	4.8	411.2	109.6	-	35.8	0.27	-	0.33	57.7
1407	T	1407	-	49.915	-0.247	62.2	22	0.9	2.1	3.7	178.9	107.6	-	-	0.60	-	-	31.8
1408	L	1189	1148	48.826	-0.247	62.2	50	0.5	2.4	6.9	1115.6	422.4	42.0	348.1	0.38	0.10	0.82	85.7
1409	B	1454	1454	49.804	-0.200	65.4	938	1.2	2.1	5.5	13853.5	6211.2	830.0	-	0.45	0.13	-	29.5
1410	L	1454	1453	49.877	-0.235	61.5	149	1.1	2.5	4.8	1641.0	851.0	86.9	-	0.52	0.10	-	29.9
1411	T	1411	-	49.575	-0.233	64.1	26	1.3	2.1	3.8	300.7	113.0	22.7	2.0	0.38	0.20	0.02	52.0
1412	T	1412	-	49.273	-0.197	66.1	150	1.3	2.1	4.9	1447.1	782.5	-	253.7	0.54	-	0.32	71.9
1413	L	486	591	49.301	-0.183	62.8	84	0.8	2.7	4.7	618.7	460.6	57.5	188.6	0.74	0.12	0.41	58.8
1414	L	486	556	49.350	-0.183	63.5	38	0.7	2.2	4.2	287.8	189.0	27.3	96.3	0.66	0.14	0.51	59.1
1415	L	486	521	49.367	-0.174	63.5	52	1.5	2.1	4.3	478.3	243.5	-	70.5	0.51	-	0.29	59.3
1416	L	486	1159	49.452	-0.136	62.8	36	0.7	2.1	3.6	281.9	119.6	-	4.3	0.42	-	0.04	52.6
1417	L	486	1166	49.426	-0.098	62.2	32	0.4	3.4	5.1	385.1	184.4	23.1	25.5	0.48	0.13	0.14	40.5
1418	L	1381	1381	49.749	-0.100	63.5	54	1.3	2.2	3.6	503.1	258.2	23.1	-	0.51	0.09	-	28.3
1419	L	486	1074	49.367	-0.079	62.8	29	0.6	2.5	4.1	335.1	151.3	-	9.9	0.45	-	0.07	45.5
1420	L	1381	1422	49.726	-0.077	63.5	53	0.8	2.3	4.0	534.2	262.1	-	-	0.49	-	-	32.4
1421	L	486	1306	49.433	-0.079	61.5	50	0.4	3.9	5.5	504.6	275.9	30.6	42.1	0.55	0.11	0.15	38.9
1422	B	1381	1381	49.726	-0.077	63.5	108	0.9	2.2	4.0	1227.1	573.7	-	-	0.47	-	-	32.4
1423	L	1381	1422	49.719	-0.067	61.5	38	0.8	2.3	3.9	388.9	193.8	-	-	0.50	-	-	32.5
1424	L	486	1209	49.384	-0.063	62.2	37	0.6	3.3	5.8	596.8	260.4	26.3	28.6	0.44	0.10	0.11	41.4
1425	L	486	1114	49.171	-0.060	60.9	24	0.5	2.2	4.2	157.2	99.3	-	-	0.63	-	-	44.8
1426	L	1039	1039	48.907	-0.048	61.5	41	0.6	2.5	4.7	758.1	226.2	-	-	0.30	-	-	72.7
1427	L	486	1214	49.303	-0.022	61.5	46	0.3	3.8	6.9	573.3	259.3	47.0	38.1	0.45	0.18	0.15	37.5
1428	T	1428	-	49.570	0.114	62.2	204	0.8	2.1	4.0	2551.0	882.9	-	-	0.35	-	-	23.5
1429	T	1429	-	49.594	0.133	62.2	50	0.7	2.1	4.1	572.2	196.9	-	-	0.34	-	-	22.5
1430	T	1430	-	49.608	0.188	61.5	95	0.5	2.1	5.9	1653.0	575.8	61.3	-	0.35	0.11	-	23.6
1431	T	1431	-	49.015	0.318	63.5	137	0.9	2.1	4.9	2445.3	863.4	-	-	0.35	-	-	36.0

1432	T	1432	-	49.480	0.412	61.5	46	0.4	2.1	3.7	310.4	176.9	-	-	0.57	-	-	29.0
1433	T	1433	-	48.661	-0.738	64.8	555	1.0	2.1	10.3	17751.7	6065.1	590.4	-	0.34	0.10	-	36.0
1434	T	1434	-	48.656	-0.632	62.2	40	0.6	2.1	3.8	522.0	173.0	24.5	-	0.33	0.14	-	42.4
1435	T	1435	-	48.585	-0.617	61.5	100	0.5	2.1	4.3	1119.3	431.6	48.5	-	0.39	0.11	-	34.1
1436	L	1435	1435	48.595	-0.613	62.2	50	0.5	2.2	4.3	517.3	201.1	20.0	-	0.39	0.10	-	33.5
1437	L	486	628	49.348	-0.514	62.8	62	0.6	2.2	4.5	912.8	290.5	-	88.0	0.32	-	0.30	34.6
1438	T	1438	-	48.720	-0.469	62.8	33	0.5	2.1	4.8	549.9	166.2	-	-	0.30	-	-	70.8
1439	L	486	1318	49.591	-0.414	64.8	29	1.1	5.9	7.9	1237.8	414.3	19.3	352.4	0.33	0.05	0.85	92.6
1440	L	1496	1531	48.791	-0.410	66.1	99	1.4	2.4	5.0	2334.8	670.1	57.8	300.7	0.29	0.09	0.45	59.8
1441	L	1442	1442	48.680	-0.391	62.2	25	0.5	2.2	6.4	318.2	141.2	15.9	-	0.44	0.11	-	59.6
1442	T	1442	-	48.680	-0.391	62.2	134	0.6	2.1	6.4	2600.0	866.8	81.7	-	0.33	0.09	-	69.0
1443	T	1443	-	49.905	-0.329	64.1	88	0.8	2.1	4.1	750.1	369.3	-	-	0.49	-	-	32.1
1444	L	486	639	49.339	-0.329	62.2	75	0.8	3.6	5.4	858.8	485.6	74.5	247.6	0.57	0.15	0.51	186.3
1445	L	486	660	49.405	-0.344	62.2	27	0.5	5.4	7.6	241.4	219.9	39.9	167.1	0.91	0.18	0.76	154.7
1446	L	486	539	49.660	-0.329	62.2	32	0.4	2.2	4.2	511.9	130.7	-	105.6	0.26	-	0.81	85.6
1447	L	486	1449	49.556	-0.313	62.2	81	0.5	4.8	8.1	1778.5	750.9	69.6	468.1	0.42	0.09	0.62	99.2
1448	B	1189	1499	48.982	-0.332	64.1	87	1.6	3.3	8.4	4280.6	1066.2	105.9	852.9	0.25	0.10	0.80	150.0
1449	B	486	635	49.556	-0.313	62.2	105	1.3	4.8	8.1	2392.4	1127.1	120.1	669.6	0.47	0.11	0.59	94.2
1450	L	486	1288	49.629	-0.287	62.2	22	0.5	4.7	6.4	517.8	165.2	-	80.6	0.32	-	0.49	69.3
1451	L	486	489	49.414	-0.294	62.8	91	0.7	2.9	5.1	934.3	514.3	91.6	120.2	0.55	0.18	0.23	211.5
1452	L	1189	1193	49.093	-0.237	62.2	77	0.6	4.4	7.3	1307.4	698.5	91.0	362.3	0.53	0.13	0.52	105.6
1453	B	1454	1409	49.804	-0.200	65.4	654	1.2	2.4	5.5	8475.8	4048.7	516.6	-	0.48	0.13	-	29.1
1454	T	1454	-	49.804	-0.200	65.4	1071	1.2	2.1	5.5	15369.3	6921.1	908.8	-	0.45	0.13	-	29.7
1455	L	1189	1150	48.793	-0.244	63.5	84	0.7	2.3	5.8	1560.9	466.4	33.6	419.5	0.30	0.07	0.90	90.1
1456	L	486	542	49.282	-0.240	65.4	85	1.2	2.9	6.5	972.6	604.6	93.5	412.1	0.62	0.15	0.68	65.4
1457	B	486	482	49.348	-0.192	62.2	119	1.7	2.3	4.1	1331.2	692.1	51.4	188.0	0.52	0.07	0.27	64.7
1458	L	486	529	49.395	-0.188	62.2	26	0.9	2.2	3.6	305.7	118.9	25.0	3.9	0.39	0.21	0.03	63.7
1459	L	486	546	49.414	-0.178	64.1	69	0.6	2.2	3.7	738.8	309.5	-	35.3	0.42	-	0.11	64.3
1460	T	1460	-	49.310	-0.162	64.1	26	0.7	2.1	3.7	157.1	111.4	-	47.0	0.71	-	0.42	59.3
1461	T	1461	-	49.263	-0.150	63.5	22	0.8	2.1	3.8	149.7	88.0	-	31.8	0.59	-	0.36	72.1
1462	T	1462	-	49.603	-0.141	61.5	29	0.4	2.1	3.9	315.7	124.7	-	18.0	0.39	-	0.14	39.9
1463	L	486	1073	49.374	-0.124	64.1	76	0.7	2.2	3.7	681.2	300.7	-	30.7	0.44	-	0.10	50.1
1464	B	486	1037	49.461	-0.143	64.8	111	1.1	2.2	4.1	1113.1	454.1	57.9	42.8	0.41	0.13	0.09	47.4
1465	L	486	1464	49.461	-0.143	64.8	81	1.1	2.2	4.1	860.3	339.6	40.6	36.9	0.39	0.12	0.11	49.1
1466	L	486	1078	49.386	-0.117	62.2	62	0.5	2.9	4.6	584.2	289.4	34.2	25.1	0.50	0.12	0.09	50.3
1467	L	486	1207	49.402	-0.098	62.2	38	0.6	3.3	5.1	552.4	247.3	-	25.1	0.45	-	0.10	44.1
1468	B	486	501	49.596	-0.079	65.4	85	1.1	2.1	4.2	1193.0	453.4	-	-	0.38	-	-	33.5
1469	B	486	1117	49.518	-0.082	62.8	250	0.7	2.4	5.4	3097.3	1329.8	112.3	154.7	0.43	0.08	0.12	33.4
1470	L	486	1305	49.405	-0.060	62.8	64	0.5	4.1	7.0	984.3	481.5	32.0	128.1	0.49	0.07	0.27	38.3
1471	L	486	1468	49.615	-0.065	62.2	49	0.7	2.2	4.1	639.0	234.6	-	-	0.37	-	-	33.2
1472	L	486	1215	49.464	-0.086	62.8	52	0.9	3.8	5.2	762.2	356.6	-	35.9	0.47	-	0.10	37.5

1473	L	486	1261	49.443	-0.060	61.5	31	0.4	4.5	6.1	384.9	196.3	23.8	42.6	0.51	0.12	0.22	37.4
1474	T	1474	-	49.587	-0.060	62.2	30	0.4	2.1	3.6	239.6	106.1	-	-	0.44	-	-	35.9
1475	L	486	1262	49.466	-0.004	62.8	27	0.6	3.9	5.5	363.7	164.7	-	20.4	0.45	-	0.12	29.6
1476	L	486	1339	49.445	0.022	63.5	88	0.7	3.1	5.3	1708.4	649.7	-	129.3	0.38	-	0.20	28.4
1477	L	1353	1353	49.296	0.100	62.8	74	0.8	2.7	4.6	1065.9	375.7	45.9	-	0.35	0.12	-	31.6
1478	L	1353	1353	49.310	0.098	62.2	64	0.9	2.7	4.7	861.2	310.2	33.9	-	0.36	0.11	-	31.0
1479	L	1428	1428	49.570	0.114	62.2	93	0.6	2.3	4.0	1031.7	371.8	-	-	0.36	-	-	23.1
1480	T	1480	-	49.528	0.126	62.8	185	0.6	2.1	5.5	2617.6	982.5	81.4	-	0.38	0.08	-	26.1
1481	T	1481	-	49.473	0.164	64.1	160	0.8	2.1	4.3	1871.9	719.3	81.4	-	0.38	0.11	-	24.8
1482	T	1482	-	48.064	0.178	62.2	60	0.4	2.1	4.5	483.4	232.2	-	-	0.48	-	-	23.2
1483	T	1483	-	49.603	0.214	62.2	104	0.5	2.1	4.1	1141.2	392.6	30.2	-	0.34	0.08	-	23.2
1484	T	1484	-	49.150	0.233	62.8	57	0.7	2.1	4.4	650.9	241.1	-	-	0.37	-	-	32.2
1485	T	1485	-	49.556	0.223	63.5	59	0.8	2.1	3.9	623.7	287.5	-	-	0.46	-	-	29.2
1486	L	1433	1433	48.630	-0.695	64.8	210	0.9	2.1	6.2	5524.3	1972.0	192.4	-	0.36	0.10	-	38.6
1487	L	1488	1488	48.680	-0.594	62.8	207	0.5	2.5	5.2	3768.6	1254.8	95.6	-	0.33	0.08	-	48.0
1488	T	1488	-	48.661	-0.542	63.5	352	0.6	2.1	6.1	6501.0	2067.0	147.9	-	0.32	0.07	-	48.3
1489	T	1489	-	48.626	-0.596	62.8	107	0.7	2.1	5.1	1948.6	680.3	49.2	-	0.35	0.07	-	35.4
1490	L	1361	1361	49.745	-0.523	63.5	27	0.4	2.9	5.2	373.7	129.2	-	-	0.35	-	-	35.7
1491	T	1491	-	48.718	-0.504	64.1	41	0.6	2.1	3.9	630.3	176.3	-	-	0.28	-	-	58.2
1492	T	1492	-	49.395	-0.504	64.1	44	0.8	2.1	5.2	1192.4	312.4	-	263.1	0.26	-	0.84	101.9
1493	L	486	503	49.480	-0.473	63.5	31	0.6	2.7	5.1	718.7	191.3	-	61.7	0.27	-	0.32	105.6
1494	B	1530	1530	49.672	-0.459	69.3	2925	1.1	2.1	11.1	113337.9	34579.3	3392.7	-	0.31	0.10	-	30.1
1495	T	1495	-	49.348	-0.398	63.5	31	0.6	2.1	3.6	181.5	119.5	21.9	6.6	0.66	0.18	0.06	127.9
1496	T	1496	-	48.737	-0.447	69.3	398	2.2	2.1	5.5	10456.1	2852.6	249.7	-	0.27	0.09	-	58.8
1497	L	1322	1322	49.764	-0.353	64.8	107	1.5	2.3	4.0	1294.9	651.6	67.2	-	0.50	0.10	-	37.3
1498	L	1189	1448	48.982	-0.332	64.1	63	1.0	3.4	8.4	2995.0	788.7	83.4	557.2	0.26	0.11	0.71	159.2
1499	B	1189	1191	48.982	-0.332	64.1	186	1.5	3.3	8.4	9045.5	2042.1	194.4	1603.8	0.23	0.10	0.79	158.5
1500	B	1189	1577	48.923	-0.277	69.3	1485	2.0	3.6	17.6	176265.1	48970.6	5052.0	58801.2	0.28	0.10	1.20	199.2
1501	B	1189	1537	48.923	-0.277	69.3	1273	1.9	4.0	17.6	155470.0	43929.9	4626.0	52804.7	0.28	0.11	1.20	205.8
1502	T	1502	-	49.990	-0.263	62.8	35	0.4	2.1	3.9	288.1	127.5	-	-	0.44	-	-	27.9
1503	T	1503	-	48.980	-0.266	63.5	50	1.0	2.1	6.9	1494.2	560.7	60.7	529.8	0.38	0.11	0.94	150.4
1504	T	1504	-	49.188	-0.247	67.4	126	1.5	2.1	5.8	2609.1	957.4	-	585.1	0.37	-	0.61	106.4
1505	L	486	463	49.461	-0.230	64.1	95	0.8	2.5	4.4	929.1	435.1	-	49.0	0.47	-	0.11	80.2
1506	L	1246	1246	49.178	-0.240	62.8	25	0.3	2.5	4.7	183.1	113.2	-	67.6	0.62	-	0.60	135.8
1507	L	486	1205	49.407	-0.237	63.5	33	0.7	2.9	4.5	410.9	193.7	-	25.3	0.47	-	0.13	73.7
1508	B	486	511	49.520	-0.192	64.1	356	1.0	2.2	4.7	4606.4	2004.3	111.9	236.1	0.44	0.06	0.12	42.5
1509	T	1509	-	49.565	-0.216	64.1	31	0.7	2.1	4.1	276.5	135.8	-	13.5	0.49	-	0.10	41.7
1510	L	486	1118	49.426	-0.174	63.5	62	0.5	2.3	4.9	527.7	256.8	-	22.6	0.49	-	0.09	67.5
1511	T	1511	-	49.631	-0.178	63.5	29	0.5	2.1	3.5	296.4	104.6	-	6.5	0.35	-	0.06	40.5
1512	L	486	1514	49.546	-0.152	64.1	81	0.8	2.3	4.3	879.5	390.4	29.1	37.9	0.44	0.07	0.10	40.0
1513	T	1513	-	49.291	-0.171	62.8	27	0.3	2.1	3.7	131.6	89.4	-	16.9	0.68	-	0.19	64.9

1514	B	486	1508	49.520	-0.192	64.1	264	1.0	2.3	4.7	3355.1	1489.0	101.1	162.6	0.44	0.07	0.11	42.4
1515	L	1454	1454	49.811	-0.141	64.8	131	0.7	2.1	4.8	1418.0	676.2	74.5	-	0.48	0.11	-	32.0
1516	L	486	1599	49.528	-0.117	65.4	55	0.8	2.4	4.1	790.2	350.6	32.8	36.2	0.44	0.09	0.10	37.1
1517	L	486	1124	49.386	-0.103	63.5	36	0.5	3.0	6.0	320.7	150.1	-	9.4	0.47	-	0.06	46.4
1518	L	486	1113	49.582	-0.084	64.1	67	0.8	2.2	4.1	920.4	348.7	-	-	0.38	-	-	37.8
1519	L	486	1121	49.549	-0.058	63.5	57	0.7	2.2	4.5	556.2	244.9	-	6.3	0.44	-	0.03	34.4
1520	T	1520	-	48.878	-0.013	64.1	18	0.8	2.1	3.9	280.3	113.0	-	37.5	0.40	-	0.33	60.8
1521	B	486	1167	49.414	0.022	65.4	159	1.2	3.0	5.1	3197.1	1391.6	174.7	-	0.44	0.13	-	29.2
1522	T	1522	-	49.216	0.077	63.5	25	0.5	2.1	3.5	280.7	95.1	-	-	0.34	-	-	37.0
1523	T	1523	-	49.690	0.077	62.8	32	0.4	2.1	3.7	283.5	115.5	-	-	0.41	-	-	29.8
1524	L	1428	1428	49.556	0.103	62.8	26	0.6	2.4	3.8	249.2	96.0	-	-	0.39	-	-	24.0
1525	T	1525	-	49.528	0.202	62.8	164	0.5	2.1	4.2	1819.0	637.7	45.8	-	0.35	0.07	-	28.6
1526	T	1526	-	49.532	0.225	63.5	40	0.4	2.1	3.6	421.8	149.5	-	-	0.35	-	-	27.3
1527	T	1527	-	49.346	-0.620	63.5	50	0.4	2.1	4.3	396.3	182.7	-	-	0.46	-	-	26.2
1528	L	1488	1529	48.661	-0.542	63.5	29	0.4	2.6	6.1	404.6	135.7	-	-	0.34	-	-	47.4
1529	B	1488	1488	48.661	-0.542	63.5	57	0.4	2.5	6.1	824.2	266.9	23.5	-	0.32	0.09	-	49.5
1530	T	1530	-	49.672	-0.459	69.3	3055	1.1	2.1	11.1	116844.5	35552.7	3459.9	-	0.30	0.10	-	29.7
1531	B	1496	1496	48.737	-0.447	69.3	330	2.0	2.3	5.5	8428.3	2343.2	189.9	-	0.28	0.08	-	58.5
1532	L	1322	1322	49.764	-0.386	64.1	63	0.7	2.3	4.5	745.5	297.3	34.0	-	0.40	0.11	-	41.3
1533	L	486	627	49.195	-0.367	65.4	110	0.9	3.3	6.4	1587.1	907.3	136.0	187.9	0.57	0.15	0.21	128.4
1534	B	486	700	49.414	-0.353	65.4	398	1.3	6.6	11.0	9361.8	6786.8	1086.6	6066.7	0.72	0.16	0.89	198.0
1535	L	1189	1149	49.065	-0.353	66.1	174	1.0	3.0	12.8	9750.7	3044.1	389.9	4048.8	0.31	0.13	1.33	181.7
1536	L	486	665	49.537	-0.322	64.8	17	0.8	5.2	7.4	248.3	216.9	34.0	169.0	0.87	0.16	0.78	87.2
1537	B	1189	1500	48.923	-0.277	69.3	1371	2.0	3.8	17.6	165630.8	46327.5	4842.3	55994.1	0.28	0.10	1.21	204.2
1538	T	1538	-	49.532	-0.252	62.8	31	0.5	2.1	4.1	291.1	124.6	-	10.9	0.43	-	0.09	64.1
1539	B	1189	1289	49.095	-0.263	64.8	190	1.0	5.5	13.1	12470.9	4382.5	403.5	4554.1	0.35	0.09	1.04	173.3
1540	L	486	527	49.388	-0.244	64.8	59	0.6	2.7	4.5	612.9	286.1	42.7	32.5	0.47	0.15	0.11	94.6
1541	L	486	545	49.339	-0.230	63.5	35	0.7	2.4	4.0	168.9	132.1	-	19.5	0.78	-	0.15	86.6
1542	L	486	1590	49.520	-0.192	64.1	119	0.9	2.4	4.7	1630.2	685.6	57.4	79.7	0.42	0.08	0.12	43.3
1543	L	486	466	49.388	-0.228	64.8	26	0.5	2.1	3.8	153.0	88.5	-	5.8	0.58	-	0.07	78.9
1544	T	1544	-	49.764	-0.211	64.1	38	0.8	2.1	3.9	402.3	145.2	-	-	0.36	-	-	30.6
1545	L	486	498	49.398	-0.200	65.4	54	0.9	2.2	4.6	555.0	294.6	25.0	22.7	0.53	0.08	0.08	70.0
1546	B	1454	1453	49.804	-0.200	65.4	468	0.8	2.5	5.5	5898.7	2817.3	391.1	-	0.48	0.14	-	28.3
1547	L	1454	1546	49.830	-0.197	64.1	201	0.6	2.7	4.8	2147.3	1106.9	145.3	-	0.52	0.13	-	26.7
1548	L	486	1590	49.549	-0.195	63.5	44	1.1	2.4	4.2	543.6	270.3	-	22.4	0.50	-	0.08	41.6
1549	B	486	1595	49.504	-0.174	66.1	343	0.8	2.3	5.4	3659.6	1876.0	130.8	231.3	0.51	0.07	0.12	44.6
1550	L	486	1549	49.504	-0.174	66.1	161	0.8	2.4	5.4	1825.5	966.5	76.4	151.2	0.53	0.08	0.16	42.7
1551	T	1551	-	48.774	-0.150	66.7	859	0.9	2.1	9.0	23540.7	8449.0	1071.2	2606.9	0.36	0.13	0.31	44.4
1552	L	486	1464	49.464	-0.124	64.1	25	0.7	2.2	4.0	185.0	92.8	18.4	5.7	0.50	0.20	0.06	44.4
1553	B	486	1172	49.537	-0.084	64.8	130	0.8	2.4	4.4	1358.5	590.8	-	53.6	0.43	-	0.09	36.7
1554	L	486	1599	49.544	-0.100	64.1	22	0.8	2.4	4.3	228.2	109.3	-	17.1	0.48	-	0.16	33.8

1555	L	486	1468	49.596	-0.079	65.4	33	0.8	2.2	4.2	352.8	150.1	-	-	0.43	-	-	33.5
1556	L	486	1553	49.537	-0.084	64.8	22	0.5	2.5	4.4	207.3	102.6	-	12.3	0.49	-	0.12	34.5
1557	L	486	1469	49.518	-0.082	62.8	25	0.4	3.3	5.4	290.9	167.3	16.6	20.8	0.58	0.10	0.12	32.1
1558	L	486	1162	49.263	-0.084	66.1	49	1.0	2.1	4.4	737.1	265.0	-	43.1	0.36	-	0.16	43.6
1559	L	486	1125	49.490	-0.079	63.5	24	0.5	2.5	4.8	304.5	113.1	-	1.2	0.37	-	0.01	31.5
1560	L	486	1521	49.407	0.006	66.7	48	1.2	3.3	4.8	768.1	331.7	59.6	59.7	0.43	0.18	0.18	28.1
1561	T	1561	-	49.306	0.129	62.8	22	0.8	2.1	3.5	235.0	89.4	-	-	0.38	-	-	34.1
1562	L	1563	1563	49.379	0.244	65.4	81	0.9	2.2	4.0	653.5	291.3	-	-	0.45	-	-	29.2
1563	T	1563	-	49.336	0.282	64.1	247	0.9	2.1	4.2	2177.4	986.8	-	-	0.45	-	-	29.8
1564	L	1563	1563	49.336	0.282	64.1	121	0.5	2.2	4.2	1043.0	505.6	-	-	0.48	-	-	30.0
1565	L	1488	1529	48.680	-0.542	63.5	22	0.4	2.6	5.4	337.5	105.5	21.8	-	0.31	0.21	-	55.5
1566	L	486	1317	49.537	-0.443	64.8	54	1.5	3.8	6.3	1521.7	647.0	47.1	547.2	0.43	0.07	0.85	129.7
1567	L	486	618	49.256	-0.412	66.7	141	1.1	3.7	11.7	7606.0	2862.8	284.1	2019.3	0.38	0.10	0.71	147.6
1568	B	486	1534	49.414	-0.353	65.4	245	1.4	6.8	11.0	4968.8	4322.5	682.9	4251.7	0.87	0.16	0.98	200.3
1569	L	486	699	49.431	-0.344	64.8	35	0.4	5.9	9.0	341.6	318.2	46.7	354.2	0.93	0.15	1.11	199.9
1570	L	1189	1537	49.032	-0.339	65.4	61	0.8	4.0	10.2	4046.6	1110.9	105.6	1686.0	0.27	0.10	1.52	196.9
1571	L	1189	1577	49.013	-0.327	64.1	23	0.5	3.6	5.6	888.5	209.4	29.6	208.6	0.24	0.14	1.00	193.5
1572	L	486	695	49.518	-0.329	64.1	18	1.2	4.9	8.1	361.5	222.6	38.3	128.3	0.62	0.17	0.58	188.5
1573	B	1189	1501	48.923	-0.277	69.3	933	1.7	5.6	17.6	100922.4	31404.2	3544.1	36888.2	0.31	0.11	1.17	211.7
1574	B	1189	1573	48.923	-0.277	69.3	478	1.6	8.0	17.6	48928.6	17258.8	2117.4	19530.3	0.35	0.12	1.13	261.4
1575	L	486	1449	49.546	-0.306	64.1	29	0.7	4.8	7.1	357.1	255.6	33.7	128.4	0.72	0.13	0.50	83.9
1576	L	486	701	49.206	-0.306	65.4	23	1.0	5.4	9.3	1236.3	452.7	32.8	330.7	0.37	0.07	0.73	164.3
1577	B	1189	1194	48.923	-0.277	69.3	1494	2.0	3.6	17.6	177672.3	49295.8	5093.3	59159.0	0.28	0.10	1.20	199.2
1578	L	486	495	49.395	-0.292	64.8	27	0.4	2.8	4.3	138.8	103.8	26.0	30.0	0.75	0.25	0.29	306.2
1579	L	486	697	49.218	-0.296	63.5	20	1.0	6.1	7.8	678.5	253.4	32.7	151.2	0.37	0.13	0.60	156.3
1580	T	1580	-	49.256	-0.287	66.1	23	0.9	2.1	3.9	209.5	99.0	17.3	24.8	0.47	0.17	0.25	108.2
1581	L	486	596	49.367	-0.292	64.8	30	0.6	3.0	4.8	212.6	135.8	23.9	53.4	0.64	0.18	0.39	260.5
1582	L	1189	1539	49.095	-0.263	64.8	111	1.0	6.5	13.1	8156.3	2951.3	263.3	2940.6	0.36	0.09	1.00	168.5
1583	L	1189	1151	48.831	-0.256	65.4	59	0.7	2.5	4.6	1083.5	277.0	-	340.9	0.26	-	1.23	93.5
1584	L	486	1625	49.424	-0.249	63.5	27	0.3	2.9	4.7	190.4	122.0	19.8	14.3	0.64	0.16	0.12	89.6
1585	T	1585	-	48.774	-0.244	64.8	28	0.6	2.1	4.1	498.5	140.5	-	97.7	0.28	-	0.70	82.9
1586	L	1454	1409	49.842	-0.230	64.8	25	0.6	2.4	4.1	277.2	142.4	27.0	-	0.51	0.19	-	32.9
1587	L	486	1631	49.502	-0.211	64.1	27	0.5	2.4	4.6	211.2	107.5	-	17.1	0.51	-	0.16	48.3
1588	L	486	483	49.414	-0.200	66.1	46	0.7	2.2	3.6	401.5	175.0	-	18.6	0.44	-	0.11	71.9
1589	L	1412	1412	49.273	-0.197	66.1	41	1.1	2.3	4.9	347.8	181.7	-	41.2	0.52	-	0.23	62.7
1590	B	486	1631	49.520	-0.192	64.1	162	1.0	2.3	4.7	2199.5	965.3	67.6	103.5	0.44	0.07	0.11	42.7
1591	T	1591	-	49.761	-0.190	64.1	57	0.5	2.1	4.1	593.2	226.8	-	-	0.38	-	-	37.1
1592	L	1246	1247	49.178	-0.190	66.1	90	1.0	4.8	10.2	1785.7	1387.6	199.7	1159.1	0.78	0.14	0.84	100.5
1593	L	486	467	49.471	-0.181	64.1	30	0.6	2.1	3.8	265.1	114.5	20.3	8.9	0.43	0.18	0.08	50.3
1594	T	1594	-	49.761	-0.162	64.8	64	0.5	2.1	4.1	536.5	233.6	37.6	-	0.44	0.16	-	32.7
1595	B	486	1036	49.504	-0.174	66.1	444	0.8	2.3	5.4	4484.6	2345.2	172.0	291.4	0.52	0.07	0.12	44.4

1596	L	486	1595	49.516	-0.133	65.4	95	0.6	2.3	4.2	729.1	424.5	34.6	55.4	0.58	0.08	0.13	42.9
1597	B	1551	1551	48.774	-0.150	66.7	715	0.9	2.3	9.0	19494.8	7201.1	926.3	2222.4	0.37	0.13	0.31	44.1
1598	L	486	1553	49.565	-0.105	64.1	89	0.9	2.5	4.3	936.1	411.7	-	34.8	0.44	-	0.08	37.3
1599	B	486	1168	49.544	-0.100	64.1	90	0.9	2.3	4.3	1186.3	526.1	30.2	58.2	0.44	0.06	0.11	36.9
1600	L	486	1160	49.452	-0.103	64.8	23	0.4	2.5	4.1	204.3	98.3	-	8.4	0.48	-	0.09	40.7
1601	L	486	1469	49.502	-0.084	63.5	28	0.3	3.3	4.9	270.6	123.7	-	16.9	0.46	-	0.14	32.3
1602	L	486	1170	49.473	-0.096	64.1	30	0.4	3.6	5.3	257.5	137.6	22.2	12.7	0.53	0.16	0.09	42.2
1603	L	486	1521	49.414	0.022	65.4	72	0.8	3.3	5.1	1082.2	511.8	58.1	104.1	0.47	0.11	0.20	30.0
1604	T	1604	-	48.951	0.027	64.8	46	0.9	2.1	4.6	660.6	263.1	23.6	-	0.40	0.09	-	54.6
1605	T	1605	-	49.823	0.081	64.8	30	0.3	2.2	4.5	363.2	134.3	17.0	-	0.37	0.13	-	29.2
1606	T	1606	-	49.379	0.223	64.8	43	0.5	2.1	3.8	335.6	156.8	-	-	0.47	-	-	28.1
1607	T	1607	-	49.242	0.336	64.1	98	0.5	2.1	3.8	789.6	339.3	29.2	-	0.43	0.09	-	32.4
1608	T	1608	-	49.265	0.414	66.7	41	0.7	2.1	4.0	394.8	193.2	-	-	0.49	-	-	27.6
1609	B	1530	1494	49.672	-0.459	69.3	2530	1.0	2.6	11.1	92013.4	29337.1	3006.4	-	0.32	0.10	-	29.8
1610	B	1530	1644	49.672	-0.459	69.3	2187	0.9	2.9	11.1	77215.9	25210.7	2652.3	-	0.33	0.11	-	29.1
1611	L	486	619	49.435	-0.388	66.1	27	0.7	3.7	6.7	489.1	275.0	25.8	272.6	0.56	0.09	0.99	345.8
1612	L	486	1568	49.414	-0.353	65.4	52	0.7	7.6	11.0	571.6	790.5	135.4	844.9	1.38	0.17	1.07	347.2
1613	L	486	739	49.369	-0.348	64.8	35	0.5	4.9	10.0	382.5	403.3	140.2	613.0	1.05	0.35	1.52	173.9
1614	B	486	685	49.273	-0.341	68.0	485	1.1	6.4	14.2	18826.4	11559.1	1850.0	9639.1	0.61	0.16	0.83	124.9
1615	L	486	1614	49.190	-0.334	67.4	40	1.1	6.9	11.5	1165.6	744.2	123.6	784.2	0.64	0.17	1.05	372.9
1616	L	1189	1499	48.928	-0.322	67.4	94	0.9	3.3	5.9	4508.1	923.5	79.8	709.5	0.20	0.09	0.77	159.9
1617	L	486	646	49.565	-0.306	66.1	25	0.6	4.3	6.9	401.8	258.8	36.8	137.6	0.64	0.14	0.53	94.2
1618	L	486	507	49.471	-0.306	64.8	32	0.6	3.2	6.0	377.6	190.7	-	73.1	0.51	-	0.38	99.8
1619	L	1189	1574	49.027	-0.308	64.1	23	0.3	9.9	13.2	1030.6	417.7	47.7	360.8	0.41	0.11	0.86	193.9
1620	L	486	1157	49.301	-0.306	66.1	24	0.5	3.9	5.7	280.7	184.5	-	41.2	0.66	-	0.22	76.6
1621	L	1189	1539	49.077	-0.292	64.8	34	0.4	6.5	10.5	821.9	370.2	47.1	420.9	0.45	0.13	1.14	188.2
1622	T	1622	-	49.724	-0.268	64.8	55	0.5	2.1	3.9	538.4	222.4	-	-	0.41	-	-	49.4
1623	T	1623	-	49.032	-0.273	64.8	35	0.5	2.1	7.4	772.6	209.5	32.9	319.4	0.27	0.16	1.52	322.0
1624	L	486	543	49.310	-0.254	66.1	260	0.7	3.2	7.8	3515.7	2472.9	283.4	1188.0	0.70	0.11	0.48	75.4
1625	B	486	1249	49.424	-0.249	63.5	50	1.0	2.9	4.7	434.5	252.9	45.4	27.5	0.58	0.18	0.11	89.1
1626	L	486	1625	49.424	-0.237	64.8	28	0.8	2.9	4.4	239.5	128.0	25.0	13.3	0.53	0.20	0.10	90.3
1627	L	1189	1500	48.850	-0.240	66.1	73	0.6	3.8	9.6	2684.4	933.1	64.2	761.7	0.35	0.07	0.82	84.8
1628	T	1628	-	49.254	-0.237	65.4	28	0.8	2.1	3.9	314.5	149.0	-	67.4	0.47	-	0.45	82.5
1629	T	1629	-	49.348	-0.209	65.4	24	0.7	2.1	3.7	218.3	129.4	-	45.4	0.59	-	0.35	65.5
1630	L	1412	1632	49.249	-0.202	64.8	25	0.4	2.5	4.2	172.0	116.7	19.9	52.6	0.68	0.17	0.45	73.0
1631	B	486	1514	49.520	-0.192	64.1	187	0.9	2.3	4.7	2414.7	1075.2	71.1	121.4	0.45	0.07	0.11	43.2
1632	B	1412	1412	49.256	-0.197	67.4	64	0.8	2.3	4.7	649.2	366.2	-	134.5	0.56	-	0.37	72.8
1633	L	1454	1546	49.804	-0.200	65.4	84	0.6	2.7	5.5	990.7	443.9	94.2	-	0.45	0.21	-	32.9
1634	L	1412	1632	49.256	-0.197	67.4	26	0.9	2.5	4.7	285.8	150.7	-	43.3	0.53	-	0.29	74.9
1635	L	486	1549	49.483	-0.126	65.4	98	0.6	2.4	4.1	813.1	427.8	35.2	29.5	0.53	0.08	0.07	48.2
1636	L	486	1119	49.388	0.046	65.4	40	0.4	2.6	5.0	382.6	171.4	18.3	-	0.45	0.11	-	30.5

1637	T	1637	-	49.395	0.211	64.8	52	0.5	2.1	4.8	413.3	186.4	23.7	-	0.45	0.13	-	27.7
1638	T	1638	-	48.189	-0.643	65.4	50	0.4	2.1	4.7	259.2	208.7	-	-	0.81	-	-	19.4
1639	T	1639	-	49.851	-0.570	66.1	380	0.5	2.1	7.3	6992.8	2581.7	276.6	-	0.37	0.11	-	20.2
1640	T	1640	-	49.934	-0.570	66.7	33	0.5	2.1	6.1	451.9	170.7	-	-	0.38	-	-	25.8
1641	T	1641	-	48.661	-0.556	65.4	33	0.3	2.1	4.6	198.2	117.0	-	-	0.59	-	-	44.1
1642	T	1642	-	49.849	-0.556	66.7	84	0.6	2.1	8.9	1262.6	426.2	53.1	-	0.34	0.12	-	25.6
1643	L	1530	1494	49.643	-0.466	64.8	20	0.4	2.6	4.0	438.6	99.6	-	78.2	0.23	-	0.79	53.1
1644	B	1530	1609	49.672	-0.459	69.3	2247	0.9	2.8	11.1	80494.5	26094.0	2754.4	-	0.32	0.11	-	29.2
1645	B	1530	1671	49.672	-0.459	69.3	1124	0.9	3.9	11.1	38283.3	13623.0	1633.0	-	0.36	0.12	-	32.7
1646	T	1646	-	48.796	-0.452	66.1	30	0.5	2.1	3.6	522.3	143.3	19.8	73.2	0.27	0.14	0.51	55.2
1647	T	1647	-	48.831	-0.445	66.1	120	0.8	2.1	5.3	2925.9	781.9	42.0	595.7	0.27	0.05	0.76	71.6
1648	T	1648	-	49.745	-0.398	64.8	27	0.4	2.1	4.3	253.7	92.8	-	16.0	0.37	-	0.17	44.0
1649	T	1649	-	48.866	-0.400	67.4	100	0.8	2.1	6.5	3064.2	744.9	-	645.6	0.24	-	0.87	90.0
1650	L	486	641	49.155	-0.370	68.0	63	1.5	3.7	7.2	3910.0	1029.4	100.0	1305.0	0.26	0.10	1.27	249.7
1651	B	486	1614	49.273	-0.341	68.0	353	0.9	6.9	14.2	13198.3	8413.4	1399.8	6974.4	0.64	0.17	0.83	115.3
1652	L	1189	1573	49.046	-0.315	64.8	18	0.4	8.0	10.9	889.5	289.1	-	302.0	0.33	-	1.04	199.2
1653	L	486	602	49.461	-0.273	66.1	77	0.8	3.0	5.0	816.5	403.7	-	64.1	0.49	-	0.16	66.9
1654	T	1654	-	48.774	-0.259	66.1	21	0.5	2.1	4.2	373.9	92.4	-	107.4	0.25	-	1.16	110.1
1655	L	1189	1152	49.140	-0.226	67.4	47	1.0	2.6	5.1	1237.8	315.5	20.6	227.0	0.25	0.07	0.72	141.6
1656	L	486	1508	49.537	-0.171	64.8	25	0.5	2.4	3.7	235.6	98.9	-	14.7	0.42	-	0.15	38.0
1657	L	1551	1551	48.692	-0.169	65.4	76	0.5	2.3	6.3	1679.5	562.2	77.2	210.3	0.33	0.14	0.37	45.4
1658	B	1551	1597	48.774	-0.150	66.7	492	0.7	2.8	9.0	13314.2	5210.2	715.5	1750.2	0.39	0.14	0.34	46.2
1659	T	1659	-	49.282	0.327	64.8	26	0.4	2.1	4.4	186.2	89.3	-	-	0.48	-	-	34.4
1660	T	1660	-	49.492	0.464	65.4	39	0.5	2.1	3.7	300.8	132.3	-	-	0.44	-	-	27.4
1661	T	1661	-	49.546	0.570	65.4	90	0.5	2.1	4.5	591.2	321.6	29.9	-	0.54	0.09	-	18.9
1662	B	1639	1639	49.877	-0.587	66.7	266	0.4	2.6	6.5	4778.2	1841.3	210.5	-	0.39	0.11	-	20.0
1663	L	1639	1662	49.924	-0.613	66.1	29	0.4	3.2	5.9	488.4	203.0	-	-	0.42	-	-	20.3
1664	B	1639	1662	49.877	-0.587	66.7	174	0.4	3.2	6.5	2771.0	1137.5	142.8	-	0.41	0.13	-	19.8
1665	L	1639	1639	49.851	-0.570	66.1	24	0.6	2.6	7.3	398.3	156.8	-	-	0.39	-	-	21.1
1666	T	1666	-	49.823	-0.542	67.4	32	0.8	2.1	4.8	702.1	211.4	-	-	0.30	-	-	27.2
1667	L	1530	1668	49.641	-0.485	66.1	51	0.7	3.1	6.4	1558.8	520.0	-	281.1	0.33	-	0.54	49.3
1668	B	1530	1609	49.629	-0.466	70.0	144	1.6	2.8	6.8	4411.4	1416.6	90.1	850.9	0.32	0.06	0.60	52.3
1669	B	1530	1610	49.672	-0.459	69.3	1787	0.9	3.3	11.1	61168.4	20801.1	2294.4	-	0.34	0.11	-	29.5
1670	B	1530	1645	49.672	-0.459	69.3	558	0.9	3.9	11.1	22507.0	7904.2	904.4	-	0.35	0.11	-	37.6
1671	B	1530	1669	49.672	-0.459	69.3	1419	0.9	3.7	11.1	46126.1	16272.7	1907.2	-	0.35	0.12	-	30.2
1672	T	1672	-	49.464	-0.455	66.7	51	0.9	2.1	5.4	1225.5	377.3	-	286.2	0.31	-	0.76	147.9
1673	L	486	581	49.516	-0.393	68.0	31	0.9	2.9	4.3	455.7	142.2	-	51.2	0.31	-	0.36	344.4
1674	L	486	662	49.294	-0.367	66.7	27	0.7	4.8	7.4	505.2	250.8	19.3	158.6	0.50	0.08	0.63	97.7
1675	B	486	887	49.424	-0.381	67.4	92	1.0	6.8	10.4	1578.6	1598.2	266.1	1665.3	1.01	0.17	1.04	324.8
1676	L	486	1675	49.433	-0.365	65.4	21	0.7	7.4	9.4	265.3	338.4	78.6	375.0	1.28	0.23	1.11	284.6
1677	L	486	767	49.509	-0.341	66.7	51	0.7	5.8	9.4	1509.7	872.9	113.6	1052.5	0.58	0.13	1.21	266.2

1678	L	486	1568	49.386	-0.344	67.4	56	0.9	7.7	10.1	851.2	864.3	129.3	792.3	1.02	0.15	0.92	163.6
1679	B	1189	1574	48.923	-0.277	69.3	314	1.3	9.9	17.6	25823.8	9815.5	1234.9	10864.0	0.38	0.13	1.11	273.6
1680	L	1189	1679	49.003	-0.306	67.4	119	1.0	11.2	15.8	8330.1	3472.4	449.0	3608.4	0.42	0.13	1.04	221.7
1681	B	1189	1192	49.077	-0.282	71.9	130	1.6	3.1	7.9	4716.0	1249.4	94.6	1803.7	0.26	0.08	1.44	168.5
1682	T	1682	-	49.235	-0.242	65.4	23	0.4	2.1	4.0	196.9	92.0	-	44.0	0.47	-	0.48	77.0
1683	L	1551	1658	48.737	-0.155	66.1	99	0.4	4.8	8.3	2359.0	921.4	132.4	330.4	0.39	0.14	0.36	56.3
1684	T	1684	-	49.147	-0.145	66.1	24	0.4	2.1	4.6	257.9	102.5	-	69.6	0.40	-	0.68	73.9
1685	L	1639	1664	49.903	-0.592	66.1	45	0.3	4.3	6.3	669.0	299.1	41.0	-	0.45	0.14	-	20.1
1686	L	1639	1664	49.877	-0.587	66.7	25	0.3	4.3	6.5	351.9	173.2	28.8	-	0.49	0.17	-	18.8
1687	L	1530	1724	49.698	-0.556	67.4	90	0.5	3.9	8.1	2262.5	771.4	87.6	-	0.34	0.11	-	26.5
1688	B	1530	1645	49.728	-0.514	68.0	520	0.6	3.9	9.7	14487.8	5315.7	685.2	-	0.37	0.13	-	30.0
1689	T	1689	-	48.623	-0.518	66.7	39	0.3	2.1	3.8	238.5	126.8	-	-	0.53	-	-	36.8
1690	B	1530	1670	49.672	-0.459	69.3	374	0.9	4.7	11.1	14680.2	5410.0	647.1	-	0.37	0.12	-	38.1
1691	B	1496	1531	48.737	-0.447	69.3	201	1.0	2.4	5.5	5270.7	1477.2	113.9	-	0.28	0.08	-	57.9
1692	L	1496	1714	48.755	-0.426	66.7	76	0.5	2.7	5.3	1734.1	504.0	-	-	0.29	-	-	60.5
1693	L	1496	1691	48.772	-0.422	67.4	17	0.6	2.6	4.5	367.7	104.9	-	44.0	0.29	-	0.42	55.0
1694	T	1694	-	48.529	-0.388	68.0	101	0.9	2.1	4.9	1291.0	575.5	70.2	-	0.45	0.12	-	26.7
1695	L	486	1675	49.424	-0.381	67.4	37	0.7	7.4	10.4	592.1	589.4	83.2	603.1	1.00	0.14	1.02	338.9
1696	L	486	663	49.502	-0.329	66.7	34	0.5	5.1	7.0	530.1	343.8	25.0	303.8	0.65	0.07	0.88	260.3
1697	L	486	1651	49.273	-0.341	68.0	137	0.8	7.3	14.2	4455.4	3427.9	647.2	2866.1	0.77	0.19	0.84	82.6
1698	B	486	1651	49.216	-0.341	67.4	170	0.7	7.3	12.5	6100.4	3507.0	534.1	2949.9	0.57	0.15	0.84	141.2
1699	T	1699	-	49.140	-0.303	68.0	19	0.7	2.1	4.4	296.1	109.7	14.9	88.2	0.37	0.14	0.80	197.2
1700	L	1189	1681	49.129	-0.282	68.0	44	0.6	3.2	6.3	1115.3	299.3	44.8	305.9	0.27	0.15	1.02	152.0
1701	L	1551	1658	48.774	-0.150	66.7	72	0.4	4.8	9.0	1209.3	692.2	123.9	264.8	0.57	0.18	0.38	43.3
1702	L	1551	1597	48.791	-0.124	66.7	39	0.4	2.8	4.3	482.2	181.1	-	33.4	0.38	-	0.18	40.3
1703	T	1703	-	49.131	0.478	66.7	60	0.4	2.1	3.8	378.3	214.9	25.5	-	0.57	0.12	-	27.0
1704	T	1704	-	49.613	-0.625	66.7	279	0.8	2.1	6.1	6103.1	1861.6	184.5	-	0.31	0.10	-	31.3
1705	L	1704	1704	49.613	-0.625	66.7	161	0.7	2.7	6.1	3302.1	1087.6	103.9	-	0.33	0.10	-	32.3
1706	L	1530	1724	49.745	-0.589	67.4	133	0.5	3.9	6.8	2721.4	1010.2	100.1	-	0.37	0.10	-	23.2
1707	L	1530	1688	49.745	-0.556	68.0	133	0.5	5.2	9.1	2597.5	1108.2	163.8	-	0.43	0.15	-	26.6
1708	L	1530	1688	49.728	-0.514	68.0	145	0.4	5.2	9.7	3960.8	1557.4	224.3	-	0.39	0.14	-	35.2
1709	T	1709	-	48.772	-0.492	69.3	90	0.8	2.1	4.9	2379.0	576.7	-	-	0.24	-	-	71.3
1710	L	1530	1670	49.700	-0.476	66.7	39	0.5	4.7	6.7	936.6	366.7	41.1	162.3	0.39	0.11	0.44	37.5
1711	B	1530	1690	49.672	-0.459	69.3	201	0.8	5.5	11.1	8013.3	3169.7	416.8	2679.5	0.40	0.13	0.85	40.9
1712	L	1530	1711	49.672	-0.459	69.3	78	0.9	5.8	11.1	4313.6	1668.4	229.7	1625.4	0.39	0.14	0.97	50.0
1713	T	1713	-	48.765	-0.455	67.4	50	0.7	2.1	4.0	1179.0	265.1	-	-	0.22	-	-	60.1
1714	B	1496	1691	48.737	-0.447	69.3	154	0.9	2.6	5.5	3889.3	1126.3	85.1	-	0.29	0.08	-	57.4
1715	T	1715	-	49.393	-0.426	67.4	28	0.4	2.1	4.1	381.7	116.4	-	81.7	0.30	-	0.70	175.8
1716	L	1530	1530	49.813	-0.433	68.7	91	0.7	2.2	5.8	1571.7	502.9	37.3	-	0.32	0.07	-	26.8
1717	B	486	691	49.471	-0.360	68.7	92	0.7	8.7	12.5	2309.9	1893.2	334.3	2144.9	0.82	0.18	1.13	217.7
1718	L	486	1717	49.471	-0.360	68.7	49	0.7	9.2	12.5	1004.0	874.6	181.1	927.2	0.87	0.21	1.06	212.9

1719	L	486	1534	49.348	-0.348	68.0	134	0.5	6.8	10.8	3644.2	2028.3	330.5	1435.1	0.56	0.16	0.71	179.5
1720	L	1189	1448	48.970	-0.344	67.4	24	0.5	3.4	5.5	767.3	169.8	-	207.7	0.22	-	1.22	134.8
1721	L	486	1698	49.237	-0.334	68.7	26	0.8	8.7	11.1	695.1	345.9	39.9	282.3	0.50	0.12	0.82	132.8
1722	L	1704	1704	49.606	-0.636	68.0	34	0.3	2.7	4.8	489.9	150.8	20.0	-	0.31	0.13	-	28.0
1723	L	1530	1610	49.662	-0.599	68.0	89	0.4	3.3	5.9	1441.9	484.1	-	-	0.34	-	-	25.5
1724	B	1530	1671	49.698	-0.556	67.4	237	0.5	3.9	8.1	5379.9	1899.6	198.4	-	0.35	0.10	-	24.5
1725	T	1725	-	49.858	-0.495	68.7	238	0.5	2.1	6.5	4498.0	1408.6	85.2	-	0.31	0.06	-	30.7
1726	T	1726	-	49.679	-0.504	69.3	33	0.7	2.1	3.8	380.0	119.5	-	55.7	0.31	-	0.47	58.0
1727	T	1727	-	49.386	-0.483	68.0	23	0.5	2.1	4.5	282.1	98.0	13.7	63.4	0.35	0.14	0.65	111.1
1728	B	1744	1744	49.842	-0.466	68.7	137	0.9	2.2	5.7	2525.4	809.7	60.2	-	0.32	0.07	-	27.6
1729	L	1530	1690	49.754	-0.476	68.0	60	0.3	5.5	8.3	1195.9	449.6	30.7	-	0.38	0.07	-	27.8
1730	L	1530	1668	49.629	-0.466	70.0	54	0.8	3.1	6.8	1510.0	542.1	46.9	353.0	0.36	0.09	0.65	55.3
1731	T	1731	-	49.771	-0.429	68.7	51	0.4	2.1	4.6	610.2	240.4	-	-	0.39	-	-	31.4
1732	L	486	689	49.471	-0.410	68.0	42	0.5	7.3	9.8	1089.1	588.1	66.0	425.7	0.54	0.11	0.72	447.5
1733	L	486	1717	49.483	-0.360	68.0	24	0.6	9.2	11.4	535.9	422.2	44.9	533.7	0.79	0.11	1.26	237.7
1734	L	486	1698	49.216	-0.341	67.4	54	0.4	8.7	12.5	1285.8	868.4	146.0	773.9	0.68	0.17	0.89	151.4
1735	T	1735	-	49.018	-0.273	70.0	74	0.7	2.1	7.9	3055.7	687.1	-	1323.3	0.22	-	1.93	316.1
1736	T	1736	-	49.136	-0.244	68.7	54	0.6	2.1	5.8	1206.8	296.6	-	312.3	0.25	-	1.05	153.7
1737	T	1737	-	49.575	-0.592	69.3	97	0.6	2.1	6.6	1498.4	507.3	-	-	0.34	-	-	35.6
1738	T	1738	-	49.957	-0.488	69.3	185	0.7	2.1	5.0	3458.9	1058.8	-	-	0.31	-	-	26.8
1739	L	1530	1644	49.662	-0.492	68.7	19	0.5	2.9	5.4	374.7	138.4	19.8	85.0	0.37	0.14	0.61	43.7
1740	L	1744	1728	49.842	-0.466	68.7	33	0.5	2.8	5.7	649.1	238.6	39.2	-	0.37	0.16	-	26.1
1741	L	1530	1669	49.794	-0.457	69.3	86	0.6	3.7	9.0	2001.6	784.3	70.2	-	0.39	0.09	-	28.2
1742	B	1530	1711	49.721	-0.462	68.7	96	0.5	5.8	9.1	2332.3	1020.9	133.0	710.0	0.44	0.13	0.70	36.1
1743	L	1530	1742	49.721	-0.462	68.7	48	0.3	6.3	9.1	953.9	451.3	74.7	319.4	0.47	0.17	0.71	34.5
1744	T	1744	-	49.842	-0.466	68.7	239	0.8	2.1	5.7	3935.3	1221.3	77.9	-	0.31	0.06	-	27.9
1745	T	1745	-	49.405	-0.462	70.0	568	1.0	2.1	11.0	31470.1	9270.3	996.6	6525.9	0.29	0.11	0.70	138.1
1746	L	1530	1742	49.707	-0.462	69.3	32	0.4	6.3	8.3	751.6	321.0	23.3	214.4	0.43	0.07	0.67	36.8
1747	L	1496	1714	48.737	-0.447	69.3	58	0.7	2.7	5.5	1575.9	473.9	48.3	-	0.30	0.10	-	55.1
1748	T	1748	-	49.872	-0.370	70.6	60	1.0	2.1	3.7	960.3	290.8	-	-	0.30	-	-	32.5
1749	L	1189	1679	48.923	-0.277	69.3	101	0.8	11.2	17.6	6459.7	2475.6	322.9	2817.4	0.38	0.13	1.14	433.2
1750	L	1189	1681	49.077	-0.282	71.9	76	1.1	3.2	7.9	3223.4	858.4	42.5	1376.5	0.27	0.05	1.60	181.5
1751	T	1751	-	49.478	-0.580	69.3	21	0.4	2.1	4.4	292.0	104.7	-	140.6	0.36	-	1.34	41.7
1752	T	1752	-	49.917	-0.473	70.0	128	0.9	2.1	5.5	2693.1	809.6	-	-	0.30	-	-	28.8
1753	L	1744	1728	49.853	-0.466	69.3	27	0.6	2.8	4.6	437.8	156.8	-	-	0.36	-	-	28.5
1754	L	1744	1744	49.851	-0.436	69.3	51	0.5	2.2	3.9	729.3	224.1	-	-	0.31	-	-	28.1
1755	T	1755	-	48.989	-0.353	70.0	22	0.7	2.1	4.2	670.3	131.8	-	203.2	0.20	-	1.54	135.8
1756	L	1745	1745	49.405	-0.462	70.0	34	0.5	7.5	11.0	1287.1	548.0	43.9	381.0	0.43	0.08	0.70	123.9
1757	L	486	616	49.452	-0.386	72.6	24	1.1	4.2	7.1	771.9	276.6	48.9	284.0	0.36	0.18	1.03	379.8
1758	L	486	722	49.407	-0.370	70.0	20	0.5	6.8	10.3	501.5	279.2	30.1	385.2	0.56	0.11	1.38	267.8
1759	L	486	669	49.263	-0.362	70.0	17	1.1	4.3	6.3	728.3	169.9	20.0	99.1	0.23	0.12	0.58	135.5

1760	L	1496	1496	48.718	-0.466	71.3	31	0.7	2.3	3.9	581.2	171.7	35.7	-	0.30	0.21	-	59.0
1761	L	1189	1501	48.999	-0.318	72.6	24	1.1	5.6	9.6	1626.2	439.7	30.6	651.5	0.27	0.07	1.48	318.3
1762	L	1745	1745	49.424	-0.436	71.3	68	0.4	7.5	10.9	1774.3	790.9	125.2	491.0	0.45	0.16	0.62	123.0
1763	T	1763	-	49.896	-0.339	71.9	34	0.6	2.1	3.9	595.7	194.2	-	-	0.33	-	-	34.7
1764	L	486	550	49.180	-0.322	72.6	27	0.9	2.7	5.4	1641.0	346.0	30.2	340.3	0.21	0.09	0.98	174.2
1765	T	1765	-	49.950	-0.452	72.6	29	0.4	2.1	4.0	405.7	111.3	-	-	0.27	-	-	25.9
1766	T	1766	-	48.734	-0.473	72.6	16	0.5	2.1	3.6	337.1	91.6	-	-	0.27	-	-	67.6
1767	T	1767	-	49.072	-0.381	73.2	25	1.0	2.1	3.8	1084.8	200.1	-	381.0	0.18	-	1.90	241.6
1768	T	1768	-	49.924	-0.346	73.2	42	0.6	2.1	3.6	585.6	195.5	-	-	0.33	-	-	28.6

Acknowledgement

I am deeply grateful to Prof. Nario Kuno, whose considerable supports and comments are indispensable to this thesis. Without his guidance and persistent help this thesis would not have been possible. I also great thank Tomofumi Umemoto, Tetsuhiro Minamidani, Kazufumi Torii, Masao Saito, Tomoka Tosaki and Prof. Naomasa Nakai for discussions and my study of doctor's programs. In particular, Kazufumi Torii gives insightful comments and suggestions about CCC. In addition, I also thank the all member of FUGIN project (PI Tomofumi Umemoto especially).

I received generous support from Atsushi Nishimura, Mitsuyoshi Yamagishi, Tatsuya Takekoshi and Mitsuhiro Matsuo. They gave me much advice for my analysis and study. On the other hand, my knowledge of the observational study of radio astronomy is based on the experience of Tsukuba 32m telescope. I am very grateful to Masumichi Seta, Makoto Nagai, Hitoshi Arai, Yusuke Miyamoto, Hiroyuki Kaneko and Yuki Terabe. Then, I am also grateful to Dr. H. Parsons and Dr. T. Jogler for providing FITS data (*JCMT* data and *Fermi*-LAT data, respectively).

Finally, I would like to thank Nobeyama Radio Observatory (NRO), National Astronomical Observatory of Japan (NAOJ), Astronomy Data Center (ADC), University of Tsukuba and Geospatial Information Authority of Japan (GSI) for preparing research opportunities and facilities.

Bibliography

- Abdo, A. A., et al. 2009, ApJ, 706, L1
- Aleksić, J., et al. 2012, A&A, 541, A13
- Arnal, E. M. and Goss, W. M. 1985, A&A, 145, 369-376.
- Bally J., 2008, in Reipurth B., ed., ASP Monograph Publications, Vol. 4, Handbook of Star Forming Regions: Vol. I. The Northern Sky. Astron. Soc. Pac., San Francisco, p. 459
- Bieging, J. 1975, in Lecture Notes in Physics 42, H II Regions and Related Topics, ed. T. L. Wilson and D. Downes (Berlin : Springer), 443
- Blitz L, Fukui Y, Kawamura A, Leroy A, Mizuno N, Rosolowsky E. 2007. Protostars and Planets V, ed. B Reipurth, D Jewitt, K Keil, p. 81. Tucson: Univ. Ariz. Press, and Houston: Lunar and Planet. Inst.
- Bonnell I. A. et al. (2001), Mon. Not. R. Astron. Soc., 323, 785.
- Burton, W. B. 1970, A&AS, 2, 291
- Carpenter, J. M., & Sanders, D. B. 1998, AJ, 116, 1856
- Colombo, D., Rosolowsky, E., Ginsburg, A., Duarte-Cabral, A., & Hughes, A. 2015, MNRAS, 454, 2067
- Elmegreen, B. G., & Lada, C. J. 1977, ApJ, 214, 725
- Fukui Y. & Kawamura A. (2010) Annu. Rev. Astron. Astrophys., 48,547
- Fukui, Y., Harada, R., Tokuda, K., et al. 2015, ApJL, 807, L4
- Fukui, Y., Ohama, A., Hanaoka, N., et al. 2014, ApJ, 780, 36
- Fukui, Y., Torii, K., Ohama, A., et al. 2016, ApJ, 820, 26
- Furukawa, N., Dawson, J. R., Ohama, A., et al. 2009, ApJL, 696, L115

- Ginsburg, A., Bally, J., Battersby, C., et al. 2015, A&A, 573, A106
- Goldreich, P., & Kwan, J. 1974, ApJ, 189, 441
- Goldsmith PF. 1987. In Interstellar Processes, ed. DJ Hollenbach, HA Thronson Jr., 134:51-70. Ap. Space Sci. Libr. Dordrecht, Neth.: Reidel
- Habe, A., & Ohta, K. 1992, PASJ, 44, 203
- Heyer, M., & Dame, T. M. 2015, ARA&A, 53, 583
- Hollenbach, D. J., & Tielens, A. G. G. M. 1999, RvMP, 71, 173
- Hou, L. G., & Gao, X. Y. 2014, MNRAS, 438, 426
- Inoue, T., & Fukui, Y. 2013, ApJL, 774, L31
- Jogler, T., & Funk, S. 2016, ApJ, 816, 100
- Kang, M., Bieging, J. H., Kulesa, C. A., et al. 2010, ApJS, 190, 58
- Kang, M., Bieging, J. H., Povich, M. S., & Lee, Y. 2009, ApJ, 706, 83
- Kim, H., Nakajima, Y., Sung, H., Moon, D.-S., & Koo, B.-C. 2007, J. Korean Astron. Soc., 40, 17
- Koo, B.-C. 1997, ApJS, 108, 489
- Koo, B.-C., & Moon, D.-S. 1997a, ApJ, 475, 194
- Koo, B.-C., & Moon, D.-S. 1997b, ApJ, 485, 263
- Koo, B.-C., Kim, K.-T., & Seward, F. D. 1995, ApJ, 447, 211
- Kuno et al. 2011, Union Radio-Scientifique Internationale, proceeding "New Observing System of the 45-m Telescope at Nobeyama Radio Observatory"
- Mehringer, D. M. 1994, ApJS, 91, 713

- MInamidani et al. Proc. SPIE 9914, Millimeter, Submillimeter, and Far-Infrared Detectors and Instrumentation for Astronomy VIII, 99141Z (19 July 2016)
- Muraoka, K., Tosaki, T., Miura, R., Onodera, S., Kuno, N., Nakanishi, K., Kaneko, H., & Komugi, S. 2012, PASJ, 64, 3
- Nagayama, T., Omodaka, T., Handa, T., Honma, M., Kobayashi, H., Kawaguchi, N., & Ueno, Y. 2011a, PASJ, 63, 719
- Ohama, A., Dawson, J. R., Furukawa, N., et al. 2010, ApJ, 709, 975
- Okumura S., Miyawaki R., Sorai K., Yamashita T., Hasegawa T., 2001, PASJ, 53, 793
- Okumura S., Mori A., Nishihara E., Watanabe E., Yamashita T., 2000, ApJ, 543, 799
- Pankonin V., Payne H. E., Terzian Y., 1979, A&A, 75, 365
- Parsons, H., Thompson, M. A., Clark, J. S., & Chrysostomou, A. 2012, MNRAS, 424, 1658
- Reid, M. J., Menten, K. M., Zheng, X. W., et al. 2009b, ApJ, 700, 137
- Rengarajan, T. N., Cheung, L. H., Fazio, G. G., Shivanandan, K., & McBreen, B. 1984, ApJ, 286, 573
- Rosolowsky E. W., Pineda J. E., Kauffmann J., Goodman A. A., 2008, ApJ, 679, 1338 (R08)
- Sato, M., Reid, M. J., Brunthaler, A., & Menten, K. M. 2010, ApJ, 720, 1055
- Sawada, T., Ikeda, N., Sunada, K., et al. 2008, PASJ, 60, 445
- Scoville, N. Z., & Sanders, D. B. 1987, in Interstellar Processes, ed. D. J. Hollenbach & H. A. Thronson, Jr. (Dordrecht: Reidel), 21
- Scoville, N. Z., & Sanders, D. B. 1987, Interstellar Processes, 134, 21
- Shimajiri, Y., Kitamura, Y., Saito, M., et al. 2014, A&A, 564, A68
- Shu F. H. et al. (1987) Ann. Rev. Astron. Astrophys., 25, 23.

- Solomon P. M., Rivolo A. R., Barrett J., Yahil A., 1987, ApJ, 319, 730
- Solomon, P. M., & Sanders, D. B. 1980, in Giant Molecular Clouds in the Galaxy, 41-73
- Stahler, S. W., & Palla, F. (ed.) 2005, The Formation of Stars (New York: Wiley), 865
- Tian, W. W., & Leahy, D. A. 2013, ApJ, 769, L17
- Torii, K., Enokiya, R., Sano, H., et al. 2011, ApJ, 738, 46
- Torii, K., Hasegawa, K., Hattori, Y., et al. 2015, ApJ, 806, 7
- Torii, K.; Hattori, Y.; Hasegawa, K., et al. 2017, ApJ, 835, 142
- Umemoto et al. submitted
- Westerhout G., 1958, Bull. Astron. Inst. Netherlands, 14, 215
- Wilking, Bruce A., “The Formation of Low Mass Stars,” Astronomical , Bruce A., “The Formation of Low Mass Stars,” Astronomical Society of the Pacific, March 1989, vol. 101, No. 637
- Wilson, T. L.,Mezger, P. G., Gardner, F. F., & Milne, D. K. 1970, Astrophys. Lett., 5, 99
- Wynn-Williams, C. G., Becklin, E. E., & Neugebauer, G. 1974, ApJ, 187, 473
- Yamada, Masaya; Oka, Tomoharu, Takekawa, Shunya, Iwata, Yuhei, Tsujimoto, Shiho, Tokuyama, Sekito, Furusawa, Maiko, Tanabe, Keisuke, Nomura, Mariko, 2017, ApJ, 834, 3
- Zhang B., Reid M. J., Menten K. M., Zheng X. W., Brunthaler A., Dame T. M., Xu Y., 2013, ApJ, 775, 79
- Zinnecker H., Yorke H. W., 2007, ARA&A, 45, 481